



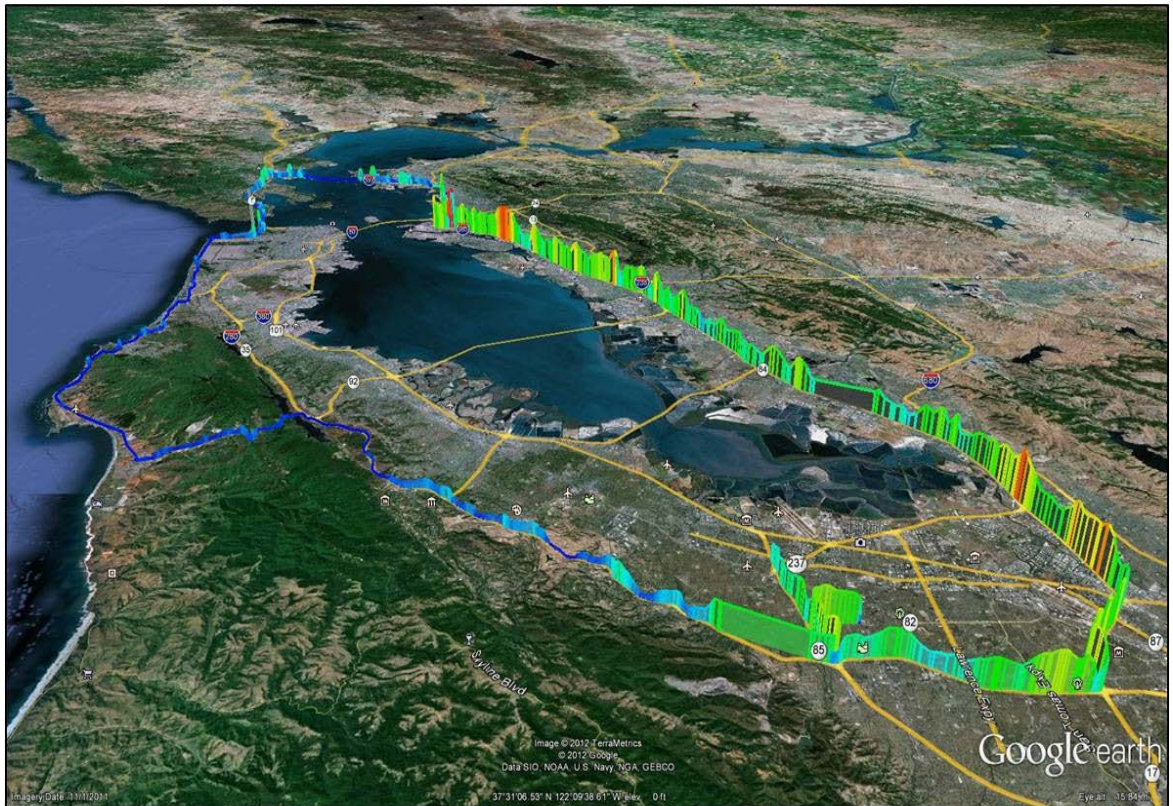
# EPA Handbook: Optical and Remote Sensing for Measurement and Monitoring of Emissions Flux of Gases and Particulate Matter

EPA 454/B-18-008  
August 2018

EPA Handbook: Optical and Remote Sensing for Measurement and Monitoring of Emissions  
Flux of Gases and Particulate Matter

U.S. Environmental Protection Agency  
Office of Air Quality Planning and Standards  
Air Quality Assessment Division  
Research Triangle Park, NC

# EPA Handbook: Optical and Remote Sensing for Measurement and Monitoring of Emissions Flux of Gases and Particulate Matter



9/1/2018

## Informational Document

**This informational document describes the emerging technologies that can measure and/or identify pollutants using state of the science techniques**

## ***Forward***

Optical Remote Sensing (ORS) technologies have been available since the late 1980s. In the early days of this technology, there were many who saw the potential of these new instruments for environmental measurements and how this technology could be integrated into emissions and ambient air monitoring for the measurement of flux. However, the monitoring community did not embrace ORS as quickly as anticipated. Several factors contributing to delayed ORS use were:

- **Cost:** The cost of these instruments made it prohibitive to purchase, operate and maintain.
- **Utility:** Since these instruments were perceived as “black boxes.” Many instrument specialists were wary of how they worked and how the instruments generated the values.
- **Ease of use:** Many of the early instruments required a well-trained spectroscopist who would have to spend a large amount of time to setup, operate, collect, validate and verify the data.
- **Data Utilization:** Results from path integrated units were different from point source data which presented challenges for data use and interpretation.

Over the years, the air monitoring community has come to accept both the challenges and overall utility of ORS technologies and applications. The emissions monitoring community and monitored sources have been employing ORS for several years and are using these technologies to answer questions that traditional instrumentation could not address. In addition, ORS technology has been applied to ambient and fence line monitoring, including near-roadway monitoring. Therefore, application of ORS technology has an expanding place with other air measurement tools.

The EPA staff and other scientists and engineers in the monitoring community recognized that a compilation of ORS material was needed to encourage wider use and understanding of ORS. Questions on how instruments generate data and how an agency or source validates and verifies data are universal, whether the instrument is optically remote or an extractive instrument on site or within the stack. With this in mind, the EPA developed this Handbook to assist the “non-spectroscopist” in understanding and using data and information generated by ORS. This Handbook is divided into five sections:

- Section 1: Discusses what ORS means and how this technology can be used. It also has several tables that have a “crosswalk” between the different technologies and their use (i.e., techniques).
- Section 2: Describes the different technologies or “hardware” that are currently available that are considered “optically remote.”
- Section 3: Explains how to use the “hardware” with different techniques and how to calculate emission flux.
- Section 4: Discusses the “other” data that needs to be collected to understand and better validate and verify the ORS data.
- Section 5: Provides a very brief overview of how to validate and verify this data once it is collected.

### ***Disclaimer of Endorsement***

Mention of, or referral to, commercial products or services and/or links to non-EPA internet sites does not imply official EPA endorsement of, or responsibility for opinions, ideas, data, or products presented at those locations, or guarantee the validity of the information provided.

Mention of commercial products/services and non-EPA websites is provided solely as a reference to information on topics related to environmental protection that may be useful to EPA staff and the public.

## ***Acknowledgement***

A document such as this requires the work and dedication of many people. This section acknowledges those that have provided their time and effort to create this document.

**Team Lead: Dennis K. Mikel, EPA-OAQPS**

**Reviewers:**

David Nash, EPA-OAQPS

Raymond Merrill EPA-OAQPS

Jason Dewees, EPA-OAQPS

**Comments and questions can be directed to:**

Steffan Johnson EPA-OAQPS

109 Alexander Drive

Research Triangle Park, NC 27711 Email: [johnson.steffan@epa.gov](mailto:johnson.steffan@epa.gov)

# Table of Contents

|   |           |
|---|-----------|
| <b>1.0 Introduction</b>   | <b>1</b>  |
| <b>1.1 Purpose of the Handbook</b>  | <b>1</b>  |
| <b>1.2 Contents and Overview of the Handbook</b>                                | <b>3</b>  |
| <b>1.3 Stationary Sources and Emissions Points</b>                              | <b>6</b>  |
| Ducted or Vented Emissions  | 7         |
| Area or Fugitive Emissions Sources  | 8         |
| <b>1.4 Why Remote Measurement?</b>  | <b>9</b>  |
| Criteria Pollutant Gases, HAPs and GHGs   | 11        |
| <b>1.5 Knowledge and Advancement of Remote Sensing to Emissions Measurement</b> | <b>15</b> |
| Active  | 15        |
| Passive   | 16        |
| Backscatter   | 17        |
| Mobile  | 18        |
| Advantages Over Closed Path Techniques  | 18        |
| <b>1.6 General Discussion of the EPA Quality System</b>                         | <b>20</b> |
| Data Quality Objectives   | 21        |
| Measurement Quality Objectives  | 22        |
| <b>1.7 Choosing the Right Tool for the Right Job</b>                            | <b>24</b> |
| What is the nature of the source?   | 24        |
| What is the required time resolution?   | 25        |
| What are the QA/QC requirements for the measurement?                            | 26        |
| How easy are the data to process?   | 27        |
| <b>1.8 Future Evolution and Updates of this Handbook</b>                        | <b>28</b> |
| <b>1.9 References</b>   | <b>28</b> |
| <br>  |           |
| <b>2.0 Optical Remote Sensing Technologies</b>                                  | <b>1</b>  |
| <b>2.1 Fourier Transform Infrared Spectroscopy</b>                              | <b>2</b>  |
| Basic Operation   | 2         |
| Extractive (Closed) Cell Measurement Applications                               | 5         |
| Open-Path Measurement Applications  | 6         |
| Pollutants and Relative Levels That Can Be Measured                             | 8         |
| Typical QA/QC   | 11        |
| Calibration Spectra   | 11        |
| QA/QC for OP-FTIR Instrumentation   | 13        |
| Data Quality Indicators for Precision and Accuracy for OP-FTIR                  | 14        |
| Example Applications and Vendors  | 14        |
| Strengths and Limitations   | 16        |
| References  | 19        |
| <b>2.2 Tunable Diode Laser</b>  | <b>21</b> |
| Basic Operation   | 22        |
| Pollutants and Relative Levels That Can Be Measured                             | 26        |
| Typical QA/QC   | 27        |
| Selection of the Laser and Absorption Line                                      | 27        |
| Calibration   | 29        |
| Quality Control Procedures  | 30        |



|  |           |
|--|-----------|
| Example Applications and Vendors Applications .....                          | 30        |
| Vendors .....  | 31        |
| Strengths and Limitations .....  | 31        |
| References .....   | 33        |
| <b>2.3 Ultraviolet Differential Optical Absorption Spectroscopy .....</b>    | <b>35</b> |
| Basic Operation .....  | 35        |
| UV-DOAS Field Implementation .....   | 38        |
| Passive UV-DOAS .....  | 40        |
| Pollutants and Relative Levels That Can Be Measured .....                    | 40        |
| Typical QA/QC .....  | 41        |
| Record Keeping .....   | 42        |
| Instrument Performance .....   | 42        |
| Example Applications and Vendors .....                                       | 43        |
| Vendors .....  | 44        |
| Strengths and Limitations .....  | 44        |
| References .....   | 46        |
| <b>2.4. Differential Absorption Light Detection and Ranging Systems.....</b> | <b>47</b> |
| Basic Operation.....   | 48        |
| Pollutants and Relative Levels That Can Be Measured.....                     | 54        |
| Typical QA/QC.....   | 55        |
| Record Keeping.....  | 56        |
| Instrument Performance .....   | 56        |
| Example Applications and Vendors Applications .....                          | 56        |
| Vendors.....   | 58        |
| Strengths and Limitations .....  | 58        |
| References .....   | 60        |
| <b>2.5 Thermal Infrared Cameras .....</b>                                    | <b>62</b> |
| Basic Operation.....   | 63        |
| Pollutants and Relative Levels That Can Be Detected .....                    | 69        |
| Typical QA/QC.....   | 70        |
| Example Applications and Vendors .....                                       | 74        |
| Vendors.....   | 75        |
| Strengths and Limitations .....  | 75        |
| References .....   | 76        |
| <b>2.6 Cavity Ring-Down Spectroscopy.....</b>                                | <b>79</b> |
| Basic Operation.....   | 79        |
| General Experimental Design .....  | 81        |
| Current Method Developments.....   | 85        |
| Pollutants and Relative Levels That Can Be Measured.....                     | 86        |
| Typical QA/QC.....   | 88        |
| Example Applications and Vendors Applications .....                          | 89        |
| Vendors.....   | 90        |
| Strengths and Limitations .....  | 90        |
| References .....   | 92        |
| <b>2.7 Particulate Matter LIDAR.....</b>                                     | <b>94</b> |
| Basic Operation.....   | 95        |
| Pollutants and Relative Levels That Can Be Detected .....                    | 101       |
| Typical QA/QC.....   | 102       |

|   |           |
|---|-----------|
| Example Applications and Vendors .....  | 102       |
| Vendors.....  | 102       |
| Strengths and Limitations .....   | 104       |
| References .....  | 104       |
| <b>3.0 Measurements Applicable to Emissions Flux .....</b>                      | <b>1</b>  |
| Reference.....  | 2         |
| <b>3.1 Radial Plume Mapping: Other Test Method 10 .....</b>                     | <b>3</b>  |
| General Description of Approach .....   | 3         |
| Horizontal RPM Algorithm .....  | 4         |
| Vertical RPM algorithm.....   | 6         |
| One-dimensional RPM algorithm .....   | 9         |
| RPM-ORS Technologies.....   | 11        |
| Verification/Validation Studies.....  | 12        |
| OP-FTIR and OP-TDLAS comparison studies.....                                    | 12        |
| OP-FTIR and UV-DOAS comparison: Colorado Springs field study .....              | 13        |
| VRPM plume capture validation study .....                                       | 13        |
| Typical QA/QC.....  | 14        |
| Siting Concerns .....   | 15        |
| Strengths and Limitations .....   | 16        |
| References .....  | 17        |
| <b>3.2 Range Resolved Measurements using Differential Absorption LIDAR.....</b> | <b>19</b> |
| General Description of Approach .....   | 19        |
| Basic DIAL algorithm to calculate backscatter.....                              | 20        |
| Verification/Validation Studies.....  | 22        |
| Verification of DIAL for Gas Species Measurements .....                         | 22        |
| Typical QA/QC.....  | 24        |
| Siting Concerns.....  | 25        |
| Strengths and Limitations .....   | 25        |
| References .....  | 26        |
| <b>3.3 Solar Occultation Flux Measurement .....</b>                             | <b>28</b> |
| General Description of Approach .....   | 29        |
| Verification/Validation Studies.....  | 34        |
| Typical QA/QC.....  | 37        |
| Siting Concerns .....   | 39        |
| Strengths and Limitations .....   | 39        |
| References .....  | 40        |
| <b>3.4 Tracer Gas Correlation .....</b>   | <b>42</b> |
| General Description of Approach .....   | 42        |
| Verification/Validation Studies.....  | 45        |
| Typical QA/QC.....  | 48        |
| Sitting Concerns .....  | 48        |
| Strength and Limitations.....   | 49        |
| References .....  | 50        |
| <b>3.5 Backward Lagrangian Stochastic Inverse-Dispersion model .....</b>        | <b>51</b> |
| General Description of Approach .....   | 51        |
| Backward LS Dispersion Model for Calculating ( $C/Q_{sim}$ ) .....              | 53        |
| bLS Model Output Units.....   | 55        |

|  |            |
|--|------------|
| Verification/Validation Study.....   | 55         |
| Flesch et al Conditions and Setup .....  | 56         |
| Flesch et al Results and Conclusions.....  | 58         |
| Typical QA/QC.....   | 59         |
| Siting Concerns .....  | 60         |
| Strengths and Limitations .....  | 61         |
| References .....   | 63         |
| <b>3.6 Geospatial Measurement of Air Pollution, Remote Emission Quantification – Other</b> |            |
| <b>Test Method 33 .....</b>  | <b>64</b>  |
| General Description of Approach .....  | 66         |
| Verification/Validation Studies.....   | 69         |
| Typical QA/QC.....   | 69         |
| Siting Concerns.....   | 70         |
| Strength and Limitations.....  | 71         |
| References .....   | 73         |
| <b>3.7 Geospatial Measurement of Air Pollution, Remote Emission Quantification: Direct</b> |            |
| <b>Assessment – Other Test Method 33A.....</b>   | <b>75</b>  |
| General Description of Approach .....  | 76         |
| Verification/Validation Studies.....   | 82         |
| Typical QA/QC.....   | 91         |
| Siting Concerns .....  | 93         |
| Strengths and Limitations .....  | 95         |
| References .....   | 96         |
| <b>3.8 Hyperspectral Imaging .....</b>   | <b>98</b>  |
| General Description of Approach .....  | 99         |
| Operating Principles.....  | 100        |
| Example Instruments .....  | 102        |
| Physical Sciences’ AIRIS.....  | 103        |
| Rebellion Photonics’ Gas Cloud Imager .....  | 104        |
| Telops’ HyperCam and MS-IR .....   | 106        |
| Additional Considerations.....   | 108        |
| Verification/Validation Studies.....   | 110        |
| Typical QA/QC.....   | 113        |
| Summary of Thermal IR Camera QA/QC.....  | 114        |
| Siting Concerns .....  | 115        |
| Strengths and Limitations .....  | 115        |
| References .....   | 116        |
| <b>3.9 Fenceline Passive Sampling – Method 325 A/B.....</b>                                | <b>118</b> |
| General Description of Approach .....  | 118        |
| Passive Tube Samplers.....   | 119        |
| Sampler Deployment .....   | 122        |
| Passive Sampler Recovery.....  | 123        |
| Meteorological Data Collection .....   | 124        |
| Passive Sampler Analysis .....   | 124        |
| Recordkeeping and Data Analysis.....   | 126        |
| Verification/Validation Studies.....   | 126        |
| Flint Hills West Refinery.....   | 126        |
| South Philadelphia PS and Sensor Study .....   | 128        |

|             |   |            |
|-------------|---|------------|
|             | Typical QA/QC.....  | 129        |
|             | Field Sampling QA/QC.....   | 129        |
|             | Laboratory QA/QC .....  | 130        |
|             | Siting Concerns.....  | 131        |
|             | Strength and Limitations.....   | 132        |
|             | References .....  | 133        |
| <b>3.10</b> | <b>Method to Quantify Particulate Matter Emissions from Windblown Dust – Other</b>    |            |
|             | <b>Test Method 30 .....</b>   | <b>134</b> |
|             | General Description of Approach .....   | 134        |
|             | Instrumentation.....  | 136        |
|             | Dispersion Modeling and K-factors.....  | 139        |
|             | Sample Collection .....   | 140        |
|             | Owens (dry) Lake, Inyo County California.....   | 141        |
|             | Mono Lake, California .....   | 141        |
|             | Typical QA/QC.....  | 142        |
|             | Siting Concerns .....   | 143        |
|             | Strengths and Limitations .....   | 144        |
|             | References .....  | 144        |
| <b>3.11</b> | <b>Determination of Emissions from Open Sources by Plume Profiling – Other Test</b>   |            |
|             | <b>Method 32 .....</b>  | <b>146</b> |
|             | General Description of Approach .....   | 146        |
|             | Sampling Equipment.....   | 147        |
|             | Sample Deployment.....  | 149        |
|             | Sample Analysis.....  | 151        |
|             | Verification/Validation Studies .....   | 151        |
|             | United Taconite and U.S. Steel Minntac.....   | 151        |
|             | Typical QA/QC.....  | 153        |
|             | Quality Control Samples .....   | 153        |
|             | Quality Assurance .....   | 153        |
|             | Precision.....  | 153        |
|             | Siting Concerns .....   | 154        |
|             | Strengths and Limitations .....   | 155        |
|             | References .....  | 156        |
| <b>3.12</b> | <b>Method to Quantify Road Dust Particulate Matter from Paved and Unpaved Roads –</b> |            |
|             | <b>Other Test Method 34.....</b>  | <b>157</b> |
|             | General Description of Approach .....   | 157        |
|             | Instrumentation.....  | 158        |
|             | Calibration.....  | 161        |
|             | Data Collection.....  | 162        |
|             | Data Analysis.....  | 162        |
|             | Verification/Validation Studies .....   | 163        |
|             | Clark County, Nevada.....   | 163        |
|             | Typical QA/QC.....  | 165        |
|             | Screening Criteria.....   | 165        |
|             | Collocation .....   | 165        |
|             | Siting Concerns .....   | 166        |
|             | Strengths and Limitations .....   | 166        |
|             | References .....  | 167        |

|   |           |
|---|-----------|
| <b>4.0 Meteorological Measurements.....</b>                             | <b>1</b>  |
| <b>4.1 Meteorological Station Siting .....</b>                          | <b>2</b>  |
| Horizontal Wind Speed and Direction .....                               | 3         |
| Vertical Wind Speed and Lateral Turbulence .....                        | 4         |
| Relative Humidity.....  | 4         |
| Temperature .....   | 4         |
| Net Solar Radiation .....   | 5         |
| Atmospheric Pressure.....   | 5         |
| Differential Global Positioning for Tracking Monitoring Locations ..... | 5         |
| Collection of Process Information .....                                 | 6         |
| Attribution of Emissions to Source of Intent.....                       | 9         |
| <b>4.2 References.....</b>  | <b>9</b>  |
| <br>  |           |
| <b>5.0 Data Validation and Verification .....</b>                       | <b>1</b>  |
| <b>5.1 General Approach .....</b>                                       | <b>2</b>  |
| <b>5.2 Data Validation Methods .....</b>                                | <b>2</b>  |
| Levels of Data Quality Review.....                                      | 3         |
| <b>5.3 Data Verification Methods .....</b>                              | <b>4</b>  |
| Data Review and Verification.....                                       | 8         |
| Validation of Primary and Ancillary Measurements .....                  | 9         |
| Final Validation and Evaluation of Measurements for Data Users.....     | 11        |
| <b>5.4 References .....</b>   | <b>12</b> |

## ***Figures***

| <b><i>Number</i></b> | <b><i>Title</i></b>  | <b><i>Section</i></b> |
|----------------------|--|-----------------------|
| 1-1                  | Types and sources of air pollutants                                  | 1.3                   |
| 1-2                  | Example of Ducted Stationary Source Stack                            | 1.3                   |
| 1-3                  | Example of Potential Fugitive Source                                 | 1.5                   |
| 1-4                  | Example of Potential Fugitive Sources                                | 1.5                   |
| 1-5                  | Block Diagram of bi-static ORS                                       | 1.5                   |
| 2-1                  | Diagram Showing Beam Path and Major Components of FTIR               | 2.1                   |
| 2-2                  | FTIR Absorption Spectrum Recorded at 1075° K                         | 2.1                   |
| 2-3                  | FTIR Closed Cell Unit Used to Monitor Stack Gas                      | 2.1                   |
| 2-4                  | Basic Setup Used to Make Monostatic Open-path FTIR Measurements      | 2.1                   |
| 2-5                  | The Corner-cube Reflector  | 2.1                   |
| 2-6                  | Typical Telescopic FTIR Transmitting and Detection Unit              | 2.1                   |
| 2-7                  | Corner Cube Reflector  | 2.1                   |
| 2-8                  | Calibration Plot of Absorbance vs. Concentration                     | 2.1                   |
| 2-9                  | TDL Bistatic Configuration   | 2.2                   |
| 2-10                 | TDL Monostatic Configuration   | 2.2                   |
| 2-11                 | The Corner-cube Reflector  | 2.2                   |
| 2-12                 | Calibration Data for an OP-TDL System                                | 2.2                   |
| 2-13                 | Opsis DOAS Unit  | 2.3                   |
| 2-14                 | Bistatic Configuration of UV-DOAS                                    | 2.3                   |
| 2-15                 | The Corner-cube Reflector  | 2.3                   |
| 2-16                 | Basic Setup Used to Make Mono-static Open-path UV- DOAS Measurements | 2.3                   |
| 2-17                 | Beam Path and Major Components of DIAL Unit                          | 2.4                   |
| 2-18                 | Monostatic Coaxial and Biaxial Configuration for DIAL                | 2.4                   |
| 2-19                 | Bistatic Configuration for DIAL                                      | 2.4                   |
| 2-20                 | Illustration of DIAL unit mapping an emission plume                  | 2.4                   |
| 2-21                 | Mobile DIAL Unit   | 2.4                   |

## **Figures**

| <b>Number</b> | <b>Title</b>  | <b>Section</b> |
|---------------|---|----------------|
| 2-22          | Overview of Thermal IR Camera Technology Basics                               | 2.5            |
| 2-23          | Image of a Controlled Gas Release where the Gas is Warmer than the Background | 2.5            |
| 2-24          | IR Spectrum for Propane with the Molecule Bond Structure                      | 2.5            |
| 2-25          | Spectral Curves for an IR Camera Window of Transmittance                      | 2.5            |
| 2-26          | Calibration/Verification Examples Configuration                               | 2.5            |
| 2-27          | Example of Quality Control Daily Operations Check Chart                       | 2.5            |
| 2-28          | Anticipated Change in Pixel Intensity for various concentrations              | 2.5            |
| 2-29          | Flare Detection by Thermal IR Camera  | 2.5            |
| 2-30          | The essential components of any CDRS experimental set-up                      | 2.6            |
| 2-31          | Schematic representation of the expected rate of decay                        | 2.6            |
| 2-32          | Comparison of Pulsed and Continuous Wave Laser Light                          | 2.6            |
| 2-33          | Optical components schematic of a cavity ring-down spectrometer               | 2.6            |
| 2-34          | Differences PMT and charge couples devices                                    | 2.6            |
| 2-35          | Simplified Schematic of LIDAR system  | 2.7            |
| 2-36          | Illustration of LIDAR System Geometry   | 2.7            |
| 2-37          | Illustration of Monostatic Coaxial and Biaxial LIDAR                          | 2.7            |
| 2-38          | Illustration of the USU AGLITE LIDAR System                                   | 2.7            |
| 2-39          | Illustration of the USU CELis LIDAR System                                    | 2.7            |
| 3-1           | Horizontal RPM setup  | 3.1            |
| 3-2           | Vertical RPM setup  | 3.1            |
| 3-3           | One-dimensional RPM setup   | 3.1            |
| 3-4           | Examples of RPM algorithm outputs.  | 3.1            |
| 3-5           | Conceptual picture on the operation of DIAL.                                  | 3.2            |
| 3-6           | Contour profile of SO <sub>2</sub> concentration measured 2.1 km downwind of  | 3.2            |
| 3-7           | <i>Solar tracker configurations</i>   | 3.3            |
| 3-8           | Rough overview of a mobile SOF system   | 3.3            |
| 3-9           | SOF cartoon   | 3.3            |
| 3-10          | An example of path-integrated calculations determined from SOF measurements   | 3.3            |

## Figures

| <b>Number</b> | <b>Title</b>   | <b>Section</b> |
|---------------|--|----------------|
| 3-11          | Tracer gas/SOF experiment measuring SF emissions in an open field over time of day             | 3.3            |
| 3-12          | Wind velocity profiles by height   | 3.3            |
| 3-13          | Tracer Gas release setup cartoon   | 3.4            |
| 3-14          | Methane concentration versus acetylene concentration<br>Tracer gas characterization using FTIR | 3.4            |
| 3-15          | Illustration of an inverse-dispersion model for estimating emission rate Q                     | 3.5            |
| 3-16          | Illustration of the WindTrax bLS Modeling Software Graphical Interface                         | 3.5            |
| 3-17          | Map of the laser paths used in the 2004 Flesch <i>et al</i> experiment                         | 3.5            |
| 3-18          | GMAP Operational Regime  | 3.6            |
| 3-19          | GMAP (OTM-33) Limitations  | 3.6            |
| 3-20          | GMAP (OTM-33) Overlapping Plume Sources  | 3.6            |
| 3-21          | GMAP (OTM-33) Limitations  | 3.7            |
| 3-22          | GMAP-REQ-DA (OTM 33A) Concentration Mapping Survey   | 3.7            |
| 3-23          | An Illustration of a Stationary EQ Observation   | 3.7            |
| 3-24          | Effect of varying atmospheric conditions   | 3.7            |
| 3-25          | Results from controlled release experiments  | 3.7            |
| 3-26          | Comparison of methane measurements by basin  | 3.7            |
| 3-27          | Density and cumulative density of methane emission measurements                                | 3.7            |
| 3-28          | Comparison of onsite measurements and remote measurements                                      | 3.7            |
| 3-29          | Source emission strength calculations for each controlled release                              | 3.7            |
| 3-30          | Source strength calculation averages by controlled release study                               | 3.7            |
| 3-31          | Example of Differences between Multi-, Hyper-and Ultraspectral                                 | 3.8            |
| 3-32          | Radiative Transfer Model Illustration for IR Remote Sensing                                    | 3.8            |
| 3-33          | Multispectral Imaging using Spectral Differentiation of Methane Gas                            | 3.8            |
| 3-34          | AIRIS Interferometer Design  | 3.8            |
| 3-35          | Illustration of the IMS Optical Layout.  | 3.8            |
| 3-36          | Example Datacube with Waveband Elements  | 3.8            |



## **Figures**

| <b>Number</b> | <b>Title</b>  | <b>Section</b> |
|---------------|---|----------------|
| 3-37          | Telops HyperCam (Left) Hyperspectral Imager and MS-IR Infrared            | 3.8            |
| 3-38          | Example Telops Software Output  | 3.8            |
| 3-39          | Detector Methods for DataCube Acquisition.                                | 3.8            |
| 3-40          | SnapShot Detection with FPA Divided into smaller collections              | 3.8            |
| 3-41          | High/Low Controlled Gas Release Platform                                  | 3.8            |
| 3-42          | ERG Controlled Leak Simulation Platform                                   | 3.8            |
| 3-43          | Example Releases as Seen from the GCI                                     | 3.8            |
| 3-44          | Cross-Section of the PS Tube  | 3.9            |
| 3-45          | Sorbent Tube Protection Cover   | 3.9            |
| 3-46          | Saltation and Dust Production Process for Windblown Dust                  | 3.10           |
| 3-47          | Schematic of CSC Placement for Sampling.                                  | 3.10           |
| 3-48          | Cut-out of a CSC and Construction Specifications                          | 3.10           |
| 3-49          | CSC Placement in the Field with a Height Adjustment Tool                  | 3.10           |
| 3-50          | BSNE Sampler Shown Sampling in the Field                                  | 3.10           |
| 3-51          | Monitoring Network at Mono Lake, CA.                                      | 3.10           |
| 3-52          | Traditional PM Sampler Configuration                                      | 3.11           |
| 3-53          | Illustration of Fixed Point Source Sampling Array                         | 3.11           |
| 3-54          | Illustration of Moving Point Source--Unpaved Road Dust                    | 3.11           |
| 3-55          | Example Sampling Array for Moving Point Source                            | 3.11           |
| 3-56          | Deployment of Collocated Plume Towers at Roadside Location                | 3.11           |
| 3-57          | Sample inlet installation behind the front tire                           | 3.12           |
| 3-58          | Sample inlet installation on a trailer pulled behind test vehicle         | 3.11           |
| 3-59          | Coefficient of Variation determined from data in Clark County             | 3.11           |
| 5-1           | Generalized Data Verification and Validation Process Flow                 | 5.1            |
| 5-2           | Level 0 Verification Checks the Most Fundamental Quality Requirements     | 5.2            |
| 5-3           | Example of Optical Remote Measurement Visual Check List                   | 5-2            |
| 5-4           | Level 1 Verification Ensures Quality Requirements are met in the Field    | 5.2            |
| 5-5           | Level 2 Quality Checks Start the Data Validation Process                  | 5.3            |
| 5-6           | Level 3 Quality Checks Ensure the Data is Usable for the Purpose Intended | 5.3            |

## ***Tables***

| <b><i>Number</i></b> | <b><i>Title</i></b>   | <b><i>Section</i></b> |
|----------------------|---|-----------------------|
| 1-1                  | Gas Phase Source Type   | 1.7                   |
| 1-2                  | Particle Phase Source Type  | 1.7                   |
| 1-3                  | Gas Phase Time Resolution Matrix  | 1.7                   |
| 1-4                  | Particle Phase Time Resolution Matrix                                   | 1.7                   |
| 1-5                  | Gas Phase QA/QC Matrix  | 1.7                   |
| 1-6                  | Particle Phase QA/QC Matrix   | 1.7                   |
| 1-7                  | Gas Phase Ease of Operation Matrix                                      | 1.7                   |
| 1-8                  | Particle Phase Ease of Operation Matrix                                 | 1.7                   |
| 2-1                  | Example List of Compounds Measured by FTIR Open-path Systems            | 2.1                   |
| 2-2                  | Typical Applications for OP-FTIR.                                       | 2.1                   |
| 2-3                  | FTIR Supply Vendors   | 2.1                   |
| 2-4                  | Summary Table of the OP-FTIR's Strengths                                | 2.1                   |
| 2-5                  | Summary Table of the OP-FTIR's Limitations                              | 2.1                   |
| 2-6                  | Example List of Gaseous Compounds Measured by Near IR<br>OP-TDL Systems | 2.2                   |
| 2-7                  | Near-IR Laser Types Available for OP-TDL Systems                        | 2.2                   |
| 2-8                  | Potentially Usable Mid-IR Lasers  | 2.2                   |
| 2-9                  | Typical Applications for OP-TDL   | 2.2                   |
| 2-10                 | Near-IR OP-TDL Vendors  | 2.2                   |
| 2-11                 | Summary Table of the TDL's Strengths                                    | 2.2                   |
| 2-12                 | Summary Table of the TDL's Limitations                                  | 2.2                   |
| 2-13                 | Species Measured with UV-DOAS Systems                                   | 2.3                   |
| 2-14                 | Approximate Detection Limits for UV-DOAS                                | 2.3                   |
| 2-15                 | Typical Applications for UV-DOAS  | 2.3                   |
| 2-16                 | UV-DOAS Vendors   | 2.3                   |
| 2-17                 | Summary Table of the UV-DOAS's Strengths                                | 2.3                   |
| 2-18                 | Summary Table of the UV-DOAS's Limitations                              | 2.3                   |
| 2-19                 | Reported Species Measured with DIAL Systems                             | 2.4                   |
| 2-20                 | Approximate Detection Limits for DIAL                                   | 2.4                   |

## **Tables**

| <b>Number</b> | <b>Title</b>   | <b>Section</b> |
|---------------|--|----------------|
| 2-21          | Typical Applications for LIDAR   | 2.4            |
| 2-22          | DIAL Vendors   | 2.4            |
| 2-23          | Summary Table of the DIAL's Strengths  | 2.4            |
| 2-24          | Summary Table of the DIAL's Limitations  | 2.4            |
| 2-25          | Example List of Gaseous Compounds that can be Detected                                       | 2.5            |
| 2-26          | Typical Applications for Thermal IR Camera   | 2.5            |
| 2-27          | Thermal IR Camera Vendors  | 2.5            |
| 2-28          | Summary Table of the IR Camera's Strengths   | 2.5            |
| 2-29          | Summary Table of the IR Camera's Limitations   | 2.5            |
| 2-30          | Example list of detectable pollutants by CRDS  | 2.6            |
| 2-31          | Typical Applications for CRDS  | 2.6            |
| 2-32          | CRDS Vendors   | 2.6            |
| 2-33          | Summary Table of CRDS Strengths  | 2.6            |
| 2-34          | Summary Table of CRDS Limitations  | 2.6            |
| 2-35          | Typical Applications for LIDAR Systems   | 2.7            |
| 2-36          | LIDAR Systems Vendors  | 2.7            |
| 2-37          | Table of LIDAR Strengths   | 2.7            |
| 2-38          | Table of LIDAR Limitations   | 2.7            |
| 3-1           | Data quality indicators for the QA/QC process  | 3.1            |
| 3-2           | Summary Table of the VPRM's Strengths  | 3.1            |
| 3-3           | Summary Table of the VPRM's Limitations  | 3.1            |
| 3-4           | Results from the comparison of DIAL and plant measurements of SO <sub>2</sub> mass emissions | 3.2            |
| 3-5           | DIAL Strengths   | 3.2            |
| 3-6           | DIAL Limitations   | 3.2            |
| 3-7           | SOF technique VOC emissions compared to DIAL   | 3.3            |
| 3-8           | Summary for measurements on the Aby field, 2002  | 3.3            |
| 3-9           | SOF traverse done on day 24-June 2002  | 3.3            |
| 3-10          | Estimation of statistical errors for the SOF measurements                                    | 3.3            |
| 3-11          | Feature strengths of using the SOF method  | 3.3            |

## ***Tables***

| <b><i>Number</i></b> | <b><i>Title</i></b>  | <b><i>Section</i></b> |
|----------------------|--|-----------------------|
| 3-12                 | Feature limitations of using the SOF method                      | 3.3                   |
| 3-13                 | Tracer Gas Correlation Strengths                                 | 3.4                   |
| 3-14                 | Tracer Gas Correlation Limitations                               | 3.4                   |
| 3-15                 | bLS Model Strengths  | 3.5                   |
| 3-16                 | bLS Model Limitations  | 3.5                   |
| 3-17                 | Summary of mobile measurement approaches                         | 3.6                   |
| 3-18                 | Strengths of the General OTM 33 Approach                         | 3.6                   |
| 3-19                 | Limitations of the General OTM 33 Approach                       | 3.6                   |
| 3-20                 | Summary of GMAP-REQ-DA Studies                                   | 3.7                   |
| 3-21                 | Pearson Correlation Coefficients of Emission and Production      | 3.7                   |
| 3-22                 | Strengths of the OTM 33A Approach                                | 3.7                   |
| 3-23                 | Limitations of the OTM 33A Approach                              | 3.7                   |
| 3-24                 | Detection Method by Instrument.                                  | 3.8                   |
| 3-25                 | Summary of Rebellion GCI EPA Controlled Release Results          | 3.8                   |
| 3-26                 | Strengths and Limitations of Hyperspectral Imaging               | 3.8                   |
| 3-27                 | Passive Sampler Manufacturers                                    | 3.9                   |
| 3-28                 | Pollutants that can be Collected with Passive Diffusive Samplers | 3.9                   |
| 3-29                 | GC/MS Tuning Criteria  | 3.9                   |
| 3-30                 | Analytical QA/QC Procedures for EPA Method 325B                  | 3.9                   |
| 3-31                 | Strengths and Limitations of EPA Method 325A/B                   | 3.9                   |
| 3-32                 | Strengths and Limitations of the OTM 30 Approach                 | 3.10                  |
| 3-33                 | Strengths and Limitations of the OTM 32 Approach                 | 3.11                  |
| 3-34                 | Strengths and Limitations of the OTM 34 Approach                 | 3.12                  |

## ***List of Acronyms***

| <b>Acronym</b>                | <b>Description</b>   |
|-------------------------------|--|
| $\mu\text{g}/\text{m}^3$      | micrograms per cubic meter                                 |
| $\mu\text{m}$                 | micrometer   |
| 2-D                           | two dimensional  |
| 3-D                           | three dimensional  |
| ANSI                          | American National Standards Institute                      |
| AOM                           | acousto-optic modulator                                    |
| ASQC                          | American Society for Quality                               |
| bLS                           | Backward Lagrangian Stochastic                             |
| BTX                           | benzene, toluene, elemental mercury and p-xylene           |
| C <sub>2</sub> H <sub>2</sub> | acetylene  |
| CCD                           | charge-coupled device                                      |
| CEA                           | cavity-enhanced absorption                                 |
| CEMs                          | continuous emissions monitors                              |
| CFCs                          | chlorofluorocarbons  |
| CH <sub>4</sub>               | methane  |
| CO                            | carbon monoxide  |
| CO <sub>2</sub>               | carbon dioxide   |
| COSPEC                        | correlation spectrometer                                   |
| CRDS                          | cavity ring-down spectroscopy                              |
| CRLAS                         | cavity ring-down laser absorption spectroscopy             |
| CW                            | continuous wave  |
| DGPS                          | differential global positioning system                     |
| DIAL                          | Differential absorption LIDAR                              |
| DIAL/LIDAR                    | differential absorption light detection and ranging        |
| DOAS                          | differential optical absorption                            |
| DQI                           | data quality indicators                                    |
| DQO                           | data quality objective                                     |
| EPA                           | Environmental Protection Agency                            |
| ETV                           | environmental technology verification                      |
| FID                           | flame ionization detectors                                 |
| FTIR                          | Fourier transform infrared                                 |
| g/s                           | grams per second   |
| GPS                           | global positioning system                                  |
| HAP                           | hazardous air pollutants                                   |
| HITRAN                        | high-resolution transmission molecular absorption database |
| HRPM                          | horizontal RPM   |
| ICOS                          | integrated cavity output spectroscopy                      |
| IR                            | Infrared   |
| LASER                         | light amplification by stimulated emission of radiation    |
| MAXDOAS                       | Multi-axis Differential Absorption Spectroscopy            |

## ***List of Acronyms***

| <b>Acronym</b> | <b>Description</b>                          |
|----------------|---|
| SBFM           | smooth basis function minimization          |
| SF6            | sulfur hexafluoride                         |
| SO2            | sulfur dioxide                              |
| SOF            | Solar Occultation Flux                      |
| SOx            | sulfur oxides                               |
| SSE            | sum of squared errors                       |
| TDC            | tracer dilution correlation                 |
| TDL            | tunable diode laser                         |
| TDLAS          | tunable diode laser absorption spectroscopy |
| UV             | ultraviolet                                 |
| VOCs           | volatile organic compounds                  |
| VRPM           | vertical radial plume mapping               |
| μs             | Microseconds                                |

## **1.0 Introduction**

This document is intended as an introductory handbook for those planning to use or review remote emissions measurement and monitoring approaches for emission sources or for data users building their expertise about current information concerning the technologies and application in these types of measurements. For the purposes of this handbook, “remote measurement” is defined as any measurement of air emissions conducted away from the point or area where the pollutant is released. This definition includes optical remote sensing (ORS), as well as other approaches such as those coupling point measurements with a mobile measurement platform. As the nation’s air quality management programs evolve, we need more measurements of non-point or unvented sources, often referred to as fugitive sources or fugitive emissions. Remote measurement technologies offer approaches that have been otherwise unavailable to measure emissions from these challenging sources.

The information presented in this document is written to be generally informative, as well as more “user friendly” than technical papers or review articles found in the open literature (i.e., peer reviewed literature and articles in periodicals that are available on the internet). Practical information is provided for those who need to understand the principles behind the use of spectroscopy or other remote measurement technologies, but who may not be trained in these technologies and their applications. This document is intended to aid readers in understanding the uses and limitations of data generated by remote measurement approaches. In this document, you will find discussion of the practical uses and operation of remote sensing equipment and applications of these and other technologies to produce emissions data. Some of the complex technical information has been provided in summary form with illustrations.

### ***1.1 Purpose of the Handbook***

The purpose of this handbook is to describe the primary remote measurement technologies and current approaches to use these technologies. This handbook also describes how potential users can assess the applicability of remote measurements and the resulting data to their emissions measurement needs. We designed this handbook for EPA, state, local, and tribal measurement

project leads, measurement contractors, industry managers planning measurements to create emission factors, and those reviewing test plans and test reports. When the term “measurement” is used in this handbook, it is referring to short-term studies (e.g., emission fluxes assessment). The term monitoring is used for long-term studies (i.e. spatial and temporal trend assessment).

Optical remote measurement techniques are most typically designed and used to measure concentrations and, when paired with meteorological data, allow calculation of mass fluxes of pollutants downwind of fugitive and non-point emission sources. Optical remote techniques provide opportunities to measure sources that are not conducive to measurement using more traditional stack testing or single point ambient techniques. Actual application, however, needs to be determined on a case-by-case basis.

This handbook describes the more prevalent and technologically demonstrated open-path, cell-based, and point measurement technologies used to make remote measurements and it provides a background for the application of remote measurement techniques for emissions measurements. Viable applications for qualitative and quantitative measurements of constituents in air are also described as examples of different ways remote measurement technologies can be applied to meet measurement and monitoring requirements. Quantitative emissions data from remote measurements may then be used for multiple purposes including possible development of emission factors, evaluation of exposure levels, compliance with ambient regulatory limits, and identification of sources of air pollution. Examples of several pollutant detection and quantification methods are provided to show the focus of current monitoring applications. Applications of ORS are relatively new, but maturing rapidly. For example, Differential Optical Absorption (DOAS) and Fourier Transform Infrared (FTIR) systems have been commercially available since the early 1990s. These earlier instruments, although designed for both background ambient and higher stationary source emission-related monitoring applications, have mostly been employed to measure stationary and fugitive source emissions. Some of the more technical information have been simplified, and illustrations have been updated and clarified to make them more understandable. Internet links and references have been added throughout the document to allow the reader to



quickly research more detailed information.

## ***1.2 Contents and Overview of the Handbook***

This handbook discusses remote measurement technologies, applications of those technologies, ancillary data necessary to use the remote measurement data, potential issues with using remote measurement data for emission factors development, models, and other atmospheric process needs. Each chapter contains information that is split into two areas. The first area focuses only on the technologies including the specific hardware, scientific principles, how the pollutant concentrations are measured, pollutant and performance capabilities. The second area discusses the current vendors of the instrument or technology, general strengths and limitations.

### **What's New?**

This is the second iteration of this handbook, which was first posted in 2011. Since that first writing, this handbook has several new chapters that appear in this edition. Below, is a list of the new features and chapters that appear in this edition:

- Decision tables that illustrate techniques and technology. These are based on ease of use, cost and time frame and quality assurance concerns;
- Chapter 2.5 has been rewritten to include Optical Gas Imaging. This section was limited to a description of Thermal Infrared Camera technology;
- Chapter 2.7 discusses ORS instrumentation that can measure PM, with size ranges to the UFPs up to PM<sub>10</sub>.
- Chapter 3.6 and 3.7 describes Other Test Methods (OTM) 33 and 33a which describe Geospatial Measurements of Air Pollution, Remote Emission Quantifications;
- Chapter 3.8, Hyperspectral Monitoring;
- Chapter 3.9, Fenceline Passive Sampling – Method 325 A/B;

- Chapter 3.10, Method to Quantify Particulate Matter Emissions from Windblown Dust;
- Chapter 3.11, Determination of Emissions from Open Source by Plume Profiling, and;
- Chapter 3.12 Method to Quantify Road Dust Particulate Matter Emissions from Vehicular Travel on Paved and Unpaved Roads.

Numerous figures and diagrams are scattered within these new sections that illustrate the techniques and technology that are utilized.

### **Structure of the Handbook**

This second edition addresses how the technologies can and are being used to measure and monitor stationary source emissions including measuring mass emissions flux, monitoring emissions concentrations, detecting fugitive emissions leaks and measuring PM from remote sources. The handbook also includes examples of remote measurement projects and readily available test reports.

Section 1.0 introduces the handbook including background information that is necessary to understand the more detailed sections to follow. In this section you will also find a description of the EPA Quality System (QS) and how it can be used to create a data collection system that gathers data of sufficient quality for its intended use. The Measurement Quality Objectives (MQOs) in Section 1.6 will be useful to organizations planning remote measurement programs. The tables will help users to quickly review the requirements of a particular program.

Section 2.0 provides an overview of the remote measurement detection technologies that are currently available for remotely measuring pollutant emissions concentrations. Included in this overview are discussions of FTIR, Tunable Diode Laser (TDL), UV-DOAS, and LIDAR (both gas and PM) spectroscopy technologies. In addition, qualitative ORS technologies including Thermal Infrared Imaging are described. Each of these technology descriptions includes information on the basic principles of operation, the pollutants that can be monitored, typical quality control (QC) and quality

assurance (QA) for the technology, strengths, limitations, example vendors, and applications.

Section 3.0 describes the predominant remote measurement applications used to deploy the detection technologies addressed on Section 2.0 and to quantify emissions concentrations and flux measurements. This section also describes how the different technologies are applied to measurement methods, which is an extremely important section in this handbook. The application descriptions briefly summarize the activity and explain how the application is verified or validated in field tests, and details typical QA/QC associated with the application. Section 3.0 also describes siting considerations or information. Each application in Section 3.0 includes a table of strengths and limitations that must be considered during the planning, implementation, and interpretation of field study results. Applications covered in Section 3.0 include RPM using EPA Other Test Method 10 (OTM-10), Differential Absorption LIDAR (DIAL), Tracer Dilution Correlation (TDC), Solar Occultation Flux (SOF), and bLS emissions modeling. Section 3.0 provides examples of how these applications are used in fugitive emissions and area source emissions flux and concentration measurement, site remediation, plant fence line monitoring, fugitive leak detection, and ambient air measurement. In addition, several methods have been added that quantify large area and mobile generated PM.

Section 4.0 presents the ancillary measurements and data that may be needed for each ORS application. Ancillary data is defined as meteorological measurements, industrial process information and source activity necessary to translate ORS results generated from the detection technique and measurement application combinations described in Sections 2.0 and 3.0, respectively, into emission data that meet project specific data quality objectives.

Section 5.0 addresses various methods to validate and verify remote measurement data.

### 1.3 Stationary Sources and Emissions Points

Stationary sources are one of the major contributors of pollution to the atmosphere. They are fixed-site (i.e., stationary), producers of air pollution such as power plants, chemical plants, oil refineries, manufacturing facilities, and other industrial facilities. Air pollution from stationary sources is produced by two primary activities: (1) stationary combustion of fuel such as coal, oil, wood, or natural gas, and (2) pollutant losses from industrial processes. Examples of industrial processes include petroleum wells, refineries, chemical manufacturing facilities, coating operations and smelters.

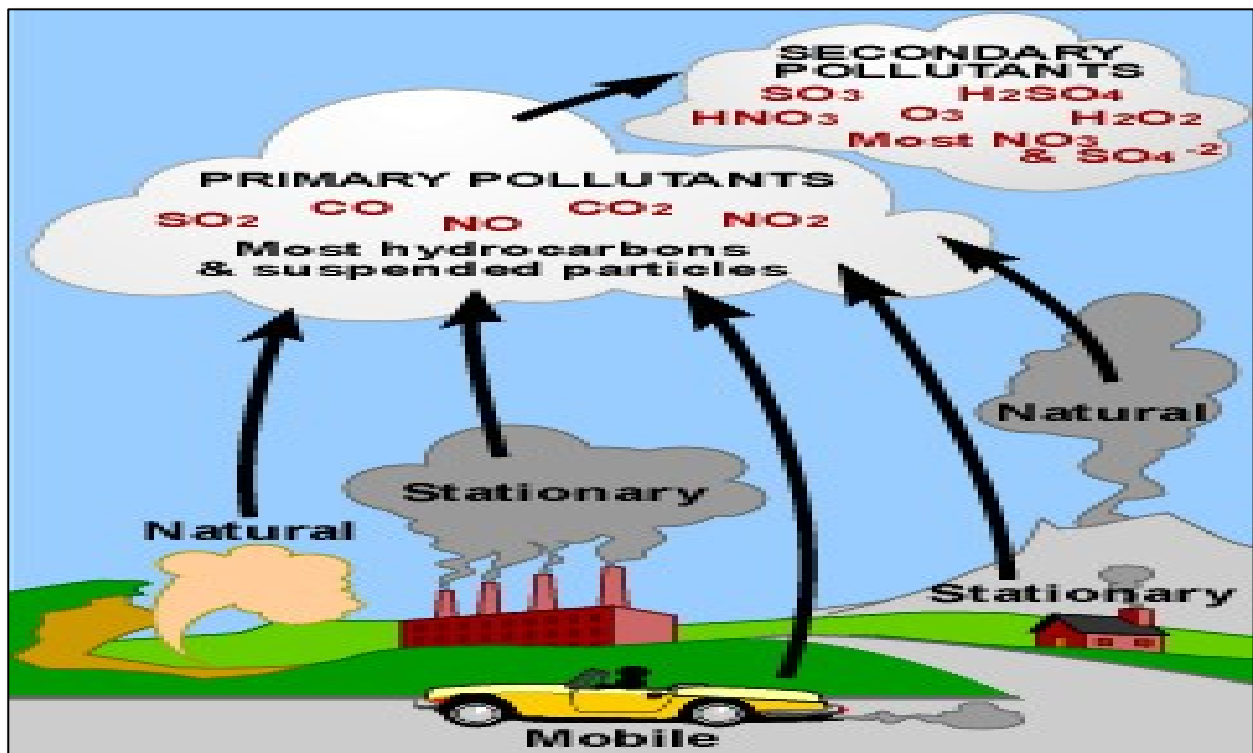


Figure 1-1. Types and Sources of Air Pollution

How the EPA defines emission points from stationary sources vary between EPA programs. An emission point is the specific place or piece of equipment from which a pollutant is emitted. Stationary sources, such as a facility or factory may have many possible emission points. Air pollutants can be emitted from smokestacks, storage tanks, equipment leaks, process wastewater handling/treatment areas, loading and unloading facilities, and process vents. These sources release various types of pollutants which are discussed in Section 1.4.

### **Ducted or Vented Emissions**

A process vent is basically an opening where substances (mostly in gaseous form) are “vented” into the atmosphere. Common process vents in a chemical plant are distillation columns and oxidation vents, for example.



***Figure 1-2. Example of a Ducted Stationary Source Stack***

Historically, ducted or vented stationary source emissions have been measured in the ducts or stacks before release into the atmosphere. These sources are also often referred to as point sources because the final release of emissions can be traced to a single or multiple defined duct or stack exhaust. Ducted sources permit emission stream parameters, such as flow rates, temperature, pressure, and other physical characteristics, to be recorded within the accuracy requirements for end data use because they are confined under relatively steady conditions.

### **Area or Fugitive Emissions Sources**

Those stationary facilities or activities whose individual air emissions do not qualify them as point sources are called area (e.g., a landfill) or fugitive sources (e.g., leaking valves at a gas or oil processing plant). Area and fugitive sources are often collections of a multitude of minor sources with individually small emissions that are impractical to consider as separate point sources. Area sources, including fugitive emissions, are those emissions that could not reasonably pass through a stack, chimney, vent, or other ducted line that could easily be characterized with conventional point source or stack sampling methods. Measurement of emissions from these sources traditionally requires total enclosure techniques, or a combination of point measurements and modeling using upwind-downwind or exposure-profiling methods.

Area sources represent numerous facilities and activities, including various unintended or irregular emissions. Fugitive and area sources may release small amounts of a given pollutant individually, but collectively can release significant amounts of a pollutant. For example, dry cleaners, vehicle refinishing, animal feeding operations and gasoline storage facilities do not typically qualify as point sources, but collectively, the various emissions from these sources are classified as area sources.<sup>1</sup>

Fugitive emissions from storage tanks are due to pollutants that can leak through the roofs and through tank openings when liquids expand or cool because of outdoor temperature changes. In addition, air pollutants can escape during the filling and emptying of a storage tank. Air pollution is also produced when wastewater containing volatile chemicals comes in contact with the air.

Both stationary point source and fugitive/area source emissions measurements have traditionally been performed using single point sampling that accumulates and integrates sampled gas for a set period of time followed by analysis for target components. Continuous point source instrumental methods have also been applied to stationary source emissions and area source measurements. Instrumental methods collect samples from a single point and provide information on the concentration of a target component of interest over relatively small increments of time. A critical issue with traditional air measurements is collection and reporting of data from a single point that is assumed to be representative of the air or emission being monitored. This assumption is verifiable when ducts or stacks are sampled but much less certain for area source and ambient measurements.

#### ***1.4 Why Remote Measurement?***

Fugitive emissions are emissions not contained or caught by a capture system and are often caused by equipment leaks, evaporative processes, and windblown disturbances. These emissions may occur from breaks or small cracks in seals, tubing, valves, or pipelines, as well as when lids or caps on equipment or tanks have not been properly closed or tightened. When natural gas escapes via fugitive emissions, methane, volatile organic compounds (VOCs), and any other contaminants in the gas (e.g., hydrogen sulfide) are released to the atmosphere. Other examples of area sources with significant fugitive emissions include landfills or waste lagoons.<sup>2</sup>



**Figure 1-3. Example of Potential Fugitive Source**

Area and fugitive emissions sources are especially challenging to monitor because the pollutants of interest are not contained within a duct or stack before release. The development of emission factors for area sources is equally difficult due to the measurement challenges. In contrast, stationary stack emissions and their related emission factors' determination are easier to measure and determine. Over the past 20 years, remote measurement approaches, including ORS methods, have been improving technologically and gaining greater use as an emissions estimation tool, especially for stationary area sources and some on-road/near-road mobile sources. A significant number of remote measurement activities have been performed for open area sources such as landfills, wastewater treatment plant ponds, agricultural waste, wastewater lagoons, oil and gas field production sites, waste ponds for mining operations, and ambient fence-line concentrations surrounding large chemical and refinery facilities.



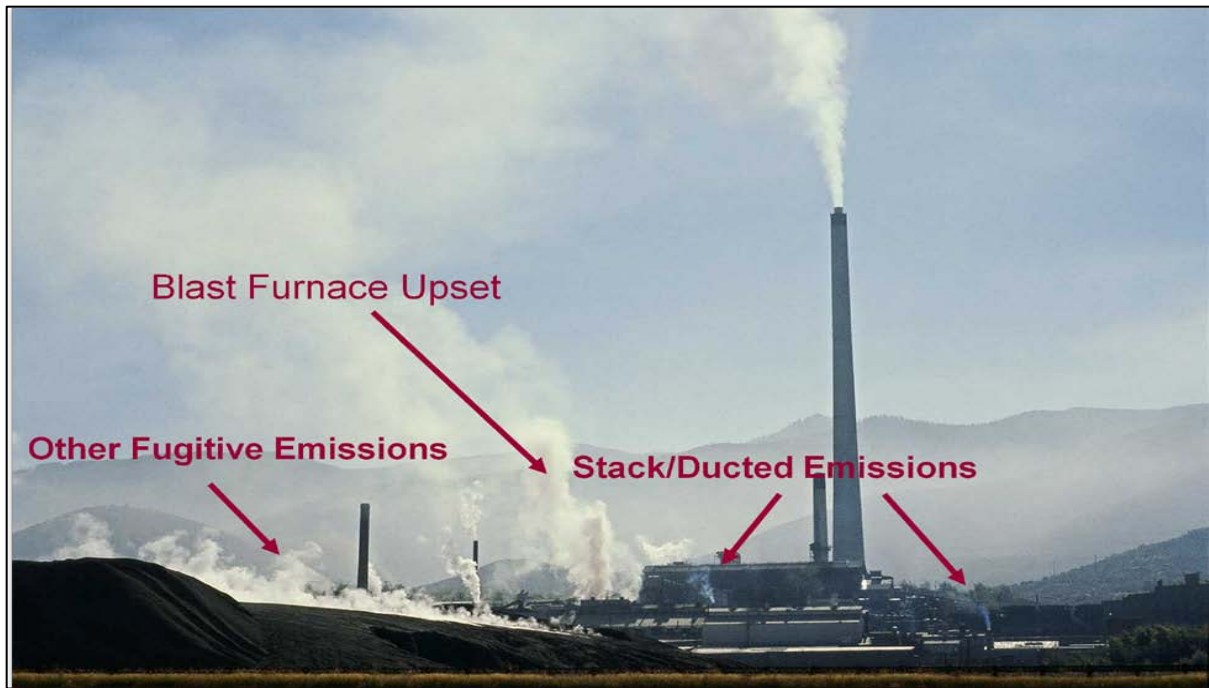


**Figure 1-4. Examples of Ducted and Fugitive Sources**

These types of sources are prime candidates for the application of remote measurement techniques because the ORS technology and techniques are small, mobile, do not take lengthy setup time and can return data quickly to the staff collecting the data and to the operators of the facilities.

### **Criteria Pollutant Gases, HAPs and GHGs**

The measurement technologies and approaches addressed in this handbook are focused on five groups of pollutants currently regulated or on the regulatory horizon under the Clean Air Act.

These four groups are:

- criteria pollutants,
- hazardous air pollutants (HAPs)
- greenhouse gases (GHGs),

- ozone-depleting substances, and
- Particulate Matter (PM).

Gaseous criteria pollutants are those inorganic pollutants (e.g., carbon monoxide, sulfur oxides, nitrogen oxides and ozone) that are commonly found all over the United States. The EPA uses these “criteria pollutants” as indicators of air quality. Each of the criteria pollutants is discussed in detail below.<sup>3</sup>

*Carbon monoxide (CO)* is a colorless, odorless gas formed when carbon in fuel is not burned completely. Motor vehicle exhaust contributes about 60 percent of all CO emissions nationwide.<sup>4</sup> Other sources of CO emissions include industrial processes (such as metals processing and chemical manufacturing), residential wood burning, and natural sources such as forest fires.

*Sulfur oxides (SO<sub>x</sub>)* are colorless gases formed when fuel containing sulfur, such as coal and oil, is burned, and when gasoline is extracted from oil or metals are extracted from ore. Sulfur dioxide (SO<sub>2</sub>) is the criteria pollutant that is the indicator of SO<sub>x</sub> concentrations in the ambient air. Other sources of SO<sub>2</sub> are industrial facilities that derive their products from raw materials like metallic ore, coal, and crude oil, or that burn coal or oil to produce process heat. Examples are petroleum refineries, cement manufacturing, sulfuric acid plants, and metal processing facilities. Also, locomotives, large ships, and some non-road diesel equipment currently burn high sulfur fuel and release SO<sub>2</sub> emissions into the air in large quantities.

*Nitrogen oxides (NO<sub>x</sub>)*, is the generic term used to describe the sum of nitric oxide (NO), nitrogen dioxide (NO<sub>2</sub>), which is a criteria pollutant, and other oxides of nitrogen. NO<sub>x</sub> is a group of highly reactive gases that play a major role in the formation of ozone. NO<sub>x</sub> form when fuel is burned at high temperatures, as in a combustion process. The primary sources of NO<sub>x</sub> are motor vehicles, electric utilities, and other industrial, commercial, and residential sources that burn fuels.

*Ozone (O<sub>3</sub>)* is a gas composed of three oxygen atoms. It is a unique criteria pollutant in that it is

exclusively a secondary pollutant. It is not usually emitted directly into the air, but at ground level is created by a chemical reaction between  $\text{NO}_x$  and VOCs in the presence of heat and sunlight.  $\text{O}_3$  has the same chemical structure whether it occurs miles above the earth or at ground level and can be “useful” or “damaging” to the environment depending on its location in the atmosphere. Useful  $\text{O}_3$  occurs naturally in the stratosphere and forms a layer that protects life on earth from the sun’s harmful rays or ultraviolet radiation. In the earth’s lower atmosphere, or troposphere, ground-level  $\text{O}_3$  is considered damaging or destructive.  $\text{O}_3$  is the most prevalent chemical found in photochemical air pollution, or smog.<sup>3</sup>

HAPs or air toxics are those pollutants that are known or suspected to cause cancer, respiratory problems or other serious health effects, or are thought to have adverse environmental or ecological effects. The presence of HAPs in the air can be more localized than criteria pollutants and the highest levels are usually found close to the emission sources. Examples of air toxics include benzene, found in gasoline; mercury from coal combustion; perchloroethylene from some dry-cleaning facilities; and methylene chloride used as a solvent by many industries. Most air toxics originate from man-made sources including mobile sources (e.g., cars, trucks, construction equipment), stationary sources (e.g., factories, refineries, power plants), and indoor sources (e.g., some buildings materials and cleaning solvents).<sup>4</sup>

GHGs are those compounds that enhance the retention of the sun’s heating of the earth. Clouds and a natural layer of atmospheric gases absorb a portion of earth’s heat and prevent it from escaping into space. This keeps our planet warm enough for life and is known as the natural “greenhouse effect.” Scientific evidence shows that the greenhouse warming effect is being increased by the release of certain gases into the atmosphere that cause the earth’s temperature to rise. This rise in temperature caused by greenhouse gases is called “global climate change.” Carbon dioxide ( $\text{CO}_2$ ), methane ( $\text{CH}_4$ ), nitrous oxide ( $\text{N}_2\text{O}$ ), sulfur hexafluoride ( $\text{SF}_6$ ), ammonium trifluoride ( $\text{NF}_3$ ), and hydro and per-fluorinated compounds, are the major compounds contributing to global climate change.  $\text{CO}_2$  emissions account for about 81 percent of greenhouse gases

released in the United States and are largely due to the combustion of fossil fuels in electric power generation, motor vehicles, and industries. Methane emissions, which result from agricultural activities, landfills, and other sources, are the next largest contributors to greenhouse gas emissions in the United States and worldwide.<sup>5</sup>

Ozone-depleting substances are compounds such as chlorofluorocarbons (CFCs), halons, carbon tetrachloride, methyl bromide, and methyl chloroform. The stratosphere contains a layer of O<sub>3</sub> gas that protects living organisms from harmful Ultraviolet-B (UV-B) radiation from the sun which has been linked to many harmful effects, including various types of skin cancer, cataracts, and harm to crops, materials, and marine life.<sup>6</sup>

Particulate matter (PM) has been shown to be deleterious to humans and the environment. In the early days of the EPA, the Agency created a NAAQS standard for total suspended particulate matter (TSP). The size cut was approximately 50 µm. However, research in the 1980 through the 1990 led the agency to adopt a smaller cut size: aerodynamic size of less than 10 µm (PM<sub>10</sub>). Some particles, such as dust, dirt, soot, or smoke, are large or dark enough to be seen with the naked eye. Others are so small they can only be detected using an electron microscope. These include:

- **PM<sub>10</sub>**: inhalable particles, with diameters that are generally 10 micrometers and smaller;
- **PM<sub>2.5</sub>**: fine inhalable particles, with diameters that are generally 2.5 micrometers and smaller; and
- **UFP**: ultrafine Particle. These are extremely fine inhalable particles that are generally in the less than 100 nanometer (nm) range.

As stated above, PM comes in many sizes and shapes and can be made up of hundreds of different chemicals. Some are emitted directly from a source, such as construction sites, unpaved roads, fields, smokestacks or fires. Most particles form in the atmosphere as a result of complex reactions of chemicals such as sulfur dioxide and nitrogen oxides, which are pollutants emitted from power plants, industries and automobiles.

### ***1.5 Knowledge and Advancement of Remote Sensing to Emissions Measurement***

There are four major sensing approaches that will be described in more detail in later sections of this handbook. They include the following:

- **Active.** Open-path ORS techniques typically use optical telescopes to transmit and receive energy beams, such as UV, infrared (IR), or visible wavelength range.
- **Passive.** Open-path ORS techniques receive light energy from pollutants activated by an external uncontrolled source such as combustion gases (e.g., Passive FTIR radiation) or the sun (e.g., Solar Occultation and mobile DOAS).
- **Backscatter.** ORS techniques use energy reflected from pollutants after activation from a controlled source of light energy (e.g., Differential Absorption Light Detection and Ranging (DIAL/LIDAR) systems).
- **Mobile.** Measurement methods do not have to be optically based. However, optical technologies have been engineered to be rugged enough to allow stable operation from a moving vehicle. Typically, these optical techniques sample the gas and PM into a confined cell while moving along a path to be measured (e.g., cavity ringdown, white cell and FTIR tracer release systems, particle counters and filter based systems).

#### **Active**

ORS techniques use the light generated under controlled conditions from one of many sources including heated glow bars for IR light, quartz lamps filled with deuterium or xenon gas, or laser light. The light energy is broadcast over relatively long distances (up to 1,000 meters) in an open-air setting. A simplified schematic of an open-path ORS technique to measure emissions from an open source is provided in Figure 1-4. In general, open-path ORS test methods involve the transmission of an energy beam across a path (straight line or two-dimensional plane) located downwind of the emission source to be measured (e.g., wastewater lagoon). The pollutant concentration along the line or plane is determined by evaluating certain qualities of the energy

beam (e.g., the amount of light absorbed) after it has passed through the sample path and is captured by a receiver. Chemical compound reference spectra and computational algorithms are used to translate the instrument signal into a pollutant path-integrated concentration (e.g., parts per billion (ppb) benzene per meter). Additionally, a mathematical calculation routine, combined with meteorological data (wind speed, wind direction) collected during the sampling event, is needed to convert the ORS instrument output (e.g., a path-integrated concentration or a flux measurement) to an emission flux rate (e.g., milligrams per second). Open-path ORS methods can be designed and applied in several different ways to capture area source emissions in both vertical and horizontal planes. The predominant measurement applications that use ORS technologies in the open-path mode include line of sight monitoring, Radial Plume Mapping<sup>7</sup> (RPM), and Backward Lagrangian Stochastic (bLS) Modeling.

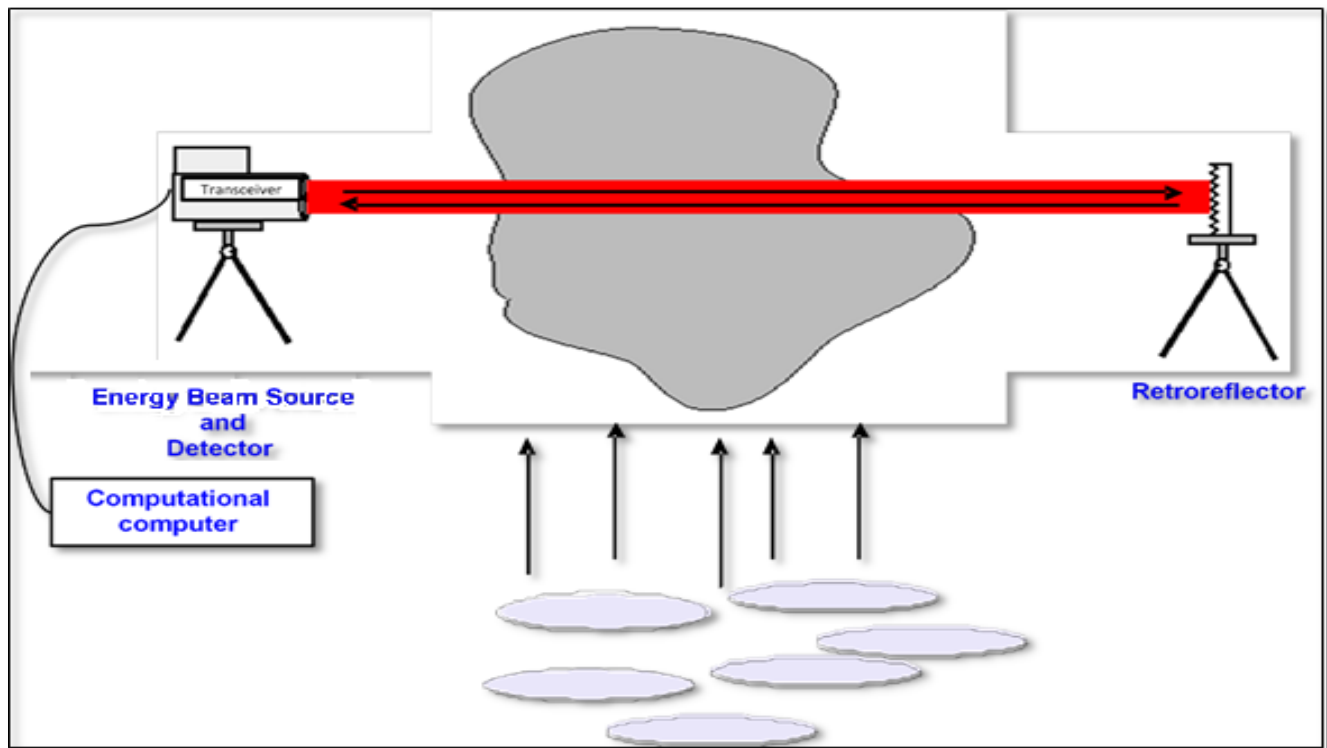


**Figure 1-5. Block Diagram of a bi-static ORS**

### **Passive**

Passive techniques use the same technology as active without the need for a controlled source of energy. The PFTIR technique is an example of this technology. PFTIR can be used to measure

infrared spectra in air at elevated temperatures because hot gases emit radiation with the same infrared signature as their absorption spectrum. Hot gases above the flame zone in an industrial flare contain combustion products such as CO<sub>2</sub>, CO, and vapor phase organic material resulting from products of incomplete combustion. For example, hot gases emitted by the flare can be identified and quantified using the radiant FTIR absorption measurements.

The primary difference that must be considered between optical remote infrared absorption (e.g., FTIR) and hot gas radiance measurements using PFTIR is the temperature dependence of the FTIR spectral measurements. The results of PFTIR are both temperature and concentration dependent. Knowing the source temperature at the location where the gas concentrations are measured is necessary to quantify the compounds of interest.

### **Backscatter**

Open-path optical measurement approaches used in this handbook refer to the use of Light LIDAR technology. DIAL is an application of LIDAR using powerful lasers directed into the atmosphere to measure reflected light energy from aerosols, dust, and gases. The DIAL measurement is achieved by the direct impingement of the laser beam on these materials and its subsequent reflection and scattering. Because the target substances vary in concentration along the axis (optical path) of the transmitted beam, the receiving telescope equipment analyzes the strength of the returning (reflected) beam continually during its reception.<sup>9</sup> The reflected beam strength is reduced from the original transmission strength by a measurable amount that is proportional to the concentration of the target matter.

LIDAR technology can also be deployed to measure PM. LIDARs that operate in the Raman and Rayleigh size ranges (i.e., wavelengths in the nanometer to micrometer range) can be utilized to measure the amount of backscatter from particles in the UFP range up to PM<sub>10</sub>. These instruments are discussed in Section 2.7.

## **Mobile**

Optical monitoring approaches use optical techniques to measure gas samples pumped into measurement cells where pressure and temperature are controlled. Unlike stationary monitoring techniques, mobile optical techniques allow the user to move along and between the emission plumes generated by area or fugitive sources. A tracer ratio application of mobile monitoring can be used to simulate emissions from a source through the release of a tracer gas at or near the center of the area source with subsequent measurement of the tracer and emission compound(s) concentrations downwind of the source. Measurements must be conducted at a distance from the source that is sufficient for the plume (e.g., from a landfill or wastewater lagoon) and tracer gas to be well mixed and close enough that emission plume is measurable well above background concentrations. These distances can range from 1 to 5 km to achieve proper mixing.<sup>9</sup>

In addition to measurements of gases, PM plume measurements techniques have become available using the current technology, such as the fast version of particle counter that are now on the market. These devices, used in conjunction with probes and plenums, can measure PM on roads instantaneously.

## **Advantages Over Closed Path Techniques**

Although open-path ORS techniques have been used for 20 years and are well-established, they are constantly improving and gaining use to characterize and quantify pollutant emissions from sources that are not conducive to traditional point source testing methods, such as large area sources.

Improvements often include changes to technologies that improve detection limits or the types of compounds detected. For large area sources, ORS methods have distinct advantages when compared with traditional single point measurement techniques, such as photo-ionization detectors (PID), PID/flame ionization detectors (FID), Summa canisters, various sorbent methods, and flux boxes. Specific advantages and disadvantages of the ORS measurement technologies and applications are addressed in Chapters 2 and 3 of this Handbook. The advantages of ORS applications should be determined on a case-by case-basis tailored to specific measurement goals



and objectives. Some of the general ORS advantages are as follows:

- More likely to identify emissions “hot spots” because measurements are collected over a large area,
- Achieve better spatial and temporal emissions resolution,
- No sample shipping costs,
- Perform direct, measurement-based emission calculations, and
- Represent personal exposure better than fixed point monitoring.

Some general issues that require consideration when ORS methods are used include the following:

- Costly initial sampling instrumentation investment,
- Experienced manpower and higher site preparation cost more to deploy,
- Dependent on weather conditions (e.g., heavy rain, fog, dust), and
- Dependent on chemical interferences (e.g., water, oxygen, O<sub>3</sub> and CO<sub>2</sub>).

As the use of open-path ORS technologies to quantify emissions from area sources has advanced, the desire to use ORS data in the development of atmospheric models and to support air quality standards has increased. However, use of remote sensing presents some challenging issues.

Classical point measurement technologies and their associated results are typically based on the size of the stack or leak, flow data, moisture, bulk gas molecular weight and stack pollutants to be measured. Performance tests for emission masses are usually snapshots of short duration and not continuous. Using ORS data, unlike point sources wherein emissions measurements are typically straightforward, a more critical evaluation of the ORS method application, the emission mechanism of the source, and the source activity is needed of the emissions developer to ensure that the resulting data provides an accurate representation of average emissions from the source. While

developing emission factors from optical remote technology applications is beyond the scope of this document, it is the aim of the handbook to provide the technology background, application examples, and quality information for optical remote measurements that can assist all data users to develop emission results comparable to those routinely generated by traditional point source testing methods.

### ***1.6 General Discussion of the EPA Quality System***

The EPA recently issued new guidance on its Quality Program (QP) policy. The document, "EPA Quality Program Policy"<sup>10</sup> states that this policy:

- Recognizes existing policies and procedures as the foundation of an Agency-wide Quality Program,
- Establishes an approach for identifying and addressing Agency quality issues,
- Provides a structure and procedures to ensure and enhance the effectiveness of the Quality Program and its application to Agency products and services.

The EPA policy is based on the national consensus standard, ANSI/ASQC E4-1994, Specifications and Guidelines for Environmental Data Collection and Environmental Technology Programs, developed by the American National Standards Institute and the American Society for Quality (ANSI/ASQC).<sup>11</sup> The ANSI/ASQC E4-1994 specification is consistent with the international standard ISO 17025. The ANSI document describes the necessary management and technical elements for developing and implementing a QS by using a tiered approach. The standard recommends documenting: (1) each organization-wide QS in a Quality Management Plan (QMP) or Quality Manual (to address requirements of Part A: Management Systems of the standard) and (2) the applicability of the QS to technical activity- specific efforts in a Quality Assurance Project Plan (QAPP) or similar document (to address the requirements of Part B: Collection and Evaluation of Environmental Data of the standard). The EPA has adopted this tiered approach for its mandatory agency-wide QS. This document addresses Part B requirements of the standard for systematic planning for environmental data operations.

In accordance with EPA Order 2106.0<sup>11</sup>, the EPA requires that environmental programs performed for or by the Agency must be supported by data of the type and quality appropriate to their expected use. The EPA defines environmental data as information collected directly from measurements, produced from models, or compiled from other sources such as databases or literature.

### **Data Quality Objectives**

EPA Order 2106.0 requires that all EPA organizations (and organizations with extramural agreements with EPA) follow a systematic planning process to develop acceptance or performance criteria for the collection, evaluation, or use of environmental data. A systematic planning process is the first component in the *planning phase* of the project tier (see the bottom tier of Figure 1.5), while the actual data collection activities take place in the *implementation phase*.

Systematic planning is a planning process based on the scientific method and includes concepts such as objectivity of approach and acceptability of results. Systematic planning is a common-sense, graded approach to ensure that the level of detail in planning is commensurate with the importance and intended use of the work and available resources. This framework promotes communication among all organizations and individuals involved in an environmental program. Through a systematic planning process, a team can develop acceptance or performance criteria for the quality of the data collected and for the quality of the decision. When these data are being used in decision-making by selecting between two clear alternative conditions (e.g., compliance/non-compliance with a standard), the EPA's recommended systematic planning tool is called the Data Quality Objective (DQO) Process.

The DQO Process is a seven-step planning approach to develop sampling designs for data collection activities that support decision-making. This process uses systematic planning and statistical hypothesis testing to differentiate between two or more clearly defined alternatives.

The DQO Process is iterative and allows the planning team to incorporate new information and

modify outputs from previous steps as inputs for a subsequent step. Although the principles of systematic planning and the DQO Process are applicable to all scientific studies, the DQO Process is particularly designed to address problems that require deciding between two clear alternatives. The final outcome of the DQO Process is a design for collecting data (e.g., the number of samples to collect and when, where, and how to collect samples).

The development and implementation of a QS should be based on a “graded approach,” that is, the components and tools of a QS (Figure 1.5) apply according to the scope and nature of an organization, program, or project and the intended use of its products or services. This approach recognizes that a “one size fits all” approach to quality management is not appropriate and that the QS of different organizations and programs should (and will) vary according to the specific needs of the organization. For example, the quality expectations of a research program are different from those of a regulatory compliance program because the intended use of the products differs. The same applies to remote sensing data. Monitoring agencies that use this Handbook are strongly encouraged to understand their data objectives, perform the DQO Process if needed, and use the MQOs described in Section 1.4.2 if they are applicable to an agency’s program. Additional explanation and details on the DQO Process can be found in EPA’s *Guidance on Systematic Planning Using the Data Quality Objectives Process*.<sup>12</sup>

When an agency or entity is monitoring for non-regulatory purposes (e.g., background concentrations, modeling applications, or exposure), these MQOs are recommended information. Meeting MQOs for non-regulatory meteorological monitoring is strongly advised.

### **Measurement Quality Objectives**

Once DQOs are designated for a program or project, measurement indicators must be determined to understand if the DQOs are being met. Most state/local/tribal agencies that collect data do so to support programs that are federally mandated or that need to meet federal requirements. However, other non-regulatory applications exist, such as modeling applications, state implementation plan development, and forecasting. These programs require different MQOs

because the application is different (i.e., different DQOs). The following prescribed objectives should be decided and discussed within the QS.

- **Measurement.** Type of measurements and/or the parameter needed to be collected.
- **Method.** The method is different from the measurement in that a particular instrument can be utilized in different methods. The method will dictate the precision, bias, and representativeness of the sampling data.
- **Reporting Units.** Reporting units must be decided before the program begins. If it is a regulatory program, then ppb or micrograms per cubic meter ( $\mu\text{g}/\text{m}^3$ ) would be the appropriate units. However, if it is a modeling exercise, then grams per second (g/s) may be the appropriate unit.
- **Detection Limits.** It is very critical to state the levels of detection (LOD) for a particular program. The LOD can be very difficult to quantify until the ORS is in the field of operation. It should also be noted that LODs can be defined in different ways. It is best to define and state LOD in the quality documents developed for a program.
- **Minimum Sample Frequency.** This objective is required to define how often data must be collected to meet the end user's requirements for precision and representativeness. Measurements must be taken often enough to meet model or modeling input criteria.
- **Completeness.** For most programs/projects, there is a minimum amount of data required to allow the data users to make decisions concerning the environment. A rule of thumb is 75 to 85 percent data completeness.
- **Precision.** Precision is the measure of agreement among repeated measurements of the same property under identical conditions. This can be very difficult to measure using ORS.
- **Bias.** Bias is the systematic or persistent distortion of a measurement process that causes errors in one direction. Bias, like precision, can be very difficult to determine with ORS.

The project or program must be able identify and determine the magnitude of its measurement bias.

- Representativeness. Representativeness is collection of the measurement location, frequency, duration, and other factors that demonstrate the results correspond to the emission characterization required by the data users.

### ***1.7 Choosing the Right Tool for the Right Job***

This section outlines recommendations on how the different technologies (i.e., instruments) stack up versus the source type (i.e., area, ducted or fugitive emissions). These table appear here in pairs; gas and particulate phase. Here is a breakdown on the information in these tables:

- Nature of the Source;
- Time Resolution;
- QA/QC Requirements; and,
- Ease of Operation.

Tables 1-1 through 1-8 aren't meant to be the final word on how these technologies and applications can be utilized, but serve as a reference for those seeking a match between the technologies and source applications.

#### **What is the nature of the source?**

Tables 1-1 illustrates the types of instruments that detect and quantify gases, while table 1-2 covers particulate sources. Three main source types are considered in this handbook: area, ducted/vented, and fugitive. Identification of the source type is an important first step towards identifying the proper technology for particular measurement needs.

Area and fugitive sources are similar in that both are often collections of minor sources that are impractical to consider as separate point sources. More specifically, area sources represent numerous facilities and activities. Fugitive sources, on the other hand, are often incidental in nature, such as leaks from valves, tank openings, or carbon sequestration sites, to name a few examples.

Ducted, or vented sources have also been referred to as point sources. Frequently, these vented

sources are distillation columns or oxidation vents in a chemical plant, for example. These sources often lend themselves to measurements under relatively stable conditions.

**Table 1-1 Gas Phase Source Type**

| Technology    | Source Type |                  |          |
|---------------|-------------|------------------|----------|
|               | Area        | Ducted or Vented | Fugitive |
| FTIR          | X           | X                | X        |
| TDL           | X           | X                | X        |
| UV-DOAS       | X           | X                | X        |
| CRDS          | X           | X                | X        |
| Passive Tubes | X           |                  | X        |
| DIAL          | X           |                  | X        |

**Table 1-2. Particle Phase Source Type**

| Technology      | Source Type |                  |          |
|-----------------|-------------|------------------|----------|
|                 | Area        | Ducted or Vented | Fugitive |
| Passive Sampler | X           | X                | X        |
| SMPS            | X           | X                | X        |
| APS             | X           | X                | X        |
| SPAMS           | X           | X                | X        |
| DIAL            | X           | X                | X        |
| Sensors         | X           | X                | X        |
| CRDS            | X           | X                | X        |
| PAS             | X           | X                | X        |
| AMS             | X           | X                | X        |
| ELPI            | X           | X                | X        |

**What is the required time resolution?**

Tables 1-3 and 1-4 illustrate which technologies perform in different time resolutions. In addition to identifying the type of source at which measurements will be taken, a second important question must do with the required time resolution of the data. Time resolution needs are often dependent upon several factors such as: available budget, expected stability of the pollutant emissions being studied, and data reporting requirements, among others. Time resolution can range from essentially continuous measurements to integrated measurements taken over a period of weeks or months. Some technologies can be employed at different time resolutions depending on current needs, and allowing the same technology to be utilized in different scenarios.

**Table 1-3. Gas Phase Time Resolution Matrix**

| Technology    | Time Resolution |         |         |                 |
|---------------|-----------------|---------|---------|-----------------|
|               | real-time       | seconds | minutes | hours or longer |
| FTIR          | X               | X       |         |                 |
| TDL           | X               | X       |         |                 |
| UV-DOAS       |                 | X       | X       |                 |
| CRDS          | X               | X       |         |                 |
| Passive Tubes |                 |         |         | X               |
| DIAL          | X               | X       | X       |                 |

**Table 1-4. Particle Phase Time Resolution Matrix**

| Technology      | Time Resolution |         |         |                 |
|-----------------|-----------------|---------|---------|-----------------|
|                 | real-time       | seconds | minutes | hours or longer |
| Passive Sampler |                 |         | X       | X               |
| SMPS            |                 | X       | X       |                 |
| APS             |                 | X       | X       |                 |
| SPAMS           | X               | X       |         |                 |
| DIAL            | X               | X       | X       |                 |
| Sensors         |                 | X       | X       |                 |
| CRDS            | X               | X       |         |                 |
| PAS             |                 | X       | X       |                 |
| AMS             | X               | X       |         |                 |
| ELPI            | X               |         |         |                 |

**What are the QA/QC requirements for the measurement?**

Tables 1-5 and 1-6 illustrate the different levels of QA and QC that are needed to obtain data that is of known quality. An important consideration when choosing a measurement technology is the level of QA/QC required of the data. The level of accuracy and precision required of a measurement will have a significant impact on the technology selected. For example, while a PID sensor and UV-DOAS instrument can both detect benzene, if the goal is to merely detect benzene, the PID sensor would be more cost effective and less labor intensive.

**Table 1-5. Gas Phase QA/QC Matrix**

| Technology        | Data Type   |                   |              |
|-------------------|-------------|-------------------|--------------|
|                   | Qualitative | Semi-Quantitative | Quantitative |
| FTIR              |             |                   | X            |
| TDL               |             |                   | X            |
| UV-DOAS           |             |                   | X            |
| CRDS              |             |                   | X            |
| Passive Tubes     |             | X                 | X            |
| DIAL              |             |                   | X            |
| Thermal IR Camera | X           |                   |              |



**Table 1-6. Particle Phase QA/QC Matrix**

| Technology      | Data Type   |                   |              |
|-----------------|-------------|-------------------|--------------|
|                 | Qualitative | Semi-Quantitative | Quantitative |
| Passive Sampler |             | X                 |              |
| SMPS            |             | X                 | X            |
| APS             |             | X                 | X            |
| SPAMS           | X           | X                 |              |
| DIAL            |             | X                 | X            |
| Sensors         |             | X                 | X            |
| CRDS            |             |                   | X            |
| PAS             |             | X                 | X            |
| AMS             | X           | X                 |              |
| ELPI            |             | X                 |              |

**How easy are the data to process?**

Tables 1-7 and 1-8 illustrate the ease of operation for each of these technologies. The experience required to process acquired data and prepare those data for presentation and interpretation is another important factor to consider prior to selecting a measurement technology. This question is crucial to recognizing the personnel required for collecting, processing, and analyzing data of the highest possible quality. In cases where much of the processing is done automatically via instrument software or settings, experience isn't as important as it is in instances where processing requires more complex calculations or a greater knowledge of the theory behind the measurement technique.

**Table 1-7. Gas Phase Ease of Operation Matrix**

| Technology             | Years of experience |     |     |
|------------------------|---------------------|-----|-----|
|                        | < 1                 | 1-3 | > 3 |
| FTIR                   |                     | X   |     |
| TDL                    |                     | X   |     |
| UV-DOAS                |                     | X   |     |
| CRDS                   |                     | X   |     |
| Passive Tubes          | X                   | X   |     |
| DIAL                   |                     |     | X   |
| Solar Occultation Flux |                     |     | X   |

**Table 1-8. Particle Phase Ease of Operation Matrix**

| Technology | Years of experience |     |     |
|------------|---------------------|-----|-----|
|            | < 1                 | 1-3 | > 3 |
| SMPS       | X                   |     |     |
| APS        | X                   |     |     |
| SPAMS      |                     |     | X   |
| DIAL       |                     | X   |     |
| Sensors    | X                   |     |     |
| CRDS       |                     |     | X   |
| PAS        |                     | X   |     |
| AMS        |                     |     | X   |
| ELPI       | X                   |     |     |

### **1.8 Future Evolution and Updates of this Handbook**

The EPA will periodically update and correct this handbook. Updates will include the addition of new information as well as feedback from stakeholders. This document will be updated, at the discretion of the EPA, depending on the availability of resources.

This document does not contain EPA policy information; it is strictly an information document. It is envisioned that in later editions, new ORS technologies and techniques will be described in this document.

### **1.9 References**

1. U.S. EPA. 2010 Sources of Pollutants in the Ambient Air – Stationary Sources, 15 July 2010
2. Earthworks. Sources of Oil and Gas Air Pollution.  
<http://www.earthworksaction.org/airpollutionsources.cfm>>.
3. U.S. EPA. Criteria Pollutants, <https://www.epa.gov/criteria-air-pollutants>
4. U.S. EPA. Hazardous Air Pollutants. <https://www.epa.gov/haps>
5. U.S. EPA. Greenhouse Gas Emissions, <https://www.epa.gov/ghgemissions>

6. U.S. EPA. Ozone Layer Protection, <https://www.epa.gov/ozone-layer-protection>
7. Other Test Method 10 (OTM 10) - Optical Remote Sensing for Emission Characterization from Non-Point Sources, FINAL ORS Protocol, <https://www3.epa.gov/ttn/emc/prelim/otm10.pdf>
8. Ednar, H., P. Ragnarson, and E. Wallinder. 1995. Industrial Emission Control Using Lidar Techniques. Environ. Sci. Technol. 29:330-337.
9. Mosher, B. W.; Czepiel, P. M.; Harriss, R. C.; Shorter, J. H.; Kolb, C. E.; McManus, J. B.; Allwine, E.; Lamb, B. K. 1999. Methane emissions at nine landfill sites in the northeastern United States. Environmental Science & Technology. 33, (12): 2088-2094.
10. US EPA. 2008. US EPA Quality Policy, CIO 2106.0, October 2008.  
[http://www.epa.gov/quality/qa\\_docs.html](http://www.epa.gov/quality/qa_docs.html)
11. Guidance on Systematic Planning Using the Data Quality Objectives Process EPA QA/G-4, EPA/240/B-06/001 February 2006, <https://www.epa.gov/quality/guidance-systematic-planning-using-data-quality-objectives-process-epa-qag-4>
12. US EPA. 2010. Implementation of Quality Assurance Requirements for Organizations Receiving EPA Financial Assistance. <http://www.epa.gov/ogd/grants/assurance.htm>.

## 2.0 Optical Remote Sensing Technologies

ORS technologies measure the concentration of chemicals in an open-air path or in contained air samples collected from discreet sampling points. They do this by measuring the interaction of electromagnetic energy (i.e., different wavelengths of light) with the air's components. Open-path technologies measure the concentrations of chemicals or particulates across an open path of air. They do this by emitting a concentrated beam of electromagnetic energy into the air and measuring its interactions with the air's components. Open-path technologies provide an average concentration over a line of sight. Point-source applications of these technologies measure the concentration of a confined sample of air drawn into the apparatus from a point or points in air. Some technologies, such as Tunable Diode Lasers (TDL), are capable of simultaneously measuring one or two compounds. Other technologies (e.g., UV-DOAS) can measure several compounds simultaneously, while others (e.g., FTIR) can measure many compounds simultaneously. ORS technologies are used to measure the average chemical concentrations over a set distance or at a stationary point. The path average over a set distance has an advantage over point-source measurements that may miss high-concentration plumes running between sampling devices. Both open-path and point-source applications of these technologies have been used to detect hotspots in area sources and to obtain path integrated averages. Each of the technologies has advantages and disadvantages for these applications. The technologies described in Chapter 2 can be used alone or in combination to provide three major types of data: plume characterization, short term flux measurements and long-term monitoring studies. In Chapter 2, we discuss how the prominent ORS technologies operates.

## ***2.1 Fourier Transform Infrared Spectroscopy***

FTIR spectroscopy is an optical spectroscopy technology adapted to perform real-time monitoring of gaseous and volatile organic compounds in air. The technique can detect and quantifying multiple compounds simultaneously, even in harsh industrial environments, using the characteristic spectral features of the individual compounds.<sup>1</sup>

FTIR spectrometers are well-suited to remote sensing applications because they are durable, portable, and do not require daily routine calibration. The technology, however, is not simple to operate and requires experienced staff to ensure correct operation and valid results. Both extractive and open-path (OP-FTIR) environmental applications of the technology have been demonstrated. The EPA test methods have been written for both open-path, such as other test method 10, (OTM10) or toxic organic 16 (TO-16) and extractive (Method 318, Method 320, EPA performance specific method 15 (PS-15), PS-18 and ASTM D6328-03) measurement by FTIR. In open-path mode, the IR radiation beam can be directed over distances of up to 400 to 500 meters to measure selected compounds in emission plumes or dispersed air parcels. Alternatively, in extractive mode, gas can be drawn into a closed cell with a folded path length of 10 to 100 meters. Optical remote spectroscopy applications focus on open-path mode. Mobile tracer applications focus on extractive mode. Compound-specific concentration is determined using standard IR spectra of known concentration. The onboard computer software and spectra library allow real time determination of concentration for preset compounds. Post-test processing of IR spectra allow other compounds in air samples to be determined. Every measurement uses calibrated reference spectra taken at conditions like the unknown field samples to determine compound concentrations therein.

### **Basic Operation**

The FTIR instrument sends an IR beam of light through a region (closed-cell or open-path) containing the compounds of interest and captures the resulting IR spectra from the sample. Figure 2-1 illustrates the basic components of an open-path FTIR spectrometer. Infrared light

generated by an IR emitting source is guided through an interferometer. The interferometer consists of an IR source, beam-splitter, mirrors, a laser, and a detector. The IR energy goes from the source to the beam-splitter, which splits the beam into two parts. One part is transmitted to a moving mirror and one part is reflected to a fixed mirror. The moving mirror oscillates back and forth at a constant velocity. This velocity is timed according to the very precise laser wavelength in the system, which also acts as an internal wavelength calibration. The beam reflected from the moving mirror and the beam reflected from the fixed mirror have traveled different distances since being generated by the source and are recombined at the beam-splitter.<sup>1,2</sup>

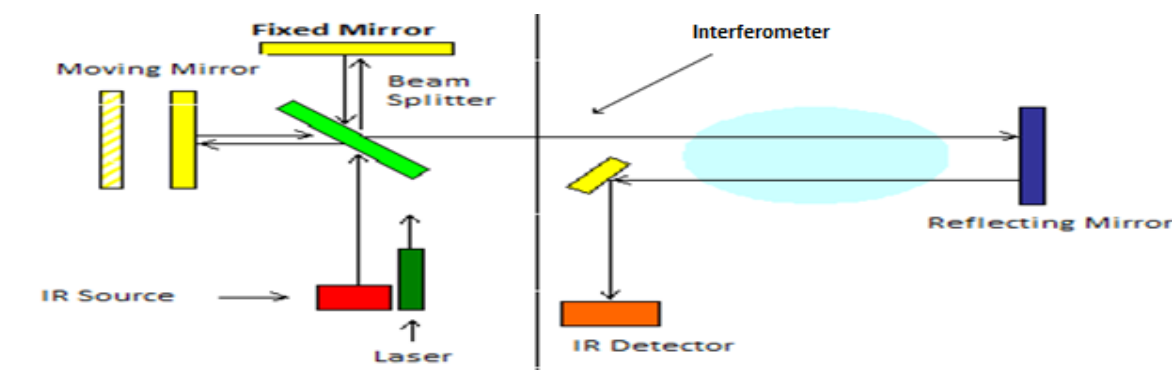


**Figure 2-1. Diagram Showing Beam Path and Major Components of FTIR**

When the beams are recombined, some of the wavelengths recombine constructively and some destructively, which creates an interference pattern. This interference pattern is called an interferogram. The recombined IR beam then passes from the beam-splitter into the open-path where a portion of the IR energy is absorbed by the gaseous compounds to be measured. The resulting IR beam reaches the IR detector where the interference pattern is detected, digitized, and transformed mathematically into a standard single beam infrared frequency spectrum using an algorithm known as a Fourier transform. A reference or background single beam spectrum is also collected without a sample and the ratio of the two single beam spectra is computed to produce a background corrected transmittance spectrum. This transmittance spectrum can be converted to absorbance by taking the negative base 10 log of the data points.<sup>2</sup>

The vibrational frequencies of all the infrared absorbing molecules in the IR beam path are captured in the IR spectrum. When a molecule absorbs light, the energy of the molecule is

increased and the molecule is promoted from its lowest energy state (ground state) to an excited state. Light energy in the infrared region of the electromagnetic spectrum stimulates molecular vibrations. Molecular species display their own characteristic vibrational structure when stimulated by IR radiation.<sup>3</sup> Figure 2-2 shows the IR absorption spectra for nitrous oxide, CO<sub>2</sub>, CO, NO, NO<sub>2</sub>, and ammonia. The units of vibrational frequency are wave number. Wave number and vibrational structure are used to identify a molecule.

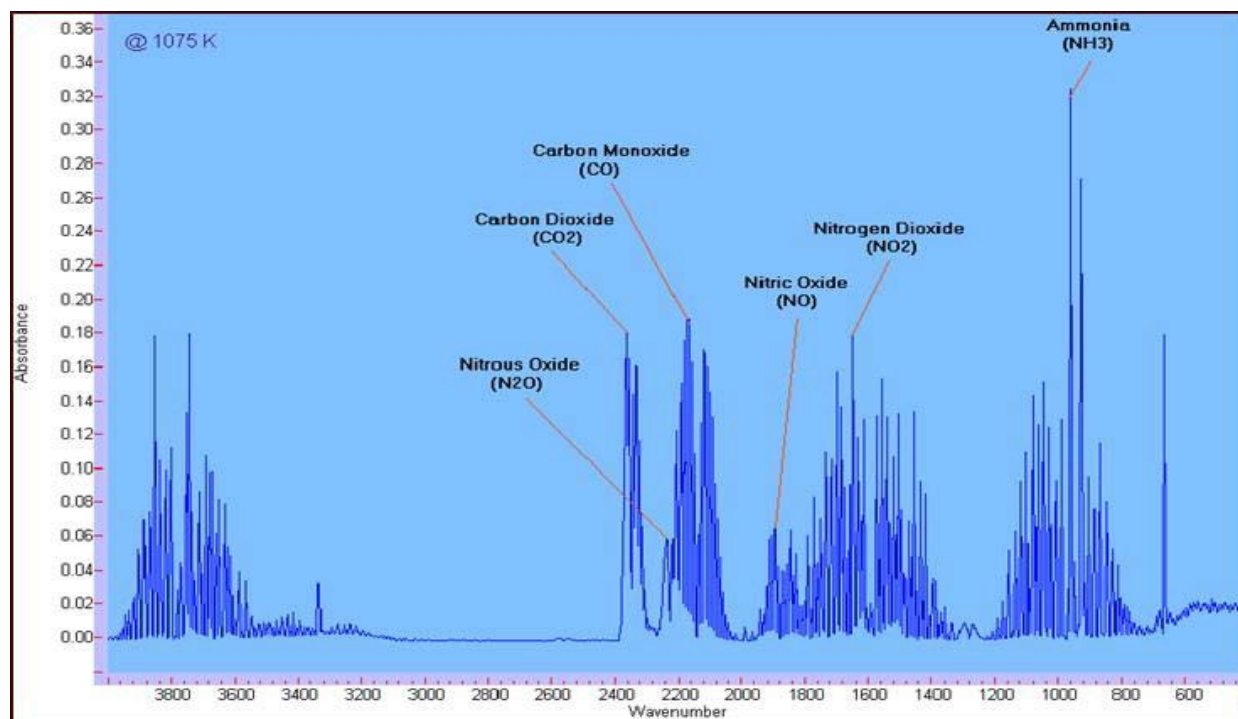


**Figure 2-2 FTIR Absorption Spectrum recorded at 1075°**

Once a compound has been identified, its spectrum can also be used to measure the compound's concentration because the amount of IR radiation absorbed from the IR beam is proportional to the concentration of the compound in the sample or open path. According to the Beer-Lambert law, there is a linear relationship between absorbance and concentration as shown in the following equation<sup>1,2,3</sup>

$$A = \epsilon * c * l$$

Where:

A = absorbance intensity

$\epsilon$  = absorption coefficient

c = sample concentration

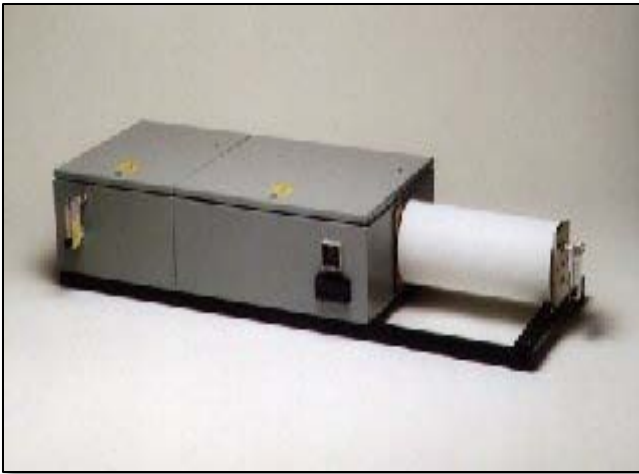
l = sample path length

FTIR systems typically operate in two modes: extractive cell or open-path. Extractive cell measurements can be conducted either from a single location or from a mobile measurement platform.<sup>4</sup> In the field, OP-FTIR systems can operate with telescopes transmitting and receiving the IR beam so monitoring of long outdoor paths is possible. The pollutants normally measured in this process are at ambient temperature and usually in the low ppb concentration range.<sup>5</sup> Typical applications of open-path monitoring include fence-line monitoring of industrial sites, landfill sites, waste lagoons, urban air monitoring in metropolitan areas, accidental release detection/identification, and detection of agents or surrogates important to homeland security monitoring applications.<sup>6,7</sup> It should be noted that moisture due to fog or high humidity will cause spectral interferences, which can limit the use of this technique to pollutants that do not have overlapping absorption features with gas-phase water.<sup>5</sup>

### **Extractive (Closed) Cell Measurement Applications**

For extractive or closed-cell FTIR measurements, the beam is sent through a cell that is mounted in the instrument itself. As shown in Figure 2-1, the IR beam passes through the cell and is focused onto the detector. Gas-phase samples are pumped into a sealed, constant temperature cell and analyzed. Sample cell path lengths can vary from 10 cm to 150 m folded-path cells. The longer the path length the more sensitive the measurement becomes because the IR beam has a greater chance of interacting with the absorbing compounds. The pollutants measured in this type of arrangement are usually at higher concentrations than those found in open-path FTIR





measurements. Typical applications of extractive FTIR monitoring include stack testing of flue gases and vehicle exhaust.<sup>6,7</sup> Figure 2-3 shows a photo of an FTIR unit used for extractive monitoring of stack gas. This unit is equipped with a 32-m folded path length cell that extends from the end of the instrument.

**Figure 2-3. FTIR Closed Cell Unit for Monitoring Stack Gases**

### **Open-Path Measurement Applications**

There are many instrumental configurations for open-path (OP) instruments. The simplest OP systems are bistatic configurations. This configuration derives its name from the fact that both the transmitter and receiver must be fixed in a static position and precisely aimed at each other. The OP-FTIR equipment projects the IR light beam directly along a path to a detector/receiver. Bistatic configurations in general have the requirement of supplying power at both the receiver and transmitter, which can be a disadvantage in some locations. Additionally, there is a requirement for alignment at both receiver and transmitter, which can be time consuming for mobile systems.<sup>8</sup> Monostatic configurations were developed to address issues raised with bistatic designs. In a monostatic configuration, all the optical components of the transmitter and receiver are in the same location, and a retro-reflector is used to return the light from the transmitter to the receiver. This configuration derives its name from the fact that only the transceiver portion of the instrument needs to be precisely pointed as the retro-reflector returns light to its source regardless of orientation. A diagram of a typical monostatic configuration is shown in Figure 2-4.

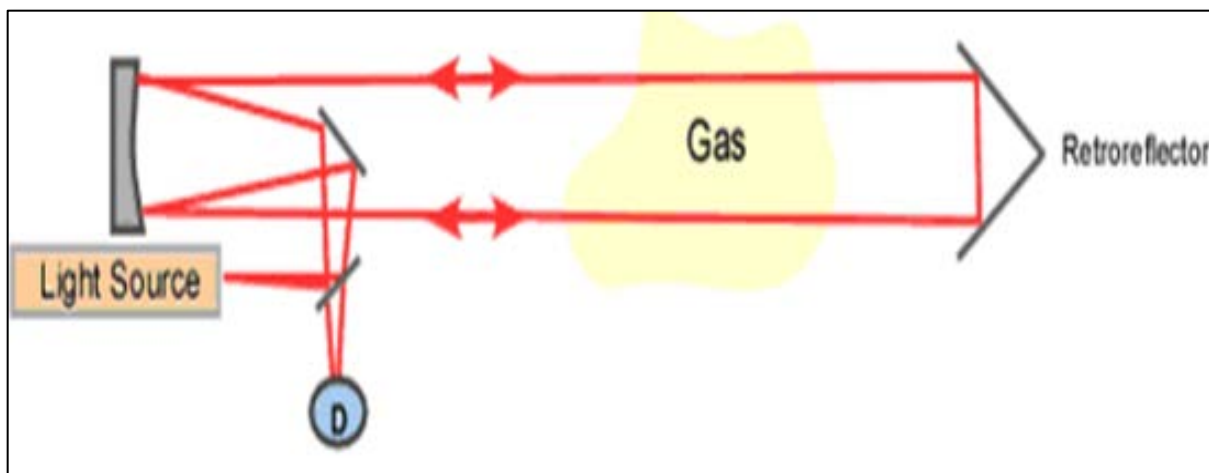


**Figure 2-4 Basic Setup for Monostatic OP-FTIR**

Retro-reflecting mirrors, as they are called, are configured with three perpendicular reflective surfaces in the shape of a corner. A combination of three mutually perpendicular mirrors reflects light incident from any direction through  $180^\circ$  as shown in Figure 2-5. Such a combination of mirrors is called a corner-cube reflector. Corner-cube reflectors beam FTIR light back to its exact point of origin. This property reduces the divergence of the beam on its return path back to the detector compared to divergence that would result from a flat mirror. Also, the retro-reflector array can be very large to capture and return essentially the entire divergent signal from the telescope.

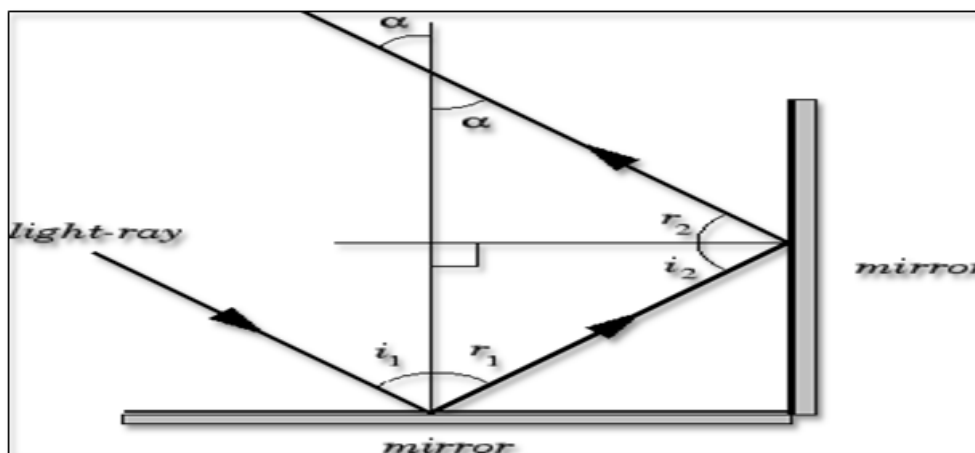


**Figure 2-5. The corner cube reflector**

<http://farside.ph.utexas.edu/teaching/316/lectures/node133.html>

In the monostatic mode, the IR laser beam is split twice, once leaving the OP-FTIR and once on turn. This design requires a beam splitter in the optical path that removes 50 percent of the light

from the outgoing beam and 50 percent of the light from the return beam for an overall loss of 75 percent of the total light intensity.



The dual-telescope monostatic configuration has lower detection limits because it does not utilize a beam splitter in the optical path. A translating retro-reflector, which is essentially a portion of a very large cube, is used to return the light beam offset to align with the receiving telescope. This single, large retro-reflector does not have the divergence reversal properties of the corner-cube array. The second telescope adds cost and complexity to the system.<sup>8</sup> However, when compared with monostatic mode, bistatic systems are harder to align and maintain

**Figure 2-6 Typical telescopic FTIR Transmitting and Detection Unit**

because any shift in the transmitter or detector can result in system misalignment.<sup>7,9</sup> Both operating modes measure only the compounds that are in the beam path. Emissions outside the beam path are not measured. In these situations, measurements have been conducted along multiple beam paths to more accurately characterize the emission plume. Figure 2-6 shows a telescopic FTIR transmitting and detection unit, which would be used for open-path field monitoring applications. Figure 2-7 shows a typical retro-reflecting mirror. The retro mirrors are surface coated with a reflective material to reduce extraneous glare from outside stray light. Retro-reflecting mirrors are often contained in a protective housing, which is closed when the unit is not in use to protect the sensitive reflecting surfaces from exposure to inclement weather conditions.

### **Pollutants and Relative Levels That Can Be Measured**

Table 2-1 provides an example list of compounds that have been measured using OP-FTIR spectroscopy.<sup>6,7</sup> This list is not all-inclusive, but shows that many compounds can be measured via OP-FTIR.

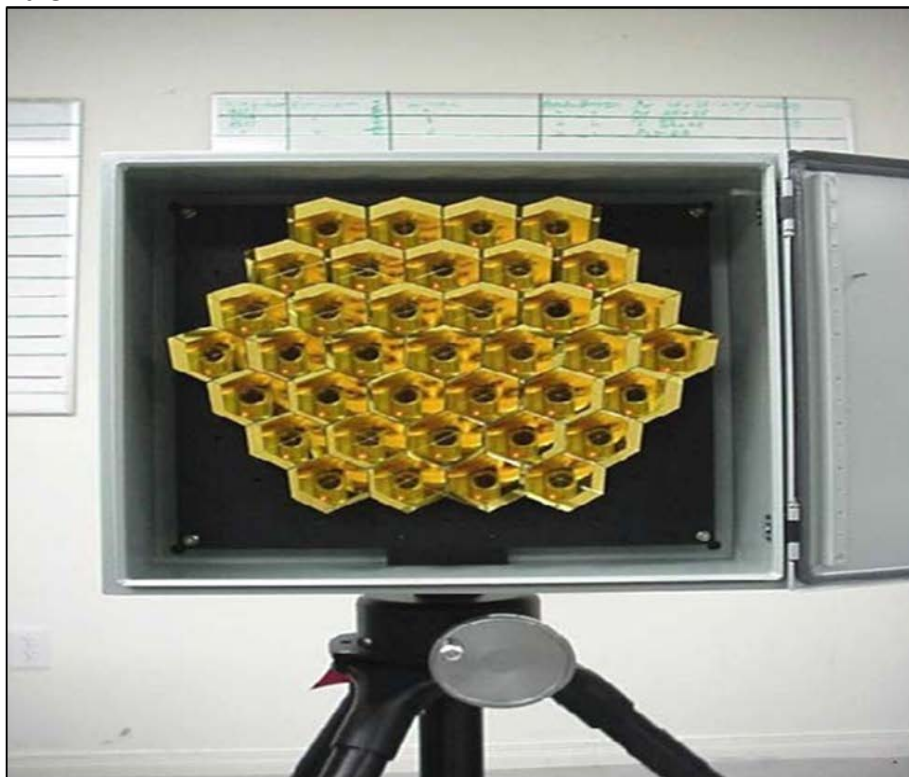


***Figure 2-7. Corner Cube Reflector***

Another feature of OP-FTIR is that many compounds can be monitored simultaneously as opposed to other beam technologies that can monitor only single compounds. As with other optical sensing systems, OP-FTIR produces a path integrated concentration (PIC) in units of parts per million (ppm) or ppb times length, i.e., ppb (meters).<sup>6</sup> Dividing the final ppb (meters) result by the total optical path length gives the path integrated gas concentration in ppb.

Detection limits can vary widely from compound to compound depending on many factors such as instrument configuration, the condition of retro-reflecting mirrors, humidity, beam path length and the absorbance strength of the target compound(s) at the wavelength chosen for analysis.

Detection limits are typically reported in ppm for one meter of path length (ppmm).

They can be determined empirically using cell based measurements or estimated by solving the equation on page 2-5 for an absorbance that is three times the mean signal noise if the absorbance coefficient and noise are known at the wavelength used to measure the compound(s) of interest. Detection limits for specific sampling episodes are calculated by dividing ppm by the actual meters of path length during field sampling.

**Table 2-1. Example List of Compounds Measured by FTIR Open-path Systems**

| Species              |                           |                           |
|----------------------|---------------------------|---------------------------|
| Acetaldehyde         | 1,4-dimethyl piperazine   | methyl mercaptan          |
| acetic acid          | 1,4-dioxane               | methyl methacrylate       |
| Acetone              | ethane                    | 2-methyl propene          |
| Acetonitrile         | ethanol                   | morphaline                |
| Acetylene            | ethyl acetate             | nitric acid               |
| Acrolein             | ethylamine                | nitric oxide              |
| acrylic acid         | ethylbenzene              | nitrogen dioxide          |
| Acrylonitrile        | ethylene                  | nitrous acid              |
| Ammonia              | ethylene oxide            | ozone                     |
| Benzene              | ethyl mercaptan           | pentane                   |
| 1,3-butadiene        | formaldehyde              | phosgene                  |
| Butane               | formic acid               | phosphine                 |
| Butanol              | furan                     | propane                   |
| 1-butene             | halocarb-11 (CCI3F)       | propanol                  |
| cis-2-butene         | halocarb-12 (CCI2F2)      | propionaldehyde           |
| trans-2-butene       | halocarb-22 (CHClF2)      | propylene                 |
| butyl acetate        | halocarb-113 (CFCl2CF2Cl) | propylene dichloride      |
| carbon disulfide     | hexafluoropropene         | propylene oxide           |
| carbon monoxide      | hydrocarbon continuum     | pyridine                  |
| carbon tetrachloride | hydrogen chloride         | silane                    |
| carbonyl sulfide     | hydrogen cyanide          | styrene                   |
| chlorobenzene        | hydrogen sulfide          | sulfur dioxide            |
| Chloroethane         | isobutene                 | sulfur hexafluoride       |
| Chloroform           | isobutanol                | 1,1,1,2-tetrachloroethane |
| m-cresol             | isobutyl acetate          | 1,1,2,2-tetrachloroethane |
| o-cresol             | isobutylene               | tetrachloroethylene       |
| p-cresol             | isoprene                  | toluene                   |
| Cyclohexane          | isopropanol               | 1,1,1-trichloroethane     |
| 1,2-dibromoethane    | isopropyl ether           | 1,1,2-trichloroethane     |
| m-dichlorobenzene    | methanol                  | trichloroethylene         |
| o-dichlorobenzene    | methylamine               | trimethylamine            |
| p-dichlorobenzene    | methyl benzoate           | 1,2,4-trimethylbenzene    |
| 1,1-dichloroethane   | methyl chloride           | vinyl chloride            |
| 1,2-dichloroethane   | methylene chloride        | m-xylene                  |
| 1,1-dichloroethylene | methyl ether              | o-xylene                  |
| dimethylamine        | methyl ethyl ketone       | p-xylene                  |
| dimethyl disulfide   | methyl isobutyl ketone    |                           |

Compounds in **bold** are EPA Hazardous Air Pollutants (HAPs) CAA -112Title 42, Chapter 85, Subchapter I, Part a U.S. Code 7412 (b).

Typically, FTIR manufacturers report detection limits for commonly monitored pollutants as part of the literature for their instrumentation. In general, open-path FTIR detection limits in the single digit ppb levels can be achieved for many strong IR absorbing compounds.<sup>7,10</sup> Extractive FTIR detection limits for a 10-meter folded path length are typically on the order of 0.1 to 10 ppm. Some compounds such as benzene have detection limits in the 30-50 ppb range because gas-phase water interferes with this measurement.<sup>7</sup> Other compounds, such as hydrogen sulfide, are weakly IR absorbing molecules and have detection limits in the 300-800 ppb range.<sup>7</sup>

### **Typical QA/QC**

To ensure measurement accuracy and data verification, instrumentation response should be verified annually (detector and IR source) using a known concentration of a standard gas mixture. Certificates of calibration should be kept on file and available for review. Maintenance records should be kept in bound notebooks for any equipment adjustments or repairs that could affect measurement performance. Maintenance notebooks should include the date and description of maintenance performed. Calibration checks should be performed after major service and regularly during analysis.<sup>11,12</sup> QA and QC procedures for the measurement of gaseous compounds by extractive FTIR are discussed in great detail in EPA Test Method 320 or ASTM D6328-03. QA and QC procedures for OP-FTIR are discussed in more detail below.

### **Calibration Spectra**

A gas-phase FTIR reference spectrum is collected at a known temperature and pressure in a fixed path length enclosed cell for the compound of interest from a sample of known concentration. A series of measurements can be made at different concentrations and a calibration curve that relates the measured absorbance and the gas concentration can be developed to confirm a linear response of signal with concentration. These calibration spectra are stored in a spectral reference library used by the computer during real-time sample processing. Unknown sample concentrations can be determined by comparing sample absorption intensities to absorption intensities in the standard reference spectra. The higher the concentration of compound being measured; the more

IR radiation characteristic of that compound is absorbed. Complex mixtures of IR sensitive compounds can be determined from a single spectrum by solving a multiple linear regression matrix using characteristic wavelengths of compounds and the relative intensities of sample IR spectral features compared to calibration spectral features.

Tables of absorbance coefficients are available, and standard reference spectra for numerous compounds can be purchased. Suppliers of reference spectra include Pacific Northwest National Laboratory, which continues to develop the Northwest Infrared (NWIR) spectral library of quantitative infrared absorption spectra<sup>13</sup> and the high-resolution transmission molecular absorption database (HITRAN) compiled by Harvard University.<sup>14</sup>

Figure 2-8 shows an example of a typical single point calibration curve where the sample absorbance is plotted against concentration. Interpolation of the curve at a given absorbance measurement gives the concentration of the molecular species being analyzed.

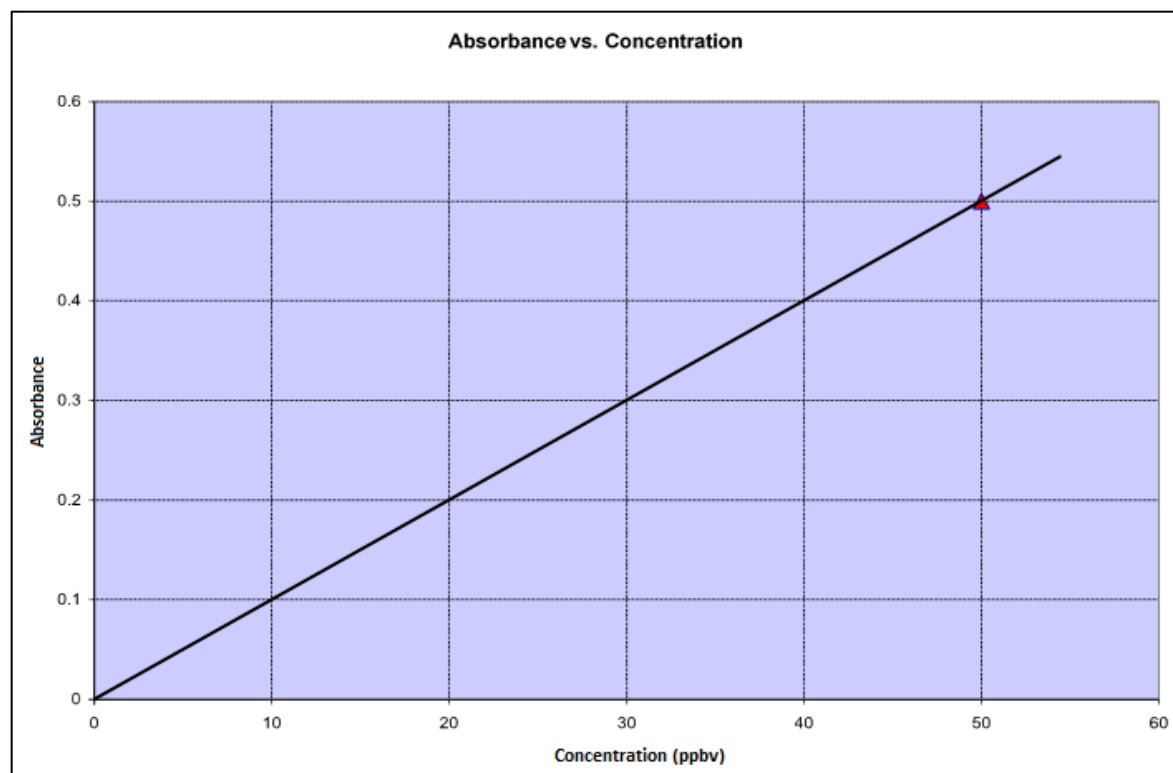


**Figure 2-8. Calibration Plot of Absorbance vs. Concentration**

### **QA/QC for OP-FTIR Instrumentation**

Several quality checks should be performed on FTIR instrumentation prior to deployment to the field and for the duration of the field campaign.<sup>15</sup> Prior to field deployment, the spectral baseline is checked to determine the amount of signal intensity, instrument noise, and baseline drift. Baseline drift is due to detector signal fluctuations that cause the signal to increase gradually over time. Typically, instruments are powered on and allowed to warm up for at least one hour prior to data collection to minimize baseline drift effects. Baseline noise should be checked prior to initial data collection and on each subsequent day of a field campaign to determine the amount of baseline signal due to the instrument's electronics and detector noise. All checks must be in accordance with the method or test protocol being performed.

On the first day of a field study, a stray light instrument check should be performed. This involves collecting, measuring, and identifying stray light as either background or instrument-related. All QC checks must be conducted prior to actual data collection and the results must indicate that the instrument is operating within the acceptable criteria range as specified in the method or protocol appropriate for the field testing campaign.<sup>15</sup> Typical quality control for this technology includes method quality objectives of 10-25 percent accuracy depending on path length and a precision target of 10 percent. Spectral quality is verified through the procedures and guidelines set by the manufacturers and specific EPA method in use.<sup>16</sup>

In addition to the QC checks performed on the FTIR, the quality of the instrument signal (interferogram) should be checked regularly during the field campaign. This is done by ensuring that the intensity of the signal is at least five times the intensity of the stray light signal and instrument noise. In addition to checking the strength of the signal, checks should be done regularly in the field to ensure that the data are being collected and stored to the data collection computer.<sup>15</sup>



### **Data Quality Indicators for Precision and Accuracy for OP-FTIR**

Instrument baseline noise and signal intensity are key data quality indicators for OP-FTIR measurements. Some investigators evaluate the precision and accuracy of the PIC measurements collected with an FTIR instrument by analyzing nitrous oxide concentrations in the atmosphere. A typical background atmospheric marker concentration for nitrous oxide is about 315 ppb.<sup>17</sup> However, this value may fluctuate due to seasonal variations in nitrous oxide concentrations or the topographical elevation of the site.<sup>17</sup>

The precision of the OP-FTIR measurements should be evaluated by calculating the relative standard deviation of ubiquitous IR active compounds (e.g., nitrous oxide) in each data subset.

A subset is defined as the data collected along one path length during one survey or sampling episode.<sup>15</sup> The number of data points in a data subset depends on the number of sample events conducted in a survey. For a stable air parcel, the standard data quality indicator (DQI) criterion set forth for precision is  $\pm 10$  percent.<sup>15</sup> The accuracy of the analyte PIC measurements can be evaluated by comparing the calculated nitrous oxide concentrations from the data subsets to the typical background concentration of 315 ppb.<sup>11</sup> The standard DQI criterion for accuracy is  $\pm 25$  percent.<sup>15</sup>

### **Example Applications and Vendors**

Details on the OP-FTIR application of open path technologies are provided in Section 3 of this Handbook. The OP-FTIR has been used for a wide variety of source emission measurements in the field including applications such as line of sight optical remote, bLS modeling and RPM. Table 2-2 summarizes optical technologies and the typical applications of each of the technologies.

**Table 2-2. Typical Applications for OP-FTIR.**

| Technology | Applications                                 |
|------------|--|
| OP-FTIR    | bLS, RPM, SOF, Tracer Gas Correlation, TO-16 |

We are aware of multiple vendors that currently manufacture OP-FTIR units; two of these vendors have verified their instrumentation through the EPA’s ETV program.<sup>18,19</sup> The cost of an OP-FTIR field ready system can range from \$75,000 to \$120,000 in 2010 U.S. dollars, depending on configuration and application. Gas standards used in fixed path length enclosed cells to confirm instrument calibration can range between \$300 and \$500. Table 2-3 lists several of these vendors and indicates which have verified their OP-FTIRs. The table also lists potential vendors for FTIR gas standards.

**Table 2-3. FTIR Supply Vendors**

| OP-FTIR Instruments            |   |
|--------------------------------|---|
| KASSAY FSI<br>*Ail Systems Inc | <a href="http://www.kassay.com">www.kassay.com</a>  |
| *Spectrex, Inc.                | <a href="http://www.spectrex-inc.com">http://www.spectrex-inc.com</a>                     |
| IMACC Instruments              | <a href="http://www.ftirs.com/">http://www.ftirs.com/</a>                                 |
| MIDAC Corporation              | <a href="http://www.midac.com/">http://www.midac.com/</a>                                 |
| Bruker Optics                  | <a href="http://www.brukeroptics.com/opag.html">http://www.brukeroptics.com/opag.html</a> |
| ABB/Bomem                      | <a href="http://www.abb.com/analytical">http://www.abb.com/analytical</a>                 |
| Gas Standard Suppliers**       |   |
| Air Gas                        | <a href="http://www.airgas.com/">http://www.airgas.com/</a>                               |
| Linde                          | <a href="http://www.linde.com/">http://www.linde.com/</a>                                 |
| Matheson Gas                   | <a href="http://www.mathesongas.com/index.aspx">http://www.mathesongas.com/index.aspx</a> |
| Spectra Gas                    | <a href="http://www.spectragases.com">http://www.spectragases.com</a>                     |
| Praxair                        | <a href="http://www.praxair.com/">http://www.praxair.com/</a>                             |

\*ETV Verified Technologies

\*\* Requires gas regulator in addition to gas cylinder

In addition to instrumentation and gas standards, tables of absorbance coefficients are available and standard reference spectra for numerous compounds can be purchased. Suppliers of reference spectra include Pacific Northwest National Laboratory, which continues to develop the NWIR spectral library of quantitative infrared absorption spectra<sup>13</sup> and Harvard University, which compiled the HITRAN database.<sup>14</sup> These spectra have been measured under tightly controlled conditions using state-of-the-art instrumentation.

### **Strengths and Limitations**

FTIR can be used as a qualitative tool to provide specific information about volatile IR energy absorbing molecules. It can also be used as a quantitative tool to provide the concentration of many gas-phase molecules. A summary of strengths and limitations is shown in Table 2-4 and Table 2-5. One of its limitations is that gas-phase water and CO<sub>2</sub> are a very strong IR absorbing species. In addition, water has strong absorption features in the 3200–4000 wave number range.<sup>5,17,20</sup>

Molecules that have coincident vibrational frequencies with water cannot be reliably analyzed using frequencies in this range. FTIR is also limited to measuring gaseous compounds that absorb IR radiation. Homonuclear diatomic gases such as nitrogen, oxygen, and halogen gases cannot be measured by FTIR.

FTIR's major strength is that it can provide real-time, simultaneous analysis of multiple gaseous contaminants<sup>6</sup>. Additionally, the FTIR is a robust field instrument that allows for unattended sampling for as long as a week period. Not only can the FTIR be used for open path concentration measurement of a variety of contaminants, but it can also be used for leak and hotspot detection.

**Table 2-4. Summary Table of the OP-FTIR's Strengths**

| Feature                          | Strength  |
|----------------------------------|---|
| Economical                       | Relatively low instrument cost (about \$80,000 - \$125,000)<br>Low-cost long-term deployment  |
| Compact Instrumentation          | FTIR equipment is rugged and easily portable  |
| Multiple Wavelength Operation    | There are many compounds that are infrared active (absorb IR light)   |
|                                  | Large number of compounds can be analyzed simultaneously. Spectra can be saved and post analyzed.   |
| Ease of Calibration              | No gas calibration standards necessary for field testing (uses standard reference spectral library). Gas standards are only needed for laboratory confirmation of instrument performance and calibration. |
| Multiple Applications            | FTIR can be used to locate discrete emissions hotspots at a facility/area source  |
|                                  | Multi-compound coverage makes FTIR ideal for leak detection or source location where the facility being monitored has multiple compounds present (e.g., chemical plants)                                  |
| Automated Real-time Measurements | Equipment can be allowed to run with minimal attention for months at a time with remote access to check instrument operation, schedule cryogen replenishment and recover data.                            |
|                                  | No sample collection, handling, or preparation is necessary.  |

**Table 2-5. Summary Table of the OP-FTIR's Limitations**

| Feature                           | Limitation   |
|-----------------------------------|--|
| Spectral Interferences            | Gas-phase water spectral interference as well as CO and CO <sub>2</sub> interference <sup>5,16,17</sup>  |
| Diatomic Molecules                | Not applicable to homonuclear diatomic gases such as chlorine, oxygen, and nitrogen <sup>1,2,3</sup>   |
| IR Wavelength Range               | Weak IR absorption features for many inorganic molecules such as sulfur dioxide and nitrogen oxides <sup>6</sup>   |
|                                   | Infrared beam has a limited range and may not be sensitive enough to meet ambient data quality objectives.   |
| Path Length Range                 | Maximum path length is on the order of 400–500 meters  |
| Field Implementation Requirements | Typical infrared detectors require cryogenic cooling to operate. Liquid nitrogen used for detector cooling must be refilled and maintained regularly (weekly).     |
|                                   | Field implementation and data collection requires highly experienced personnel   |
| Setup Time Consuming and Costly   | Typical set-up time usually requires about 5 to 8 hours and a minimum of two people  |
|                                   | Multiple vertical or horizontal path measurements necessary to calculate plume flux, can require significant time and cost to set up and implement                 |
| Measurement Limitations           | Single beam open-path method measures concentration along a path. The path must capture most if not all an analyte plume to provide accurate measure of emissions. |

## References

1. Bell, R. J. 1972. Introductory Fourier Transform Spectroscopy. New York, NY: Academic Press.
2. Hollas, M. J. 1992. Modern Spectroscopy. 2nd ed. New York, NY: John Wiley & Sons.
3. Laidler, J. K. 1995. Physical Chemistry. 2nd ed. Toronto, Canada: Houghton Mifflin Company.
4. Galle, B., J. Samuelsson, B. Svensson, and G. Borjesson. 2000. Measurements of Methane Emissions from Landfills Using a Time Correlation Tracer Method Based on FTIR Absorption Spectroscopy. Environmental Science and Technology. 201, 35 (1): 21- 25.
5. U.S. EPA. 2009. Measurement and Monitoring Technologies for the 21st Century, CLU- IN. <http://www.clu-in.org/programs/21m2/openpath/op-ftir/>
6. Liptak, B. 1995. Instrument Engineers' Handbook: Process Measurement and Analysis. Boca Raton, FL: CRC Press.
7. Spellicy, R. 2003. IMACC Industrial Monitoring Corporation, Round Rock Texas. <http://www.ftirs.com/>
8. Liptak, B. 2003. Instrument Engineer's Handbook: Process Measurement and Analysis. Radnor, PA: Chilton Book Company.
9. Liptak, B. 1995. Instrument Engineers' Handbook: Process Measurement and Analysis. Boca Raton, FL: CRC Press.
10. Minnich, T. and R. Scotto. 1999. Use of Open-Path FTIR Spectroscopy to Address Air Monitoring Needs During Site Remediations. Invited Article Published in Remediation. Summer 1999.

11. U.S. EPA. 2007. Evaluation of Fugitive Emissions Using Ground-Based Optical Remote Sensing Technology. EPA/600/R-07/032.
12. U.S. EPA. 2005. Evaluation of Fugitive Emissions at a Former Landfill Site in Colorado Springs, Colorado Using Ground-Based Optical Remote Sensing Technology. EPA- 600/R-05/041.
13. U.S. DOE Pacific Northwest National Laboratory. 2009. Optics and Infrared Sensing. Richland WA. <http://infrared.pnl.gov/>
14. Harvard University. 2009. The HITRAN Database. <http://www.cfa.harvard.edu/HITRAN/>
15. U.S. EPA. 2004. Optical Remote Sensing Facility Manual, U.S. EPA National Risk Management Research Laboratory, Air Pollution Prevention and Control Division, Emissions Characterization and Prevention Branch. Contract No. EP-C-04-023, Work Assignment 0-33.
16. U.S. EPA. 2006. Optical Remote Sensing for Emission Characterization from Non-Point Sources. <http://www.epa.gov/ttn/emc/prelim/otm10.pdf>
17. Godish, T. 2004. Air Quality, Fourth Edition. Boca Raton, FL: Lewis Publishers - CRC Press.
18. U.S. EPA and Battelle. 2000. Environmental Technology Verification Report: RAM 2000 Fourier Transform Open-Path Monitor. Report prepared by AIL Systems, Inc. [http://www.epa.gov/etv/pubs/01\\_vr\\_ail.pdf](http://www.epa.gov/etv/pubs/01_vr_ail.pdf).
19. U.S. EPA and Battelle. 2001. Environmental Technology Verification Report: SafEye 227 Infrared Open-Path Monitor. Report prepared by Spectrex, Inc. [http://www.epa.gov/etv/pubs/01\\_vr\\_safeyetwo.pdf](http://www.epa.gov/etv/pubs/01_vr_safeyetwo.pdf).
20. Jaakkola, P., T. Vahlman, A. Roos, P. Saarinen, J. Kauppinen. 1998. On-line Analysis of Stack Gas Composition by a Low Resolution FT-IR Gas Analyzer. Water, Air, & Soil Pollution. 101 (1-4): 79-92.

## **2.2 Tunable Diode Laser**

Light amplification by stimulated emission of radiation (LASER) is a technique to generate a narrow wavelength of light with a small cross-sectional area. Diode lasers generate this beam of light using a semiconductor material that emits light when electrical current is “injected” into the semiconductor junction. When the TDL was first introduced, its measurement applications were limited to laboratory functions because of the instrument functionality and cost. The rise of the fiber-optics communication industry in the 1980s led to the development of open-path TDL (OP-TDL) instrumentation that is compact and affordable.<sup>1</sup> Since that time, the OP-TDL has become recognized as a reliable technology for use in the field for *in situ* measurement of a variety of gaseous pollutants. New laser development demonstrated in 1994 using a repeated stack of thin semiconductor layers (Quantum cascade lasers) offers the possibility to produce laser beams at additional wavelengths and add to the list of compounds that can be measured.<sup>2</sup>

Laser-based gas detectors are now being used in a wide variety of applications for process and quality monitoring, and safety and environmental compliance. Laser detectors combine semiconductor TDLs and optical fibers developed by the telecommunications industry with detection techniques based on frequency or wavelength modulation (similar to radio). Laser detectors measure gas concentrations by shining a laser beam through a sample of gas and measuring the amount of laser light absorbed. Lasers emit light at a single wavelength. In TDLs, the wavelength can be “tuned” over a small range to match the exact absorption wavelength of a target compound by adjusting temperature and bias current. The wavelength of the laser is tuned over a selected absorption feature of the target species. The measured absorption spectra are recorded and, combined with measured gas temperature and pressure, effective path length, and known line strength, used to determine a quantitative measurement of concentration. These properties give laser detectors a combination of selectivity, sensitivity, dynamic range and rapid response time. The OP-TDL can make quantitative measurements of select gases based on the principals of Beer-Lambert law. Gas molecules absorb energy at specific wavelengths based on rotational and vibrational motion within the molecule. By measuring the energy absorbed for a



compound-specific wavelength over a laser's path, the OP-TDL can determine the concentration present of a specific gaseous compound. This technology can be used for several open-path and point monitoring applications.

The OP-TDL is a relatively inexpensive technology that emits very narrow wavelengths in the near IR ranges. While mid-IR wavelength lasers are available, they are much more difficult to operate or are currently cost prohibitive for general use. Because the wavelength emitted is very narrow and can be chosen specific to a vibration or rotation of a specific compound, the OP-TDL eliminates most interference. Lack of interference and high intensity of the laser beam allows longer open path lengths, up to 1 to 2 km and therefore, higher sensitivity for the compounds TDL can measure. The near-IR OP-TDL units currently in use are limited by the small number of compound specific wavelengths available from commonly available TDLs and the necessity to use a different TDL for each compound of interest.

### **Basic Operation**

TDL Absorption Spectroscopy instruments rely on spectroscopic principles and sensitive detection techniques, coupled with advanced diode lasers and optical fibers developed by the telecommunications industry. Gas molecules absorb energy at specific wavelengths in the electromagnetic spectrum. At wavelengths slightly different than these absorption lines, there is essentially no absorption. Measurement of the relative strengths of off-line to on-line transmission yields a precise and highly sensitive measure of the target gas concentration along the path transited by the laser beam. Measurements are made by (1) transmitting a beam of light through a gas mixture sample containing a quantity of the target gas, (2) tuning the beam's wavelength to one of the target gas's absorption lines, and (3) accurately measuring the absorption of that beam. The concentration of target gas molecules can then be integrated over the beam's path length.

While results generated by traditional optical instrumentation are generally in concentration units such as ppb, the output generated by the OP-TDL, like all open-path technologies, represents units of concentration over distance, such as ppb(m). This is also known as a PIC.

Each gaseous compound absorbs energy at different wavelengths, usually more than one, depending on vibrational and rotational excitement within the molecule. Therefore, each compound has its own “signature” of bands from which energy may be absorbed. Each band is highly selective, with virtually no absorption occurring outside of a specific wavelength. Because the OP-TDL emits a laser at a very narrowly tuned wavelength range, it is an ideal instrument for single compound measurement. The OP-TDL’s laser is selected for an overtone band specific to the compound of interest. The absorption of energy over the laser’s path length is measured by the instrument’s detector. The absorption is used to determine the concentration of the target gaseous compound using the principals of Beer-Lambert Law as described in the equation below.

$$A = \epsilon * c * l$$

Where:

A = absorbance intensity

$\epsilon$  = absorption coefficient

c = sample concentration

l = sample path length

There are many instrumental configurations for OP instruments. The simplest OP-systems are bistatic configurations. The arrangement of the components of this design for OP-TDL is shown in Figure 2-9. This configuration derives its name from the fact that both the transmitter and receiver must be fixed in a static position and precisely aimed at each other. The OP-TDL equipment projects the laser beam directly along a path to a detector/receiver. Bistatic configurations, in general, have the requirement of supplying power at both the receiver and transmitter, which can be a disadvantage in some locations. Additionally, there is a requirement for alignment at both receiver and transmitter, which can be time-consuming for mobile systems.<sup>3</sup>

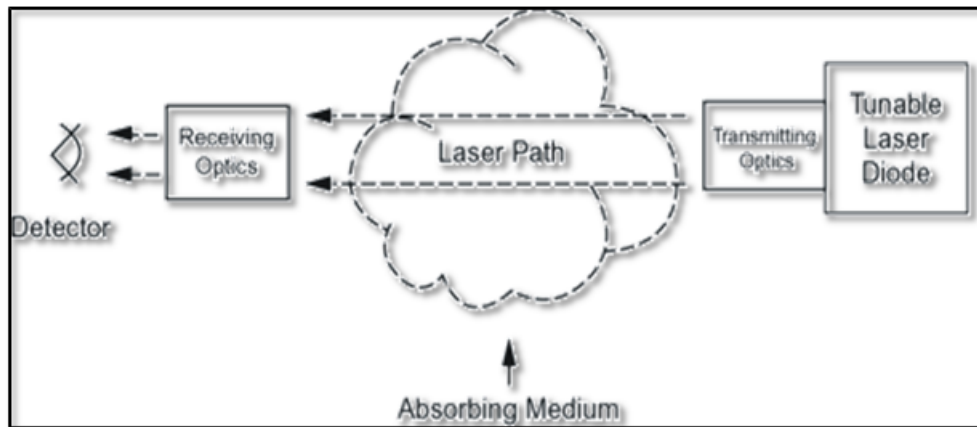


**Figure 2-9. TDL Bistatic Configuration**

Monostatic configurations were developed to address issues raised with bistatic designs. In a monostatic configuration, all the optical components of the transmitter and receiver are in the same location, and a retro-reflector is used to return the light from the transmitter to the receiver. This configuration derives its name from the fact that only the transceiver portion of the instrument needs to be precisely pointed as the retro-reflector returns light to its source regardless of orientation. A diagram of two monostatic configurations is shown in Figure 2-10.

Retro-reflecting mirrors, as they are called, are configured with three perpendicular reflective surfaces in the shape of a corner. A combination of three mutually perpendicular mirrors reflects light incident from any direction through  $180^\circ$  as shown in Figure 2-11. Such a combination of mirrors is called a corner-cube reflector. Corner-cube reflectors beam TDL light back to its exact point of origin. This property reduces the divergence of the beam on its return path back to the detector compared to divergence that would result from a flat mirror. Also, the retro-reflector array can be very large to capture and return essentially the entire divergent signal from the telescope.

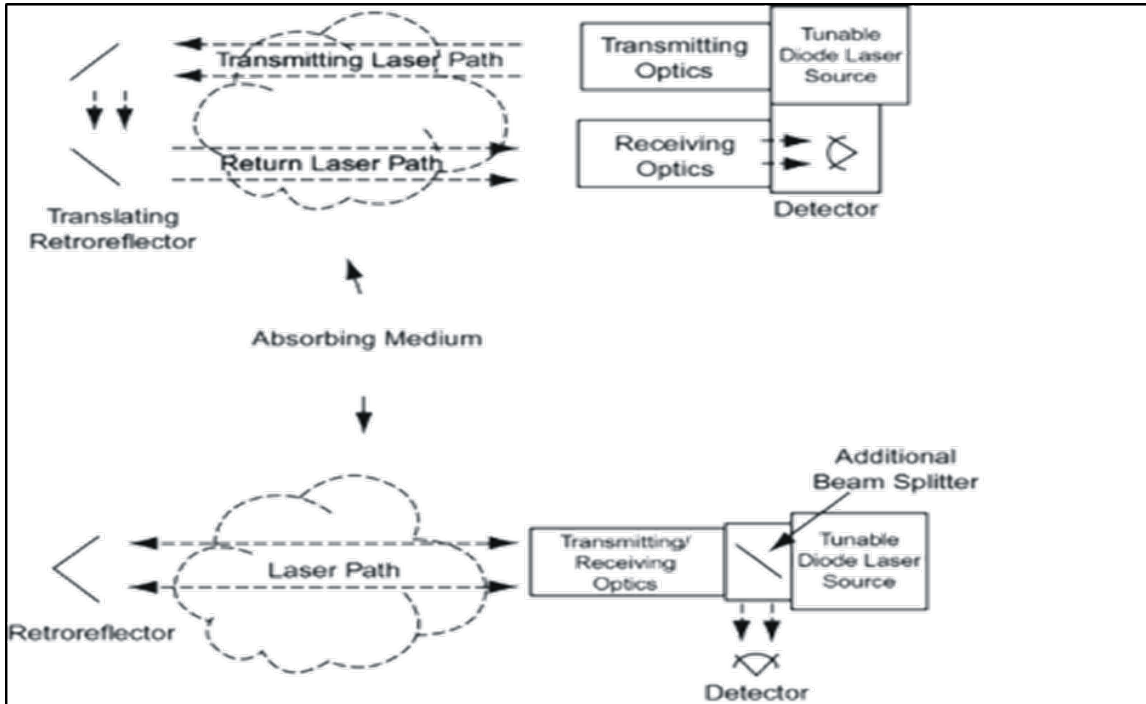


**Figure 2-10. TDL Monostatic Configuration**

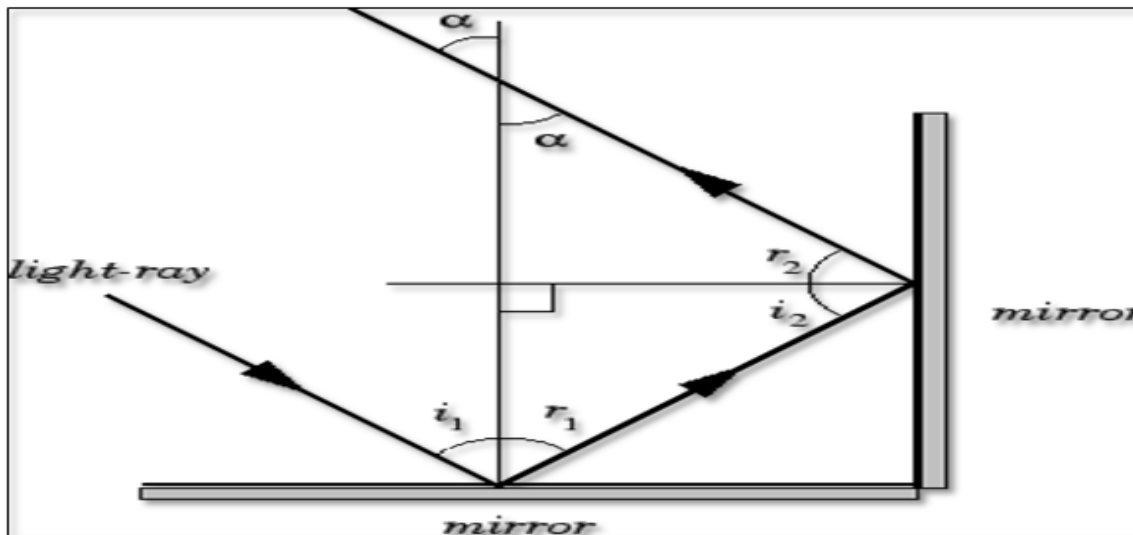


**Figure 2-11. The corner reflector cube**

In the mono-static mode, the IR laser beam is split twice, once leaving the OP-TDL and once on its return. This design requires a beam splitter in the optical path that removes 50 percent of the light from the outgoing beam and 50 percent of the light from the return beam for an overall loss of 75 percent of the total light intensity.

The dual-telescope monostatic configuration has lower detection limits because it does not utilize a beam splitter in the optical path. A translating retro-reflector, which is essentially a portion of a

very large cube, is used to return the light beam offset to align with the receiving telescope.

This single, large retro-reflector does not have the divergence reversal properties of the corner-cube array. The second telescope adds cost and complexity to the system.<sup>3</sup> However, when compared with mono-static mode, bi-static systems are harder to align and maintain because any shift in the transmitter or detector can result in system misalignment.<sup>4,5</sup> Both operating modes measure only the compounds that are in the beam path. Emissions outside the beam path are not measured. In these situations, measurements have been conducted along multiple beam paths to more accurately characterize the emission plume.

OP-TDL units are designed to operate under computer control, where the interfacing software controls the function of the OP-TDL, controls the tuning of the laser, and collects resulting data from the detector. Commercially available OP-TDL units can be equipped with multiple lasers, allowing the measurement of several compounds at one time. Field units typically include a hardware controller, a laptop, a telescope receiver, and a reflector. Instruments can run unattended via computer control for extended periods of time.<sup>6</sup>

### **Pollutants and Relative Levels That Can Be Measured**

Near-IR TDLs have been used to measure approximately 20 compounds that have absorbencies in the 1.4 – 1.8 micrometer ( $\mu\text{m}$ ) wavelength range. Using an open-path setup, concentrations into the low ppm range can be detected over a path length of approximately 1000 m to 2000 m. Table 2-6 lists airborne compounds that can be measured by OP-TDL systems and their approximate wavelengths. The compounds measured by TDLs are limited by the wavelength range commonly available using electrical current driven semiconductor lasers. Quantum Cascade Laser (QC-Laser) development offers the possibility of expanding the list by extending available laser wavelengths into the mid-infrared range, where many compounds of interest strongly absorb these wavelengths. However, one issue is that the measurements are also limited by the ability of fiber optic cables to transmit the raw LASER energy in those instruments using remote modules. Current TDL light sources cost \$2,000 to \$3,000. Experimental QC-Lasers are available at a cost up to

\$100,000.

**Table 2-6. Example List of Gaseous Compounds Measured by Near IR OP-TDL Systems**

| Species           | Approximate near-IR $\lambda$ (nm) | Reported Detection Limit (ppm-m)  |
|-------------------|------------------------------------|---|
| ammonia           | 760, 1500                          | 0.5-5.0   |
| carbon monoxide   | 1570                               | 40-1,000  |
| carbon dioxide    | 1570                               | 40-1,000  |
| hydrogen chloride | 1790                               | 0.15-1  |
| hydrogen cyanide  | 1540                               | 1.0   |
| hydrogen fluoride | 1310                               | 0.1-0.2   |
| hydrogen sulfide  | 1570                               | 20  |
| methane           | 1650                               | 0.5-1   |
| nitric oxide      | 1800                               | 30  |
| nitrogen dioxide  | 680                                | 0.2   |
| oxygen            | 760                                | 50  |
| water             | 970, 1200, 1450                    | 0.2-1.0   |
| acetylene         | 1520                               | These compounds are not commonly measured; therefore, detection limits are not readily available. |
| ethylene          | 1693                               |   |
| formaldehyde      | 1930                               |   |
| hydrogen bromide  | 1960                               |   |
| hydrogen iodide   | 1540                               |   |
| nitrous oxide     | 2260                               |   |
| phosphine         | 2150                               |   |
| propane           | 1400, 1500, 1700                   |   |

**Typical QA/QC**

Three major QA requirements are necessary when using a TDL system: (1) selection of the appropriate laser and absorption line for the compound of interest, (2) establishment and use of an appropriate calibration procedure, and (3) establishment of QC procedures that ensure the instrument's performance as measurements are made.<sup>6</sup>

**Selection of the Laser and Absorption Line**

A TDL optical system is typically built to generate one wavelength at a time. The range of wavelengths from each type of laser limits measurement to one compound at a time. Therefore, laser and instrument selection must be carefully considered. A few lasers can be configured for one of a limited range of wavelengths, while others provide a wider selection of wavelengths. It is also important to note that many compounds have multiple absorption bands in both the near-

and mid-IR regions. However, the availability of mid-IR lasers is limited and may not be available for open-path monitoring or measurement programs. Table 2-7 lists commercially available lasers producing wavelengths in the near-IR range. Table 2-8 lists other laser types that have been developed for mid-IR applications. While this list covers most of the lasers available, TDLs represent a limited set from a larger array of laser types.

**Table 2-7. Near-IR Laser Types Available for OP-TDL Systems**

| Laser Type  | Tunable $\lambda$ Range (nm) | Target Compounds   |
|-------------|------------------------------|--|
| InGaAsP     | 1200-2000                    | CO, CO <sub>2</sub> , NO, CH <sub>4</sub> , C <sub>2</sub> H <sub>2</sub> , HF, HCl, HBr, HI, HCN, NH <sub>3</sub> , H <sub>2</sub> CO, PH <sub>3</sub> , H <sub>2</sub> O |
| Antimonide* | 2000-4000                    | CO, CO <sub>2</sub> , NO, N <sub>2</sub> O, CH <sub>4</sub> , HCl, HBr, H <sub>2</sub> CO  |

\*Laser emits wavelengths in both the near-IR and mid-IR spectrums.

**Table 2-8. Potentially Usable Mid-IR Lasers**

| Laser Type        | Tunable $\lambda$ Range (nm) | Target Compounds   |
|-------------------|------------------------------|--|
| AlGaInP           | 630-690                      | NO <sub>2</sub>  |
| AlGaAs            | 750-1000                     | O <sub>2</sub> , NH <sub>3</sub>   |
| Vertical Cavity   | 650-1680                     | H <sub>2</sub> O, C <sub>2</sub> H <sub>2</sub> , HF, H <sub>2</sub> S, O <sub>2</sub> , H <sub>2</sub> O, NH <sub>3</sub>   |
| Antimonide*       | 2000-4000                    | CO, CO <sub>2</sub> , NO, N <sub>2</sub> O, CH <sub>4</sub> , HCl, HBr, H <sub>2</sub> CO  |
| Quantum Cascade** | 4000-12000                   | H <sub>2</sub> O, CO, CO <sub>2</sub> , NO, NO <sub>2</sub> , N <sub>2</sub> O, SO <sub>2</sub> , C <sub>2</sub> H <sub>2</sub> , HCN, NH <sub>3</sub> , PH <sub>3</sub> , O <sub>3</sub>  |
| Lead-salt**       | 3000-30000                   | H <sub>2</sub> O, CO, CO <sub>2</sub> , NO, NO <sub>2</sub> , N <sub>2</sub> O, SO <sub>2</sub> , CH <sub>4</sub> , C <sub>2</sub> H <sub>2</sub> , HCl, HBr, HCN, NH <sub>3</sub> , H <sub>2</sub> CO, PH <sub>3</sub> , O <sub>3</sub> |

\*Laser emits wavelengths in both the near-IR and mid-IR spectrums.

\*\* Laser emits wavelengths in the mid-IR spectrum

Because compounds often have multiple absorption bands that can be detected by a TDL system, it is also important to consider which band is best for quantitative purposes.<sup>7</sup> Higher intensity absorption bands provide the best sensitivity. However, interference from other compounds may eliminate the use of the most sensitive wavelengths. It also may be worthwhile to measure the concentrations from a second absorption band to verify the nonexistence of interferences. It is

highly unlikely that the same interference would exist for both absorption bands.<sup>6</sup>

### **Calibration**

In a closed-gas cell TDL instrument, known concentrations of the compound of interest are introduced into the white cell used for sample analysis. Calibration gas is added through the same line used to collect the sample. Varying concentrations of one compound can be introduced by adjusting the inlet flow of the calibration gas relative to the dilution gas. For each concentration step in the calibration curve, the absorption trend should be recorded and the mean and standard variation calculated.<sup>8</sup>

The calibration factors are typically determined in the laboratory with short path length gas cells. One instrument vendor provides an insertion slot that can contain a gas cell of known concentration into the path of the optical beam during measurement. Other OP-FTIR instruments can also be calibrated with gas cells of known concentration by introducing the cell into the laser's path for measurement. Field calibration checks can be accomplished using the absorption signal provided by the calibration gas cell added to the open path field absorption signal. The signal increases above the open path signal, proportionally to the gas concentration and path length of the gas cell. The instrument response is checked using the difference of the measurements with and without the gas cell. An example of a calibration curve for methane is provided as Figure 2-12.



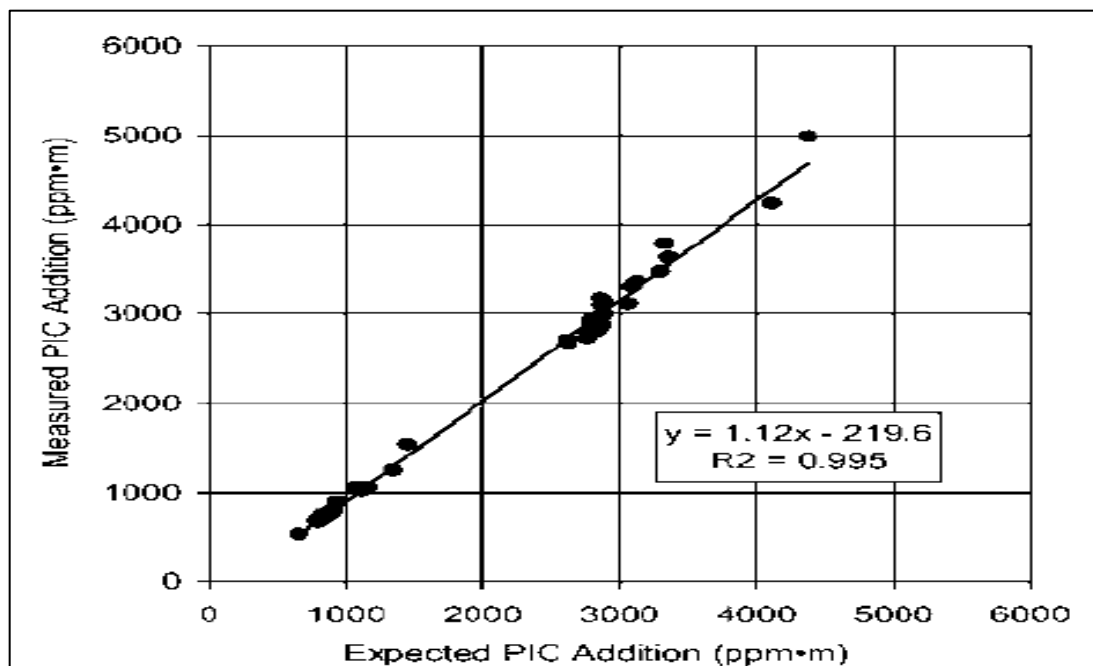


**Figure 2-12. Calibration Data for an OP-TDL System**

Calibration frequency depends on the duration of the measurement period as well as the concentrations of compounds that are measured. Shorter term measurements projects need calibration verification at the beginning of a measurement episode. Also note that regulatory requirements may also dictate calibration frequencies. Low concentrations in ambient conditions may require background and calibration determinations on a weekly or monthly basis because a small drift in instrument response is more significant at lower measured concentrations.

### **Quality Control Procedures**

Each OP-TDL manufacturer recommends its own QC procedures; however, it is necessary to verify the accuracy of the calibration throughout a set of field measurements. This can be done by reinserting a calibration standard cell periodically during a measurement episode to ensure correct measurement. Recalibration during field measurements may be necessary due to instrument drift and is typically performed using the instrument's system software.

### **Example Applications and Vendors Applications**

Details on the near-IR TDL application of open path technologies are provided in Section 3 of this

Handbook. The OP-TDL has been used for a wide variety of source emission measurements in the field including applications such as line of sight optical remote, bLS modeling, RPM, and mobile tracer release correlation. Table 2-9 summarizes optical technologies and the typical applications of each of the technologies.

**Table 2-9. Typical Applications for OP-TDL.**

| Technology | Applications                            |
|------------|---|
| OP-TDL     | bLS, RPM, Tracer Gas Correlation, TO-16 |

**Vendors**

While there are many sources for TDL instrumentation that is suitable for laboratory applications, there are only a few vendors currently offering field ready OP-TDL instrumentation. Vendors offering instrumentation exclusive to fire detection and monitoring have not been included. The cost of a TDL field ready system can range from \$35,000 to \$75,000 in 2010 U.S. dollars depending on the configuration and application. Table 2-10 lists example vendors and their internet contact address.

**Table 2-10. Near-IR OP-TDL Vendors**

| Vendors  |                               |
|--|-------------------------------|
| Boreal Laser                                   | www.boreal-laser.com          |
| OP SIS AB                                      | www.opsis.se                  |
| Leister Process Technologies, Axetris Division | www.ir-microsystems.com       |
| Norsk Elektro Optikk (NEO, Norway)             | www.neo.no                    |
| PKL Technologies, Inc.                         | www.pktechnologies.com        |
| PSI Physical Sciences, Inc.                    | www.tdlas.com www.psicorp.com |
| Senscient                                      | www.senscient.com             |
| Simtronics group                               | www.simtronics.eu             |
| Unisearch Associates, Inc. (Concord, Canada)   | www.unisearch-associates.com  |

**Strengths and Limitations**

The TDL has an array of strengths and limitations that must be considered for each OP-TDL application. A summary of strengths and limitations is shown in Table 2-11 and Table 2-12,

respectively. Perhaps the most striking limitation is the fact that each TDL laser can detect only one compound at a time and each laser can scan only a limited range of wavelengths. It is also true that only compounds with overtone absorbencies in the near- and mid-IR ranges can be detected and quantified, of which there are approximately twenty.<sup>9</sup> The instrument's sensitivity is limited because of noise created by the laser<sup>10</sup>, though this can be improved by either of the modulations described above. However, because the laser emits such a narrow bandwidth, interferences from other gaseous compounds are unlikely and limited to compounds with absorbance at that wave number.

**Table 2-11. Summary Table of the TDL's Strengths**

| <b>Feature</b>                          | <b>Strength</b>  |
|---|--|
| Automated Real-time Measurements        | 24/7 remote monitoring   |
|   | Can provide near real time data  |
|   | Unattended measurements collection   |
| Compact instrumentation                 | Field units are lightweight, typically under 75 Kg, and relatively easy to transport and setup |
| Economical                              | 0.5 to .01 the cost of alternative technologies  |
| High intensity light source             | Wide linear response over a wide dynamic range resulting in measurements from 0.1 to 1000 ppm  |
|   | The ability to measure longer path lengths (1 km compared to other ORS technologies)           |
| Solid state technology                  | Robust field use with low maintenance, minimal consumables to operate                          |
| Low response times                      | Rapid response – typically 1 second  |
| High spectral resolution                | Minimizes interference from other gases resulting in high compound specificity                 |
| Uses fiber optics for signal processing | Lower equipment cost per measurement, ability to multiplex signals                             |
| Vendor-specific calibration cells       | Self-calibration, zero and span drift correction   |

The TDL's strengths in field application are numerous. Technological developments originating

from the fiber optics communication field have allowed the TDL to become compact, robust, and economical compared to other technologies. The TDL can be used for several applications, including open-path, RPM, and cavity ring-down spectroscopy (CRDS) measurements. The high-powered laser source also promotes fast instrument response times (as low as one measurement per second) and longer path lengths up to 1,000 meters.

**Table 2-12. Summary Table of the TDL’s Limitations**

| Feature                               | Limitation   |
|---------------------------------------|--|
| Single wavelength operation           | Detects only one compound per laser, fewer measurable compounds, and limited sensitivity   |
| Mid-IR wavelength range               | Quantitation limited to compounds with overtone absorbencies in the near- and mid-IR range |
| Dust and objects block the laser beam | With all open path optical measurements, blocked beams result in no measurements           |

**References**

1. Harris, Shores and Thoma. 2007. Using Tunable Diode Lasers to Measure Emissions from Animal Housing and Waste Lagoons, 16th Annual International Emission Inventory Conference Emission Inventories: “Integration, Analysis, and Communications” Raleigh.<<http://www.epa.gov/ttn/chief/conference/ei16/session12/harris.pdf>>. May 14-17.
2. Faist, Jerome, Federico Capasso, Deborah L. Sivco, Carlo Sirtori, Albert L. Hutchinson, and Alfred Y. Cho. 1994. "Quantum Cascade Laser" Science 264 (5158): 553–556.
3. Liptak, B. G. 2003. Instrument Engineer’s Handbook: Process Measurement and Analysis. Radnor, PA: Chilton Book Company
4. Liptak, B. G. 1995. Instrument Engineers’ Handbook: Process Measurement and Analysis. CRC Press.
5. Spellicy, R. 2003. IMACC Industrial Monitoring Corporation, Round Rock Texas.

6. Schiff, H. I. 1987. Measurement of Atmospheric Gases by Tunable Diode Laser Absorption Spectrometry. Monitoring of Gaseous Pollutants by Tunable Diode Lasers: Proceedings of the International Symposium held in Freiburg, F.R.G, 13-14 November 1986. D. Reidel Publishing Company.
7. Ku, R. T., E. D. Hinkley, and J.O. Sample. 1975. Long-Path Monitoring of Atmospheric Carbon Monoxide with a Tunable Diode Laser System. Applied Optics. 14 (4).
8. Mock, A., C. Roller, J. Jeffers, N. Khosrow. P. McCann, and J. Grego. 2001. Real-time ground level atmospheric nitric oxide measured by calibrated TDLAS system. Optical Society of America.
9. Thoma, E. D., Shores, R. C.; Thompson Jr, E. L.; Harris, D. B.; Thorneloe, S. A.; Varma, R. M.; Hashmonay, R. A.; Modrak, M. T.; Natschke, D. F. and Gamble, H. A. 2005. Open-Path Tunable Diode Laser Absorption Spectroscopy for Acquisition of Fugitive Emission Flux Data. J. Air & Waste Manage. Assoc. 55: 658-668.
10. Cappellani, F., G. Melandrone, and G. Restelli. 1987. Post Detection Data Handling Techniques for Application in Derivative Monitoring. Monitoring of Gaseous Pollutants by Tunable Diode Lasers: Proceedings of the International Symposium held in Freiburg, F.R.G, 13-14 November 1986. D. Reidel Publishing Company.

### ***2.3 Ultraviolet Differential Optical Absorption Spectroscopy***

The UV-DOAS is an optical remote sensing technology that quantifies concentrations of gaseous compounds by measuring the absorption of UV light by chemical compounds in the air and applying the Beer-Lambert law.<sup>1</sup>

A significant strength of the UV-DOAS is its extremely long path-length capability – typically 500 meters with some research applications up to 10 kilometers.<sup>2</sup> UV-DOAS has been deployed in a wide variety of environmental measurement applications. It is most frequently used to measure or monitor criteria and smog-related air pollutants. It is also able to accurately monitor several pollutants that do not produce ideal IR absorption bands. However, because the absorption bands for UV-DOAS are very wide, there are many compounds that cannot be accurately quantified by UV-DOAS. Nitrogen and oxygen molecules in the air cause broad spectral scattering and interfere with many of the compounds that can be measured. The UV-DOAS is reported to have detection limits in the low (ppb) range and can reach parts per trillion in some research applications when used with optimum measurement path lengths.<sup>2</sup>

#### **Basic Operation**

In general, UV, visible, and near-IR light is that radiation within the 180-780 nanometer wavelength range that causes changes in energy between the bonding electrons in molecules that absorb the light. While wavelength ranges produced by UV-DOAS instrumentation include the rotational and vibrational transitions caused by near-IR light, the typical application of UV-DOAS restricts the UV light to a wavelength range of 245 to 380 nanometers. Due to the range of excitations measured, molecular absorption bands tend to be far broader than that of IR instrumentation. Compounds that can be accurately detected and measured with the UV-DOAS possess specific chemical structure characteristics that allow for unique absorption bands, which limits the number of compounds that can be monitored.<sup>3</sup>

DOAS is based on the principal that the Beer-Lambert Law (Equation below):

$$A = \epsilon * c * l$$

Where:

A = absorbance intensity

$\epsilon$  = absorption coefficient

c = sample concentration

l = sample path length

Interferences in the atmosphere cause absorption to occur at all points in the measurement spectrum. In the atmosphere, the light of the beam undergoes extinction processes by air molecules and aerosols, turbulence, and absorption by many trace gases. DOAS overcomes the effects of the beam extinction by mathematically separating and removing the nonspecific beam extinction from the target gas absorption.<sup>4</sup> To address this issue, DOAS measures the difference between the absorption peak caused by the compound of interest and absorption peaks at wavelengths on either side of that targeted peak.<sup>3</sup> The concentration is determined by the light intensity in the absence of a structured absorption band, rather than the light intensity in the absence of all absorption.

A typical UV-DOAS system consists of a light source, optics, a spectrometer, and depending on the system configuration, a retro-reflector. Most systems employ a tungsten halogen or xenon arc lamp, though some use deuterium lamps.<sup>2</sup> From the source, the light is focused and directed into the atmosphere by means of a transmitting telescope. A receiving telescope retrieves and focuses the attenuated light beam and the spectrometer measures the change in absorbance caused of the UV light. Data collected by the UV-DOAS can be stored in the analyzer and can be transferred off-site via external storage or Internet connection.<sup>5</sup> The digital signal from the spectrometer is

collected by a computer system and compared to laboratory-developed reference spectra to ensure a match between all absorption bands associated with a targeted compound are present to confirm its identification and quantification.<sup>7</sup> Some technologies use specific gas calibrations to fine tune the library reference spectra and improve instrument performance. Figure 2-13 shows an Opsis DOAS<sup>6</sup> source unit.



**Figure 2-13. OPSIS DOAS Instrument**

UV-DOAS instruments can practically measure path lengths up to 500 meters. Optimum light path length depends on the compound of interest, the desired detection limit, the clear line of sight available, and the expected interferences (e.g., dust and fog). Measurement noise increases and beam intensity decreases as path length increases.<sup>1</sup>

Certain chemical species can also pose interference issues at particular wavelengths. For example, when trying to measure nitrous oxide ( $N_2O$ ) in the presence of other nitrogen oxides ( $NO$ ,  $NO_2$ ), absorption from  $NO$  and  $NO_2$  can cause interference.<sup>8</sup> Special considerations must also be made when measuring concentrations of aliphatic hydrocarbons in ambient air since oxygen is a major interferent for these compounds.<sup>5</sup>

Additionally, there are several operational concerns that must be considered when operating a UV-DOAS in the field. These instruments are approved for use in temperatures of 5 - 30°C with humidity ranging from 0 - 80 percent. High humidity can cause fog to build up on the receiver



mirrors and windows, which can substantially decrease the detected light intensity and deteriorate the condition of the instrument optics and mirrors. This can be corrected by installing heaters on the mirrors and windows or by changing the site where the UV-DOAS is installed.<sup>5</sup>

### UV-DOAS Field Implementation

There are many instrumental configurations for open-path UV-DOAS instruments. UV-DOAS instrumentation can be deployed in both bistatic and monostatic open-path configurations.

The simplest OP-systems are bistatic configurations. The arrangement of the components of this design for UV-DOAS is shown in Figure 2-14. This configuration derives its name from the fact that both the transmitter and receiver must be fixed in a static position and precisely aimed at each other. The UV-DOAS equipment projects the light beam directly along a path to a detector/receiver. Bistatic configurations, in general, have the requirement of supplying power at both the receiver and transmitter, which can be a disadvantage in some locations. The receiver and transmitter must be accurately aligned to optimize signal intensity.<sup>9</sup>

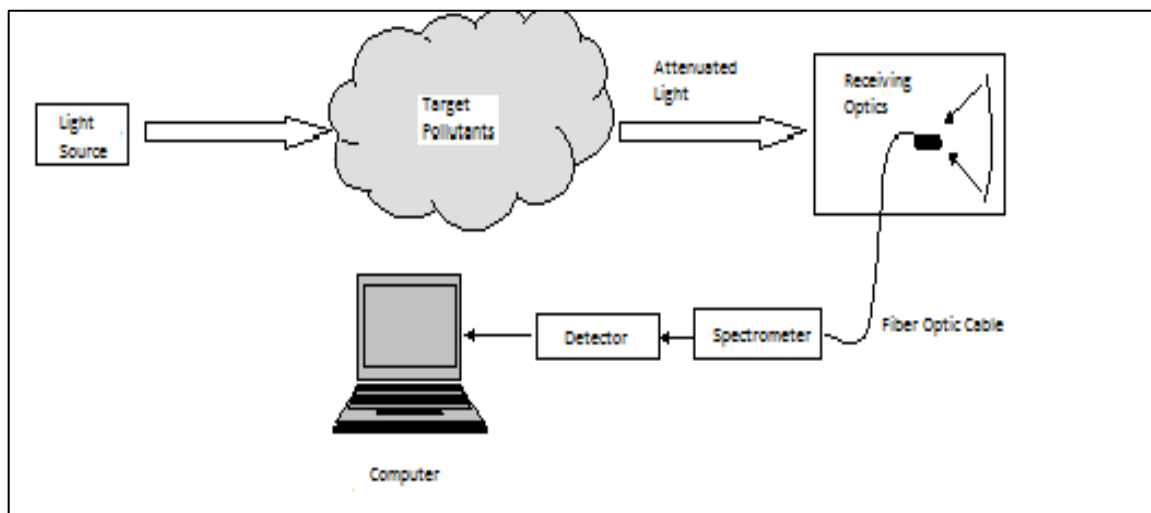


**Figure 2-14. Bistatic Configuration of UV-DOAS**

Monostatic configurations were developed to address issues raised with bistatic designs. In a monostatic configuration, all the optical components of the transmitter and receiver are in the same location and a retro-reflector is used to return the light from the transmitter to the receiver. A noted disadvantage of a monostatic system is that the physical path is only half the distance of a

bistatic system.

“Retro-reflecting” mirrors are configured with three perpendicular reflective surfaces in the shape of a corner. A combination of three mutually perpendicular mirrors reflects light incident from any direction through  $180^\circ$  as shown in Figure 2-15. Such a combination of mirrors is called a “corner-cube reflector.” Corner-cube reflectors beam light back to its exact point of origin. This property reduces the divergence of the beam on its return path back to the detector compared to divergence that would result from a flat mirror. Also, the retro-reflector array can be very large to capture and return essentially the entire divergent signal from the telescope.

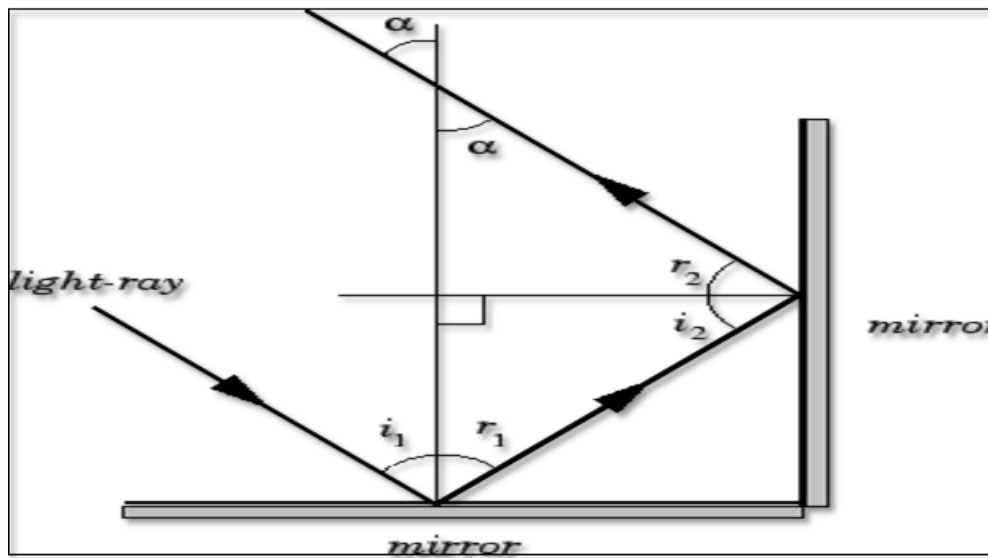


**Figure 2-15. The Corner-cube Reflector**

The monostatic configuration derives its name from the fact that only the transceiver portion of the instrument needs to be precisely aimed because the retro-reflector returns light to its source.

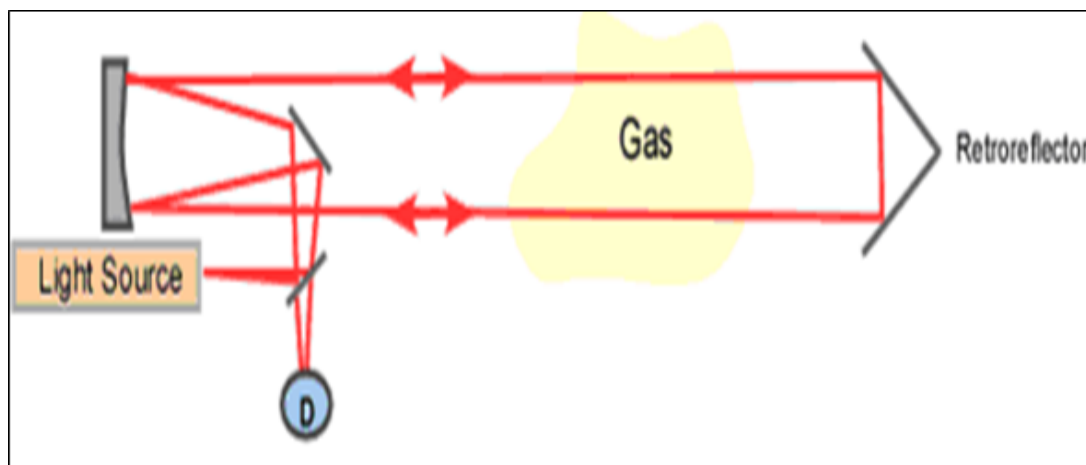


**Figure 2-16. Basic Setup Used to Make Monostatic Open-path UV-DOAS Measurements**

When compared with monostatic mode, bi-static systems are harder to align and maintain because any shift in the transmitter or detector can result in system misalignment.<sup>10,11</sup> Both operating modes measure only the compounds that are in the beam path. Emissions outside the beam path are not measured. Siting and additional QA procedures for ambient measurements found in 40 CFR Part 58 provide basic guidance for criteria pollutants using open-path measurements. In addition, EPA QA Handbook Volume II12 has siting requirements and other useful information on using UVDOAS in ambient/background monitoring situations.

### **Passive UV-DOAS**

A third configuration is known as passive UV-DOAS. Passive UV-DOAS uses ambient lighting, such as sunlight, as its light source and does not require a transmitting telescope. Passive UV-DOAS instruments can be fitted into balloons and used to measure concentrations of pollutant gases at differing heights in the atmosphere.<sup>12</sup>

### **Pollutants and Relative Levels That Can Be Measured**

Table 2-13 lists compounds that have been measured with UV-DOAS systems. The list is not exhaustive and includes only compounds reported in recent literature.<sup>2,12</sup> UV-DOAS systems have the most widespread environmental use in the detection and measurement of inorganic gases and vapors, monoaromatics (i.e., benzene), and aldehydes.

**Table 2-13. Species Measured with UV-DOAS Systems**

|                  | Species           |                |
|------------------|-------------------|----------------|
| 1,3-Butadiene    | Formaldehyde      | Ozone          |
| Acrolein         | Hydrogen Fluoride | Sulfur Dioxide |
| Ammonia          | Isoprene          | Styrene        |
| Benzene          | Mercury           | Toluene        |
| Carbon Disulfide | Nitric Oxide      | m, p-Xylene    |
| Chlorine         | Nitrogen Dioxide  | o-Xylene       |
| Ethyl Benzene    | Nitrous Acid      |                |

Detection limits have been reported in the ppb with at least one research application reporting cases of detection down to parts per trillion ranges.<sup>2</sup> Detection limits vary based on factors such as the deployment configuration, light path length, measurement noise, and meteorological conditions.<sup>1,2</sup> Table 2-14 gives example detection limits found in the literature.

**Table 2-14. Approximate Detection Limits for UV-DOAS**

| Pollutant        | Lower Detection Limit (ppb) | Path Length (m) |
|------------------|-----------------------------|-----------------|
| Ammonia          | 800                         | 200             |
| Benzene          | single digit ppb            | 500             |
| Carbon Disulfide | 500                         | 5000            |
| Formaldehyde     | single digit ppb            | 500             |
| Nitrous Acid     | single digit ppb            | 500             |
| Nitrogen Dioxide | single digit ppb            | 1000            |
| Nitrogen Oxide   | 240                         | 200             |
| Ozone            | single digit ppb            | 1000            |
| Sulfur Dioxide   | single digit ppb            | 1000            |
| Toluene          | single digit ppb            | 200             |
| m, p-Xylene      | 10                          | 500             |
| o-Xylene         | single digit ppb            | 500             |

**Typical QA/QC**

QA/QC ensure the validity of data and calculations performed by UV-DOAS systems. Each instrument manufacturer establishes its own quality assurance procedures based on the specifications of the individual instrumentation, but there are several procedures that should be

followed universally.

### **Record Keeping**

As with all environmental measurements, it is necessary to keep accurate records during measurement periods to ensure accurate data collection. For UV-DOAS, information such as meteorological conditions, path lengths, UV filter numbers, lamp type, light intensities and measurement times should be recorded.<sup>5</sup> Light intensities must be recorded anytime the UV emitter or receiver is adjusted and compared to the intensities measured when the UV-DOAS was installed. The measured recoveries of standard gas cells with known concentrations should also be documented.

### **Instrument Performance**

Before measurements are begun and throughout the measurement process, several instrument performance checks are required to make sure the instrument is accurately collecting data. Individual vendors recommend specific instrument performance checks such as correcting for slight variances in the reference spectrum (i.e., the lamp spectrum with no concentration bands) caused by changes in the spectrometer and instrument electronics. This is performed by periodically re-recording the lamp spectrum and comparing it to the initial reference spectrum for agreement. The reference spectrum is critical to the analysis of collected data and performing regular reference checks also minimizes noise collected by the instrument.<sup>5</sup>

Calibration checks are also very important for the collection of accurate data. The analyzer is checked by measuring gas standards of known concentrations for accuracy. Calibration cells are filled with the gas standard, allowed to stabilize, and the absorption is measured. A valid calibration curve should contain six equally-spaced calibration points, including zero, and cover at least 80 percent of the perceived measurement range. Because UV-DOAS measurements are based on absorption and, therefore, the number of target compound molecules in a specific path length, the calibration points can be obtained either by decreasing the measurement path or

diluting the gas standard.<sup>5</sup>

A function check is also required to periodically validate the instrument's performance. During a function test, a cell with a known concentration of gas is placed in front of the receiver. The instrument measures the concentration of the compound in the cell plus the concentration of the compound in ambient air. This check serves two purposes: (1) to ensure that the analyzer is producing accurate measurements and (2) to ensure that no cross-sensitivities occur between the test gas in the cell and other gases. Function tests must be performed in stable ambient pollution conditions because spikes in pollutants may cause the results of the function test to be difficult to interpret.<sup>5</sup>

Accuracy and precision tests are defined by the EPA regulations at 40 CFR part 58 (Ambient Air Quality Surveillance). Often these values are determined by performing calibration checks against known gas standards and verifying the MDL provided by the instrument manufacturer. Instrument manufacturers provide their own instructions on how to perform accuracy and precision tests in accordance with EPA regulations.

### **Example Applications and Vendors**

UV-DOAS has been deployed in a wide variety of environmental measurement applications which are discussed for specific applications in Chapter 3 of this Handbook. UV-DOAS is most frequently used for monitoring smog-related air pollutants, where its long range is used to verify Eulerian models that are used in air quality management. Multiple pathways have been used to create 2 dimensional (2-D) and 3 dimensional (3-D) tomographic depictions of pollutants around a large area source or urban area. UV-DOAS is used for fence-line monitoring of air pollutant emissions. Benzene has been measured in residential areas downwind of chemical manufacturing plants and ammonia has been monitored in areas around large-capacity swine feeding operations. UV-DOAS was also used to measure mercury emissions from a chloro-alkali plant.<sup>7</sup> These types of ambient and fugitive or area source measurements have been useful to government agencies to identify places where harmful levels of pollution exist and determine the level of injunctive relief necessary.<sup>2</sup>

Table 2-15 summarizes those applications that utilize UV-DOAS technology.

**Table 2-15. Typical Applications for UV-DOAS.**

| Technology | Application             |
|------------|-------------------------|
| UV-DOAS    | OTM 10, Tracer Gas, bLS |

One developing application for UV-DOAS is known as Multi-Axis Differential Optical Absorption Spectroscopy (MAX-DOAS). The application provides the ability to derive a vertical profile of pollutants by completing multiple scans simultaneously using either passive or active techniques.<sup>2</sup>

**Vendors**

There are currently five vendors of field-ready UV-DOAS instruments, as summarized by Table 2-16. Opsi, Inc., has had two separate instruments verified through the EPA’s ETV program.<sup>13</sup> The Opsi System has also been designated as an “Equivalent Method” for the measurement of SO<sub>2</sub>, NO<sub>2</sub> and O<sub>3</sub> in ambient air.

**Table 2-16. UV-DOAS Vendors**

| Vendors                                  | Websites   |
|--|--|
| Argos Scientific                         | <a href="http://www.argos-sci.com">www.argos-sci.com</a>               |
| Environnement S.A. Sanoa UV/Visible DOAS | <a href="http://www.environnement-sa.com">www.environnement-sa.com</a> |
| ETG Risorse e Tecnologia                 | <a href="http://www.etgrisorse.com">www.etgrisorse.com</a>             |
| IMACC                                    | <a href="http://www.ftirs.com">www.ftirs.com</a>                       |
| Opsi, Inc.                               | <a href="http://www.opsi.se">www.opsi.se</a>                           |
| Spectrex                                 | <a href="http://www.spectrex-inc.com">www.spectrex-inc.com</a>         |
| Cerex Monitoring Solutions               | <a href="http://www.cerexms.com">www.cerexms.com</a>                   |

**Strengths and Limitations**

Tables 2-17 and 2-18 summarize the strengths and limitations associated with the use of the UV-DOAS. Some UV-DOAS can provide concentration data for up to three compounds simultaneously. In the field, the instrument is portable<sup>15</sup> and can be deployed long-term for continuous remote *in situ* monitoring.<sup>13</sup> UV-DOAS quantifies compounds more successfully that have strong UV light and weak infrared absorption characteristics. Since NO<sub>2</sub> measurement by UV-DOAS does not require conversion to NO and measurement by difference, as conventional chemiluminescent monitors operate, this ORS technology provides a direct rather than indirect measurements.

**Table 2-17. Summary of UV-DOAS Strengths**

| <b>Feature</b>                   | <b>Strengths</b>  |
|----------------------------------|---|
| Automated Real-time Measurements | 24/7 remote monitoring  |
|                                  | Can provide near real time data   |
|                                  | Unattended measurements collection  |
| Economical                       | Relatively low instrument cost (about \$60,000 - \$200,000)<br>Low-cost long-term deployment  |
| Multiple Wavelength Operation    | Broad spectrum instruments allow monitoring of three criteria pollutants and trace species simultaneously. Spectra can be saved and post analyzed |
| Range of Measurement             | Long measurement path length – up to 500 m.   |
| Detectability                    | Many compounds are detectable in the low ppb range  |
| Compact Instrumentation          | Portable  |

However, the number of species that can be analyzed with UV-DOAS is limited due to the lack of appropriate absorption characteristics in the UV-visible wavelength range of many compounds.

**Table 2-18. Summary of UV-DOAS Limitations**

| <b>Feature</b>             | <b>Limitations</b>   |
|----------------------------|--|
| Difficulty in Deployment   | Alignment of remote receiving optics or reflectors can be difficult at long path length.                                       |
| Meteorological Limitations | Fixed observation area. Long term deployment depends on constant wind direction.   |
|                            | Affected by poor visibility conditions   |
| Limited Compounds          | Many species do not have appropriate UV-visible absorption structures making them undetectable by UV-DOAS                      |
| Application Limitations    | Some bistatic systems are more difficult to use for radial plume mapping due to difficulty aligning optics from multiple paths |



## References

1. Sigrist, M. W. (Eds.). 1994. Air Monitoring by Spectroscopic Techniques. New York, NY: John Wiley & Sons, Inc.
2. U.S. EPA. 2009. Measurement and Monitoring Technologies for the 21<sup>st</sup> Century (21M<sup>2</sup>). Open Path Technologies: Measurement at a Distance UV-DOAS.
3. <http://www.clu-in.org/download/misc/21M2flier.pdf>. Washington, DC.
4. Finlaysson-Pitts, B.J., J.N. Pitts. 1986. Differential Optical Absorption Spectroscopy, from Atmospheric Chemistry; Fundamentals and Experimental Techniques. John Wiley & Sons.
5. Stutz, J., The Stutz Research Group, <http://www.atmos.ucla.edu/~jochen/research/doas/DOAS.html>
6. Opsis AB. 1996. Quality Assurance and Quality Control using Opsis Analyzers for Air Quality Monitoring. Version 1.1. Furulund.
7. Thoma, Eben, Measurement of Total Site Mercury Emissions from a Chlor-alkali Plant Using Open-Path UV-DOAS, EPA/R-07/077, July 2007, <http://www.epa.gov/ord/NRMRL/pubs/600r07077/600r07077.pdf>
8. Pundt, I. 2006. DOAS tomography for the localization and quantification of anthropogenic air pollution. Analytical and Bioanalytical Chemistry, 385 (1) 18-21. doi:10.1007/s00216-005-0205-4
9. US DOE/ORNL. 1999. NARSTO Measurement Methods Compendium.
10. Liptak, B. 2003. Instrument Engineer's Handbook: Process Measurement and Analysis. Chilton Book Company. Radnor, PA.
11. Liptak, B. 1995. Instrument Engineers' Handbook: Process Measurement and Analysis. Boca Raton, FL: CRC Press.
12. Spellicy, R. 2003. IMACC Industrial Monitoring Corporation. Round Rock, TX <http://www.ftirs.com>.
13. ETG Resource Tecnologia. 2007. The UV DOAS SENTINEL System Represents the Most Cost Effective.

## **2.4. Differential Absorption Light Detection and Ranging Systems**

LIDAR is a technology used to measure area source, fugitive or ambient air pollutants without the requirement for line of sight or retro-reflector measurement paths. LIDAR operates on the same principles as radio detection and ranging (RADAR) except light is used rather than radio waves. In early applications of LIDAR, investigators used search lights, a telescope, and a photoelectric light detector to collect information about Earth's atmosphere. The technology was used to determine atmospheric density by studying the backscattered light intensity along the path of the searchlight beam. Since the 1930s, the use of LIDAR has expanded to applications in aerial surveying, three-dimensional imaging, chemical warfare agent detection, and forestry. LIDAR is also used to study atmospheric parameters such as aerosol and cloud properties, temperature, wind velocity, and species concentration.<sup>1,2</sup>

There are three generic LIDAR applications:

- range finders
- Differential absorption LIDAR (DIAL)
- Doppler LIDARs

In 1964, a new LIDAR application called DIAL was proposed to locate and measure trace chemical concentrations in the atmosphere.<sup>1</sup> The goal of LIDAR-based DIAL technique was to precisely measure constituents of ambient air using a simple remote sensing technique that lacked the complexity of traditional optical techniques such as FTIR. Since then, DIAL has developed into a commercially available technology capable of mapping concentrations of multiple atmospheric pollutants.

DIAL uses lasers directed into the atmosphere to measure species concentrations of target aerosols, dust, and gases in the lower few kilometers of the atmosphere. Using the DIAL approach, spatial concentrations are obtained from the reflected or backscattered light from two wavelengths of light: one that is strongly absorbed by the species of interest and the other just outside of the

absorption range of the target compound, which is used to measure background light scattering. As these wavelengths of light are emitted from the laser source, the ratio of the backscattered light intensity between the two wavelengths is measured and coupled with the time delay of the return signal. The target compounds absorb or reflect and scatter the light back to a telescope or receiving optics, where intensity of the backscattered light is detected and evaluated. Concentration is determined based on the amount of light absorbed and the location of the observed compounds is based on the time delay of the backscattered light at the detector.<sup>3</sup> By measuring the backscatter at different angles from the source, the data can be processed to show the two-dimensional plume shape of the target compound emission profile.

The main advantage of DIAL over other ORS technologies is the ability to spatially resolve the concentration of a single compound, or class of compounds, based on the radiation absorption characteristics of the pollutants being measured.<sup>3,4</sup> The ability to spatially resolve concentration data is a unique advantage when compared to alternate remote sensing methods, which yield average concentration data over a predetermined path length. The main limitation in using DIAL is the limited number of wavelengths that can be generated by current laser technology at the precise wavelength for compounds of environmental interest to be monitored. Additionally, the use of DIAL in the United States has been limited due to limited availability and the high cost of the associated equipment.<sup>5</sup>

### **Basic Operation**

LIDAR technology operates by transmitting a laser into a medium containing gaseous compound. The laser light can be transmitted in the UV, visible, or IR wave range.<sup>6</sup> For the DIAL application of LIDAR, an appropriate wavelength is chosen for the species to be measured along with a nearby wavelength that will not be absorbed by the target compound.<sup>7</sup>

During operation, light generated by a laser is directed through a wavelength switching unit. As the laser pulses, the switching unit alternates the laser between the two different wavelengths designated as “on” (the wavelength that is absorbed by the target compound) and “off” (the

wavelength just outside of the target compound's absorption). Some DIAL systems use separate lasers to produce both wavelengths. A continuous laser is used when the measurement range is short or for long measurement time periods. A pulsed laser is used when higher energy is needed for long measurement ranges or short time intervals.<sup>6</sup>

A small portion of the laser output is directed to a calibration cell. The cell is filled with a known concentration calibration gas and the absorption for a given path length is measured. The remaining narrow beam of laser light is expanded or widened to make it "eye safe" and then directed into the atmosphere by a series of mirrors and optics.<sup>7</sup> The expanded laser beam interacts with molecules and particles, and is scattered by them. As the light travels through the atmosphere, the "off" wavelength is scattered elastically by atmospheric particles. The "on" wavelength is absorbed by the target gaseous compound(s) and scattered at a reduced intensity.<sup>3</sup> Light is scattered in various directions and a small portion is reflected back towards its source. This backscattered light is collected, focused, and a detector converts the light information into a digital signal for use in determination of pollutant location and concentration.<sup>7</sup>

DIAL laser systems are chosen based on the absorption characteristics of the compounds under study. Requirements for lasers include low beam divergence, adequately low pulse repetition frequency (PRF), and appropriate wavelength specificity.<sup>1</sup> Capture of the entire beam by the receiving optics is preferable to reduce background noise. A low beam divergence (narrow beam) is necessary to retain the beam in the receiving optics field of view. If a pulsed laser is used, a low PRF ensures measurement cycles are separated by a sufficient length of time to avoid inference from one measurement to the next.

Wavelength specificity defines which compounds can be measured by DIAL systems. Although other applications of LIDAR, such as measuring aerosols, are operated across a range of wavelengths, DIAL wavelengths are specific to the absorption characteristics of the pollutants being measured.<sup>1</sup> Advances in tunable laser technology have allowed simultaneous multi-wavelength, hence multi-component, measurements to be made.<sup>8</sup>

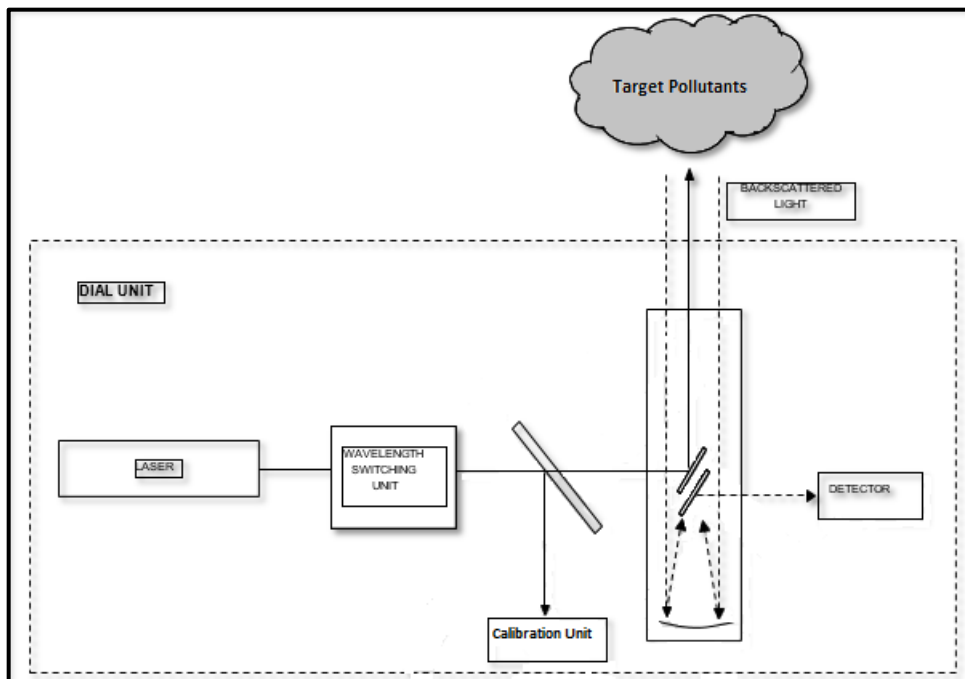


**Figure 2-17. Beam Path and Major Components of DIAL Unit.**

The difference in the backscattered intensity between the “on” and “off” wavelengths allows for a concentration of the compound to be calculated. The “off” wavelength is reflected predictably and decreases in intensity ( $P$ ) by the inverse square of the distance the light has traveled. The two intensities are divided by one another and transformed into concentration data using the Beer-Lambert law.<sup>9</sup> When the time delay of backscattering is added into the calculation, the distance from the laser to the compound can be determined.<sup>3,10,11</sup>

DIAL measurements collect pollutant concentration data over a relatively long path length. Beam path lengths range from a few hundred meters to 3,000 meters.<sup>5</sup> Since DIAL systems do not require a remote detector/reflector, 2-D scans can be completed in approximately 10 minutes.<sup>4,5,8</sup> Pollution emission flux is calculated by collecting wind speed data and plume concentration during DIAL testing. Wind speed is multiplied by the pollutant concentration across the emission plane to obtain a flux value.<sup>3</sup>

Most of atmospheric sensing DIAL systems operate in a monostatic mode where light is emitted and received at the same location. A monostatic mode may be deployed in two sub-configurations; monostatic coaxial mode, where light is received by the same optics through which

it was emitted, and monostatic biaxial mode, where light is received by optics located adjacent to the originating optics. The monostatic system allows multiple measurements to be completed quickly without the need of retro-reflectors or line of site detection systems. Figure 2-18 illustrates the monostatic coaxial and biaxial modes.

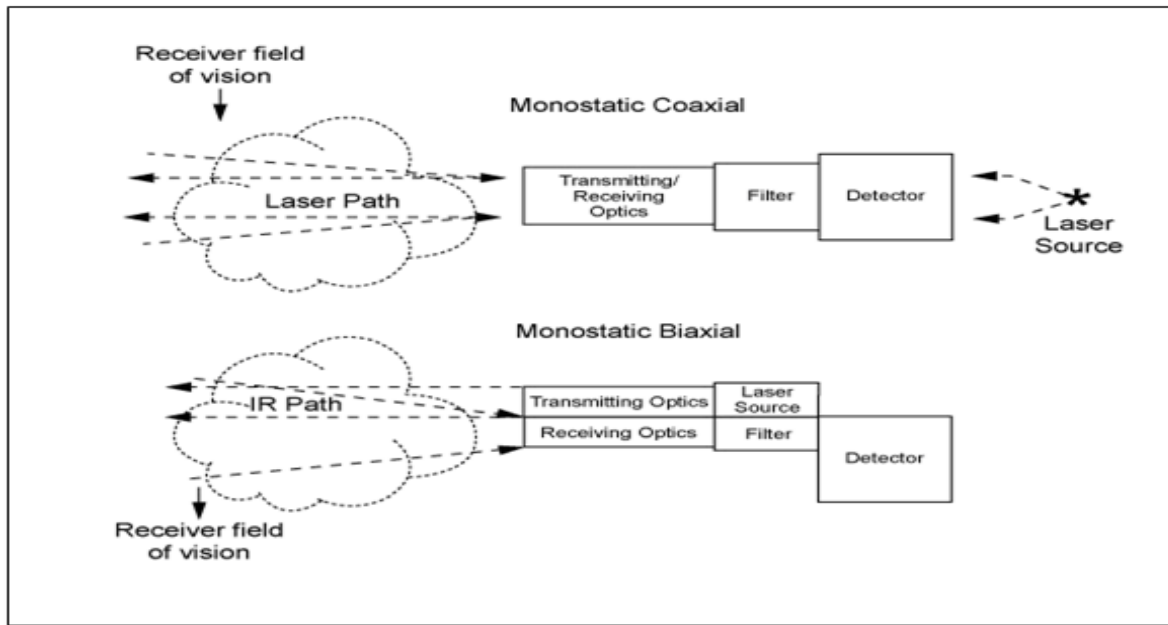


**Figure 2-18. Monostatic Coaxial and Biaxial Configuration for DIAL**

The use of a bistatic DIAL configuration is less common. In bistatic mode light is produced and detected at separate locations. The bistatic configuration requires frequent repositioning of the detector to obtain an emissions concentration profile.<sup>1, 5</sup> Figure 2-19 illustrates a bistatic DIAL system.

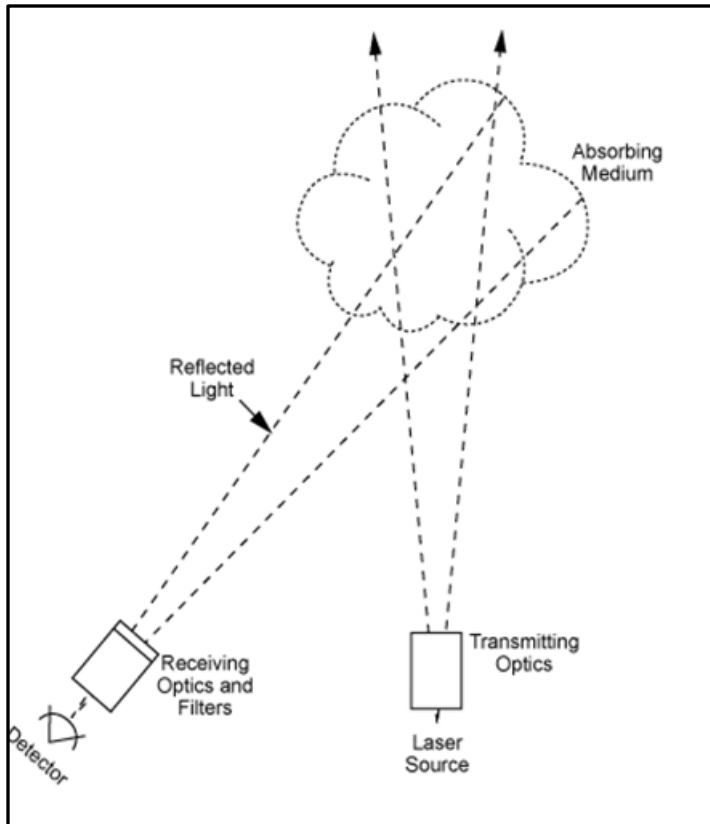


**Figure 2-19. Bistatic Configuration for DIAL**

The signal receiving and detection system consists of primary optics, a spectral filtering unit, a detector, and a photon counter. Receiving optics collect the backscattered light for analysis.

Primary optics vary by application and can include Cassegrain or Newtonian telescopes, multiple small mirrors, and liquid mirror telescopes among others.<sup>1, 6</sup> Spectral filtering systems remove background light and reduce signal noise. Spectral filtering can be accomplished by using simple systems such as narrow bandwidth interference filters or more complicated systems such as depolarization techniques.<sup>1</sup> A detector converts the incoming spectral signal into a digital signal for photon counting. Typical detectors include traditional Photomultiplier Tubes (PMTs), Charge Coupled Devices (CCDs), mercury-cadmium-telluride (MCT) detectors, or avalanche photodiodes.<sup>1, 6</sup> The photon counter performs two steps. The first step removes dark counts, which are a type of signal noise created by the detector. The second step counts the number of photons based on the time they were received. By counting photons on a sequential basis, range resolved measurements are realized.<sup>1</sup>

The DIAL system yields a spatially resolved concentration measurement along the specified path length. Multiple closely spaced scans are often performed over a cross section of an emission plume to produce concentration maps as illustrated in Figure 2-20. This type of output is unique compared to that of measurements such as OP-FTIR spectroscopy, for which the output is a PIC without spatial resolution along the path length.

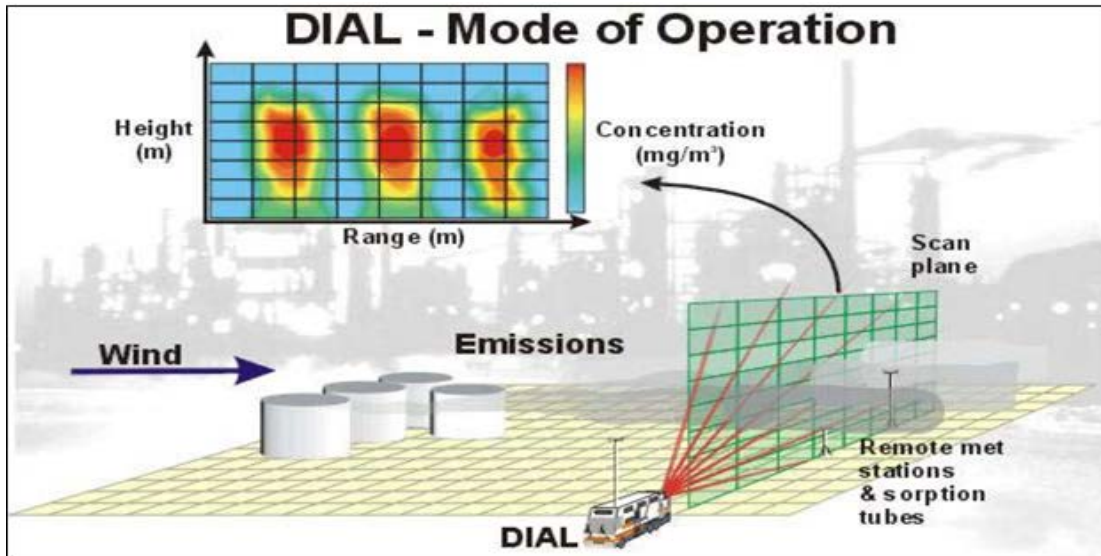


**Figure 2-20. Illustration of DIAL unit mapping an emission plume**

Wind characteristics play a major role in how the DIAL system should be positioned to take measurements, as well as the validity of data obtained from those measurements. Equipment set up is recommended to be at least 50 meters from the plume cross section and measurements should be taken perpendicular to the wind direction. During the measurement period, wind direction may change, which effectively skews the measurement plane.<sup>12</sup> Therefore, wind direction is typically analyzed throughout the measurement process to accurately adjust the measurement plane for skew.<sup>12,13</sup> Changes in wind direction and speed may cause variation in the emission plume over time and affect the results of a scan along a measurement plane, which takes about 10 to 15 minutes to complete. Averaging multiple scans of the same cross section helps to suppress the error associated with a dynamic emission plume.<sup>12</sup> Wind speed analyzed using dual wind monitors typically do not vary more than 20 percent between the independent wind measurements. Wind data from three elevations ranging from 15 to 25 meters, provide sufficient information to determine plume flux through the plane.<sup>14</sup>



**Pollutants and Relative Levels That Can Be Measured**

A variety of atmospheric parameters can be measured with DIAL techniques including: temperature, pressure, water-vapor concentration, and selected atmospheric gases. Additionally, back scatter and light absorption of cloud particles and aerosols can be investigated.

DIAL has historically been used to measure criteria pollutants in the upper atmosphere. Approximately 15 species in the spectral range of ultraviolet to infrared can be detected by DIAL systems. Table 2-19 lists compounds that can be measured with DIAL systems. The list is not all-inclusive but displays compounds reported in literature.

**Table 2-19: Reported Species Measured with DIAL Systems**

|               | Compounds         |                |
|---------------|-------------------|----------------|
| Acetylene     | Hydrogen Chloride | Nitrous Oxide  |
| Alkanes       | Mercury           | Ozone          |
| Benzene       | Methane           | Sulfur Dioxide |
| Ethane        | Methanol          | Toluene        |
| Ethyl Benzene | Nitric Oxide      | Xylenes        |
| Ethylene      | Nitrogen Dioxide  |                |

Detection limits in the ppb range have been reported at distances of 500 to 3000 meters.<sup>6,15</sup>

Detection limits vary based on many factors. Atmospheric effects, such as laser beam wander from atmospheric turbulence, influence the accuracy of DIAL measurements. Laser type and internal instrument noise can also have a negative influence on detection limits.<sup>16,17</sup> The path length also affects the resolution of the system. Reported minimum detection limits range from 0.001 ppb for mercury to 90 ppb for hydrogen chloride gas at a 200-meter absorption path length.<sup>9</sup> Detection limits are given as estimates in Table 2-20 and are based on various absorption path lengths.

**Table 2-20. Approximate Detection Limits for DIAL<sup>6</sup>**

| Compound          | Reported Minimum Detection Limit (ppb) | Detection Range (m) |
|-------------------|--|---------------------|
| Acetylene         | 26                                     | 800                 |
| Alkanes           | 10                                     | 800                 |
| Benzene           | 3                                      | 800                 |
| Ethane            | 16                                     | 800                 |
| Ethylene          | 9                                      | 800                 |
| Hydrogen chloride | 13                                     | 1,000               |
| Mercury           | 0.06                                   | 3,000               |
| Methane           | 76                                     | 1,000               |
| Methanol          | 153                                    | 500                 |
| Nitric Oxide      | 4                                      | 500                 |
| Nitrogen Dioxide  | 5                                      | 500                 |
| Nitrous Oxide     | 56                                     | 800                 |
| Ozone             | 3                                      | 2,000               |
| Sulfur Dioxide    | 4                                      | 3,000               |
| Toluene           | 3                                      | 800                 |
| Xylenes           | 5                                      | 500                 |

The specific wavelength used for detection depends upon the absorption characteristics of the target compounds. The number of identifiable pollutants is further limited by the number of absorbing wavelengths that are unique to a specific compound without additional interferences, as well as the laser technology that is currently available. This technology is improving with expectation that the range of detectable pollutants will expand.<sup>6</sup> DIAL systems can also be used in a mode like a fugitive source monitor. In this mode, an entire class of chemicals can be measured using a single laser wavelength that the entire chemical class absorbs. DIAL results from such a study must be interpreted as an average.

**Typical QA/QC**

While the EPA provides information by general reference in Other Test Method 10 (OTM10)<sup>13</sup>, the verification of DIAL measurements is challenging due to its unique ability to produce spatially resolved concentration data. Limited QA/QC guidelines exist that verify such data in the literature. Information specific to LIDAR technology has been published by the Association of German Engineers (VDI) in VDI 4210 Part 1 (1999) Remote sensing, Atmospheric measurements with LIDAR, Measuring gaseous air pollution with DAS LIDAR.<sup>18</sup>

### **Record Keeping**

As with all environmental measurements, it is necessary to keep accurate records during measurement periods to ensure accurate data collection including records of calibrations, meteorological conditions, path lengths, and measurement times.

### **Instrument Performance**

Initial measurements should be conducted over a period so that emission source fluctuations may be considered during data analysis; one half to an entire day is recommended for an initial measurement.<sup>14</sup> Scanning the same plume over different days and varying conditions is also recommended to assess the impact of varying conditions on measurement results.<sup>12</sup> An initial site assessment should also be conducted to determine any interference that may disrupt data acquisition. Interferences include geographic constraints and off-site upwind emissions sources.<sup>13</sup>

Some DIAL systems are programmed with verification systems to ensure that quality measurements are taken. One reported DIAL system employs an internal “wavelength” verification system, known as a wavemeter, to identify and dispose of any data produced from the emission of an inconsistent wavelength.<sup>8</sup> This prevents erroneous data from being produced if the light source emits radiation outside of the specified wavelength.

### **Example Applications and Vendors Applications**

With the ability to develop spatial concentration information of air pollutants, DIAL systems have been implemented in a variety of applications including fence line monitoring, fugitive emissions measurement, and plume fate analysis. DIAL may also be used to measure flare efficiency from industrial processes.<sup>5,11</sup> For each application, the strengths and limitations of a DIAL system must be considered to produce results that meet users' DQOs. For example, the use of CO<sub>2</sub> laser assumes sufficient aerosol concentration in the atmosphere to provide sufficient backscatter. High wavelength visible and UV light sources rely on molecular backscatter.

**Table 2-21. Typical Applications for LIDAR.**

| TECHNOLOGY | APPLICATIONS |
|------------|--------------|
| LIDAR      | DIAL         |

DIAL systems are either in a fixed or mobile arrangement. Fixed DIAL units used in laboratories are typically less complicated than mobile systems used for field operation.<sup>9</sup> Many mobile systems have been constructed based on an enclosed truck platform. The truck is driven to the testing site and positioned accordingly to obtain emissions data.<sup>3, 7, 19</sup> DIAL systems have also been implemented onboard ocean vessels and in airborne systems, collecting emissions information while flying over a target area.<sup>11, 20</sup> Figure 2-21 illustrates a truck-based mobile DIAL platform.



**Figure 2-21. Mobile DIAL Unit**

Specific field implementation examples include studies completed on gas processing plants and oil refineries. These studies used DIAL systems and plume mapping techniques in Canada and European nations. Measured fugitive emissions were four to 20 times greater than factor estimated fugitive emissions.<sup>5,6,14,21</sup> While these studies have concluded emissions factors may underestimate actual fugitive emissions, objection to using annual emissions figures calculated by DIAL measurements is apparent. Industry objects to using DIAL-based calculated emissions due to the short time-period of measurement relative to the long time-period of annual operation.<sup>6</sup>

In other studies, DIAL systems have been implemented to measure emissions from mobile sources such as air and highway traffic. Additional DIAL systems have been developed to detect chemical warfare agents as well as natural gas pipeline leaks from airplane mounted platforms<sup>6</sup>

**Vendors**

Many vendors manufacture laboratory-scale DIAL applications; however, field-ready measurement instruments are only offered by a small number of vendors. Table 2-22 lists vendors that manufacture or provide field-ready DIAL instruments.

**Table 2-22: DIAL Vendors**

| Vendors                      |   |
|------------------------------|---|
| Spectrasyne                  | <a href="http://www.spectrasyne.ltd.uk/">http://www.spectrasyne.ltd.uk/</a> |
| LASEN                        | <a href="http://www.lasen.com/">http://www.lasen.com/</a>                   |
| National Physical Laboratory | <a href="http://www.npl.co.uk/">http://www.npl.co.uk/</a>                   |
| ITT                          | <a href="http://www.itt.com/">http://www.itt.com/</a>                       |

**Strengths and Limitations**

A significant limitation of DIAL technology is the cost and limited availability of the measurement service. Multiple measurements in North America have relied on importing the instrumentation from the United Kingdom<sup>12,15,21</sup> Additionally, the number of chemical species measurable by DIAL is restricted to the unique absorption characteristics of those species and the availability of laser technologies able to produce the absorption wavelengths.

The most notable strength of a DIAL system is the ability to spatially resolve pollutant concentration information in three dimensions in a short period of time. Concentration gradient data obtained in short periods of time enables DIAL to be deployed in many applications and many configurations. DIAL has been used in scenarios from ground-based emissions plume monitoring to helicopter and fixed-wing aircraft aerial surveys. Table 2-23 and Table 2- 24 summarize the strengths and limitations of DIAL systems.

**Table 2-23: Summary of the DIAL Strengths**

| <b>Feature</b>                           | <b>Strength</b>  |
|--|--|
| Concentration data is spatially resolved | In contrast to PIC measurements taken by other instrumentation system, DIAL relay concentration data as a function of distance along the beam path   |
| Beam Path                                | Reported path lengths up to 3000 meters  |
| Receiving Optics                         | Collects backscattered light without the use retro- reflectors   |
| Measurement Time                         | Scan along measurement plane requires 10 to 15 minutes   |
| Mobile Platform                          | Instrumentation is moved around measurement site obtaining multiple plume scans from various locations increasing accuracy of plume characterization |
|  | Instrumentation can also be mounted on airborne platform for increased mobility and expanded applications  |
| Near Real Time Data                      | Real time data allows for leak identification and inputs to process change decisions   |
| Multi-Wavelength Operation               | Allows for simultaneous concentration measurements of multiple species and classes of species  |

**Table 2-24: Summary of the DIAL Limitations**

| <b>Feature</b>                           | <b>Limitation</b>  |
|--|--|
| Unique Chemical Absorption Bands         | Measurable species are limited to those with unique absorption bands. Chemical species with common absorption characteristics can only be measured as classes of compounds   |
| Chemical Species Absorption Dependencies | The absorption wavelengths of species are temperature and pressure dependent. It is necessary to check the applicability of wavelengths selected for measurement based on temperature and pressure variation in target absorption. |
| Backscatter Requirements                 | Sufficient aerosol or molecular material must be in the atmosphere to create sufficient backscatter  |
| Wind speed and direction                 | Rapidly changing wind speed or direction may cause measurements to change rapidly and may affect mixing ratios of measured surrogates to compounds of interest.  |
| Vendors                                  | Small number of vendors providing DIAL systems and services  |
| Expense                                  | High system cost has limited to amount of commercial DIAL studies in the United States   |

## References

1. Argall, P. and R. Sica. 2002. LIDAR in the Encyclopedia of Imaging Science and Technology. Ed. J.P. Hornak. John Wiley & Sons Inc. New York, NY.
2. Moskal, L., T. Erdody, A. Kato, J. Richardson, G. Zheng, and D. Briggs. 2009. Lidar Applications in Precision Forestry. <[http://depts.washington.edu/rsgal/pubs/Moskaletal\\_Silvilaser2009.pdf](http://depts.washington.edu/rsgal/pubs/Moskaletal_Silvilaser2009.pdf)>.
3. Edner, H., K. Fredriksson, A. Sunesson, S. Svanberg, L. Uneus, and W. Wendt, W. 1987. Mobile remote sensing system for atmospheric monitoring. Applied Optics. 26(19): 4330-4338. doi:10.1364/AO.26.004330.
4. SIRA, Ltd. 2004. Recommendations for best practice in the use of open-path instrumentation. <<http://www.spectrasyne.ltd.uk/BestPractisev13.pdf>>.
5. U.S. EPA. 2006. VOC Fugitive Losses: New Monitors, Emission Losses, and Potential Policy Gaps – 2006 International Workshop.
6. <[http://www.epa.gov/ttn/chief/efpac/documents/wrkshop\\_fugvocemissions.pdf](http://www.epa.gov/ttn/chief/efpac/documents/wrkshop_fugvocemissions.pdf)>
7. U.S. EPA. 2009. Measurement and Monitoring Technologies for the 21<sup>st</sup> Century (21M<sup>2</sup>). Open Path Technologies: Measurement at a Distance UV-DOAS.
8. <<http://www.clu-in.org/download/misc/21M2flier.pdf>>.
9. Fredriksson, K., B. Galle, K. Nyström, and S. Svanberg. 1981. Mobile lidar system for environmental probing. Applied Optics. 20(24): 4181-4189.
10. Weibring, P., H. Edner, and S. Svanberg. 2003. Versatile mobile lidar system for environmental monitoring. Applied Optics. 42(18): 3583-3594. doi: 10.1364/AO.42.003583.
11. Sigrist, M. W. (Eds.). 1994. Air Monitoring by Spectroscopic Techniques. New York, NY: John Wiley & Sons, Inc.
12. Spectrasyne, Ltd. 2007. The Technique.
13. <<http://www.spectrasyne.ltd.uk/html/technique.html>>.
14. Weibring, P., H. Edner, S. Svanberg, G. Cecchi, L. Pantani, R. Ferrara, and T. Caltabiano. 1998. Monitoring of volcanic sulfur dioxide emissions using differential absorption lidar (DIAL), differential optical absorption spectroscopy (DOAS), and correlation spectroscopy (COSPEC). Applied Physics B: Lasers and Optics. 67(4): 419- 426. doi:

10.1007/s003400050525.

15. Chambers, A. 2003. Well Test Flare Plume Monitoring Phase II: DIAL Testing in Alberta. Alberta Research Council Inc. Prepared for Canadian Association of Petroleum Producers. <<http://www.ptac.org/env/dl/envp0402fr.pdf>>.
16. U. S. EPA. 2006. Other Test Method (OTM) 10 Optical Remote Sensing for Emission Characterization for Non-Point Sources. <<http://www.epa.gov/ttnemc01/prelim.html>>.
17. Frisch, L. 2003. [Fugitive VOC-Emissions Measured at Oil Refineries in the Province of Västra Götaland in South West Sweden - A Success Story: Development and Results 1986 - 2001](#). County Administration of Västra Götaland, Report No. 2003:56.
18. Chambers, A., M. Strosher, T. Wootton, J. Moncrieff. and P. McCready. 2008. Direct measurement of fugitive emissions of hydrocarbons from a refinery. Journal of the Air and Waste Management Association. 58: 1047-1056. doi: 10.3155/1047- 3289.58.8.1047.
19. Fredriksson, K. A. 1985. DIAL technique for pollution monitoring: improvements and complementary systems. Applied Optics. 24(19): 3297-3304. doi: 10.1364/AO.24.003297.
20. Ahmad, S. R. 1997. Application of lidar to atmosphere pollutant mapping: a review. Proceedings of the SPIE. The International Society for Optical Engineering. doi: 10.1117/12.283904.
21. VDI 4210 Part 1. 1999. Remote sensing, Atmospheric measurements with LIDAR, Measuring gaseous air pollution with DAS LIDAR.



## ***2.5 Thermal Infrared Cameras***

Thermal infrared (IR) cameras that are used for environmental measurements come from a class of camera known as thermographic or forward-looking IR, which use IR radiation to form an image in a manner like the way photographic cameras use visible light. The original thermal IR camera development was funded largely by the astronomy and defense communities for the purposes of “night-vision” for aircraft and other vehicles and development of heat-seeking missiles.<sup>1</sup> Private companies have adapted military IR technology that does not require sophisticated cooling or optics to produce commercial IR cameras for environmental applications.

IR cameras are useful for a wide range of applications, including to monitor watershed temperature in game habitats, to detect energy loss or insulation defects in buildings, to detect biomedical abnormalities, to track and aid in target acquisition by the military, to improve piloting of aircraft in low visibility conditions, to pinpoint ignitions sources during firefighting, and to aid in search and rescue operations of missing persons.

Environmental applications of IR cameras include the detection of industrial gas leaks that are invisible to the naked eye. By filtering incoming light to permit only regions of IR radiance characteristic of hydrocarbon or volatile organic compound (VOC) gases to reach the camera’s detector, the IR video camera allows the user to see images of hydrocarbon gases on the camera screen in real time.<sup>2</sup> These cameras can identify the source and flow path of escaping gases in a wide variety of applications,<sup>3</sup> such as tank vents and gas line leaks.

The major advantages to using the thermal IR camera for leak detection are the technology’s portability and its qualitative ability to display a wide field of view that allows major leaks to be detected more efficiently than classical leak detection and repair procedures that require each equipment component to be tested individually. Additionally, IR camera technology allows leak detection in parts of facilities that may be difficult or hazardous for personnel to access. The thermal IR camera’s major drawback is its inability to measure the quantity or concentration of gas present in a gas plume. A second limitation is the technology’s inability to identify individual chemicals in a complex gas leak mixture due to the simple optics employed in portable IR cameras. A third limitation is the technology’s inability to detect leaks when the background temperature is the same as the gas temperature. A fourth limitation is the

technology's inability to detect leaks when ambient wind conditions are stronger than a moderate breeze.

### **Basic Operation**

All objects that have a temperature above absolute zero (or 0 Kelvin) have a thermal profile by emitting IR radiation. In the case of IR cameras designed for the visualization of hydrocarbon gases, a special band-pass optical filter is placed between the outer lens optic (made of optically-transmissible germanium) and a focal plane array (FPA) detector that allows only IR radiation in the range of about 3.2 to 3.4 micrometers ( $\mu\text{m}$ ) to pass to the detector (Figure 2.22).<sup>4</sup>

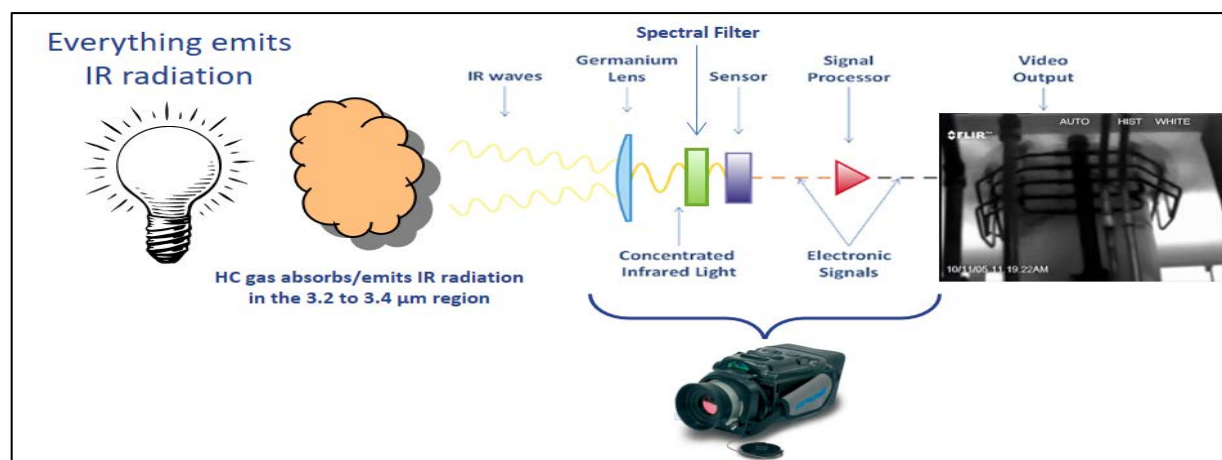


**Figure 2.22. Overview of Thermal IR Camera Technology Basics.**

The detector passes along the information as an electrical signal that is then processed by the camera software to produce a live video image of the thermogram. The thermogram is an image of the thermal radiation in the field of view and will display normally invisible gas emissions on the camera's screen as a clouded area or smoke in real time, as shown in Figure 2.23.<sup>10</sup> If the IR camera is set to display hotter areas on a thermogram as whiter than the cooler areas in black and white, then a gas plume that is colder than the surrounding background will appear like a dark cloud or smoke. If the opposite is true and the gas is hotter than the background, then the gas plume will appear lighter like a white cloud or steam. The presence of hydrocarbon gas in the thermogram are represented as a change in heat, similar to how a shadow with a normal camera represents a change in visible light.<sup>4-9</sup>

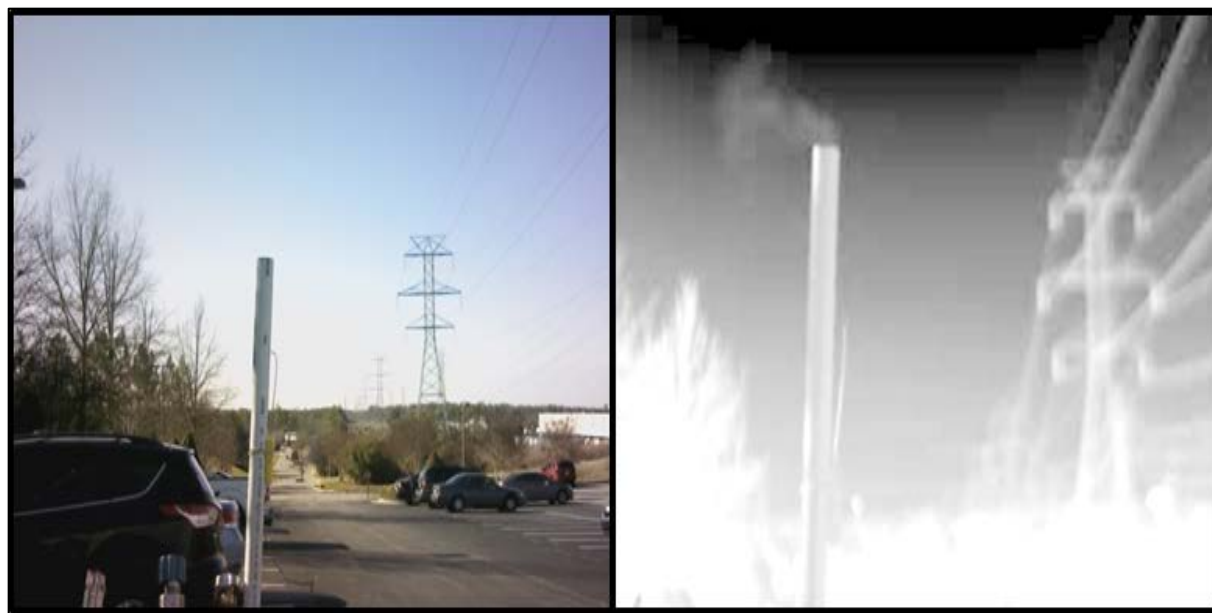


**Figure 2.23. Image of a Controlled Gas Release where the Gas is Warmer than the Background.**

The IR gas sensing camera creates images based on the IR absorption/emission characteristics of chemical species within the camera's field of view. IR detection typically occurs in the 3 – 5  $\mu\text{m}$  wavelength range for hydrocarbon gases,<sup>11</sup> but the special lens and filter arrangements represented by the spectral filter in Figure 2.22 are used to narrow the IR spectrum of wavelengths detected to about 3.2 to 3.4  $\mu\text{m}$ , thereby allowing the camera to image specific compounds or compound classes that have electromagnetic signatures in that region.<sup>12</sup> Other wavebands are available in different camera models ranging from 1 to 14  $\mu\text{m}$ . For example, 3.2 to 3.4  $\mu\text{m}$  is used for hydrocarbon detection, 4.52 to 4.67  $\mu\text{m}$  is used for carbon monoxide detection, 8.0 to 8.6  $\mu\text{m}$  is used for the detection of refrigerant gases, and 10.3 to 10.7  $\mu\text{m}$  is used for sulfur hexafluoride and anhydrous ammonia detection.<sup>13</sup>

Each chemical compound has a unique response to radiation from the electromagnetic spectrum based on the rotational and vibrational energy transition characteristics of the bonds in each molecule to generate rotating and vibrational “ro-vibrational” spectra. For example, many hydrocarbon molecules are electromagnetically active in the 3.2 to 3.4  $\mu\text{m}$  range due to the structure of the carbon-hydrogen bonds. One such chemical, propane, is a short chain of three carbon atoms with single bonds to each other and to hydrogen atoms (as shown in Figure 2.24). Figure 2.24 also shows the areas where the propane molecule has the greatest amount of IR absorbance by the peaks in the blue line. Over the IR spectrum (1 to 14  $\mu\text{m}$ ), propane has its

highest peak in the 3.2 to 3.4  $\mu\text{m}$  region with a secondary peak around 6.5 to 7.5  $\mu\text{m}$ . This indicates that targeting one of these two bandwidths (but especially the primary peak) with the optics of the IR camera should result in the detection of propane, assuming there are no gases that may cause interference.

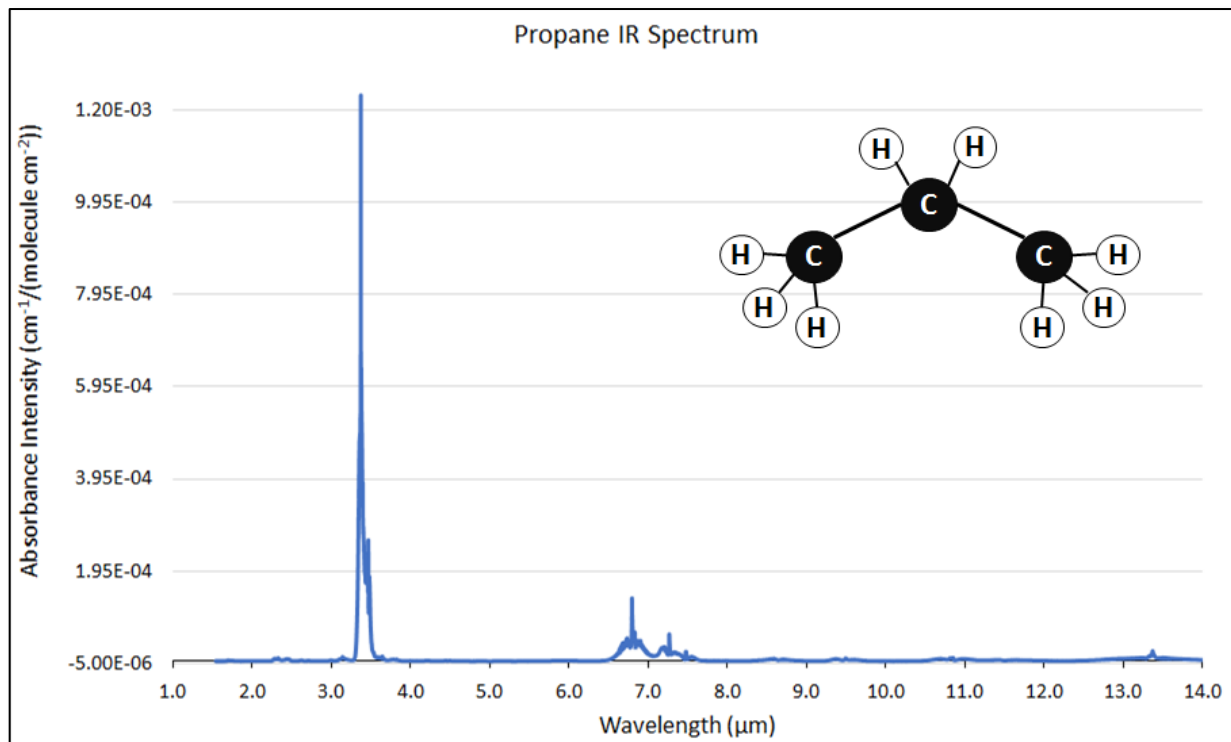


**Figure 2.24. IR Spectrum for Propane with the molecule Bond Structure (not to Scale).**

An IR camera that targets the detection of hydrocarbon gases and has optics that focus the imaging bandwidth to the 3.2 to 3.4  $\mu\text{m}$  region will have an optical window of transmission like that presented in the top left panel of Figure 2.24.<sup>14</sup> The top middle panel of Figure 2.25<sup>14,15</sup> illustrates the IR camera window of transmission overlaid with the propane spectrum and the top right panel is the same but with the spectrum for methane. All three curves are represented in the bottom panel of Figure 2.25 to illustrate that, although each curve will be different, if the compound absorbs IR radiation in the window of transmission for the camera, then the IR camera should theoretically be able to detect and make visible the gas emission of that compound.

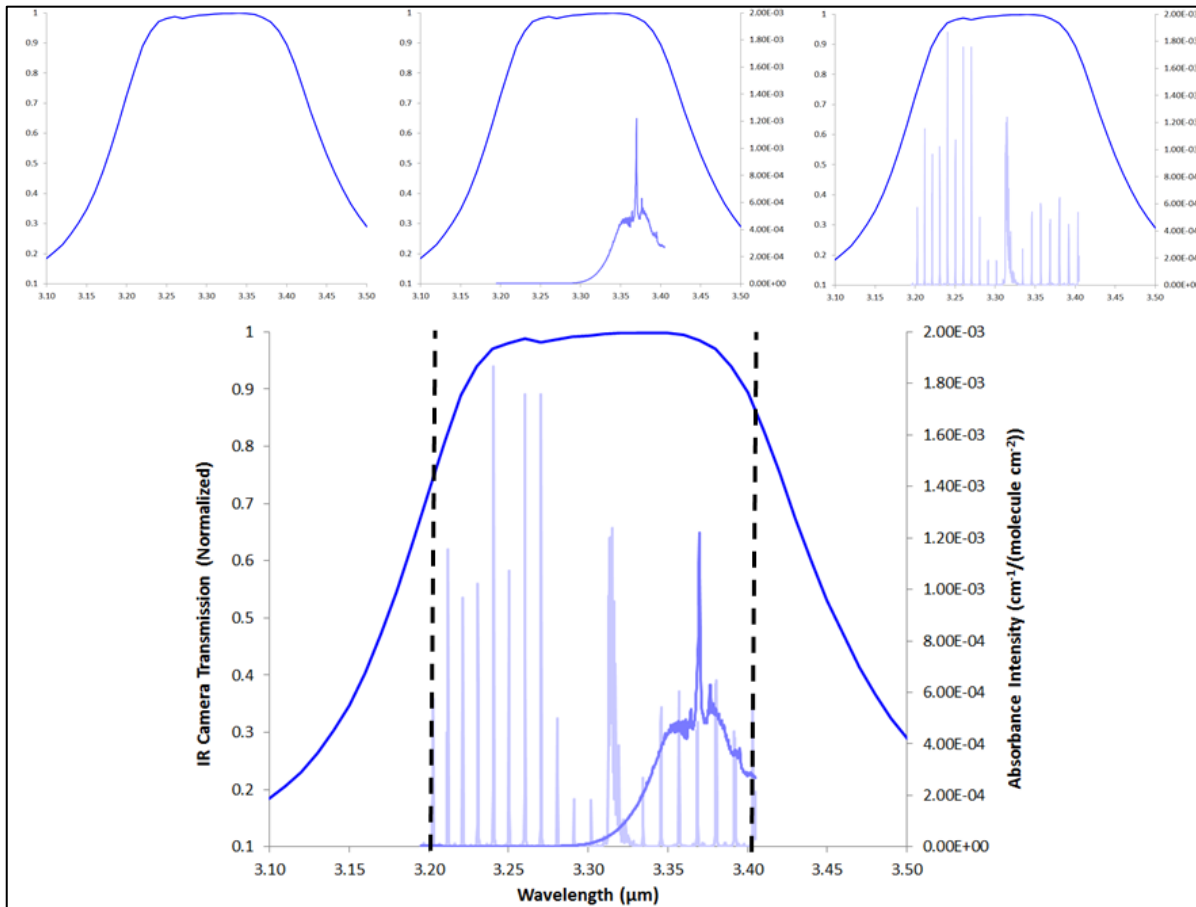


**Figure 2.25. Spectral curves for (top Left) an IR Camera Window of Transmission, (Top Middle) a Propane Spectral Curve, (Top Right) a Methane Spectral Curve, and (Bottom) All Three Curves put together with the Dashed Line Indicating the 3.2 – 3.4 Region.**

It is expected that, if the IR camera window of transmission and a major peak in the IR spectrum of a compound overlap, then the IR camera will be able to image a gaseous fugitive emission of that compound. However, several factors affect the IR camera's imaging and, therefore, the sensitivity of the technology. These are:

- **Ambient thermal energy** plays an important role in the sharpness or resolution of the IR camera's image.
- **Variations in the thermal profile** of the image (called a thermogram) can require that any of a number of settings be adjusted, such as focusing the lens, changing the viewing angle, adjusting the temperature range setting, and switching between automatic and high sensitivity (or enhanced) camera modes to ensure no leaks were missed.<sup>12</sup>

- **The IR camera's leak detection sensitivity** is affected by the temperature of the target gas and the equipment surface and/or surrounding background in the field of view.
- **Reflectivity** (reflection of IR light) and emissivity (emission of thermal energy due to the absorbance of IR radiation) of surrounding materials also play a role in the camera's sensitivity.
- **Gas concentration, distance from the leak source, leak pressure**, play a role in the ability to measure using this technology.
- **Meteorology**, such as cloud cover, and wind speed and direction.<sup>16</sup>

It is possible under certain conditions that the thermal radiance of the leaking gas and the background are equal. Because the camera uses the temperature differentials to image a gas plume, the leak will be invisible to the IR camera and, therefore, the operator under these conditions. The temperature differential between the target gas and the background is commonly called  $\Delta T$  ("delta-T") and is a major influence on the sensitivity of the IR camera.<sup>4,13,15</sup> Proper IR camera operator training is required to ensure each of these factors are considered during leak detection surveys to make sure all possible leaks or vapor clouds are detected.<sup>10</sup>

The operation of an IR camera is straightforward. At start up, the IR camera must be allowed to reach operating temperature since the camera's detector is cooled by a Stirling engine to reduce analytical noise. This start-up process takes an average of about 8 to 10 minutes to complete, depending on the conditions of the surrounding environment. An additional wait of 10 to 15 minutes after the camera has reached the cooling set point is suggested to allow for thermal stabilization. At this point, it is recommended that the operator perform a non-uniformity correction (NUC) to spatially homogenize the detector response to thermal differences.

IR camera models' basic operation modes can include additional contrast adjustments allowing easier visualization of leaking gaseous compound against the stationary backgrounds. There are three potential modes on any given IR camera: Auto or Normal mode, Manual mode, and High Sensitivity (HSM) or Enhanced (ENH) mode. As the name implies, Auto or Normal mode is like the Auto mode on a digital camera where software algorithms optimize the image display;

in the case of IR cameras, this is based on a histogram evaluation of the thermogram in the field of view. Manual mode indicates the ability to adjust the brightness and contrast (called level and span, respectively) of the image output. This mode is useful when the temperature of the target gas is in the bulk of the histogram and not easily distinguishable from the thermal profiles of other objects in the surrounding scene. An example is the presence of a very hot object that skews the histogram to one extreme and effectively “washes out” the objects with a thermal profile on the opposite end. Instead of using Manual mode, it is often the preference of IR camera operators to use the HSM or ENH mode almost exclusively.

The HSM/ENH mode is executed differently by each individual manufacturer, but, basically, algorithms in the camera software can perform a type of scene-subtraction whereby the camera display results in only those objects that are time-dependent. For example, if the only object moving in a scene is the escaping gas, then the HSM/ENH mode highlights only those gas pixels that have changed over a series of frames. The camera operator can control how many frames are included in the analysis, thereby increasing the camera sensitivity by increasing the number of frames. The highest settings for sensitivity come at the cost of image object resolution, potential interference, and larger file size. Because this mode can greatly enhance the sensitivity of the IR camera, it is common that heat convection and the various phase changes and air mass transportations related to heat are imaged. Frequent examples of this interference are water evaporation, heat convection from hot or cold objects relative to the ambient temperature, and water sublimation. There is also a training or warm-up period associated with using HSM/ENH mode where the operator’s brain needs some time to become accustomed to the features of the HSM/ENH images. Just like an athlete must practice a certain skill to learn the skill and then warm-up before using the skill during a sporting event, so too should the IR camera operator practice and warm-up before surveying with an IR camera.<sup>10</sup>

Operators are trained to scan each piece of relevant equipment or area of potential leaks from one end to another, pausing frequently on each new scene of equipment to detect time-dependent changes, and to perform the scan from a minimum of two different viewing angles or locations relative to air flow or wind direction to ensure all leaks are detected.<sup>2</sup> The first field of view is often from a wider angle with a larger viewpoint, while the second field of view

is at a closer viewing angle. The same areas can be scanned repeatedly to improve the likelihood that all leaks are detected.<sup>12</sup>

The images collected by modern IR cameras are digital. Even older IR cameras generated a video feed that was recordable and allowed archiving for remote viewing and review. The cameras can operate using battery power for up to eight hours of continuous use, or connected to AC power for 24-hour monitoring purposes.<sup>8</sup> Additionally, IR cameras used for vehicle inspections have been adapted to use a 12-volt power source. Some IR cameras are available with global positioning systems (GPS) to automatically record the location of the camera's use.<sup>9</sup>

If quantification of a leaking gas is required, it is also possible to couple the IR camera with additional technology, such as a passive FTIR system, different optical elements, modeling software, or more traditional leak detection and repair instrumentation such as a portable instrument meeting EPA Method 21 requirements or mass flow measurement using a bagging technique. Coupling the IR camera with another technology not only provides means for quantification, but can verify a detected leak as well as determine its chemical composition.<sup>5</sup>

### **Pollutants and Relative Levels That Can Be Detected**

Thermal IR cameras can be designed to detect chemical compounds that have absorptions anywhere in the 1 – 12  $\mu\text{m}$  wavelength IR absorption range. Typically, the 3 – 5  $\mu\text{m}$  wavelength range is used for organic VOC. Depending on a variety of factors, including lens focal point,<sup>17</sup> distance from the source, and meteorological conditions, gaseous compound concentrations in the hundreds of ppm range (> 500 ppm) or leaks above an emission rate of about 12 grams per hour (g/hr) are detectable by the camera.<sup>4,5</sup> Table 2-25 provides a list of example compounds that have been detected using IR cameras with different wavebands. This list is not all-inclusive, but shows that many compounds can be detected with the technology.



**Table 2-25. List of Example Gaseous Compounds that can be Detected by Thermal IR Cameras at Different Wavebands**

| 3.2 – 3.4 $\mu\text{m}$ | 4.52 – 4.67 $\mu\text{m}$ | 10.3 – 10.7 $\mu\text{m}$                 |
|-------------------------|---------------------------|---|
| 1-Pentene               | Carbon Monoxide           | SF <sub>6</sub> (Sulfur Hexafluoride)     |
| Benzene                 | Nitrous Oxide             | Acetic Acid                               |
| Butane                  | Ketene                    | Anhydrous Ammonia                         |
| Ethane                  | Ethenone                  | Chlorine Dioxide                          |
| Ethanol                 | Butyl Isocyanide          | Dichlorodifluoromethane "FREON-12"        |
| Ethylbenzene            | Hexyl Isocyanide          | Ethyl Cyanoacrylate "Superglue"           |
| Ethylene                | Cyanogen Bromide          | Ethylene                                  |
| Heptane                 | Acetonitrile              |   |
| Hexane                  | Acetyl Cyanide            | <b>8.0 – 8.6 <math>\mu\text{m}</math></b> |
| Isoprene                | Chlorine Isocyanate       |   |
| MEK                     | Bromine Isocyanate        | R404A                                     |
| Methane                 | Methyl Thiocyanate        | R407C                                     |
| Methanol                | Ethyl Thiocyanate         | R410A                                     |
| MIBK                    | Chlorodimethylsilane      | R134A                                     |
| Octane                  | Dichloromethylsilane      | R417A                                     |
| Pentane                 | Silane                    | R422A                                     |
| Propane                 | Germane                   | R507A                                     |
| Propylene               | Arsine                    | R143A                                     |
| Toluene                 |                           | R125                                      |
| Xylene                  |                           | R245fa                                    |

### **Typical QA/QC**

Maintenance records should be kept for any equipment adjustments or repairs that could affect measurement performance. Records should include the date and description of maintenance performed. When the instrument is turned on, it must be allowed to warm up to the manufacturer's recommended operating temperature and the duration of this initial period should be regularly noted in the instrument logbook. Once at the appropriate temperature, the camera can be used to scan a known concentration of a detectable gaseous compound or the butane from a standard BIC® lighter to demonstrate that the IR camera is producing a visible image.<sup>4,12</sup>

When a leak is detected, a video record should be taken from an angle and distance that promotes optimum leak visibility. The video should be at least 10 seconds long and stored with a unique video tag.<sup>2</sup> Information about the leak (such as component type, model or style of component, service, size, process unit, process stream, pressure, vent location and ambient or

process temperature<sup>18,19</sup>) should also be entered into a log sheet to further document the leak.<sup>12</sup> For leak detection and repair (LDAR) applications, once the leak has been identified, the leaking component should be marked with a leak detection ID tag so that it can be easily identified by maintenance and then repaired.<sup>2</sup> For vents, tanks or other major gas emissions detected by the IR camera, the GPS location and a visible light photograph should be used to document the observation.

Although no prescribed method exists, a couple theories have proposed the unbiased evaluation of thermal camera performance using pixel intensity values. The first theoretical method described is based on a white paper from Dr. Yousheng Zeng,<sup>20</sup> and the second is based on the noise equivalent temperature difference (NETD) method used to quantify the thermal sensitivity of a thermal imager called the noise equivalent concentration length (NECL)<sup>21</sup> for a gas leak imager. Detailed discussion of these theories is available in reference 13, however, a summary of these methods is provided below.

An experimental configuration where the filling optical gas cells in front of a controlled background with a known concentration of test gas (Figure 2.26<sup>4</sup>) yields a pixel intensity response is the keystone of Dr. Zeng's white paper method. A daily operations quality control chart (Figure 2.27<sup>20</sup>) is developed by measuring the change in pixel intensity of the camera response to the gas concentration in the test cells over different  $\Delta T$  set points. Similarly, by repeating the intensity measurements over different  $\Delta T$  set points with different concentrations can help to define a pixel intensity change over various concentration-path lengths for a specific gas and camera model.

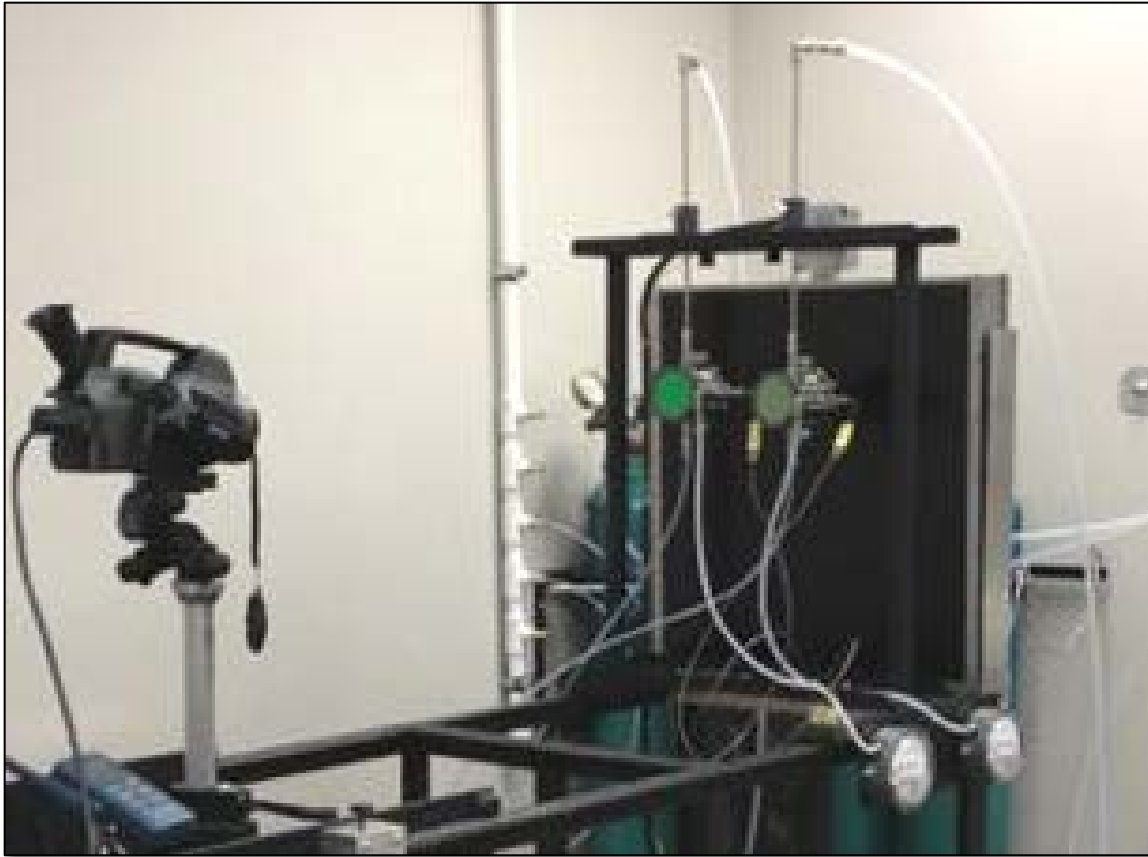


Figure 2.26. Calibration/Verification Example Configuration, with IR Camera, Test Cells, Temperature-Controlled Background, and a Gas Delivery System.

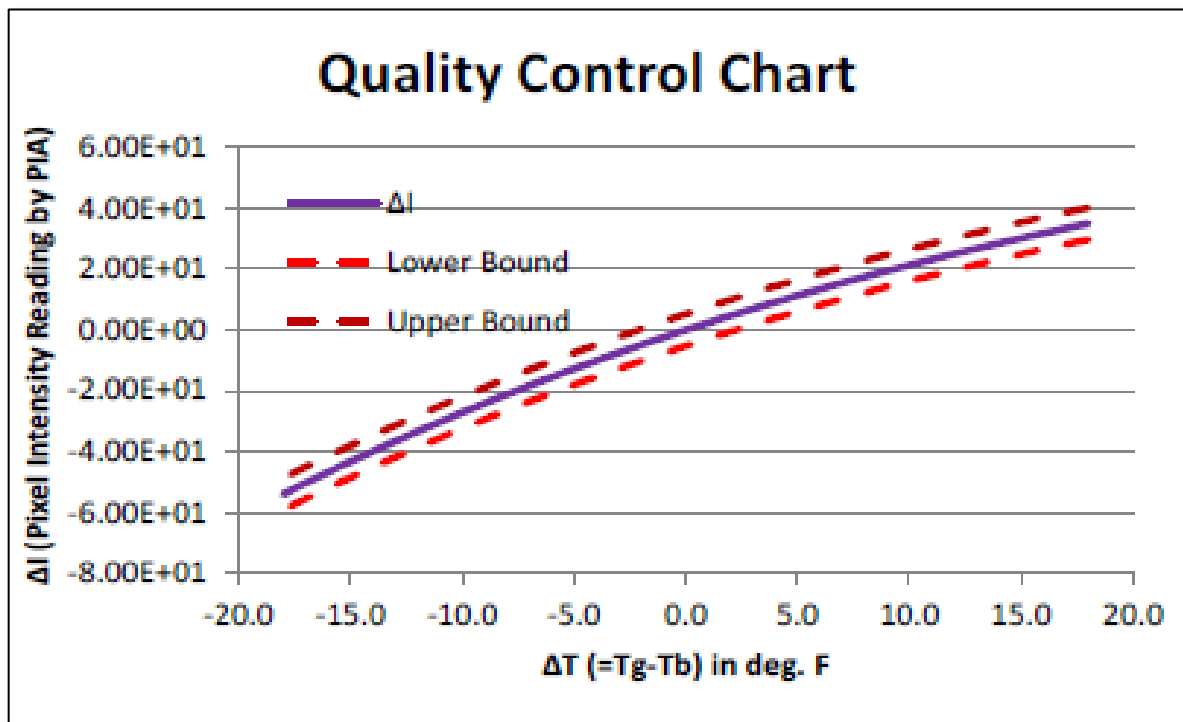
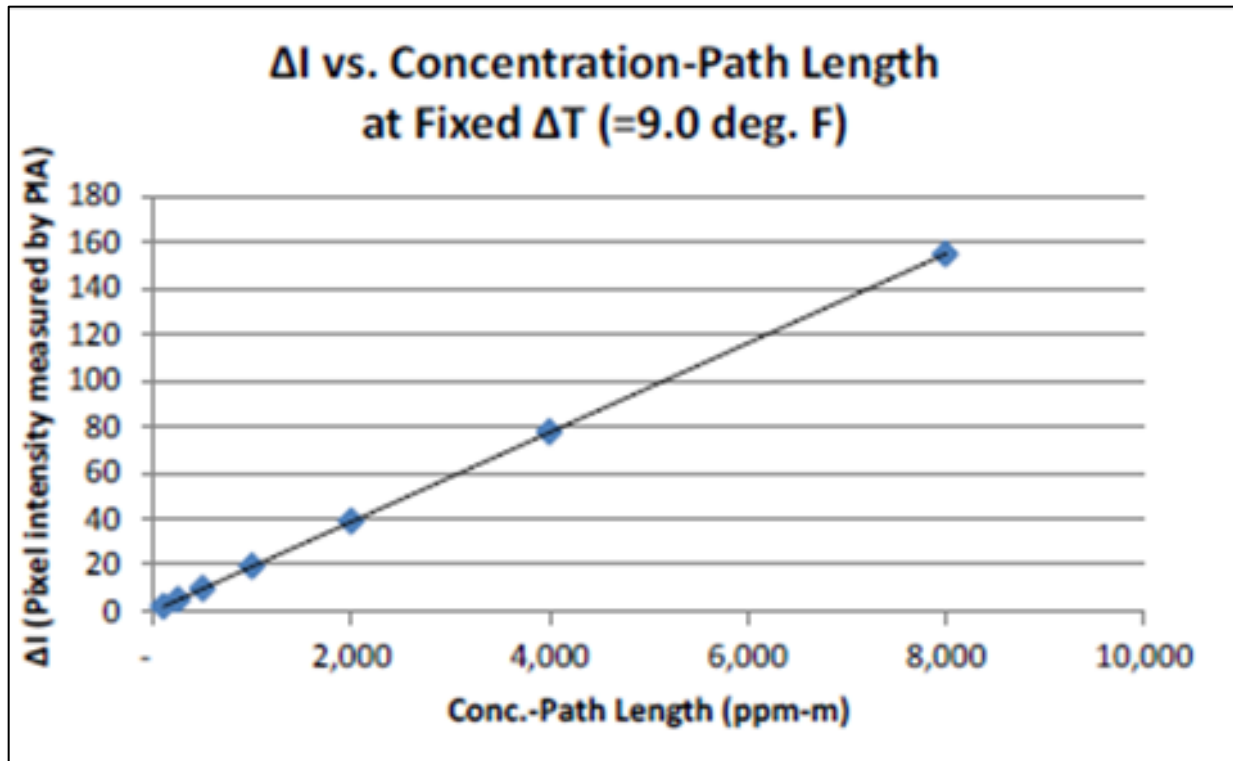


Figure 2.27. Example Quality Control Daily Operations Check Chart with Performance Boundaries.



**Figure 2.28. Anticipated Change in Pixel Intensity for various concentration-path lengths at a Specific  $\Delta T$ .**

The objective of the NECL method is to allow for the unbiased comparison of various OGI camera sensitivities from different suppliers. By developing absorption curves that describe an OGI camera response to set conditions (like the Zeng method), the NECL method uses these absorption curves to calculate a single number that describes the minimum concentration-path length that would be detectable above the baseline noise level. The proposed standardized conditions for developing the absorption curve of a camera for comparison are:

- $\Delta T = 10^{\circ}\text{C}$ .
- The OGI camera to be tested is set up 1.0 m from the gas cell.
- After the line of best fit is optimized through the data, the NECL is evaluated at a concentration-path length (CL) = 0 ppm·m.<sup>21</sup>

The line of best fit through the experimental absorption curve data is extrapolated to CL = 0 ppm·m to yield the minimum concentration-path length (NECL) that is multiplied by the optical thickness of the gas plume (path length) to result in the minimum concentration that is theoretically detectable for that OGI camera. For example, the authors of the study<sup>21</sup>

determined that 13 ppm·m is the NECL for methane using a FLIR GF320 OGI camera. Dividing the concentration-path length by the path length results in the concentration. Therefore, conducting an OGI survey in the field with a gas plume that is 10 cm in optical depth translates to the OGI camera being technically capable of detecting the plume if it has a concentration greater than 130 ppm (13 ppm·m / 0.1 m). This limit of detection will increase, however, in a manner commiserate with field conditions at the time of detection (e.g., wind speed, leak exit velocity, background temperature and uniformity, distance from targeted equipment).<sup>21,13</sup>

### **Example Applications and Vendors**

Thermal IR gas imaging cameras have a wide range of applications, though they are most commonly used to detect large leaks from process equipment and storage tanks at refineries and chemical plants.<sup>5</sup> The technology is now allowed as a replacement in the current LDAR requirements for federal rules.<sup>4,12,19</sup> The cameras have also been used to detect leaks in natural gas pipelines through aerial viewing on helicopters.<sup>2,3,5</sup> Thermal IR cameras can also be used to monitor other plant activities that could potentially create fugitive emissions such as truck and barge loading and unloading and incinerator activities. The cameras can also identify flares that would otherwise be unnoticed by the naked eye.<sup>22</sup> An image of such a flare is included as Figure 2.29.<sup>22</sup> Table 2-26 provides a general description of the applications for thermal IR camera.



**Figure 2.29. Flare Detection by Thermal IR Camera.**

**Table 2-26. Typical Applications for Thermal IR Camera.**

| TECHNOLOGY | APPLICATIONS   |
|------------|----------------|
| IR Camera  | Leak Detection |

**Vendors**

Although there are several vendors for standard thermal imaging IR cameras, only a few companies promote their products primarily as optical remote sensing IR cameras for pollutants. A standard thermal imaging IR camera used for pollutant detection costs approximately \$80,000. Table 2-27 summarizes these vendors and their website information.

**Table 2-27. Thermal IR Camera Vendors**

| VENDORS                        |  |
|--------------------------------|--|
| FLIR, Inc.                     | <a href="http://www.flir.com">www.flir.com</a>                             |
| Opgal Optronic Industries Ltd. | <a href="http://www.opgal.com">www.opgal.com</a>                           |
| IR Cameras, Inc.               | <a href="http://www.ircameras.com">www.ircameras.com</a>                   |
| Infrared Cameras, Inc.         | <a href="http://www.infraredcamerasinc.com">www.infraredcamerasinc.com</a> |

**Strengths and Limitations**

The thermal IR camera has a variety of strengths and limitations that should be considered for each application. A summary of strengths and limitations is shown in Table 2-28 and Table 2-29, respectively. Utilizing a thermal IR camera is typically a more economical approach to leak detection than traditional methods. The camera can identify the exact source of a leak from safe distances within a plant. However, training is required for operating personnel, and quantitative results cannot be obtained without introducing additional measurement technology. Additionally, for outdoor use, gas detection becomes more challenging on overcast days and the IR camera is not waterproof and therefore has limited use on rainy days.

**Table 2-28. Summary Table of the IR Camera's Strengths**

| Feature                        | Strength  |
|--------------------------------|---|
| Economical                     | Fast screening speed compared to conventional leak detection methods <sup>18</sup>  |
|                                | Leak assessment can be done without interruption to plant operations <sup>2,3</sup>   |
|                                | Cost-effective compared to traditional leak detection methods. <sup>2,3</sup>   |
| Qualitative Results            | Accurately assess the size of each leak <sup>18</sup>   |
| Leak Identification            | Better able to isolate the exact source of a leak, despite proximity to other leaking sources, in real time and record in a video format. <sup>2,3,18</sup> |
| Leak Detection from a Distance | Wide field of view: More likely to identify leaking components in unconventional places. <sup>3,18</sup>  |
|                                | Exposure risk minor because leaking components can be viewed at a distance. <sup>2,3,18</sup>   |

**Table 2-29. Summary Table of the IR Camera's Limitations**

| Feature                    | Limitation   |
|----------------------------|--|
| Qualitative Results        | Cannot quantify the concentration of a leak without additional technology <sup>3</sup>                             |
| Training Requirements      | Camera use requires individuals with specific training. Some models are easier to use than others. <sup>3,18</sup> |
| Meteorological Limitations | Cannot be used during rain or fog and is not as effective during overcast skies. <sup>18</sup>                     |
|                            | The camera has a specified nominal operating range for ambient temperature. <sup>18</sup>                          |
| Safety Requirements        | Operation is not intrinsically safe and use is limited in hazardous areas. <sup>18</sup>                           |

**References**

1. Miseo, E. V. and N. A. Wright. 2003. Developing a Chemical-Imaging Camera. The Industrial Physicist. 29-32.
2. Trefiak, T. 2006. Pilot Study: Optical Leak Detection & Measurement. Prepared by ConocoPhillips (October 16).
3. U.S. EPA. 2005. Natural Gas STAR Partner Update.
4. Footer, T.L., J.M. DeWees, E.D. Thoma, B.C. Squier, C.D. Secrest, and A.P. Eisele. 2015. Performance Evaluations and Quality Validation System for Optical Gas Imaging Cameras

that Visualize Fugitive Hydrocarbon Gas Emissions. In Proceedings of the 108<sup>th</sup> Annual Conference of the Air & Waste Management Association. Raleigh, NC, June 25, 2015.

5. U.S. EPA. 2009. Infrared Spectroscopy and Imaging. <http://www.clu-in.org/characterization/technologies/infrared.cfm>. December 21.
6. FLIR Systems. 2008. Data sheet: ThermaCam GasFindIR CO Infrared Camera for Leak Detection and Repair.
7. FLIR Systems. 2007. Data sheet: ThermaCam GasFindIR LW Infrared Camera for Leak Detection and Repair.
8. FLIR Systems. 2008. Data sheet: ThermaCam GasFindIR HSX Infrared Camera for Leak Detection and Repair.
9. FLIR Systems. 2009. Data sheet: ThermaCam GasFindIR GF300 Infrared Camera for Leak Detection and Repair.
10. Footer, T.L. 2016. "Recent Observations from Optical Gas Imaging Camera Evaluations for Hydrocarbon Leak Detection." Presented at the ITC InfraMation Conference, September 27-29, 2016, Las Vegas, NV.
11. Coffey, Tom. 2009. Alternative Applications for GasFindIR. Presented at the 3<sup>rd</sup> Annual PetroTherm Conference in League City, Texas (February).
12. Reese, D., C. Melvin, and W. Sadik. 2007. Smart LDAR: Pipe Dream or Potential Reality? Exxon Mobil Corporation.
13. Footer, TL. 2015. DRAFT Technical Support Document: Optical Gas Imaging Protocol (40 CFR Part 60, Appendix K). Prepared for the U.S. EPA and available as docket document EPA-HQ-OAR-2010-0505-4949.
14. Rothman, L.S., I.E. Gordon, Y. Babikov, et al. 2013. "The HITRAN 2012 Molecular Spectroscopic Database." *Journal of Quantitative Spectroscopy and Radiative Transfer*, 130, 4-50.
15. Footer, T.L., and J. DeWees. 2014. "Recent Observations on the Performance of Optical Gas Imaging Cameras for Visualizing Fugitive Hydrocarbon Gas Emissions." Presented at the 14<sup>th</sup> ISA LDAR Fugitive Emissions Symposium, May 19-22, New Orleans, LA.
16. Spectral Remote Sensing & Detection. 2009. Sensitivity Reliability of Gas Imaging Leak Detection of SF<sub>6</sub>. Presented to the 2009 Workshop on SF<sub>6</sub> Emission Reduction Strategies (February).
17. Benson, R., R. Madding, R. Lucier, J. Lyons, and P. Czeripuszko. 2006. "Standoff Passive Optical Leak Detection of Volatile Organic Compounds using a Cooled InSb Based Infrared Imager." Proceedings of the 99<sup>th</sup> A&WMA Annual Conference and Exhibition, June 21-23, New Orleans, LA.



18. Picard, D., J. Panek, and D. Fashimpaur. 2006. Directed Inspection and Maintenance Leak Survey at a Gas Fractionation Plant Using Traditional Methods and Optical Gas Imaging. Presentation for AWMA Annual Conference (June 22).
19. Federal Register Volume 73, No. 246 (73 FR 78199–78219 [E8–30196]), QA/QC Requirements Alternative Work Practice to Detect Leaks from Equipment. 12/22/2008.
20. Zeng, Y. 2012. White Paper on A Calibration/Verification Device for Gas Imaging Infrared Cameras. Providence Photonics, Inc., June 25, 2012.
21. Sandsten, J., U. Wållgren, M. Barenthin Syberg, and H. Hagman. 2015. Optical Gas Imaging Standard for Sensitivity and Detection of Gases. Proceedings of the Air & Waste Management Association 108<sup>th</sup> Annual Conference and Exhibition, Raleigh, NC, June.
22. Bullock, Adam. 2009. TCEQ and Thermal Imaging Technology. Presentation FLIR Petrotherm 2009 Conference (February 24-25).

## **2.6 Cavity Ring-Down Spectroscopy**

There are multiple variations on cavity enhanced absorption techniques based on the property of the time required to reduce the signal due to the absorption or scatter of laser light. CRDS and Integrated Cavity Output Spectroscopy (ICOS) are examples of laser absorption spectrometry that measures optical extinction of compounds that scatter and absorb light in a closed sample path. This chapter describes first generation Cavity Ring-Down Laser Absorption Spectroscopy (CRLAS) as an example of this widely used optical technology to measure *in situ* concentrations of gaseous samples that absorb light at specific optical wavelengths down to the part-per-trillion level. Although noteworthy for a broad range of applications, this technology is most often used for measurements of weakly-absorbing or highly-dilute atmospheric samples.

Traditional absorption spectroscopy techniques measure the absolute change in light intensity after passing through a sample relative to the original intensity of the light. CRDS techniques improve on these methods by measuring the rate of decay of light intensity exiting from a high-finesse optical cavity. Using the rate of decay rather than the change in light intensity makes the CRDS technique less sensitive to fluctuations in the source laser intensity or variations in ambient conditions (such as humidity). Moreover, the reflectivity of the closed optical (or ring-down) cavity yields much longer effective sample path lengths for greater detection sensitivity.

In CRDS applications, the measured rate of decay of light intensity over time is a function of the cavity length, the ability of the optical mirrors to achieve perfect reflectance, and the absorptivity ( $\epsilon$ ) of the sample. Because the cavity length and mirror reflectance are constant between successive analyses, the amount of time required for the light intensity to decay to  $1/e$  of its initial intensity (herein referred to as the 'rate of decay') within an empty ring-down cavity and one where the target sample is present is entirely the result of the sample absorbance.<sup>1</sup>

### **Basic Operation**

Each gaseous compound absorbs energy at different wavelengths, usually more than one, depending on vibrational and rotational excitement within the molecule. Therefore, each

compound has its own “signature” of bands from which energy may be absorbed. Each band is highly selective, with virtually no absorption occurring outside of a specific wavelength. Once a compound has been identified, its spectrum can also be used to measure the compound’s concentration because the amount of infrared radiation absorbed from the IR beam is proportional to the concentration of the compound in the sample or open path.

the absorption path length may or may not be equal to the cavity length, depending on the experimental design; the total reflection pathway may be used instead, as with prism cavities.<sup>2</sup> The CRDS technique enhances sensitivity to target analytes by significantly increasing the pathlength using an optical resonator (or ring-down cavity). Increased sensitivity of the CRDS technique relative to that of conventional absorption spectroscopy was demonstrated in the inaugural experiments published by O’Keefe and Deacon in the visible region of the electromagnetic spectrum<sup>3</sup>.

The absorption spectrum (or collection of spectral features for a single species over a range of wavelengths) of a gaseous molecule is the spectroscopic equivalent to a fingerprint as each compound will absorb energy at different wavelengths depending on the quantum properties of that compound. Given the simplicity of CRDS systems, there are no intrinsic limitations to the spectral region of which CRDS can be applied.<sup>4</sup> Indeed, studies have proven that successful measurements from the far-IR (12  $\mu\text{m}$ )<sup>5</sup> to UV (197 nm)<sup>6</sup> are possible with current technologies.

Theoretically, any spectral region can be probed with CRDS if the following three conditions are satisfied:

1. Mirrors of sufficiently high reflectivity are available in the spectral region of interest. High-speed detectors are employed that can confidently measure very small differences in duration on the order of microseconds ( $\mu\text{s}$ ) or less.
2. Tunable pulsed lasers or optical wavelength modulation for continuous-wave CRDS applications are available.

### General Experimental Design

A general schematic diagram of the essential components of a CRDS apparatus is shown in Figure 2-30. The heart of this technique is the sample cell which is bounded by highly reflective, dielectric-coated, concave mirrors. Traditionally, the technique evolved using two of these mirrors as depicted in Figure 2-30, but many mirror configurations that employ three or more mirrors have been attempted (some of which are available through commercial vendors) and are shown to improve the measurement quality from CRDS applications. Regardless of how many mirrors are utilized, the ability of the highly reflective mirrors to achieve maximum reflectivity over the full wavelength range of interest largely depends on the nature of the dielectric coating selected.

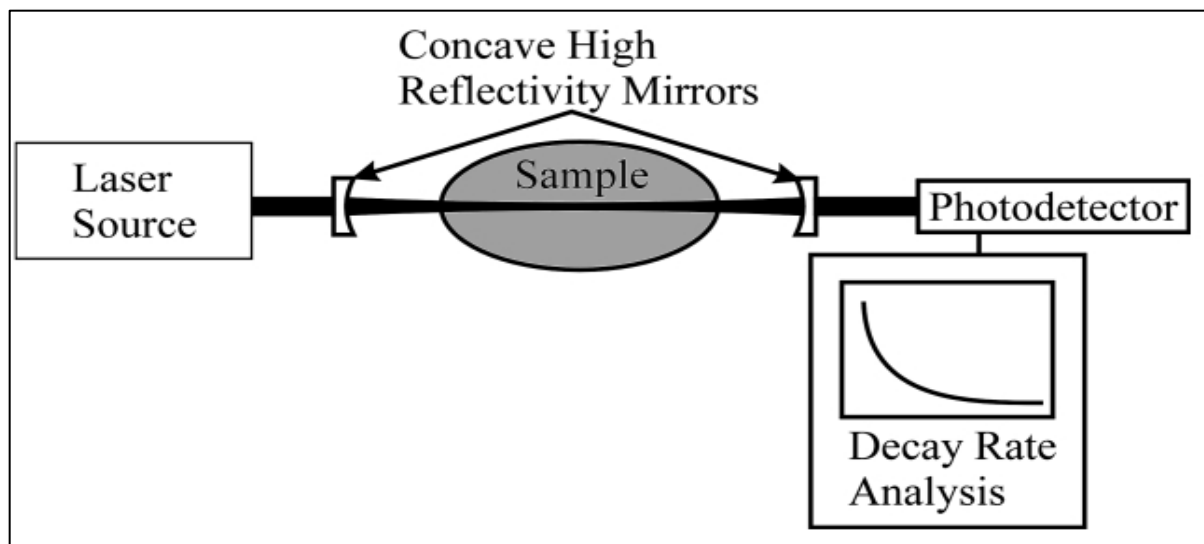


**Figure 2-30. The essential components of any CRDS experimental set-up**

As shown in Figure 2-30, basic CRDS measurements are acquired by optically coupling laser light through the input mirror of a closed sample chamber bounded by two (input and output) non-cofocal, highly-reflective optical mirrors and measuring the rate of light intensity decay over time. To achieve proper optical coupling and cavity reflectance, the bandwidth of the laser radiation needs to be sufficiently narrow enough to excite only a single optical mode of the cavity while also being sufficiently narrower than that of the spectral features of the sample to obtain well-resolved results (this is illustrated later in Figure 2-31).

When the laser light enters the closed optical cavity, it reflects off the bounding mirrors with a

known amount of light exiting the cavity on each reflection (defined by the mirrors' reflectance). If the optical cavity is empty, this rate of light intensity decay is characterized by a steady, exponential decrease to zero (like the single-exponential function plotted in Figure 2-25). If a gaseous species that absorbs the laser light is introduced into the cavity, then the intensity decay rate will be faster depending on the concentration of the absorbing species.

The time it takes for the light intensity in an optical cavity to decay to  $1/e$  of its original value is called the cavity ring-down time (RDT or  $\tau$ ) and is illustrated in Figure 2-25. This illustration depicts the light lost from the cavity with each pass of the reflecting light as measured by a PMT detector. The smoothed exponential curve above the oscillating data in the figure was derived from an algorithm applied to the data by instrumental software. The difference between the RDT curve of an empty cavity and the RDT curve of a cavity that contains sample is directly proportional to the concentration of the absorbing gas species in the sample. If the empty cavity ring-down time,  $\tau$ , is known, measurements of the decay rate of light intensity obtained as each laser wavelength is scanned yields a complete absorption spectrum for each analyte.

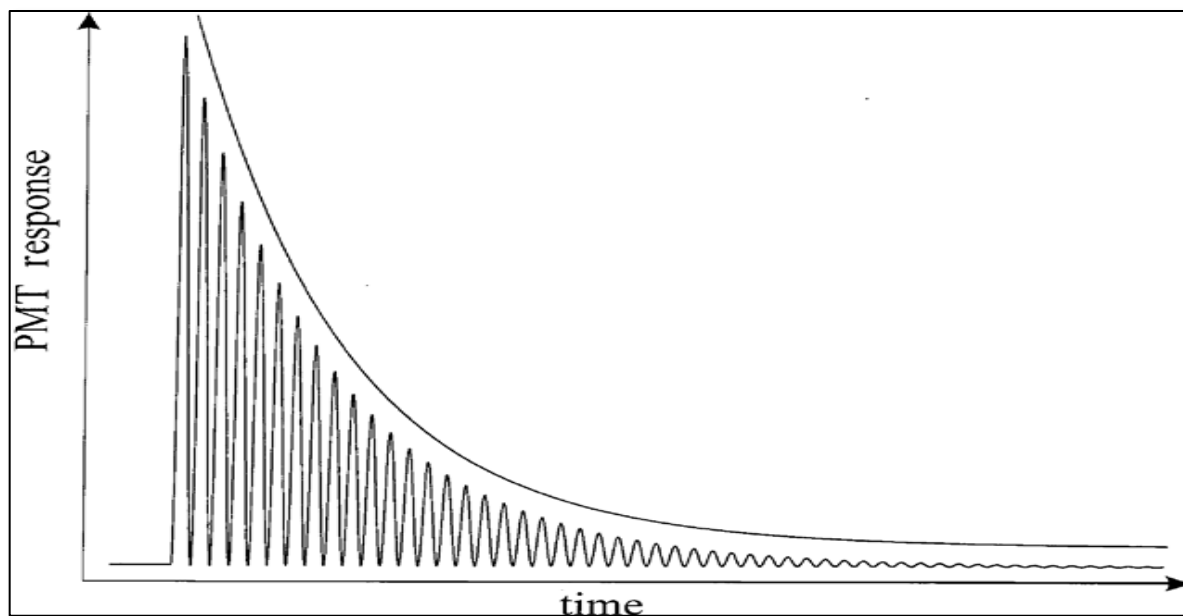


**Figure 2-31. Schematic representation of the expected rate of decay.**

The laser light source can be pulsed or continuous wave (CW), the differences in the experimental design between the two techniques is mostly in the number and arrangement of optical components. Romanini *et al*<sup>7</sup> demonstrated the first application of CRDS with a continuous laser

source (or CW-CRDS) such as a TDL. In their study, Romanini *et al.* found that this change in the laser light source lead to gains in spectral resolution, signal intensity, and data acquisition rate. Instead of receiving a signal in the shape illustrated in Figure 2-32, the instantaneous power of a continuous laser is lower, but usually concentrated into a narrower bandwidth.<sup>2,8</sup> Figure 2-26 illustrates the difference between the incident pulsed laser light and that of the CW laser light.

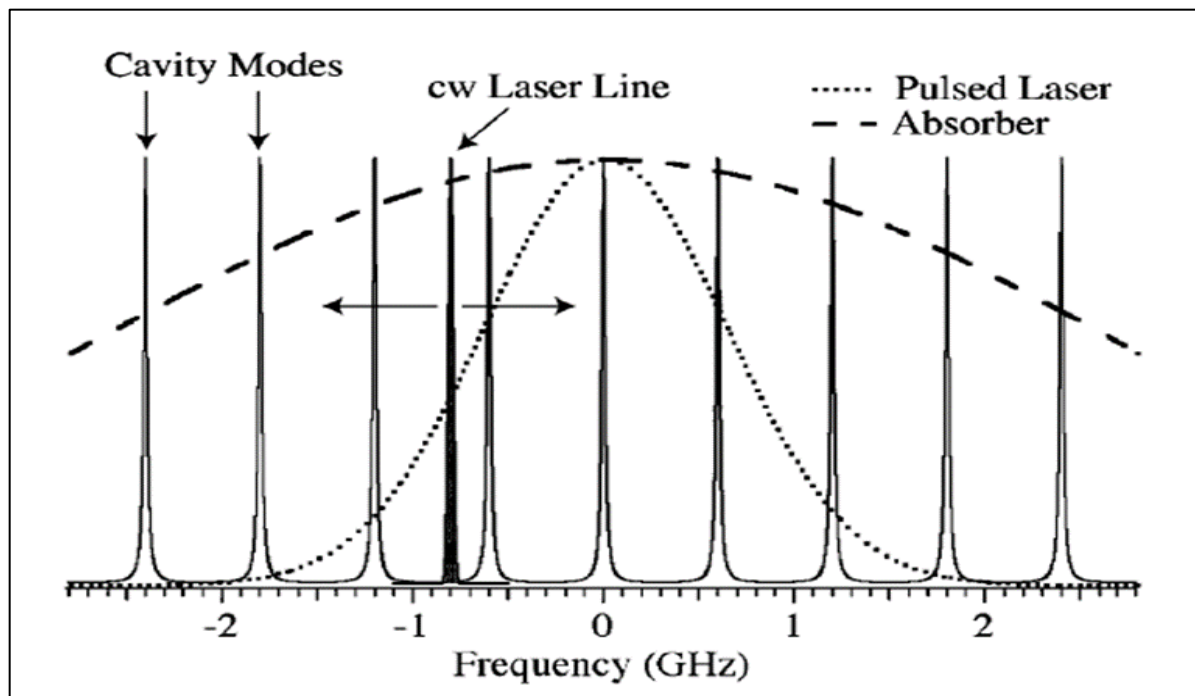


**Figure 2-32. Comparison of Pulsed and Continuous Wave Laser Light. Illustrating the overlap between the bandwidths of the absorbing species (Absorber), the pulsed laser source, the CW laser source, and the optical cavity resonance frequency modes.**

The CW laser bandwidth must be matched to the narrow transmission limits of the optical cavity to allow injection of the light into the cavity; this can be done by adjusting the length of the optical cavity, modulating the laser properties, or a combination of both.<sup>2</sup> Looking at Figure 2-26, it is easy to observe the more passive mode matching of the pulsed laser source with a wider bandwidth capturing a complete cavity mode versus the more difficult mode matching of the thinner CW laser source to superimpose on a narrow cavity mode.<sup>9</sup> While the CW-CRDS method is more optically complicated than the pulsed CRDS method, the low-cost, high-performance, and practical energy requirements of the TDL allows more flexibility for field applications.<sup>2</sup>

Once the light is transmitted into the cavity, the light source must be turned off to observe the

decay in light intensity in one of two ways: the operator can either configure the optics to allow build-up of the light intensity through constructive interference to a predetermined threshold before extinguishing the light source, or he can turn the light source off immediately once a signal is produced from the detector. There are many ways to turn off the light source, but the most common is using an acousto-optic modulator (AOM) as a laser 'shutter.'

Figure 2-33 provides a more detailed illustration of the experimental design for CW-CRDS applications.<sup>8</sup> An optical isolator can be installed immediately after the laser source to reduce on-axis back reflections and increase the signal-to-noise ratio.<sup>10</sup> A piezoelectric transducer (PZT) is added to modulate the cavity length with a triangular signal to achieve greater cavity resonance, increasing sensitivity, and further improving the signal-to-noise ratio.<sup>11</sup> Optical filters and lenses can be added immediately before the PZT to augment the laser spectral line selectivity and improve cavity mode-matching if necessary/desired. Additional optics may be incorporated into the experimental design after the ring-down cavity for similar purposes, depending on the experimental application and the selection of the optical detector type. It is important to note that the PZT is included for CW applications only.

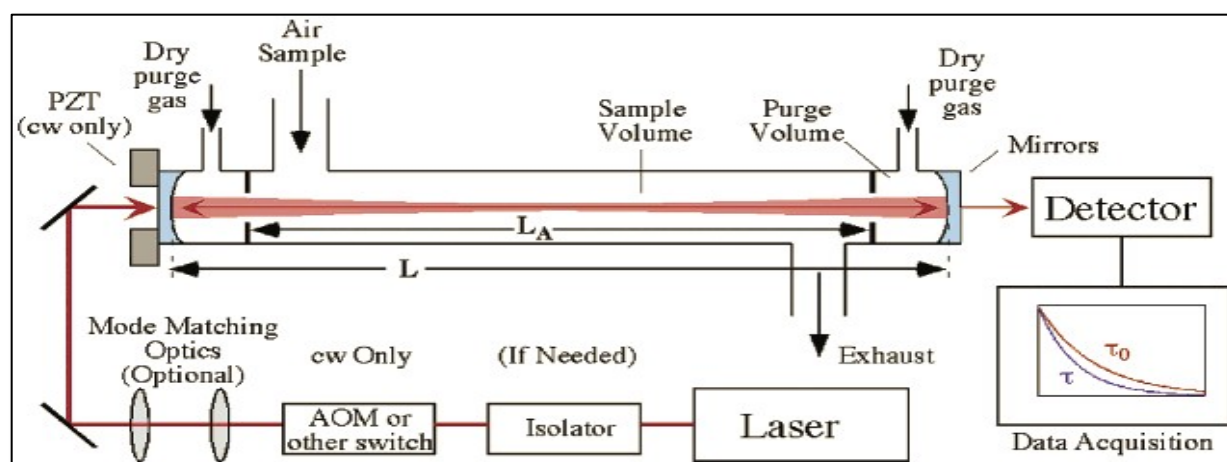


**Figure 2-33. Optical components schematic of a cavity ring-down spectrometer**

When the light is coupled out of the laser, a detector generates a signal that is ultimately relayed to a personal computer for processing and storage. The type of detector integrated into the experimental design largely depends on the application and the required signal format. Most commonly, researchers will use a PMT to detect the CRDS signal because it has good quantum

efficiency, good spectral range, and a high gain in addition to being lower in cost. Alternatively, a CCD has comparable, if not better, spectroscopic properties while providing a two-dimensional read-out and having multiple channel capabilities. PMT and CCD detectors are the two most frequently cited detectors used in CRDS studies. Figure 2-34 illustrates the difference between the signals received by either detector.

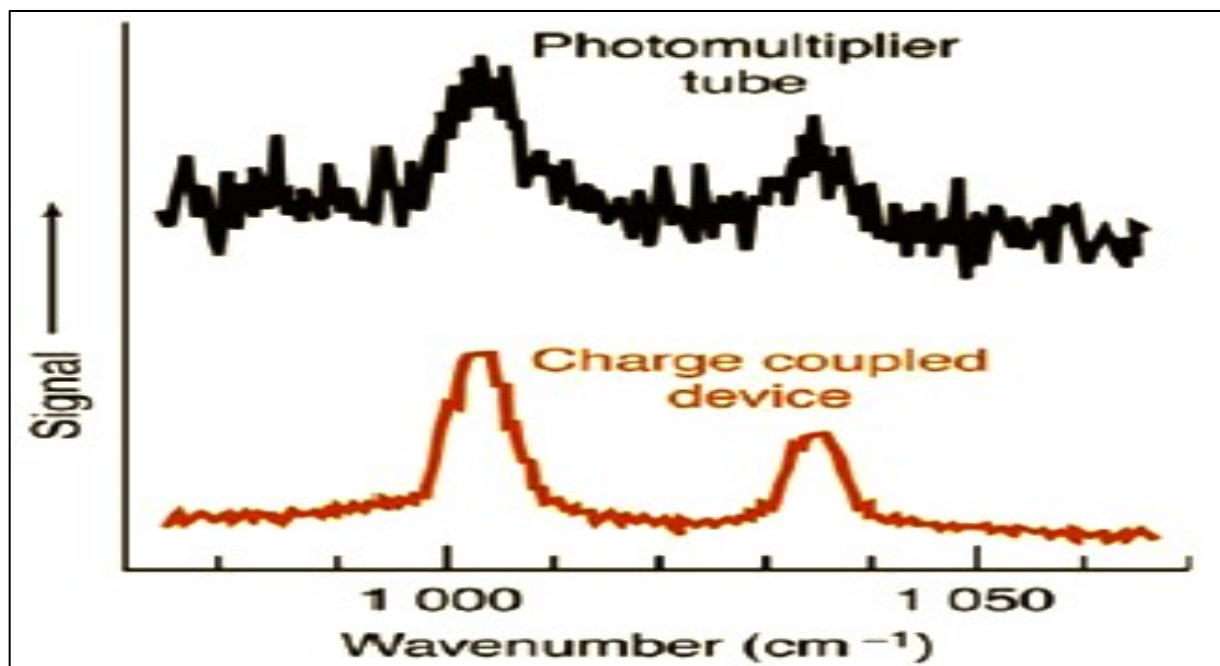


**Figure 2-34.** Differences between photomultiplier tube (PMT) and charge-coupled device (CCD) detector outputs. (Adapted from Pemberton, 1989)

### Current Method Developments

Developments of CRDS technology for vast disciplines and environments have led to many variations to the aforementioned experimental design. Due to the simplicity of the CRD approach, there are only three zones in the experimental design where changes can be made that would significantly alter the technology:

1. (a) the light source (laser technology, spectral design, and the incorporation of input/output optical components);
2. (b) the construction and design of the internal components to the ring-down cavity; and
3. (c) the methods and algorithms utilized for data processing.



The most extensive application of CRDS technology has been atmospheric studies. Pulsed laser CRDS has evolved through many design permutations and is currently manufactured using off-axis cavity-enhanced absorption (OA-CEA) techniques with advancements to the construction of the reflective cavity components. Although appropriate for both pulsed and continuous wave light source applications, CEA or ICOS and off-axis integrated cavity output spectroscopy (OAICOS or OA-CEA) are more frequently used with the CW approach.<sup>8</sup>

Most CRDS experiments are performed on gaseous samples due to the simplicity with which gases can be introduced into the sampling cell. However, attempts to broaden the applicability of the technology have led to a few studies that sample surfaces, thin films, liquids, and solids, although no sample medium has been as extensively studied with CRDS than air.

### **Pollutants and Relative Levels That Can Be Measured**

The applications for pulsed CRDS and its numerous variants (such as CW-CRDS, FT-CRDS, CEA/ICOS, etc.) and the studies performed on these techniques are limitless. Therefore, the list of detectable pollutants provided in Table 2-30 is only a cursory list and does not represent all possibilities.<sup>8</sup>

**Table 2-30. Example list of detectable pollutants by CRDS. Wavelength ( $\lambda$ ), sensitivity, and minimum detectable mixing ratio at  $1\sigma$  noise level for common gaseous species.**

| Species                       | Method                   | Approximate $\lambda$ ( $\mu\text{m}$ ) | Sensitivity ( $\text{cm}^{-1}$ ) | Mixing Ratio (ppbv) |
|-------------------------------|--------------------------|---|----------------------------------|---------------------|
| CH <sub>4</sub>               | CW CRDS                  | 1.65                                    | $1.5 \times 10^{-8}$             | 52                  |
| C <sub>2</sub> H <sub>2</sub> | CW CRDS <sup>a</sup>     | 1.5                                     | $\sim 4 \times 10^{-9}$          | 4                   |
| TNT                           | Pulsed CRDS <sup>b</sup> | 6 – 8                                   | $9 \times 10^{-9}$               | 0.075               |
| Chlorobenzenes                | Pulsed CRDS              | 0.266                                   | --                               | ppmv levels         |
| CO <sub>2</sub>               | CW CRDS                  | 1.57                                    | $\sim 4 \times 10^{-9}$          | 2500                |
| CO                            | CW CRDS <sup>c</sup>     | 1.57                                    | $\sim 4 \times 10^{-9}$          | 2000                |
| NH <sub>3</sub>               | CW CRDS <sup>c</sup>     | 1.5                                     | $\sim 4 \times 10^{-9}$          | 19                  |
| NO                            | CW CRDS <sup>d</sup>     | 5.2                                     | $5 \times 10^{-8}$               | 0.7                 |
| NO <sub>2</sub>               | CW CRDS <sup>c</sup>     | 0.41                                    | $7 \times 10^{-9}$               | 0.4                 |
| NO <sub>3</sub>               | CW CRDS <sup>c</sup>     | 0.662                                   | $1 \times 10^{-9}$               | 0.002               |
| N <sub>2</sub> O <sub>5</sub> | CW CRDS                  | 0.662                                   | $1 \times 10^{-9}$               | 0.0012              |
| HONO                          | Pulsed CRDS <sup>c</sup> | 0.354                                   | $2 \times 10^{-8}$               | 1.7                 |
| OH                            | Pulsed CRDS              | 0.309                                   | --                               | ppmv levels         |
| Hg                            | Pulsed CRDS              | 0.254                                   | --                               | 0.001               |
| H <sub>2</sub> O              | Pulsed CRDS <sup>e</sup> | 0.95                                    | --                               | 7 ‰                 |
| Aerosol                       | Pulsed CRDS              | 0.532                                   | $1 \times 10^{-10}$              | --                  |

Samples were analyzed ambient or lab air unless otherwise noted. <sup>a</sup> Sampled in a flame matrix. <sup>b</sup> Synthetically prepared sample. <sup>c</sup> Sampled from a lab source, pure gas or carrier gas mixture matrix. <sup>d</sup> Sampled in human breath. <sup>e</sup> Sampled from prepared standard.

The sensitivity of the CRDS method is determined by the fractional loss of light intensity per round-trip in the cavity. The absorption of laser light intensity for a single pass through the optical cavity is given by the Beer-Lambert law, which is used to approximate the minimum detectable absorption in CRDS. The equation below shows that the minimum detectable absorbance per pass is dependent upon the reflectivity (R) of the mirrors and the accuracy in the determination of  $\tau$  and the precision of  $\Delta\tau$  (or the precision of the number of round trips in the cavity (N)).<sup>13</sup>

$$\delta I_m \approx (1-R) \frac{\Delta \tau_{\min}}{\tau} = (1-R) \frac{\Delta N_{\min}}{N}$$

Where:

$\delta I_m$  = the minimum detectable change in absorbance

R = mirror reflectivity

$\Delta \tau_{\min}$  = minimum detectable change in the ring-down time (i.e., precision of  $\Delta \tau$ )

N = the number of round trips in the cavity

$\Delta N_{\min}$  = the accuracy to which N can be measured

### **Typical QA/QC**

There are three main requirements in the experimental design when CRDS is used. First, the laser source must emit the wavelength absorbed by the target analyte or a range of wavelengths that includes the absorption wavelength. Also, the cavity mirrors must be able to reflect the light in the wavelength region of interest. Finally, the detector must be fast enough to detect changes that occur in very short time intervals ( $\mu$ s). The rest of the instrumental configuration involves adjustments (such as cavity length modulation or cavity resonance mode matching) to achieve an absorbance signal. The optical modes of the entire system must then be harmonized to acquire a signal from the detector.

Accuracy, precision, linearity, zero/calibration drift, and response time can be evaluated using known concentrations of gas standards and/or zero air. Simultaneous measurements based on a reference method such as EPA CTM-027 could provide the reference data for assessing CRDS comparability. The data completeness is simply a measure of the amount of valid data points achieved versus the total amount of data points expected for a given period. Other factors that become important during operation such as maintenance requirements, consumables used, ease-

of-operation, and frequency of repairs are being assessed through EPA verification tests.<sup>15</sup>

### **Example Applications and Vendors Applications**

Although the technology is new to regulated environmental applications, it is not foreign to experiments involving the direct monitoring of environmental contaminants. A work by Berden *et al.* [2000] lists a comprehensive overview of published findings with CRDS technology from the official date of inception (with O'Keefe and Deacon in 1988) to the date of publication (2000).<sup>3,4</sup> This list contains well over 200 spectral features detected by CRDS and includes absorption wavelengths, almost continuously, from 205 nm to 10,617 nm. Moreover, Atkinson [2003] and Brown [2003] individually identified chemical divisions for the most potential applications of CRDS in direct environmental contaminant monitoring into the following classes:<sup>2,8</sup>

- Nitrogen oxides and Nitrous Acid (HONO)
- Ammonia
- Elemental mercury and volatile mercury compounds
- Carbon monoxide and carbon dioxide
- Methane, hydrocarbons, and formaldehyde
- Atmospheric aerosol particulates

The limitations to the application of CRDS technology depend on the development of individual optical system components. The overall applicability and usefulness of the method has only begun to be explored and various transfigurations of CRDS will enjoy extensive application in environmental analytical chemistry as the merits of these methods are proven in time. Table 2-31 summarizes the common applications for CRDS technology.

**Table 2-31. Typical Applications for OP-TDL.**

| Technology | Applications            |
|------------|-------------------------|
| CRDS       | Tracer Gas Correlations |

**Vendors**

There are currently three known proprietors of commercial CRDS systems: (1) Picarro, Inc., (2) Los Gatos Research, Inc., and (3) Tiger Optics, Inc. Each manufacturer has developed a system different from the others. The main technological differences between each manufacturer’s designs have primarily to do with the ring-down cavity configuration and construction materials. The cost of a CRDS system ready for field use ranges between \$40K to \$150K, depending on specific application and configuration. Table 2-32 lists CRDS vendors and their internet contact information.

**Table 2-32. CRDS Vendors**

| Vendors                   |  |
|---------------------------|--|
| Picarro, Inc. (CRDS)      | <a href="http://www.picarro.com">www.picarro.com</a>         |
| Tiger Optics              | <a href="http://www.tigeroptics.com">www.tigeroptics.com</a> |
| Los Gatos Research (ICOS) | <a href="http://www.lgrinc.com">www.lgrinc.com</a>           |

**Strengths and Limitations**

CRDS can be used as a qualitative tool to provide specific information about volatile IR energy-absorbing molecules. It can also be used as a quantitative tool to provide the concentration of many gas-phase molecules. A summary of strengths and limitations is shown in Tables 2-33 and 2-34. One of the main strengths of CRDS is that it measures time and not absorbance, making the technique immune to environmental variations and laser intensity fluctuations while concurrently increasing the linear dynamic range. Moreover, using a high-finesse optical cell, CRDS has greatly increased the technology sensitivity to target compounds without adding complicated sample pre-conditioning steps. The use of the optical cell further enhances the technological design to withstand vibration making field applications of the technology simpler.

The CRDS application is limited mostly by the properties of the high-reflectivity optical mirrors. The mirrors used for CRDS have a high amount of wavelength specificity but lack the flexibility

necessary to allow simultaneous multiple species detection and/or a broad species application range. High-reflectivity optical mirrors currently are only able to reflect about 15 percent of the target wavelength on either side.

**Table 2-33. Summary Table of CRDS Strengths**

| <b>Feature</b>                                | <b>Strength</b>  |
|---|--|
| Simple design                                 | Minimal maintenance required and no consumables are needed. Turnkey operation with the potential for remote access and control. "User friendly."       |
| Fast detector                                 | Ability to measure very small changes in short time frames. Can rapidly scan spectra continuously for high temporal resolution and real- time results. |
| Multi-pass, high-finesse, stable optical cell | Greatly increases sensitivity with much longer effective pathlengths. Insensitive to vibrations during measurements.                                   |
| Broad-band source capable                     | Allows for extended wavelength range scanning, increasing sensitivity by probing multiple absorption lines while also eliminating other interferences. |
| Internal temperature and pressure controls    | Minimal-to-no drift making frequent calibration unnecessary. Enhanced accuracy and system stability.   |
| Measures time, not absorbance                 | Renders the method immune to ambient changes (such as relative humidity and temperature) and laser intensity fluctuations.                             |
| Direct sampling                               | Little-to-no sample pre-conditioning or treatment required before analysis.  |

**Table 2-33. Summary Table of CRDS Strengths (continued)**

| Feature                           | Strength   |
|-----------------------------------|--|
| Compact system                    | Easy field deployment and installation. Quick sample exchange in a smaller volume cavity with moderate flow rates. Advances in components allow for a rugged portable system |
| Can use low power optical sources | Logistically simpler for field use to eliminate the need for a large power source.   |

**Table 2-34. Summary Table of CRDS Limitations**

| Feature                         | Limitation   |
|---------------------------------|--|
| Measures only total extinction  | May need to apply sample filtering components to avoid interferences.  |
| Laser light source              | Limits the method to the laser spectral ranges available.  |
| High-reflectivity mirrors       | Are only able to reflect over a small wavelength range (about $\pm 15\%$ ) relative to the center wavelength.<br>Multiple species detection difficult. |
| High quality lasers and mirrors | Key components that typically drive up the cost of the instrumentation, depending on application.  |

**References**

1. Wheeler, M.D. S.M. Newman, A.J. Orr-Ewing, and M.N.R. Ashfold; (1998). "Cavity ring-down spectroscopy." *Journal of the Chemical Society, Faraday Transactions*, **94(3)**: 337.
2. Atkinson, D.B.; (2003). "Solving chemical problems of environmental importance using cavity ring-down spectroscopy." *Analyst*, **128**: 117.
3. O'Keefe, A., and D.A.G. Deacon; (1988). "Cavity ring-down optical spectrometer for absorption measurements using pulsed laser sources." *Review of Scientific Instruments*, **59(12)**: 2544.
4. Berden, G., R. Peeters, and G. Meijer; (2000). "Cavity ring-down spectroscopy: Experimental schemes and applications". *International Reviews in Physical Chemistry*, **19(4)**: 565.

5. Bisson, S.E., T.J. Kulp, O. Levi, J.S. Harris and M.M. Fejer; (2006). "Long-wave IR chemical sensing based on difference frequency generation in orientation-patterned GaAs." *Appl. Phys. B - Lasers and Optics*, 85(2-3): 199.
6. Snee, M., S. Hannemann, E.J. van Duijn, and W. Ubachs; (2004). "Deep-ultraviolet cavity ringdown spectroscopy." *Optics Letters*, 29(12): 1378.
7. Romanini, D., A.A. Kachanov, N. Sadeghi, and F. Stoeckel; (1997). "CW cavity ring down spectroscopy." *Chemical Physics Letters*, **264**: 316.
8. Brown, S.S.; (2003). "Absorption Spectroscopy in High-Finesse Cavities for Atmospheric Studies." *Chemical Reviews*, 103(12): 5219.
9. Paldus, B.A, and A.A. Kachanov; (2005). "An historical overview of cavity-enhanced methods." *Canadian Journal of Physics*, **83**: 975.
10. Hippler, M., and M. Quack; (1999). "Cw cavity ring-down infrared absorption spectroscopy in pulsed supersonic jets: nitrous oxide and methane." *Chemical Physics Letters*, 314: 273.
11. Thiebaud, J., and C. Fittschen; (2006). "Near infrared cw-CRDS coupled to laser photolysis: Spectroscopy and kinetics of the HO<sub>2</sub> radical." *Applied Physics B*, 85: 383.
12. Pemberton, J.E., and R.L. Sobocinski; (1989). "Raman Spectroscopy with Helium-Neon Laser Excitation and Charge-Coupled Device Detection." *Journal of the American Chemistry Society*, **111**(2): 432.
13. Crosson, E.R.; (2008). "A cavity ring-down analyzer for measuring atmospheric levels of methane, carbon dioxide, and water vapor." *Applied Physics B*, 92: 403.
14. Chen, H., J. Winderlich, C. Gerbig, A. Hofer, C.W. Rella, E.R. Crosson, A.D. van Pelt, J. Steinbach, O. Kolle, V. Beck, B.C. Daube, E.W. Gottlieb, V.Y. Chow, G.W. Santoni, and S.C. Wofsy; (2010). "High-accuracy continuous airborne measurements of greenhouse gases (CO<sub>2</sub> and CH<sub>4</sub>) using the cavity ring-down spectroscopy (CRDS) technique." *Atmospheric Measurement Techniques*, 3: 375.



## **2.7 Particulate Matter LIDAR**

Light detection and ranging (LIDAR) technology is based on measuring the speed and wavelength of a laser signal that has reflected off compounds of interest. LIDAR operates on the same principles as radio detection and ranging (RADAR) except laser light is used as the energy source instead of radio waves. The laser light is aimed toward a material of interest and the properties of the backscattered (or reflected) light correspond to the physical characteristics of the encountered material (e.g., gas concentration, density, temperature, humidity, and wind). LIDAR can operate across many wavelengths, from ultraviolet (UV) to far-infrared (IR), and is therefore utilized in a variety of applications. From high-resolution mapping to atmospheric content measurements and from range-finding to autonomous vehicle navigation, the flexibility of LIDAR technology and the simplicity of its application relative to other remote sensing methods result in a wide distribution of LIDAR to a multitude of disciplines. This section discusses LIDAR technology as its application to the measurement of particulate matter (PM) from ground-based sources, with emphasis on tropospheric applications. LIDAR is well suited to measure tropospheric PM concentrations due to the high spatial resolution and ability to monitor temporal variations.

The use of LIDAR technology to detect PM in the atmosphere was first explored in the 1960s (e.g., Collis and Ligda, 1966).<sup>1</sup> The detection of this PM led to some of the first ground-based observations of the stratospheric structure, but did not have good sensitivity for heights less than about 20 kilometers (km). Since then, LIDAR technology has advanced with the development of laser technology to include the following remote sensing techniques:

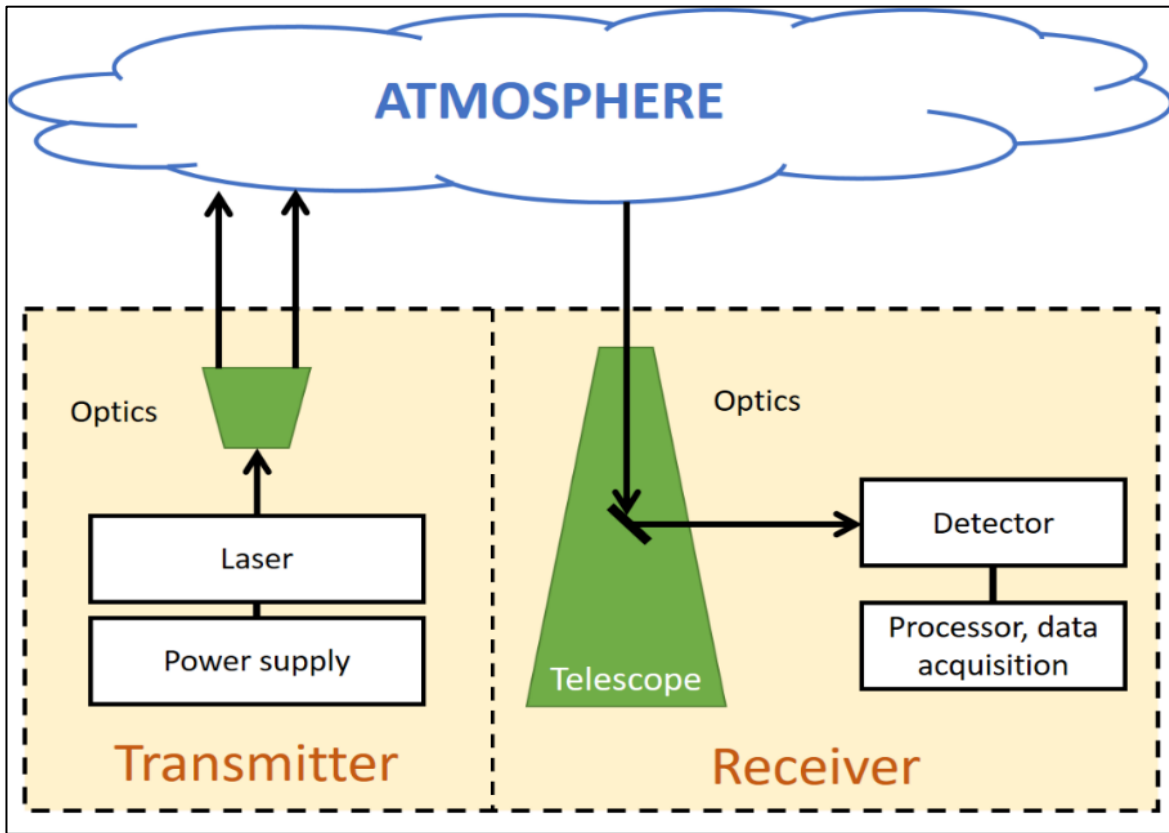
- Elastic-backscatter LIDAR
- Coherent, Raman, or Doppler LIDAR
- Differential absorption LIDAR (DIAL).

Elastic LIDAR simply measures the changes in magnitude of the reflected light, while coherent and Raman LIDAR provide information on changes in the wavelength of the reflected light. DIAL, discussed in Section 2.4, was developed primarily for the spatial measurement of trace chemicals

in the atmosphere and achieves results by calculating a ratio between two different wavelengths of laser light. One wavelength is strongly absorbed by the species of interest and is used to probe for concentration, while the other is just outside of the absorption range of the species of interest and is used to collect background light scattering. The time-adjusted ratio of these two wavelengths indicates the location and concentration of the species of interest.<sup>2</sup> The increase in instrumental complexity for the DIAL systems limits the use of this technique due to limited availability and the prohibitive cost of associated equipment.<sup>3</sup>

### **Basic Operation**

LIDAR-based systems consist of two basic components: the transmitter and the receiver. The transmitter consists of the power supply, laser light source (typically a neodymium-doped yttrium aluminum garnet; Nd:Y<sub>3</sub>Al<sub>5</sub>O<sub>12</sub> (Nd:YAG)), and any modulating optics required to direct the laser light into the material to be sampled. The receiver consists of a sensor, processor, and any optics required to detect the reflected light. In the simplified illustration of a LIDAR system in Figure 2.35<sup>4</sup>, the laser light source transmitted to the atmosphere is passed through optics that expand and collimate the light to deliver even light distribution across the laser beam path diameter and to disperse the laser power over a larger area for eye-safe applications.<sup>4</sup> Eye-safe configurations also include micro-pulsed lasers, wherein the energy transmitted with the laser pulse is below the ANSI 2136.1-1986 laser exposure safety standard in which the maximum permissible exposure is  $5 \times 10^{-7}$  J/cm<sup>2</sup> in the 520-530 nanometer (nm) wavelength range.<sup>5</sup> The transmitted light is backscattered by the dust, gases, and aerosols present in the target atmosphere and collected by return optics, such as a Newtonian or Cassegrain telescope and spectrally separating optical components, and directed into the detector (typically, photomultiplier tube or avalanche photodiode) for signal detection. The electronic signal is then processed and converted to a digital output for analysis.<sup>4</sup>



la

**Figure 2-35. Simplified Schematic of LIDAR System.**

Currently, the calculation of emission concentrations from LIDAR signals represents the largest amount of uncertainty in the LIDAR system processing equations.<sup>4</sup> The retrieval algorithms must consider the geometry of the instrumental optics in addition to the geometry of the target material. Typically, general assumptions on particle “sphericity” and/or *a priori* information related to the material extinction coefficient and backscatter coefficient may be required to calculate the desired measurement results, depending on the LIDAR system design.<sup>4</sup>

The conventional LIDAR method, elastic-backscatter LIDAR, was the first technology design and served as the foundation from which other configurations were developed. The simplified equation for detecting the LIDAR signal from the elastic-backscatter LIDAR system is:

$$P_R = KG_R\beta_R T_R$$

Where:

$P_R$  = power  $P$  received at distance  $R$  from the object.

- $K$  = measure of the LIDAR system performance.
- $G_R$  = range-dependent measurement geometry.
- $B_R$  = backscatter coefficient at distance  $R$ .
- $T_R$  = amount of transmitted laser light that is lost when traveling distance  $R$  and back.

The geometry term ( $G_R$ ) in the LIDAR equation is described as  $O_R/R^2$ , where  $O_R$  is the overlap function to account for the area where the laser transmission beam and the receiver field of view overlap. This term refers to the geometry of the LIDAR system (Figure 2.XX2) and, along with the  $K$  term, is adjustable by the LIDAR developer/operator. At the point of transmission, the overlap function is zero and approaches unity with distance away from the LIDAR. Therefore, a section called the “blind zone” exists in every LIDAR system where the overlap function is insufficient for providing robust measurements and the amount of calculation error is too great to report a result with adequate certainty. This would occur if the distance to  $R$  in Figure 2.36<sup>4</sup> was short enough such that the diameter of backscatter area reflected from one particle (and illustrated with the return perception angle in Figure 2.XX2) did not exceed the diameter of the laser beam at the point of transmission. Where this area occurs relative to the position of the LIDAR depends on the design optics and can range from <50m to 20 km.<sup>6</sup>

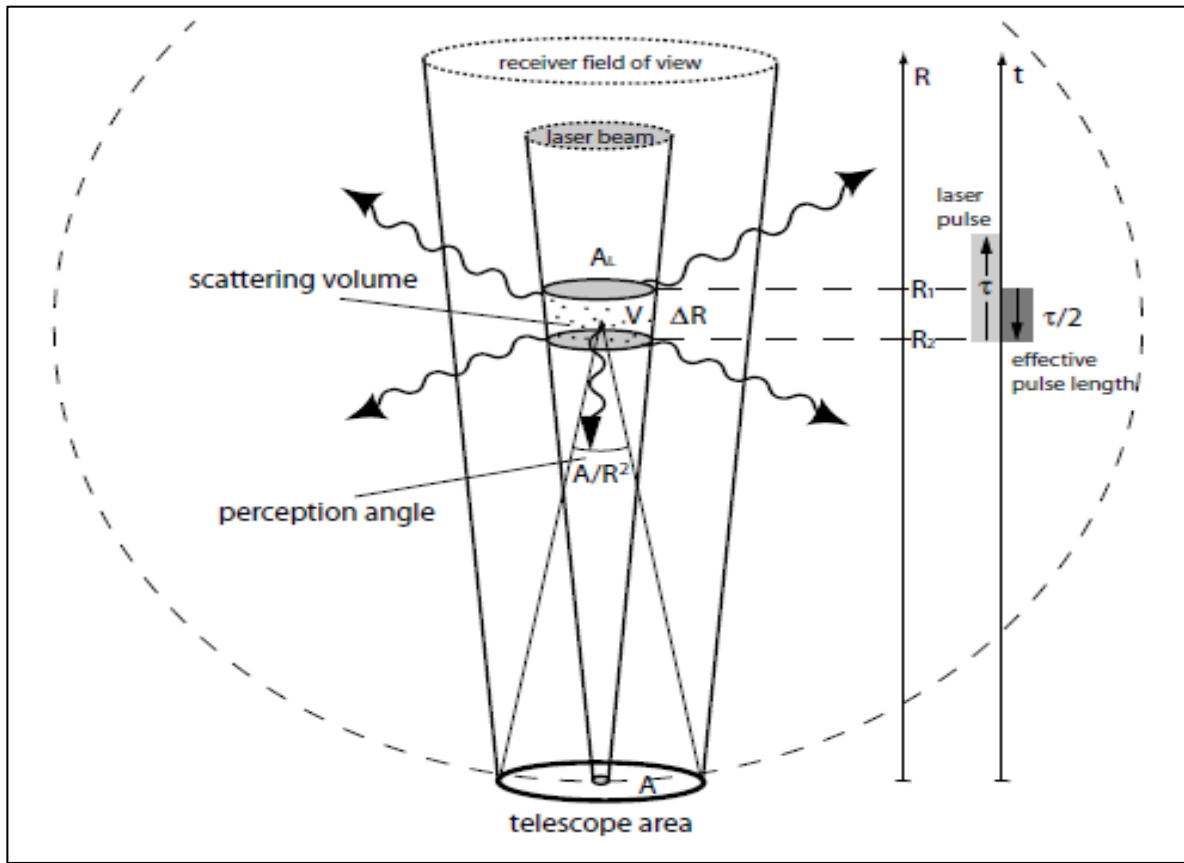


Figure 2-36. Illustration of LIDAR System Geometry.

The variable  $K$  describes the performance of a LIDAR system and can be described in more detail with the following equation:

$$K = P_0 \frac{c\tau}{2} A\eta$$

Where:

- $K$  = measure of the LIDAR system performance
- $P_0$  = average power of a single laser pulse
- $c$  = speed of light
- $\tau$  = duration of the laser pulse
- $A$  = area of the primary return optics responsible for the collection of the backscattered light
- $\eta$  = overall system efficiency.

The term  $c\tau/2$  describes the amount of atmospheric volume that is illuminated by the laser light, known as the effective laser pulse length. The telescope area  $A$  and the average laser power (energy \* pulse repetition frequency) are typical LIDAR system design parameters, with the optimization of  $\eta$  for achieving the best possible LIDAR signal.<sup>4</sup>

There are two general designs for LIDAR systems, monostatic coaxial and monostatic biaxial, as shown in Figure 2.37.<sup>7</sup> In coaxial systems, the path for the transmitted laser light and the path for the returning backscatter received are the same and are separated by optics within the instrument. Biaxial systems have separate pathways for the transmitted laser light and received backscatter signal.

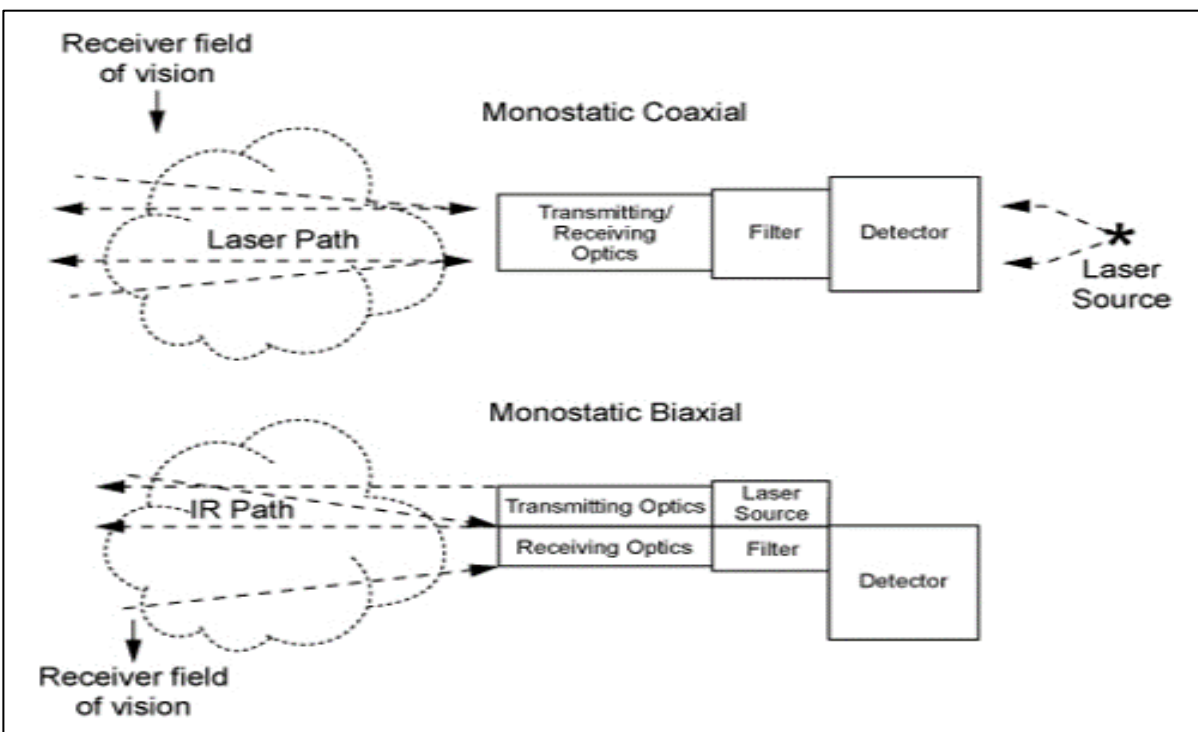


**Figure 2-37. Illustrations of Monostatic Coaxial and Monostatic Biaxial LIDAR Configurations.**

Researchers at the Utah State University's Space Dynamics Laboratory investigated systems of both monostatic types. The coaxial system (the AGLITE, Figure 2.38<sup>11</sup>) has a three-wavelength design derived from a Nd:YAG 1064 nm laser that is frequency-doubled and tripled to produce transmissions that cover UV, visible, and IR wavelength regions for agricultural aerosol monitoring applications. Light that is elastically backscattered from the quick (~ 10 nanosecond) laser

transmission pulses is collected into a Newtonian telescope at a repetition rate of 10 kilohertz (kHz). The operating range for the AGLITE system to produce confident results is about 500 meters (m) to about 15 km with a resolution of about 5 m given the prototype specifications. Measurements characterizing the density of probed aerosols as a function of distance from the LIDAR system are derived from the temporal properties of each laser transmission "return."<sup>11</sup>

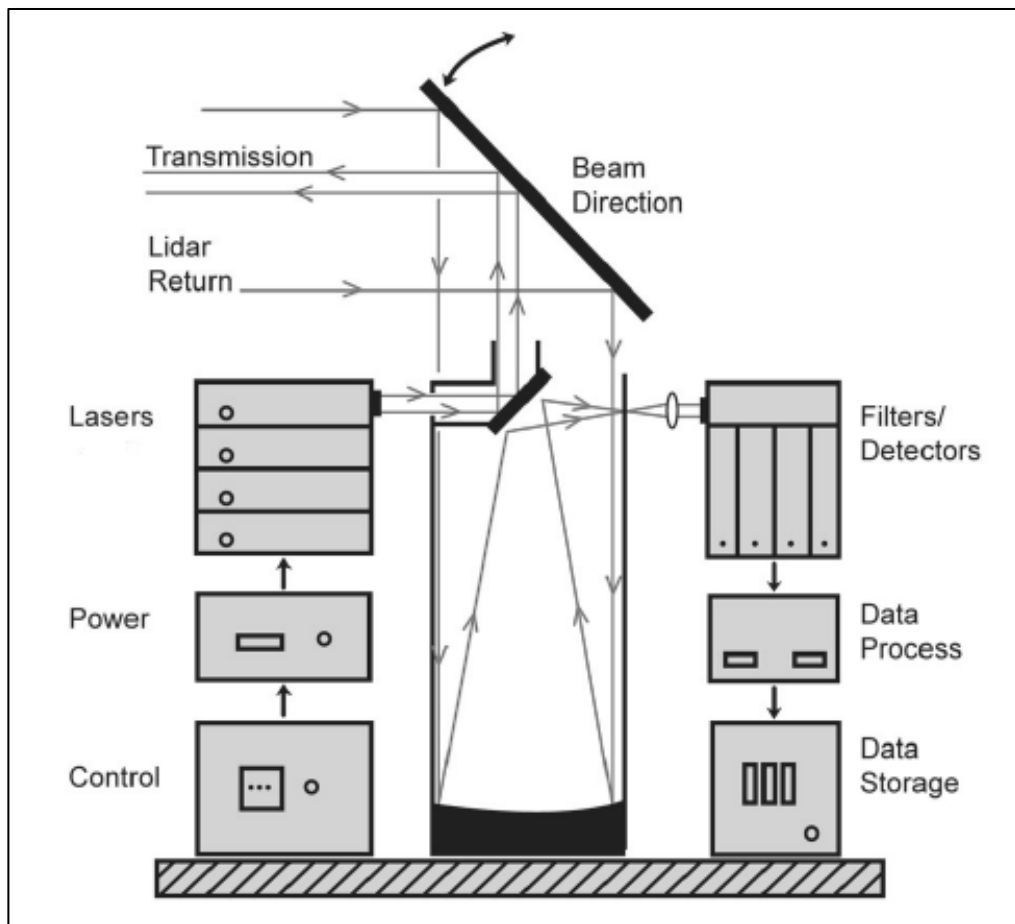


**Figure 2-38. Illustration of the USU AGLITE LIDAR System.**

The biaxial system (the Compact Eyesafe Lidar System, or CELiS) was developed for PM emissions fence-line monitoring (Figure 2.39).<sup>12</sup> Some of the optical components and performance specifications are comparable to the AGLITE (i.e., Nd: YAG laser source, about 7 nanosecond pulse width, range resolution of about 5 m), but with a single wavelength transmission at 1,574 nm and a laser pulse repetition rate of 20 Hz.<sup>12</sup>

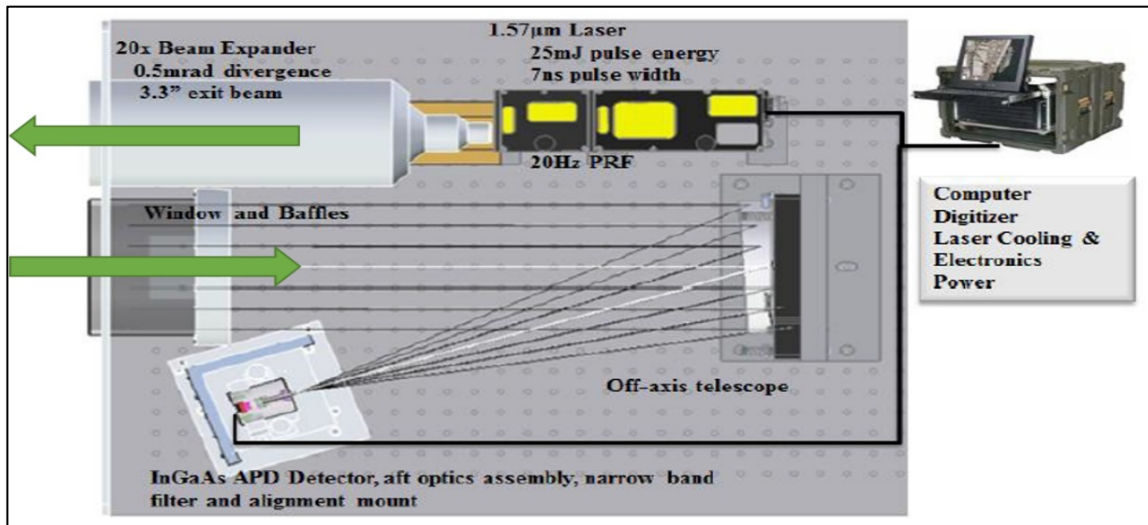


*Figure 2.39. Illustration of USU CELiS LIDAR System.*

### Pollutants and Relative Levels That Can Be Detected

LIDAR technology can measure atmospheric concentrations of trace gases, aerosols, and clouds in addition to properties such as density, temperature, humidity, and wind. The flexibility of LIDAR technology to probe for compounds in the UV, visible, and IR region of the spectra allows for the detection of unlimited number of pollutants. LIDAR is also sensitive enough to distinguish between water droplets and ice crystals in clouds and probe stratospheric air masses from the ground or tropospheric concentrations from satellite. The European EARLINET network of LIDAR measurement stations detected the 2013 forest fires occurring in the United States.<sup>13</sup>

Currently, very few commercial options are available for LIDAR PM monitoring systems, because most LIDAR-only instruments are still in the research phase of development.<sup>4</sup> The current systems are predominantly airborne or satellite-based technologies. USA-based TSI Inc. offers light-scattering laser photometers, which, instead of transmitting a laser beam of light into the atmosphere, draw in a sample of the atmosphere and performs the laser light scattering measurements internally.<sup>8</sup> Components are available for laboratories, researchers, and hobbyists to build their own systems, but manufacturers specifications for detection levels may not be



available. US company Micro Pulse LiDAR and French companies Leosphere and Cimel Electronique offer the most complete packages with their models MPL, EZ LIDAR and CE376 Compact Aerosol Analyzer, respectively. Although, both SES (USA) and Raymetrics (Greece) offer components and/or services to build a custom modular system.

**Typical QA/QC**

Some LIDAR instruments (e.g., micro-pulse LIDAR) can achieve a few photons per microsecond detection or less<sup>5</sup> and can spatially resolve measurements down to 2 cm.<sup>6</sup>

Trace gases and water vapor measurements in the atmosphere can be compared to *in situ* measurements from balloon sondes and airborne-based monitors for quality control purposes. The complexity of aerosol measurements, however, are less straight-forward.<sup>10</sup> In these cases, the instrument performance can be verified either with collocated sun photometer measurements (in the absence of clouds) or intercomparison with a different LIDAR system.

**Example Applications and Vendors**

LIDAR systems have an extraordinary wide range of applications, though they are most commonly used to conduct 3D wind and topography surveys. Table 2-35 provides a general description of the applications for LIDAR systems.

**Table 2-35. Typical Applications for LIDAR Systems.**

| TECHNOLOGY | APPLICATIONS  |
|------------|---|
| LIDAR      | DIAL, Elastic-backscatter, Raman-backscatter, Ranging, Optical Density Monitoring |

**Vendors**

Vendors offering complete solutions for PM measurements via LIDAR are currently very few. Most systems discussed in the literature are laboratory research developments that are not commercially available yet. The vendors in Table 2-36 offer either a commercial system

(Leosphere, Micro Pulse LiDAR, and Cimet), services to build a custom LiDAR (SES), or modules to incorporate into a custom system (Raymetrics).

**Table 2-36. LiDAR Systems Vendors**

| VENDORS            |  |
|--------------------|--|
| Micro Pulse LiDAR  | <a href="http://www.micropulselidar.com">www.micropulselidar.com</a> |
| Leosphere          | <a href="http://www.leosphere.com">www.leosphere.com</a>             |
| Cimet Electronique | <a href="http://www.cimet.fr">www.cimet.fr</a>                       |
| SES, Inc.          | <a href="http://www.sesincusa.com">www.sesincusa.com</a>             |
| Raymetrics         | <a href="http://www.raymetrics.com">www.raymetrics.com</a>           |

**Strengths and Limitations**

As with every technology, the strengths and limitations depend on application and design.

**Table 2-37. Table of LIDAR Strengths**

| <b>FEATURE</b>                   | <b>STRENGTH</b>  |
|----------------------------------|--|
| Reliable                         | Safe and reliable method for dust concentration measurements, even for very low levels.            |
| User-friendly                    | Easy to install and user-friendly operation. Low maintenance, infrequent maintenance requirements. |
| Spatial Concentration Resolution | Able to provide density and/or concentration heat mapping down to very small spatial increments.   |
| Laser Transmission Range         | Can cover a wide range of area with one configuration.   |
| Receiving Optics                 | Does not require retroreflectors.  |
| Near Real-time Response          | Can provide results within minutes of measurement, depending on sample averaging time.             |

**Table 2-38. Table of LIDAR Limitations**

| <b>FEATURE</b>                       | <b>LIMITATION</b>   |
|--------------------------------------|---|
| Backscatter Requirements             | Sufficient PM must be in the laser path to create sufficient backscatter for detection. |
| Wind Speed and Direction Variability | Rapidly changing wind speed or direction may cause measurements to change rapidly.      |
| Vendors                              | Small number of vendors providing LIDAR systems and services.                           |
| Blind Zone                           | Unable to make accurate measurements in the near-field.                                 |
| Expense                              | Prohibitive cost for complete system solutions.   |

**References**

1. Collis, R.T.H. and M.G.H. Ligda. 1966. Note on Lidar Observations of Particulate Matter in the Stratosphere. *Journal of the Atmospheric Sciences*. 23: 255—257.
2. Edner, H., K. Fredriksson, A. Sunesson, S. Svanberg, L. Uneus, and W. Wendt. 1987. Mobile remote sensing system for atmospheric monitoring. *Applied Optics*. 26(19): 4330—4338.
3. U.S. EPA. 2006. VOC Fugitive Losses: New Monitors, Emission Losses, and Potential Policy

Gaps – 2006 International Workshop.

[http://www.epa.gov/ttn/chief/efpac/documents/wrkshop\\_fugvocemissions.pdf](http://www.epa.gov/ttn/chief/efpac/documents/wrkshop_fugvocemissions.pdf)

4. Weitkamp, C (ed). 2005. Lidar: Range-Resolved Optical Remote Sensing of the Atmosphere. Springer Series in Optical Sciences. Springer, NY, USA.
5. Spinhirne, J.D. 1993. Micro Pulse Lidar. IEEE Transactions on Geoscience and Remote Sensing. 31(1): 48—55.
6. Cimel Electronique. [www.cimel.fr](http://www.cimel.fr).
7. U.S. EPA. 2013. Measurement and Monitoring Technologies for the 21<sup>st</sup> Century (21M<sup>2</sup>) – Open Path Technologies: Measurement at a Distance, Lidar. Available from <https://clu-in.org/PROGRAMS/21M2/openpath/lidar/>.
8. TSI, Inc. [www.tsi.com](http://www.tsi.com).
9. Sicard, M., Md. Reba, M., Tomas, S., Comeron, A., Batet, O., Muñoz, C., Rodriguez-Gomez, A., Rocadenbosch, F., Muñoz-Tuñón, C., J. Fuensalida, J. 2010. Monthly Notices of the Royal Astronomical Society. 405(1): 129—142.
10. Matthais, V., V. Freudenthaler, A. Amodeo, I. Balin, D. Balis, J. Bösenberg, A. Chaikovsky, G. Chourdakis, A. Comeron, A. Delaval, F. De Tomasi, R. Eixmann, A. Hågård, L. Komguem, S. Kreipl, R. Matthey, V. Rizi, J.A. Rodrigues, U. Wandinger, and X. Wang. 2004. Aerosol Lidar Intercomparison in the Framework of the EARLINET Project. 1. Instruments. Applied Optics. 43(4): 961—976.
11. Wilkerson, T.D., G.E. Bingham, V.V. Zavyalov, J. Swasey, J.J. Hancock, B.G. Crowther, S.S. Cornelsen, C. Marchant, J.N. Cuttis, D.C. Huish, C.L. Earl, J.M. Andersen, and M.L. Cox. 2006. AGLITE: A Multiwavelength Lidar for Aerosols. Space Dynamics Lab Publications, Utah State University, Paper 143. [http://digitalcommons.usu.edu/sdl\\_pubs/143](http://digitalcommons.usu.edu/sdl_pubs/143).
12. Wojcik, M.D. and A.W. Bird. 2012. CELiS (Compact Eyesafe Lidar System): A Portable 1.5  $\mu\text{m}$  Elastic Lidar System for Rapid Aerosol Concentration Measurement. Space Dynamics Lab Publications, Utah State University, Paper 144. [http://digitalcommons.usu.edu/sdl\\_pubs/144](http://digitalcommons.usu.edu/sdl_pubs/144).
13. Ancellet, G., J. Pelon, J. Totems, P. Chazette, A. Bazureau, M. Sicard, T. Di Iorio, F. Dulac, and M. Mallet. Long-range transport and mixing of aerosol sources during the 2013 North American biomass burning episode: analysis of multiple lidar observations in the western Mediterranean basin. Atmospheric Chemistry and Physics, 16, 4725—4742.

### **3.0 Measurements Applicable to Emissions Flux**

Optical remote technologies have been applied to answer a variety of fugitive and area source emissions questions. The range of applications spans both short-term characterization and measurement of emission flux (which is defined as measurement of pollutants that are either constant or changing concentration over time) to long-term monitoring of trends in control strategy performance. Technologies described in this chapter have been used in mobile applications to screen pipelines or industrial sites for leaks or major sources and in stationary applications to measure flux from landfills, waste lagoons, and petrochemical plants. In addition, the PM methods described in this section can also be used in mobile or stationary settings to understand PM flux in area sources.

Please note that technologies described in Chapter 2 can be used alone or in combination of the techniques and methods described within this chapter. The techniques and methods in this chapter also provide three major types of data: plume characterization, short-term flux measurements and long-term monitoring studies.

Short-term flux measurement applications (e.g. DIAL, RPM, SOF, Tracer Release Correlation etc.) are useful to determine the emissions from a complex area sources at one point in time. These measurements provide an estimate of the emissions plume size and concentration of selected target compounds or surrogates. Concentration profiling involves using ORS such as line of sight open-path optical techniques. Profiling periodic changes of emissions in one dimension is often the precursor of pilot stage of long-term monitoring at an area or fugitive emissions site.

Long-term monitoring is used to determine average trends of area sources emissions and to provide an indication of seasonal or industrial cycle emissions profiles. Continuous concentration profiling is also useful to determine process upsets or to diagnose the potential source of emissions from a complex industrial area using back trajectory calculations. Typically, long-term monitoring needs to be associated with a short-term measurement characterization of the size and composition of the emissions plume to relate trends in monitoring data to emissions and emission factors.<sup>1</sup>

These three types of data provide essential information on the annual emissions rate of fugitive and area sources as well as a measure of the effect of emissions reductions efforts.

Chapter 3 of this Handbook introduces the use of technologies by describing applications that measure short-term flux or mass emission rates from open or un-ducted gas and PM sources.

### **3.0.1 Reference**

1. Hashmonay, Ram, Long Term Monitoring of Greenhouse Gas Emissions from Fugitive and Area Sources, presented at the AWMA Symposium on Air Quality Measurements Methods and Technology, Los Angeles, CA November 2010

### ***3.1 Radial Plume Mapping: Other Test Method 10***

RPM is an ORS method used to determine fugitive emissions from non-point emissions sources including fugitive emissions and area source emissions. Its main goals are to identify emission “hot spots” over large scanned areas and measure emission fluxes. Fugitive emissions include air pollutants released into the ambient air from pressurized equipment due to leaks and various other unintended or irregular releases of gases. Examples of fugitive emissions include O<sub>3</sub> precursors, benzene, and methane.<sup>1</sup> For some source categories, fugitive and/or area source emissions are a significant portion of the total pollutant emissions; therefore, it is important to be able to locate and quantify these emissions.

The open-path configuration for ORS technologies was originally used to determine the average concentration of a compound of interest over a path of known length. The line-of-sight, or one-path, configuration provides an average of the compound of interest concentration per path length (i.e., ppm). Open-path monitoring expanded to include the measurement of the average concentration over several distances along the open path length. These interval measurements enabled estimation of the concentration profile of the plume. However, the survey of leaks and hot spots over a large area is not possible with just one optical path. Directing the ORS path over different lengths, as well as different horizontal and vertical paths, allows additional characterization of the horizontal or vertical emissions plume profile. RPM, as discussed in this section, is the outgrowth of multidirectional, multi-pathlength ORS and is used in combination with mathematical algorithms to characterize the concentration profile over a horizontal or vertical optical path plane.

#### **General Description of Approach**

Measuring the total amount of a fugitive emission over a large area is not simple. Earlier efforts used traditional point sampling techniques such as canisters, sorbents methods, flux boxes, PID/FID instruments and others.<sup>2</sup> However, the traditional point methods only provide concentrations from

a single point and fail to capture the temporal and spatial distribution of fugitive emissions over a large area. These methods also fail to identify, if any, “hot spots” of fugitive emissions. RPM provides a more complete survey of a large area. Open-path ORS measurement technology mounted on a programmable aiming platform or scanner can be configured in a vertical plane to measure emissions flux. When scanning in the horizontal plane (HRPM), results can be used to locate hot spots at ground level. Emission fluxes are obtained when scanning in the vertical plane (VRPM) downwind of the area source along with meteorological measurements data.

One-dimensional RPM, which scans along one line, such as an industrial fence line, is used to profile pollutant concentrations downwind from a source and coupled with wind direction may also be useful in locating emissions sources.<sup>2</sup> Determining which scanning setup to use depends entirely on the objectives of the project and data quality indicators.

### **Horizontal RPM Algorithm**

The HRPM approach provides horizontal differentiation to path-integrated measurements by optical remote sensing. This technique yields information on the two-dimensional distribution of the concentrations in the form of chemical-concentration contour maps. In this application, the plume mapping identifies chemical “hot spots,” the location of high emissions. Horizontal radial scanning is usually performed with the ORS beams located close to the ground. The survey area is divided into a Cartesian grid of rectangular cells. A mirror is located in each of these cells and the OP-FTIR sensor scans to each of these mirrors, dwelling on each for a set measurement time. The measurement equipment scans to the mirrors in the order of either increasing or decreasing azimuth angle. The path-integrated concentrations measured at each mirror are averaged over several scanning cycles to produce time-averaged concentration maps. Meteorological measurements are made concurrent with the scanning measurements.

The equation on page 3-5 illustrates how the measurements are made.



$$PIC_k = \sum_m K_{km} c_m$$

Where:

PIC = path integrated concentration

K = Kernel matrix

k = number of index for the pixels

m = number index for the pixels

c = average concentration in the m<sup>th</sup> pixel

The kernel matrix includes the specific beam geometry as shown in Figure 3-2 where the diagonal lines represent the  $K$ . Each value in the kernel matrix  $K$  is the length of the  $k$ <sup>th</sup> beam within the  $m$ <sup>th</sup> pixel; therefore, the matrix is specific to the beam geometry. The HRPM procedure solves for the average concentrations (one for each pixel) by solving the non-negative least squares-best fit for the data. Then the algorithm multiplies the resulting vertical vector of averaged concentration by the matrix  $K$  to yield the end vector of predicted PIC data. The second stage of the plume reconstruction involves interpolation among the reconstructed pixel's average concentration, providing a peak concentration not limited to the center of the pixels. A triangle-based cubic interpolation procedure (in Cartesian coordinates) is currently used in the HRPM procedure.<sup>2</sup> The ORS instrument is typically placed at the origin (in the first quadrant of the Cartesian convention) of the rectangular area to be measured. Once the HRPM measurement area and the number of path-determining components (PDCs) have been determined, the area is divided into smaller rectangular areas called pixels. The total number of pixels required is smaller or equal to the total number of beam paths.<sup>6</sup>

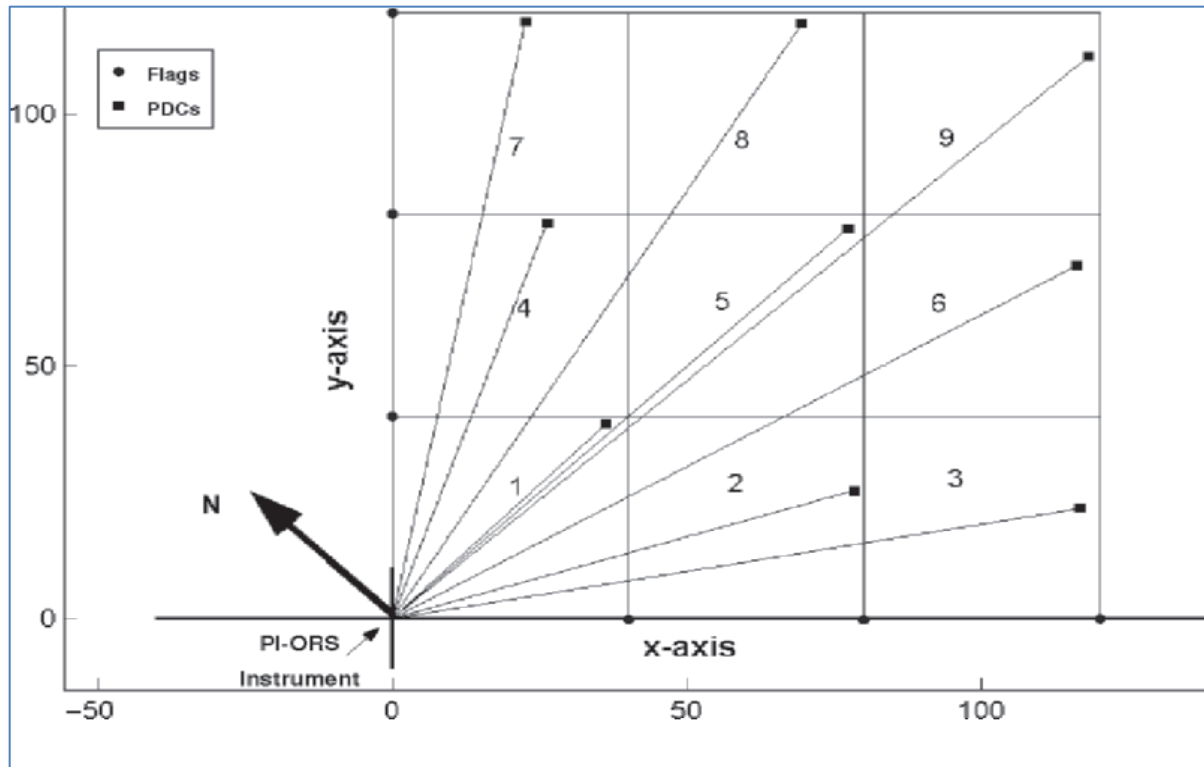


**Figure 3-1. Horizontal RPM setup**

### **Vertical RPM algorithm**

The VRPM algorithm uses multiple beam paths to survey the vertical pollutant concentration profile as a function of distance from the measurement equipment. Two different beam configurations of the VRPM methodology have been used: the five-beam (or more) and the three-beam VRPM configuration. Figure 3-1 shows a VRPM configuration using six beams.<sup>3</sup> In the five-beam (or more) configuration, the ORS instrument sequentially scans the paths of five PDCs. Three PDCs are along the ground-level crosswind direction, and the other two are elevated on a vertical structure. Additional beam configurations provide better spatial definition of the plume in the crosswind direction. In the three-beam configuration, the ORS instrument sequentially scans over three PDCs. Only one beam is focused at ground level, while the other two are elevated on a vertical structure. Pollutant data are collected over time as the measurement equipment cycles between each PDC.<sup>2</sup>

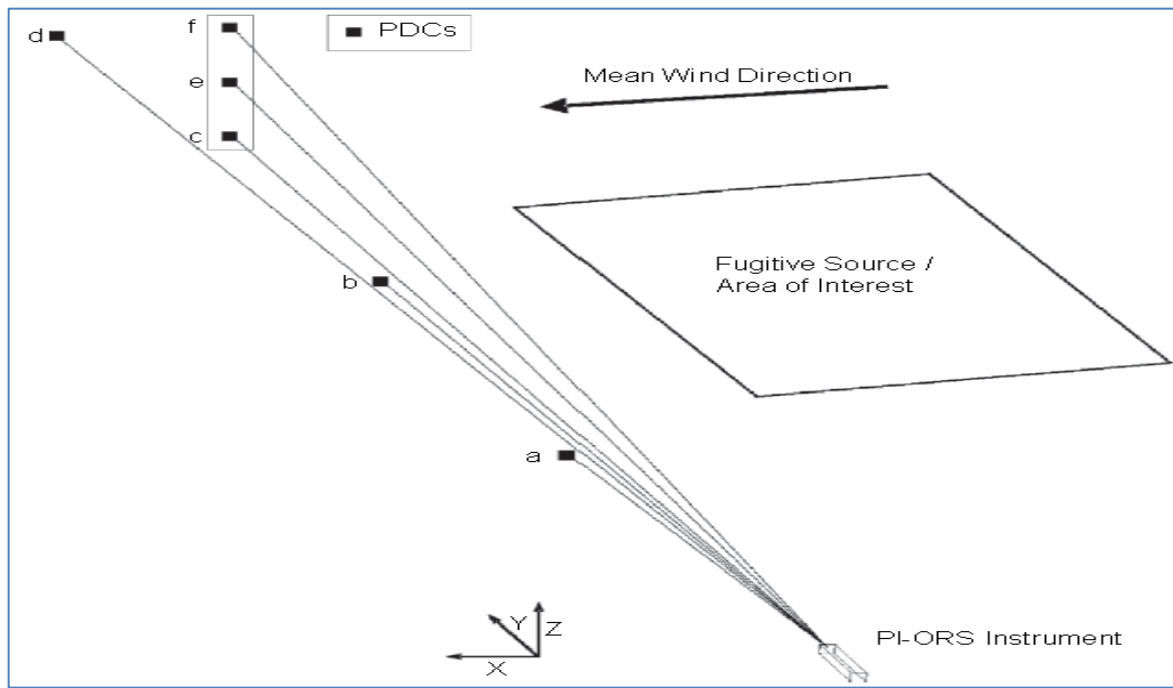


**Figure 3-2. Vertical RPM setup**

Figure 3-2 illustrates a vertical mapping configuration.<sup>4</sup> Once the PIC for all beam paths are averaged for the gas species of interest, the VRPM calculations reconstruct a plume map in the vertical downwind plane. A two-phase smooth basis function minimization (SBFM) approach is applied when there are three or more beams focused along the ground level (5-beam or more configurations). In the two-phase SBFM approach, a one-dimensional SBFM (1D-SBFM) reconstruction procedure is applied to reconstruct the smoothed ground level and crosswind concentration profile. The reconstruction is applied to the ground level segmented beam paths of the same beam geometry to find the crosswind concentration profile. A univariate Gaussian function is fitted to measured PIC ground level values.<sup>2</sup> The 1D-SBFM is also the sum of the squared errors (SSE), which is also the error function for the minimization procedure. The equation for calculating SSE is:

$$SSE(B_j, m_{yj}, \sigma_{yj}) = \sum_i \left( PIC_i - \sum_j \frac{B_j}{\sqrt{2\pi}\sigma_{yj}} \int_0^{r_i} \exp \left[ -\frac{1}{2} \left( \frac{m_{yj} - r}{\sigma_{yj}} \right)^2 \right] dr \right)^2$$

Where:

B = area under the one-dimensional Gaussian distribution

$r_i$  = pathlength of the  $i^{\text{th}}$  beam

$m_y$  = mean (peak location)

$\sigma_y$  = standard deviation of the  $j^{\text{th}}$  Gaussian function

$PIC_i$  = measured PIC value of the  $i^{\text{th}}$  path

The SSE function is minimized using the simplex minimization procedure to solve for the unknown parameters. When there are more than three beams at the ground level, two Gaussian functions are fitted to retrieve skewed and sometimes bi-modal concentration profiles. This is the reason for the index  $j$  in equation above.<sup>2</sup>

Once the 1D-SBFM phase is completed, the 2-D phase is applied. The bivariate Gaussian function used in the second phase is:

$$G(A, \sigma_z) = \frac{A}{2\pi\sigma_{y-1D}\sigma_z} \exp \left\{ -\frac{1}{2} \left[ \frac{(r \cdot \cos \theta - m_{y-1D})^2}{\sigma_{y-1D}^2} + \frac{(r \cdot \sin \theta)^2}{\sigma_z^2} \right] \right\}$$

Where:

$\sigma_{y-1D}$  is the standard deviation along the crosswind direction found in the 1D-SBFM;

$m_{y-1D}$  is the peak location along the crosswind direction found in the 1D-SBFM procedure, and

$\sigma_z$  are the unknown parameters to be retrieved in the second phase of the fitting procedure.

To solve for the unknowns an error function (SSE) is used which is minimized using the simplex method to solve for the two unknowns. If measurement equipment uses the three-beam setup (one at the ground level and the other two elevated), the one-dimensional phase calculation can be skipped, assuming a wide plume. The standard deviation in the crosswind direction is assumed to be about 10 times that of the ground-level beam path (length of vertical plane). Thus, if  $r_1$  is the length of the vertical plane, to determine the vertical gradient in concentration we use:

$$G(A, \sigma_z) = \frac{A}{2\pi(10r_1)\sigma_z} \exp \left\{ -\frac{1}{2} \left[ \frac{(r \cdot \cos \theta - \frac{1}{2}r_1)^2}{(10r_1)^2} + \frac{(r \cdot \sin \theta)^2}{\sigma_z^2} \right] \right\}$$

When the parameters of the function are found for a specific run, the VRPM algorithm calculates the concentration values for every square unit in a vertical plane (pixels). Then, the algorithm integrates the values incorporating wind speed data at each height to calculate the flux.

### **One-dimensional RPM algorithm**

For 1 dimensional (1-D) plume mapping, the scanning ORS instrument and three or more PDC are placed in a crosswind direction along a line, such as an industrial site fence line, and PIC measurements are made. A minimum of three PDCs are needed, but four to six are recommended, as shown in Figure 3-3, to provide a more detailed concentration profile. PDCs should be placed on the line-of-sight with an equal distance between each subsequent PDC, if possible. The 1D-RPM configuration uses the same equations for the VRPM, 1D-SBFM, which reconstructs a mass-equivalent plume concentration profile along a line-of-sight measurement.

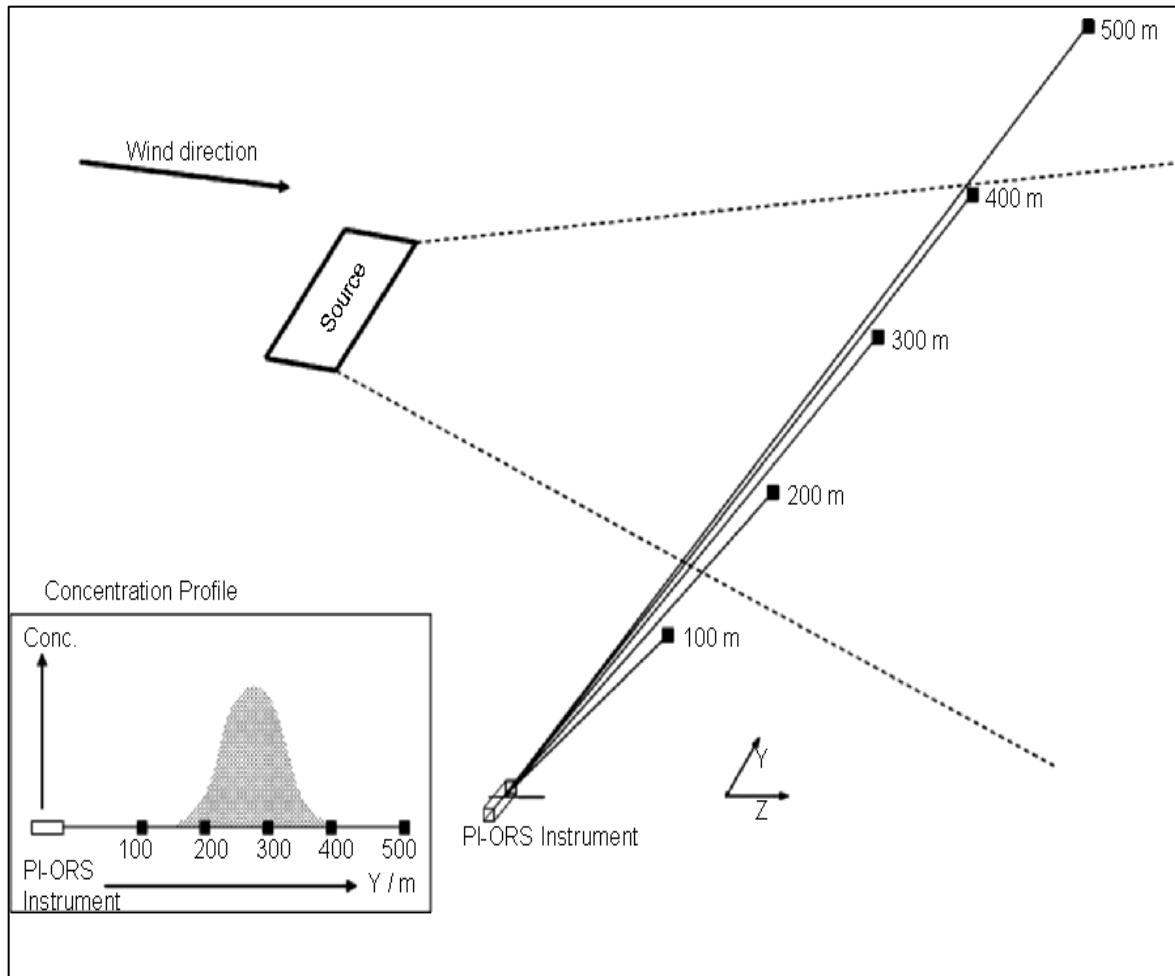


**Figure 3-3. One-dimensional RPM setup**

The RPM model and ORS technique are coupled together by a series of steps. First, the ORS pollutant concentration data along with wind vector information are processed with the VRPM algorithm to yield a mass emission flux for the source.<sup>2,5,6,7</sup> In a similar way, HRPM and 1D-RPM algorithms are processed with the concentration data to provide hot spots info or concentration downwind for the source. The output of the concentration data and algorithm process looks like a contour map. Figure 3-5 displays VRPM and HRPM contour map outputs where the concentration patterns are evidence of the distribution of the fugitive emission.

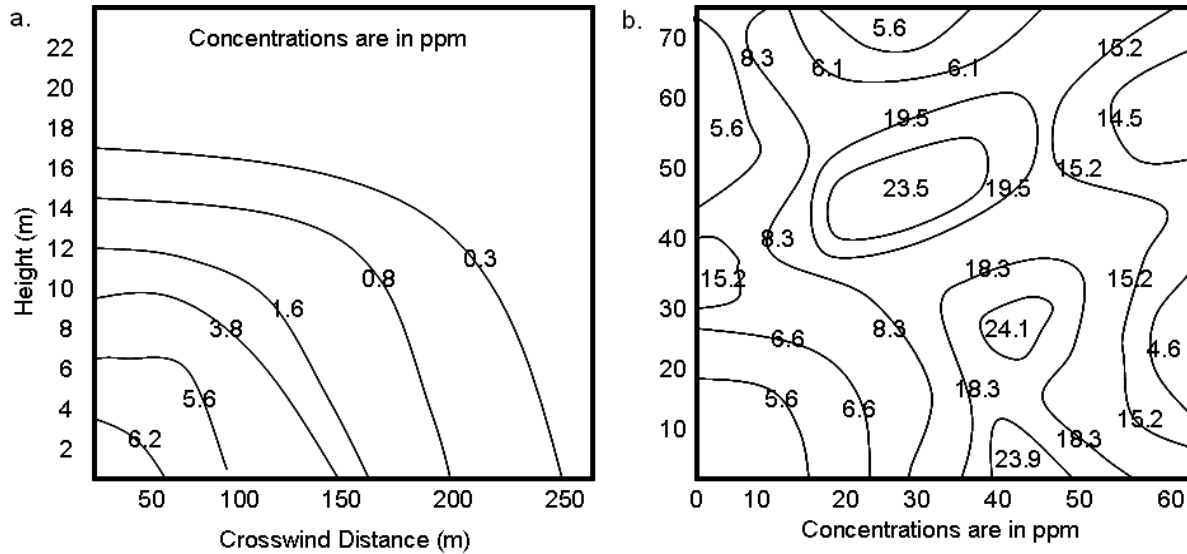


**Figure 3-4. Examples of RPM algorithm outputs. Panel a. corresponds to the VRPM output and panel b. is HRPM output.**

### **RPM-ORS Technologies**

Technologies appropriate for characterizing ground-level area sources and non-point emission sources such as landfills, lagoons, and industrial complexes; using RPM methodologies are: OP-FTIR, open-path Tunable Diode Laser Absorption Spectroscopy (OP-TDLAS), UV-DOAS, and DIAL. Each technology has its own strengths and limitations and, depending on the objective of the project, some are more effective than others. The following is a discussion of the conditions and requirements to deploy each technology.

OP-FTIR has an optical range of 100 – 500 m; it can detect multiple compounds simultaneously at high temporal resolution with detection limits in the ppb range. The instrument setup is time-consuming and it requires liquid nitrogen to cool the instrument, so OP-FTIR is best for campaigns that do not require constant relocation and multiple setups. Another consideration is that CO<sub>2</sub> and water are interfering species in FTIR measurements. OP-FTIR data must be processed to quantify path-integrated concentrations, so if real-time is needed, OP-FTIR is not the best choice. For more details about OP-FTIR technology see section 2.1.

OP-TDL has an optical range of up to 1 km. Depending on the topography and location of physical barriers at the survey area, the distance between the control box and the telescopes may require a

large amount of fiber optic cable, which can be difficult to deploy<sup>2</sup>. OP-TDL can detect CO, CO<sub>2</sub>, NO<sub>x</sub>, ammonia, methane (CH<sub>4</sub>) and hydrogen sulfide with detection limits in the ppb range, but can only detect one compound of interest at a time. The instrument can produce multiple beam paths, is lightweight, and is easily deployed. The OP-TDL generates real-time path-averaged concentration data in the field. When only a single gas is of interest, OP-TDL offers a cost-effective choice compared to OP-FTIR. OP-TDLAS has been used to monitor the exhaust from natural and mechanical ventilation systems used in houses, farms and other facilities. The technique has also been used to measure the flux from a traveling gun sprayer applying swine lagoon liquid to the farm field.<sup>4</sup> For more details about OP-TDLAS technology, see section 2.2.

UV-DOAS detects unstable species like radicals, nitrous acid, aromatic species, and BTX at low concentrations in the ppb levels. The UV-DOAS can be setup to scan multiple or single beam paths. For more details about UV-DOAS technology, see section 2.3.

### **Verification/Validation Studies**

The RPM algorithm's capacity to locate/identify sources of fugitive emissions and provide accurate measurement of emissions flux of fugitive emissions and area sources has been assessed in two different ways: (1) measurement of known concentration tracer gas releases and (2) comparison with the measurement results of selected instruments in collocated systems. RPM data is verified by assessing if the collected data satisfies the objectives of the study.<sup>1</sup> The following are several examples of studies performed to test RPM and the selected ORS instruments to survey fugitive emissions.

### **OP-FTIR and OP-TDLAS comparison studies**

During the Fort Collins measurement campaign<sup>8</sup>, methane measurements from two OP-FTIR instruments were compared.<sup>7</sup> Both OP-FTIR instruments contain a Nicolet bench, 12-inch telescope, and collected data at resolutions of 0.125 cm<sup>-1</sup>, 0.25 cm<sup>-1</sup>, 0.5 cm<sup>-1</sup>, 1 cm<sup>-1</sup>, 2 cm<sup>-1</sup>, 4 cm<sup>-1</sup>, and 8 cm<sup>-1</sup>. The data comparison showed that the instruments were extremely stable and reliable



for the duration of the campaigns. In separate studies, investigators used OP-TDLAS and OP-FTIR to compare methane measurements obtained by both instruments and found similar results.<sup>6,7</sup> During the experiments, the two instruments were deployed side-by-side and aligned to an identical mirror. Methane concentration data were collected with each instrument for a period of 30 minutes.<sup>7</sup> The results of the experiment found that methane concentrations measured with the OP-TDLAS were slightly higher (3 percent) than concentrations measured with the OP-FTIR instrument. These results are significant because they show that methane concentration data collected by the two instruments are comparable, and that both can be used interchangeably in RPM configurations:

### **OP-FTIR and UV-DOAS comparison: Colorado Springs field study**

The Colorado Springs field campaign occurred in September 2003 at a former landfill site as part of an effort to rehabilitate the site for recreational use. The current owners of the landfill and the State of Colorado requested assistance from the EPA to perform a site assessment to search for the presence of any fugitive gas emissions from the site. The study used OP-FTIR, OP-TDLAS, and UV-DOAS instruments. The UV-DOAS instrument was deployed at the site to collect data concurrently with the OP-FTIR instrument. The UV-DOAS detected the presence of BTX. The concentrations of toluene measured with the UV-DOAS instrument correlated well with gasoline concentrations measured with the OP-FTIR instrument during the same period.

### **VRPM plume capture validation study**

During June and July 2006 at Orange County Municipal Landfill, the EPA and ARCADIS performed a VRPM plume capture validation study. The objective was to capture the emissions from hot spots located a large distance upwind of the measurement configuration. The experimental design used OP-FTIR for VRPM measurements and a known concentration of tracer gas released to determine plume capture. The effectiveness of the RPM configuration in capturing plumes (horizontal and vertical planes) was evaluated by comparing the actual release rate of the tracer gas to the

calculated flux values as tracer gases were released at different distances upwind of the configuration. Releases were made at different distances; 20, 60, 100, and 140 m from the VRPM measurement plane. The study found that if there is no statistical significant difference between the averaged concentrations along each beam (i.e., no vertical concentration gradient), the VRPM configuration is not vertically capturing the plume. If the difference between the average concentrations along each beam is less than 10 percent (i.e., a slight vertical concentration gradient exists), the VRPM configuration is sufficiently capturing the plume from the upwind release point. If the difference between the average concentrations along each beam is greater than 10 percent (i.e. a substantial vertical concentration exists), the VRPM configuration is vertically capturing the plume from the upwind release point and the releasing location is not close enough to the maximum upwind location for complete plume capture.

### **Typical QA/QC**

This section describes the QA/QC activities that pertain to the RPM as described above. QA/QC activities normally depend on pre-determined data quality indicators that address the project unique objectives. The technologies used for RPM have their own specific QA/QC associated with the instruments. If interested in the technology QA/QC for OP-FTIR, refer to section 2.1; for OP-TDLAS, refer to section 2.2; and for UV-DOAS, refer to section 2.3.

The general QA/QC steps are: (1) equipment calibration, (2) assessment of DQI goals and (3) DQI check for analyte path-integrated concentration measurement. Each ORS instrument has its own calibration procedure as discussed in Chapter 2 of this Handbook, thus is important to follow the instrument's manufacturer instructions. DQI goals depend on the compound of interest and the expected concentration ranges, thus detection limits, accuracy, and precision need to be determined using appropriate traceable standards. On-site verification using a known concentration tracer gas release provides a sampling episode specific QC confirmation of test results.

Because meteorological data is part of RPM calculations, instruments used to measure ambient conditions need to be calibrated and their accuracy and precision tested regularly. Table 3-1 shows the recommended DQIs for the different aspects associated with the measurement of the path-integrated concentration and RPM.<sup>2</sup>

**Table 3-1. Data quality indicators for the QA/QC process, taken from EPA-OTM10**

| Measurement parameter | Analysis Method                              | DQI                             |
|-----------------------|--|---------------------------------|
| PI-ORS Instrument     | Instrument specific                          | Instrument specific             |
| Wind speed            | Side-by-side comparison of two wind monitors | Within 20%                      |
| Wind direction        | Comparison to magnetic north                 | Within 10%                      |
| Optical path-length   | Measure and compare to known path            | Within 2%                       |
| Beam angle            | Measure and compare known angle              | Within 2°                       |
| HRPM, VRPM and 1D-RPM | CCF*   | ≥0.8                            |
| VRPM flux measurement | Wind direction                               | -10° to +25° from perpendicular |
| 1D-RPM                | Peak location variability                    | Reconstructed peak locations    |

\* Concordance correlation factor (CCF) indicates the goodness of fit between measured and predicted path-integrated concentration,  $CCF = rA$ .

### **Siting Concerns**

Certain weather conditions such as rain, fog or snow can obscure the optical beam of the utilized instrument and affect its ability to continuously measure gaseous concentrations. Transient, but significant, obscuration can occur during heavy precipitation events, particularly with longer path measurements. This limits the sensitivity of the PIC measurements or the instrument's ability to collect data.<sup>2</sup>

Wind conditions can greatly affect the results of field measurements and should be taken into account when interpreting data. Calm wind conditions do not affect the HRPM methodology algorithm for hot spot source location. However, very low wind speeds are not ideal for the VRPM methodology for emission rate estimation, as the source plume may not be carried through the vertical plane in the absence of measurable wind. Very high wind speed conditions are not ideal

for any of the RPM methodologies. High winds may displace or vibrate the optical alignment of the components of the ORS system used in the setup, and affect the quality of the PIC values acquired in multiple beam paths. They may also cause displacement of any hot spot identified by HRPM. Based on controlled studies performed in the past, the following wind speed ranges are recommended for optimal results:

- HRPM methodology: Near 0 to 5 m/s
- VRPM methodology: 1 to 8 m/s
- 1D-RPM methodology: 1 to 8 m/s

In optimal conditions, the prevailing wind direction should be as close as possible to perpendicular to the VRPM measurement plane. The wind direction needs to be determined for each field study measurement configuration. These requirements present a challenge when determining sites and setup locations. HRPM data should be collected for at least one hour in ideal conditions, which can be difficult when considering locations with highly variable conditions.

### **Strengths and Limitations**

Strengths of RPM-ORS are the ability to measure high time resolution and spatially distributed emission data, directly calculate emission rates, capture the distribution of all major emissions in an area and isolate emissions from specific measurement areas. Depending on the ORS instrument, it can provide real-time PIC data for multiple compounds simultaneously. RPM is limited because it relies on good wind conditions, it has difficulties characterizing emissions from complex terrain, and has larger uncertainty when capturing emissions for sources located a large distance upwind of the VRPM configuration. Depending on the RPM-ORS instrument used, some ambient compounds cause interferences. No ORS instrument can measure all the possible compounds of interest, which may create the need for two systems depending on the experimental design. A summary of these strengths and limitations is presented in Tables 3-2 and 3-3.

**Table 3-2. Summary Table of the VRPM’s Strengths**

| Feature                  | Strength  |
|--------------------------|---|
| Measurement Capabilities | Measures high time resolution and spatially distributed emission data.  |
|                          | Directly calculates emission rates.   |
|                          | Characterizes the distribution of all major emissions in a large area and isolates emissions from specific areas. |
|                          | May provide real-time PIC data depending on the technology used.  |

**Table 3-3. Summary Table of the VRPM’s Limitations**

| Feature                   | Limitation   |
|---------------------------|--|
| Meteorological Challenges | Characterization is reliant on optimal wind conditions.  |
| Interferences             | Each OP technology used has its own interferences that must be considered.                         |
| Topographical Concerns    | Difficulties associated with characterizing a plume from complex terrain (e.g., a side slope)      |
|                           | Large uncertainty when capturing emissions from sources a large distance upwind of the VRPM Setup. |

**References**

1. Thoma, E. D., Green, R. B., Hater, G. R., Goldsmith, C. D., Swan, N. D., Chase, M. J. Hashmonay, R. A. 2009. Development of EPA OTM 10 for Landfill Applications. Journal of Environmental Engineering, 10.1061/(ASCE)EE.1943-7870.0000157.
2. U.S. EPA. 2006. ORS Protocol, Optical Remote Sensing for Emission Characterization from Non-Point Sources. June 14.
3. Hashmonay, R. A., R. M. Varma, M. T. Modrak, R. H. Kagann, R. R. Segall, and P. D. Sullivan. 2008. Radial Plume Mapping: A US EPA Test Method for Area and Fugitive Source Emission Monitoring Using Optical Remote Sensing, Advanced Environmental Monitoring. 2:21 – 36.
4. U.S. EPA. Using Tunable Diode Lasers to Measure Emissions from Animal Housing and Waste Lagoons. <<http://www.epa.gov/ttn/chief/conference/ei16/session12/harris.pdf>>.

5. Hashmonay, R.A., and M.G. Yost. 1999. Innovative approach for estimating fugitive gaseous fluxes using computed tomography and remote optical sensing techniques. *J. Air Waste Manage. Assoc.*, 49: 966- 972.
6. Thoma, E.D., R.C. Shores, E.L. Thompson, D.B. Harris, S.A. Thorneloe, R.M. Varma, R.A. Hashmonay, M.T. Modrak, D.F. Natschke, and H.A. Gamble. 2005. Open-Path Tunable Diode Laser Absorption Spectroscopy for Acquisition of Fugitive Emission Flux Data; *Journal of Air and Waste Management Association*. 55: 658-668.
7. Modrak, M. T.; Hashmonay, R. A.; Varma R.; Kagann, R. 2005. Evaluation of Fugitive Emissions at a Brownfield Landfill in Ft. Collins, Colorado Using Ground-Based Optical Remote Sensing Technology. EPA-600/R- 05/042. U.S. Environmental Protection Agency, Research and Development, Work Assignment No. 0-025. March.

### 3.2 Range Resolved Measurements using Differential Absorption LIDAR

The term "range resolved," refers to vertical and horizontal profiles of concentrations for compounds of interest coupled with meteorological parameters. Generally, range resolved measurements are performed to study emission rates and fate and transport of the compounds of interest. LIDAR technology is often paired with the DIAL application to measure range resolved concentrations of trace species in the atmosphere. DIAL has been used to monitor pollution species in the lower atmosphere such as water vapor, NO, O<sub>3</sub>, SO<sub>2</sub> and CH<sub>4</sub>.<sup>1</sup> DIAL can also be used to measure O<sub>3</sub> concentrations in the middle and high troposphere.<sup>1</sup> Atmospheric temperature measurements are possible by the DIAL technique if the absorption line selected is temperature-dependent.<sup>1</sup>

#### General Description of Approach

Range resolved measurements of plume flux typically employs some technology to measure a surrogate gas in the plume to estimate the concentration of compounds of interest. DIAL is a dual-wavelength, elastic (the atom absorbs the photon and instantly emits another photon at the same frequency), backscatter LIDAR that transmits one wavelength at the absorption line of the target compound ( $\lambda_{on}$ ) and one wavelength slightly off-line ( $\lambda_{off}$ ) of the target compound to measure backscatter ( $\lambda_{off}$ ). The on-line wavelength is absorbed by the gas of interest, while the off-line wavelength is not absorbed as shown in Figure 3-5.<sup>2</sup>

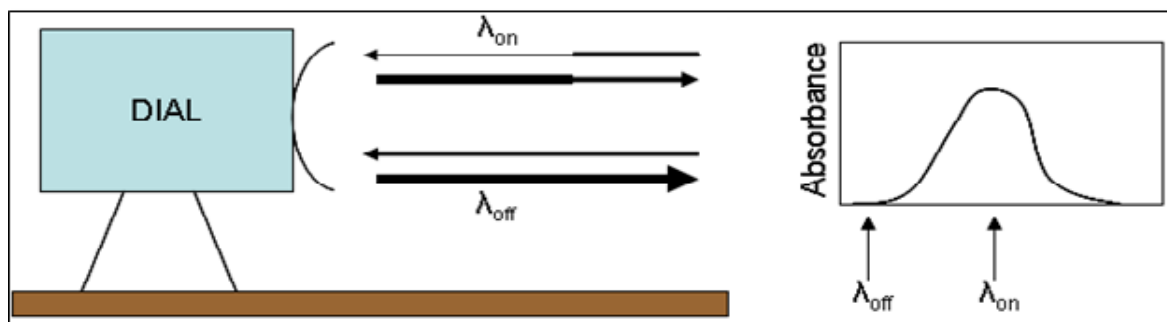


**Figure 3-5. Conceptual picture on the operation of DIAL.**

The differential absorption between the two wavelengths is a measure of the concentration of the gas as a function of range.<sup>2</sup> DIAL can provide a 2-D measure or “contour” of concentrations across a scanning plane. By combining this concentration contour with separately obtained wind speeds, a contaminant flux can be calculated for the measured compound<sub>3</sub>, see Figure 3-6.<sup>3</sup>

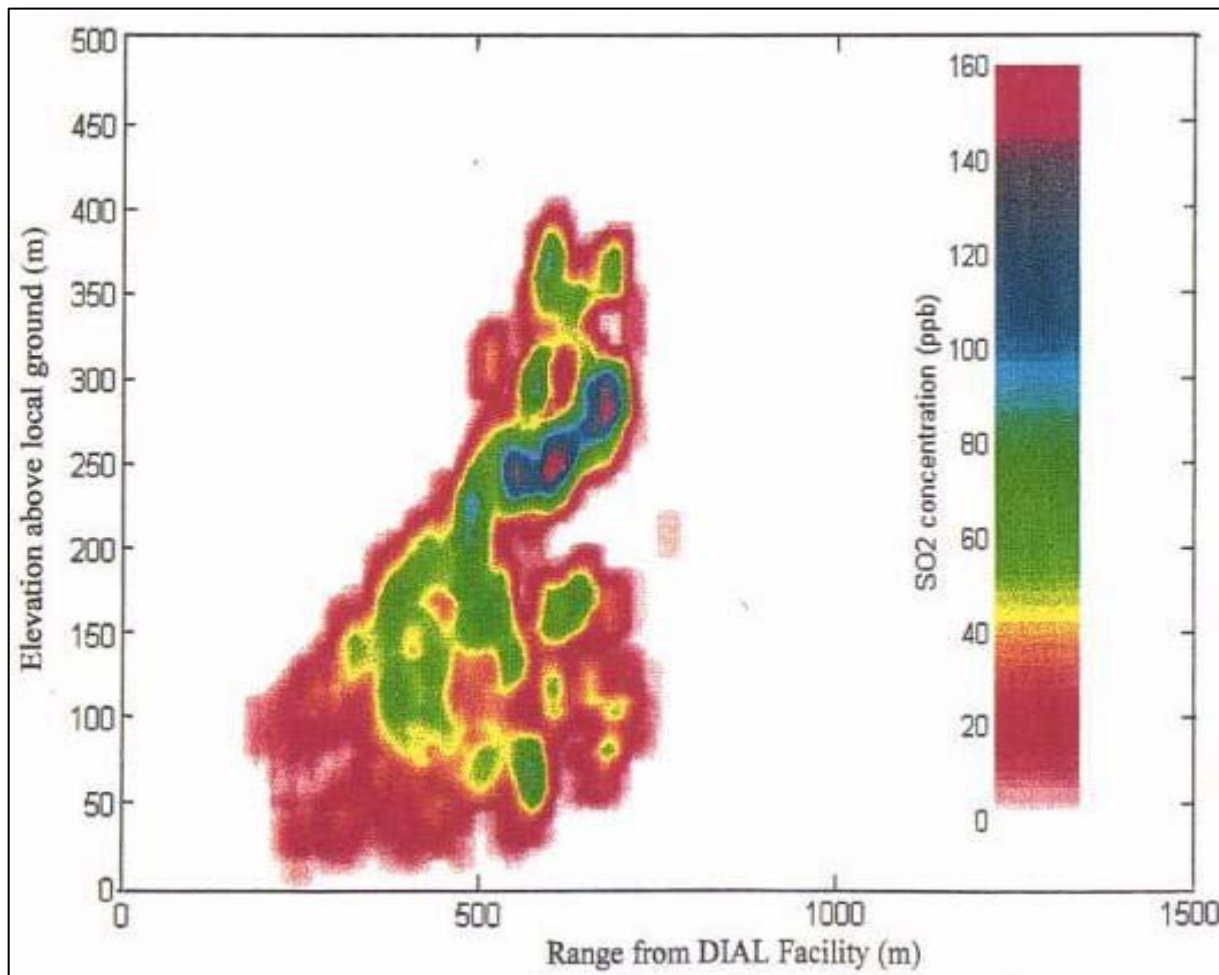


**Figure 3-6. Contour profile of SO<sub>2</sub> concentration measured 2.1 km downwind of source, at Cement Works, by Environmental Measurements Group National Physical Laboratory, UK.**

#### **Basic DIAL algorithm to calculate backscatter**

The number of photons backscattered correlates to the compound concentration. The basic equation to calculate number of photons backscattered per unit solid angle due to scattering of type *i* (forms of radiation like light, sound) is:



$$P\tau_t(\lambda_l) \int_{R_1}^{R_2} \tau_a(r, \lambda_l) \sigma_{\pi}^i(\lambda_l) N^i(r) dr$$

Where:

$\lambda_l$  = wavelength

$\tau_t$  = transmission coefficient of the LIDAR transmitter optics

$r$  = range interval

$\tau_a$  = optical transmission of the atmosphere

$\sigma_{\pi}^i$  = backscatter cross section at the laser wavelength

$N^i(r)$  = number density of scattering centers at range  $r$ .

However, to calculate the number of photons incident on the collecting optic of the LIDAR due to scattering of type  $i$ , one must consider the area of the collecting optic ( $A$ ):

$$P\tau_t(\lambda_l)A \int_{R_1}^{R_2} \frac{1}{r^2} \tau_a(r, \lambda_l) \tau_a(r, \lambda_s) \zeta(r) \sigma_{\pi}^i(\lambda_l) N^i(r) dr$$

Where:

$\lambda_s$  = wavelength of the scattered light

$\zeta(r)$  = overlap factor

There are two typical types of detectors: photomultiplier and analog. When using photomultiplier detectors, the number of photons detected is:

$$P\tau_t(\lambda_l)A\tau_t(\lambda_s)Q(\lambda_s) \int_{R_1}^{R_2} \frac{1}{r^2} \tau_a(r, \lambda_l) \tau_a(r, \lambda_s) \zeta(r) \sigma_{\pi}^i(\lambda_l) N^i(r) dr$$

Where:

$\tau_t$  = transmission coefficient of the reception optics

Q = quantum efficiency of the photomultiplier

Quantum efficiency refers to the percentage of photons incident (hitting) the receiver (photo reactive surface) and it measures the LIDAR electrical sensitivity to light. When using analog detectors, the equations replace the quantum efficiency of the photomultiplier by the gain of the photomultiplier ( $G(\lambda_s)$ ) combined with the gain of any amplifiers used. After some approximations, the analog detector version of equation is:

$$P\tau_t(\lambda_l)A\tau_t(\lambda_s)Q(\lambda_s)\tau_a(R, \lambda_l)\tau_a(R, \lambda_s)\frac{1}{R^2}\zeta(R)\sigma_\pi^i(\lambda_l)N^i(R)\delta R$$

Where:

R = range of the center of the scattering volume

### **Verification/Validation Studies**

This section presents studies designed to validate the DIAL technique under various conditions. Some studies aim to verify that the applications can provide accurate results, thus most of these studies will have other technologies to compare measured concentrations and emission rates.

### **Verification of DIAL for Gas Species Measurements**

DIAL has been validated in European studies<sup>5,6</sup> for hydrocarbon emissions with calculated results ranging from  $\pm 3$  to  $\pm 12$  percent of the actual value.<sup>3</sup> Two validation studies were performed in Alberta with measured fluxes agreeing within +1 to -10 percent of the known source.<sup>3</sup> Over a four-week period during May-June 2003 in Alberta, Canada, DIAL surveys were performed at four gas processing plants, one gas well test site located in the foothills, and two solution gas flare sites. The objective of this project was to field test DIAL technology as a means to:

- monitor ambient SO<sub>2</sub> concentrations in the vicinity of sour gas well test flares and track

the SO<sub>2</sub> plume position,

- measure the combustion efficiency of well test and solution gas flares,
- measure fugitive emissions of methane and other hydrocarbons from gas processing facilities.<sup>6</sup>

The DIAL measurements were performed by Spectrasyne Ltd., UK. When measuring plume concentration profiles, Spectrasyne generally located the DIAL equipment at least 50 meters from the area of interest and relative to the plume source and wind direction so scans could be taken roughly at right angles to the direction of plume travel.<sup>6</sup> Often meteorological changes make this impossible and the measurements were taken at an oblique angle, which results in profiles that appear stretched in the horizontal direction.<sup>4</sup>

The DIAL system included two DIAL lasers, one emitting in the IR range and one in the UV range, and a self-contained weather station for measuring wind speed and temperature. Meteorological parameter data is used in mass rate calculations to reprocess the data to account for the angle relative to the plume direction.<sup>4</sup> With this system, total contaminant flux can be calculated and portions of the plume assigned to specific sources.<sup>4</sup>

The accuracy of the DIAL system was checked by comparing SO<sub>2</sub> mass emissions calculated from the DIAL measurements of the SO<sub>2</sub> plume with SO<sub>2</sub> mass emissions calculated from gas plant CEM instrumentation installed in the incinerator stack.<sup>4</sup> Direct comparison between DIAL and fence line point source concentration measurements is not possible, since the DIAL measures gas concentration in a relatively large volume in the atmosphere against a point sampling type instrument such as a gas chromatograph.<sup>4</sup> However, the combination of point source measurements for a target compound, combined with meteorological data and dispersion modeling, can provide comparisons useful to verify the DIAL results. Table 3-4 shows some of the results, the scan time, and calculated fluxes for the DIAL and point source. The DIAL and point measurements showed a difference of 11 percent, which is within the range of -18 to +5 percent

from other calibration studies performed by Spectrasyne Ltd.<sup>6</sup> According to this Spectrasyne study and others, DIAL plume measurements generally underestimate the total mass because some areas of the plume contain compound concentration below DIAL’s detection limit and are not included in the plume mass. Additional variability among DIAL measurements is believed to originate from variation in wind speed and direction, combined with the 4 - 20 minutes required to do a full DIAL scan across the plume.

**Table 3-4. Results from the comparison of DIAL and plant measurements of SO<sub>2</sub> mass emissions**

| SCAN NUMBER | SCAN TIME   | WIND SPEED (M/S) | WIND DIRECTION (DEG)       | SO <sub>2</sub> FLUX (KG/HR) |
|-------------|-------------|------------------|----------------------------|------------------------------|
| 1           | 12:37-12:48 | 5.2              | 331                        | 372                          |
| 2           | 13:00-13:21 | 2.2              | 350                        | 223                          |
| 3           | 13:31-13:51 | 4.3              | 346                        | 394                          |
| 4           | 14:00-14:04 | 5.6              | 359                        | 196                          |
| 5           | 14:07-14:19 | 3.9              | 359                        | 145                          |
| 6           | 14:42-14:51 | 4.0              | 350                        | 333                          |
| 7           | 15:10-15:21 | 3.9              | 0                          | 394                          |
|             |             |                  | Time Weighted Mean of DIAL | 304                          |
|             |             |                  | <b>Plant Data</b>          | <b>340</b>                   |

*Note: collected on May 26 about 190 m downwind of incinerator stack. Adapted from Chambers, 2003.*

### **Typical QA/QC**

This section describes the QA/QC steps that pertain to the applications described above. QA/QC steps for applications normally depend on pre-determined data quality indicators that address the project unique objectives. The technology used for the applications presented above have their own QA/QC associated to specifics of the instruments. If interested in the technology QA/QC for DIAL, refer to section 2.4.

DIAL measurements are typically verified by running two collocated DIAL systems or one DIAL system along with another ORS instrument, like FTIR or CRDS. Arcadis has verified DIAL measurements using OTM10 and developed QA/QC information for conducting DIAL measurement projects.<sup>7</sup> However, as noted in OTM10, the unique setup of DIAL requires project specific QA/QC steps with data quality indicators that meet study objectives.

### **Siting Concerns**

The DIAL equipment, optical housing, electronics, computer equipment and other components require a climate control enclosure such as a trailer or an aircraft. Therefore, the operating temperature is controlled to human comfort level  $\sim 22^{\circ}\text{C}$ . Trailers require relatively flat surfaces and road access. Changing weather conditions, physical interferences like buildings, trees, traffic and changing terrain, and interfering chemical species at certain wavelengths will increase variability in the measurement and possibly result in less accurate results.

### **Strengths and Limitations**

The most significant limitation to DIAL application is the cost and limited availability of measurement systems. Multiple measurements in North America have relied on importing the instrumentation from the United Kingdom.<sup>4,5,6</sup> Additionally, the number of chemical species measurable by DIAL is restricted to those that are detectable by the Lidar technology. The most notable strength of a DIAL system is the ability to quickly resolve pollutant concentrations in two dimensions. Concentration gradient data obtained in short periods of time enables DIAL to be deployed in many applications and a number of configurations. Tables 3-3 and 3-4 summarize these strengths and limitations.

**Table 3-5. DIAL Strengths**

| Feature                     | DIAL Strengths   |
|-----------------------------|--|
| Measurement Capabilities    | DIAL provides spatially resolved pollutant concentration in two dimensions |
|                             | Measurements are provided in a relatively short period of time.            |
| Flexibility                 | DIAL is deployable in many different applications and configurations.      |
| High intensity light source | The ability to measure longer path lengths (1 to 3 km)                     |

**Table 3-6. DIAL Limitations**

| Feature                          | Dial Limitations   |
|----------------------------------|--|
| Limited Availability and Expense | Due to limited availability, DIAL systems used in North America are typically imported, which increases the expense of using DIAL for measurements.  |
| Range of Measurement             | Chemical species that can be characterized and limited to those compounds with the unique chemical properties required to be detected by the LIDAR instrument. Only a few wavelengths are measured; spectral artifacts cannot be fixed or investigated |

**References**

1. Argall, P. S. and R. J. Sica. 2002. LIDAR in the Encyclopedia of Imaging Science and Technology. J.P. Hornak John Wiley & Sons Inc., New York. January.
2. Argall, P. S. and R. J. Sica. 2003. LIDAR in The Optics Encyclopedia. Wiley-VCH, New York, NY.
3. Robinson, R. 2006. The Application of DIAL for industrial emissions monitoring. Presentation at the VOC Fugitive Losses: New Monitors, Emission Losses, and Potential Policy Gaps, 2006 International Workshop. Office of Air Quality Planning and Standards, Research Triangle Park and Office of Solid Waste and Emergency Response, Washington, DC. October 25 – 27.
4. Chambers, A. 2003. Well Test Flare Plume Monitoring Phase II: DIAL Testing in Alberta. Alberta Research Council Inc. Prepared for Canadian Association of Petroleum Producers.

<<http://www.ptac.org/env/dl/envp0402fr.pdf>>.

5. Chambers, A., M. Strosher, T. Wootton, J. Moncrieff. and P. McCready. 2008. Direct measurement of fugitive emissions of hydrocarbons from a refinery. *Journal of the Air and Waste Management Association*. 58: 1047-1056. doi: 10.3155/1047-3289.58.8.1047.
6. Chambers, A. K., M. Strosher, T. Wootton, J. Moncrieff, and P. McCready. 2006. DIAL Measurements of Fugitive Emissions from Natural Gas Plants and the Comparison with Emission Factor Estimates.
7. <<http://www.epa.gov/ttn/chief/conference/ei15/session14/chambers.pdf>>.

### **3.3 Solar Occultation Flux Measurement**

Characterizing and quantitatively measuring fugitive VOC emissions from non-point sources are challenging. The ability to accurately calculate the flux rate of VOC emissions from large area sources such as landfills, refineries, waste retention ponds, process areas, and product holding tanks is highly pursued by government and industry alike. The development and advancement of optical measurement technologies have increased environmental VOC monitoring capabilities and are applied in many new monitoring methods. SOF is a method where optical spectroscopic technologies are used to directly speciate and quantify the chemicals present in a gaseous emission plume using the sun as a light source.

Because the SOF method uses the sun as a broadband light source, the target compound possibilities are limited only by the detection equipment and interferences. Depending on the spectrometer used, the SOF can detect many different gaseous species, even at the same time, including: ammonia, formaldehyde, VOCs, terpenes, vinyl chloride, CO, ethylene, ethylene oxide, hydrofluoric acid, (HF) hydrochloric acid, HCl, CH<sub>4</sub>, SO<sub>2</sub>, propane, propylene, and hydrocarbons up to C<sub>15</sub>.<sup>1,2</sup> Due to the ease of mobility with the SOF method, the technique can be used in applications such as total CO columns of megacities, petrochemical industries, agriculture, refineries, ships, and volcanoes.<sup>3</sup>

Volcanic emissions research is a rich source of information on monitoring techniques to determine emission rates of fugitive gases in atmospheric plumes including SOF. Several measurement techniques have been employed to measure volcanic gases such as SO<sub>2</sub> (i.e., correlation spectrometer (COSPEC), DOAS, and DIAL). However, the SOF method was developed to improve volcanic activity forecasting capabilities because multiple gas species can be detected using passive FTIR, and direct flux measurements can be made based on movement of the instrument view through the emissions plume.<sup>4</sup>

Environmental applications of the SOF technique have previously focused on measuring fugitive VOCs from oil refineries and industry processes.<sup>5</sup> VOC gases emitted from these source types



mostly consist of alkanes, alkenes, and some aromatic compounds.<sup>5</sup> These fugitive VOCs have historically been measured using the DIAL method.<sup>6</sup> The DIAL method, described in Chapter 3.2 of this Handbook, employs short laser pulses directed through the gas plume at different wavelengths to calculate mass flux measurements by multiplying the resulting concentration integrated over the plume cross section at different angles by the wind speed.<sup>7</sup> However, DIAL is rather complex and expensive relative to SOF and is not ideal for periodic regulatory monitoring.<sup>7</sup> In comparison to DIAL, the SOF technique uses solar broadband IR or UV/visible spectral radiation as the light source instead of a laser source, making the SOF method potentially more cost-effective, faster than DIAL, and easier to automate.<sup>7</sup> From the solar spectra, it is possible to retrieve the PIC (molecules/cm<sup>2</sup>) of VOCs between the sun and the spectrometer.<sup>8</sup> Multiplying this PIC by the local wind speed results in the mass-flux of target VOCs through the area.

Agricultural application studies have established that the SOF method has a detection limit for measured hydrocarbons of 0.3 mg/ meter <sup>2,3</sup>. Similarly, in applications pertaining to refineries and leak detection, studies conclude that a point source emission of measured hydrocarbons at 0.5 kg/ hour can be measured 50 meters downwind with a precision of three percent and an accuracy of 30 percent.<sup>1</sup> For simple sources and several traverses, it has been found that the accuracy can be better than 10 percent. Under more complicated conditions, with emissions occurring from a complex structure with an unknown plume lift, larger systematic errors will occur, primarily due to uncertainties in assessing the plume lift and the associated wind field. Uncertainty in the wind speed in more complex terrain and wind stability can be 15 – 30 percent. Consequently, the accuracy in the SOF method depends on the amount of error associated with the ancillary meteorological measurements which can dominate the uncertainty in the emissions results.<sup>1,3</sup>

### **General Description of Approach**

There are three main components to the SOF system: an FTIR spectrometer to capture solar radiation spectra, a sun tracker to maintain instrumental orientation to the solar zenith, and a GPS for accurate measurement location relative to the gas plume.<sup>5</sup> Two different sun tracker configurations are shown in Figure 3-7, and a rough schematic of the entire SOF system is provided in Figure 3-8<sup>1</sup>.

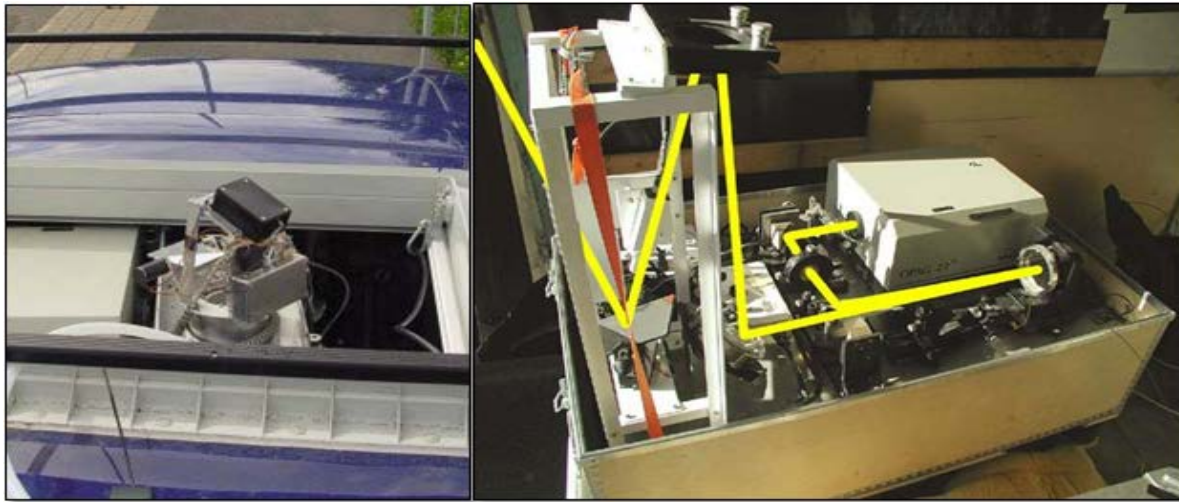


**Figure 3-7. Solar tracker configurations**

Note: The left panel shows the sun tracker and mirrors extending out the top of the vehicle to maintain orientation<sup>9</sup> while the right panel shows the path of the sunlight (in yellow) first striking the mirror of the solar tracker before being directed into the spectrometer<sup>5</sup>

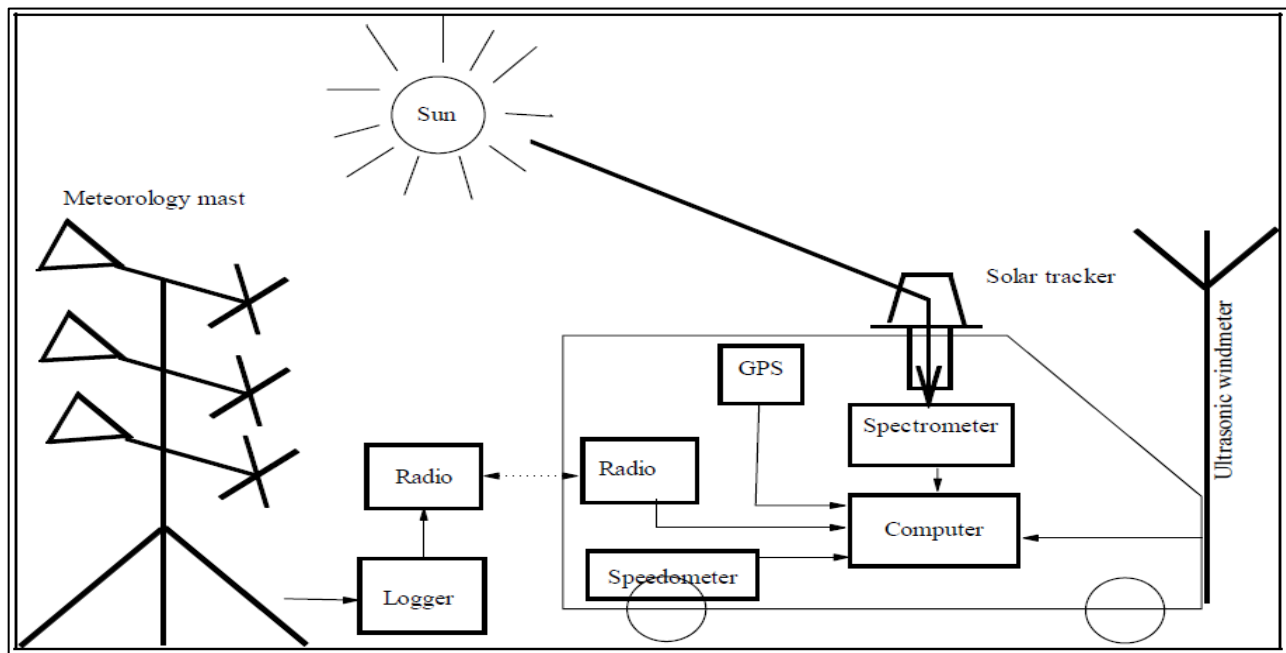


**Figure 3-8. Rough overview of a mobile SOF system.**

Flux measurements are difficult to measure in an atmospheric plume using stationary instrumentation. Figure 3-9 illustrates the capture of a complete plume transect for better constrained source flux calculations using the SOF technique. In the illustration of Figure 3-9<sup>9</sup>, the solar tracker maintains the solar zenith, reflecting the solar light into the spectrometer regardless of the vehicle position as it traverses the width of the plume column.<sup>1,9</sup> As previous methods

combined stationary plume measurements with dispersion modeling or tracer gas ratios, the mobile aspect of the SOF technique allows for direct measurements of gaseous flux emissions if the full plume column is captured.<sup>3</sup>

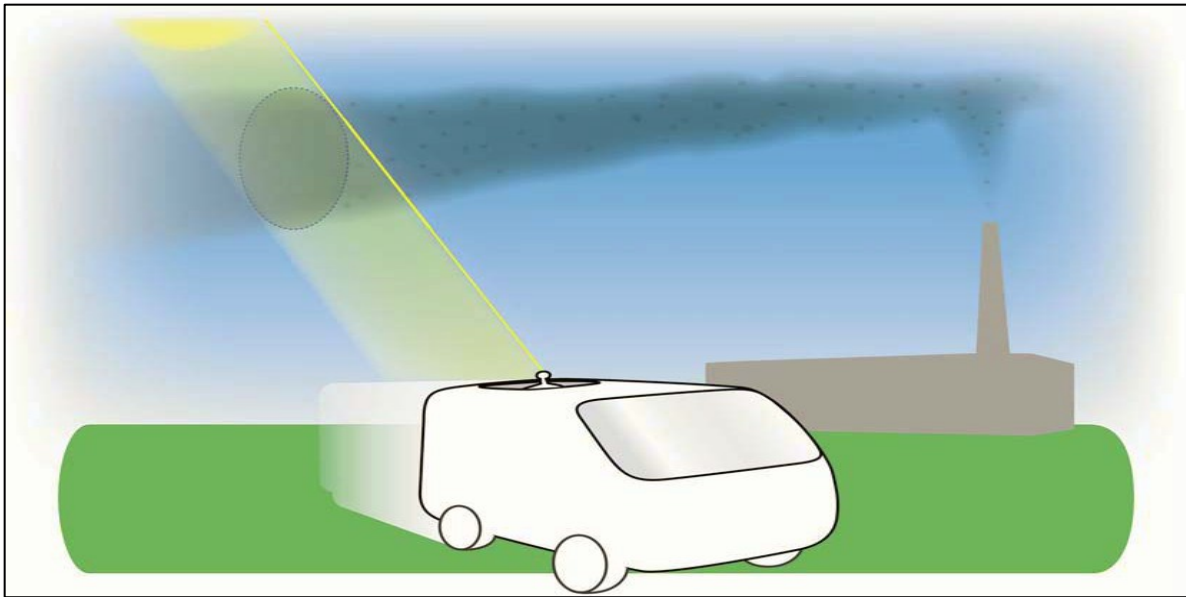


**Figure 3-9. Solar Occultation Flux method. The instrument is placed in a vehicle which travels across the gas plume to capture the plume cross-section (Illustration Karin Sjöberg).**

Each gaseous compound absorbs energy at different wavelengths, usually more than one, depending on vibrational and rotational excitement within the molecule. Fundamentally, this measurement is a passive form of IR or UV spectroscopy. Therefore, each compound has its own “signature” of bands from which energy may be absorbed. Each band is highly selective, with virtually no absorption occurring outside of a specific wavelength. When molecules intercept the solar radiation before it reaches the detector, the molecular absorption is an extinction (or occultation) of the solar radiation intensity at the signature wavelengths. Once a compound has been identified, its spectrum can also be used to measure the compound’s concentration because the amount of radiation absorbed from the solar ray is proportional to the concentration of the compound in the sample or open path. According to the Beer-Lambert law, there is a linear relationship between absorbance and concentration as shown in Equation below<sup>1</sup>:

$$A = \epsilon * c * l$$

Where:

- $\epsilon$  = absorption coefficient
- $c$  = sample concentration
- $l$  = sample path length

SOF measurements acquired from within the plume column are divided by a reference (background) spectrum recorded outside the plume. This prevents any background sources— such as the atmosphere, inherent structures of the sun, and instrument functionality—from interfering with accurate measurements.<sup>5</sup> Multiple species are simultaneously evaluated for each spectral acquisition using non-linear, least-squares fit routines with published reference spectra from HITRAN 2000, Pacific Northwest National Laboratory, National Institute of Standards and Technology, and Hanst library databases.<sup>7</sup> The resulting spectra are evaluated for gas species absorption intensity to determine concentration using Equation below:

$$I_m(\nu) = I_L(\nu) * \exp\left(-\nu^4 * \alpha_R * L_R - \alpha_{Mie} * L_{Mie} - \sum_i \sigma_i(\nu) * conc_i * L_i\right)$$

Where:

$I_m(\nu)$  = light intensity at each wave number  $\nu$  after it has passed through the gas

$I_L(\nu)$  = light intensity at each wave number  $\nu$  for the light source

$\sigma_i(\nu)$  = absorption cross section ( $\text{cm}^2/\text{molecule}$ ) fo the gas with index  $i$ .

$L_i$  = path length where the gas with refractive index  $i$  is present

$conc_i$  = concentration of the gas with refractive index  $i$  ( $\text{molecules}/\text{m}^3$ )

$\alpha_R L_R$  = Rayleigh scattering which occurs on particles and molecules with a size smaller than the wavelength of the light

$\alpha_{Mie} L_{Mie}$  = Mie scattering which occurs on particles and molecules with a size about equal to the wavelength of the light

The PIC is determined by evaluating spectrum measurements individually along a path of continuous analysis to derive the line-integrated concentration represented by each spectrum. GPS measurements taken at the beginning and end of each measured spectrum determine the surface length represented by the spectrum. This value is then multiplied by the line-integrated concentration and summed over the total plume transect to calculate the PIC. An example of this process is shown in Figure 3-11.<sup>8</sup> Multiplying this PIC by the local wind speed results in the mass-flux of target VOCs through the measurement plane.

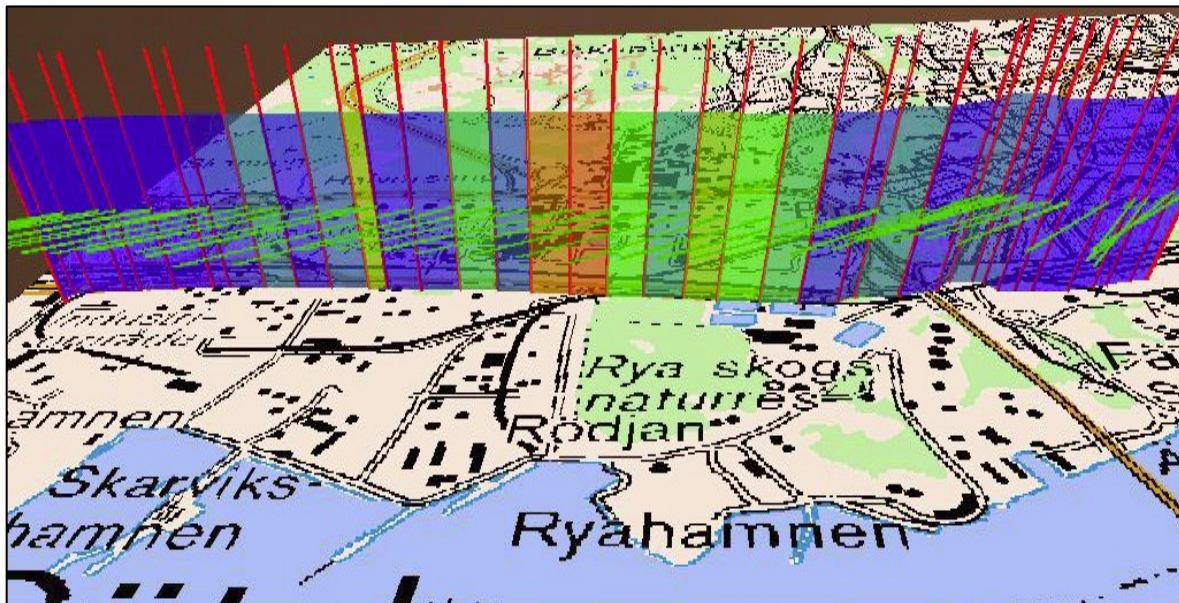


**Figure 3-10. An example of path-integrated calculations determined from SOF measurements.**

*Note: The red lines indicate individual spectra, the area between the red lines correspond to the surface-integrated concentration, and the green lines illustrate the wind direction vector<sup>8</sup>*

As shown in Figures 3-9 and 3-10, SOF mobile measurements are made crosswind and near downwind (about 0.5 to 3 km) from the target source. The total cross-sectional mass of key species is obtained by summation of all the species measurements over the plume traverse.<sup>10</sup> The process of determining the emissions flux is summarized mathematically by the Equation below. The assumption that the wind speed is equivalent to the gas plume velocity is necessary for both the DIAL and SOF techniques as this value is required to calculate the mass flux by multiplying the plume velocity by the cross-sectional integrated gas concentration<sup>5</sup> Therefore, both methods will

be susceptible to the same measurement error associated with the wind speed parameter.

$$Emission = \int_{x_1}^{x_2} column(x) \cdot \bar{u} dx$$

Where:

Column(x) = the total column at distance x across the plume

$\bar{u}$  = average wind speed for plume at plume height

### Verification/Validation Studies

Because DIAL measurements are a standard method of monitoring VOC emissions at refineries in Europe, performed a comparison between the results of the two different methods during a 2001 SOF field study.<sup>5</sup> SOF measurements by this group were made at the Preem refinery in Göteborg, Sweden for four days starting August 1, 2001. DIAL emissions measurements from 1995 and 1999 were recalculated with the annual average wind speed to compare with the 2001 SOF results; this comparison is shown in Table 3-7.<sup>1</sup>

**Table 3-7. SOF technique VOC emissions compared to DIAL.**

| Area            | SOF (no of scans)<br>2001 | DIAL 1999                  | DIAL 1995                  |
|-----------------|---------------------------|----------------------------|----------------------------|
| Crude oil tanks | 56 ±16 (8)                | 56 (wind normalised 4 m/s) | 62 (wind normalised 4 m/s) |
| Process plant E | 54 ±19 (7)                | 52                         | 56                         |
| Process plant W | 20 ±5 (5)                 | 35                         | 7.5                        |
| Water treatment | 19 ±3 (3)                 | 25                         | 11                         |

Although comparing environmental data that is up to six years apart is not recommended, the data in Table 3-7 shows that the emissions measured using SOF are generally consistent with previous DIAL results.<sup>1</sup> Regardless of the amount of measurement error imposed on the SOF result by wind speed approximations, all SOF measurements either match a previous DIAL result exactly or are very near to the average of the 1995 and 1999 DIAL results.

Annual VOC emissions from the Port of Göteborg were reported to be 1100 tons in 1999 and 2300 tons in 1995 by Shell Global Solutions and Spectrasyne, respectively. Researchers used an SOF system mounted on a ship to calculate an annual flux of 1770 tons per year based on two

measurements—that were not temperature corrected—performed on the same day in August 2001.<sup>5</sup> Again, more than two measurements on a variety of days distributed throughout the year would yield a more accurate snapshot of annual emissions. Nonetheless, a result of 1770 tons per year is almost the exact equivalent to the average of the reported 1999 and 1995 values and is a satisfactory result, validating the application of SOF to measure oil refinery gas emissions flux.

The results from two tracer gas correlation studies plus other validation studies were discussed by researchers<sup>3,8</sup> During these studies, sulfur hexafluoride ( $\text{SF}_6$ ) was released in an open field and from the roof of a crude oil tank at the previously mentioned Göteborg refinery in May and June of 2002. Each experiment released  $\text{SF}_6$  at a rate of about 2.0 kg/h. Tables 3-8 and 3-9 display the results from the open field and tank roof tracer experiments, respectively.<sup>8</sup> As shown in Table 3-8, tracer correlation measurements over four days in an open field validated that the SOF method can accurately retrieve emissions flux measurements within  $\pm 20$  percent error; whereas crude oil tank measurements done on a single day shown in Table 3-9 yields emissions flux measurements with up to 50 percent error.<sup>3,8</sup> It is worth noting that the crude oil tank measurements were conducted in the near field as opposed to a medium or far distance from the emission source in addition to being conducted on only one day. Figure 3-12 illustrates a combination of both scenarios where a tracer experiment in an open field resulted in 72 percent agreement (within 20 percent) of SOF measurements to the actual tracer gas emission, while other measurements can vary up to 50 percent from the actual emission.<sup>1</sup> When averaged together, however, the resulting value is within three percent of the actual emission rate.

**Table 3-8. Summary for measurements on the Åby field, 2002.**

| Day     | Emitted SF <sub>6</sub> | Calculated Average (kg/h) | Number of Accepted Traverses | Ave. Wind Speed (m/s) | Ave. Wind Direction | Error |
|---------|-------------------------|---------------------------|------------------------------|-----------------------|---------------------|-------|
| May 22  | 1.92                    | 2.3±1.3                   | 4                            | 4.9-8.6               | 152°-169°           | 20 %  |
| May 23  | 1.97                    | 2.2±0.6                   | 15                           | 3.9-5.6               | 120°-142°           | 10 %  |
| June 03 | 1.97                    | 1.6±0.9                   | 16                           | 2.7-5.3               | 235°-273°           | -20 % |
| June 04 | 1.89                    | 2.0±1.4                   | 9                            | 5.9-7.8               | 152°-191°           | 5 %   |

**Table 3-9. SOF traverse done on day 24-June 2002. True emitted SF<sub>6</sub> was determined to be 2.0 kg/hr.**

| Time    | Emission SF <sub>6</sub> | Ave. Wind Speed (m/s) | Ave. Wind Direction |
|---------|--------------------------|-----------------------|---------------------|
| 12:45   | 3.1                      | 6.5                   | 252°                |
| 12:54   | 1.8                      | 7.2                   | 252°                |
| 13:05   | 1.3                      | 6.0                   | 259°                |
| 13:17   | 2.7                      | 7.5                   | 253°                |
| 13:29   | 3.1                      | 5.4                   | 255°                |
| 13:56   | 5.2                      | 7.4                   | 264°                |
| 14:05   | 3.7                      | 7.4                   | 251°                |
| 14:24   | 2.6                      | 7.3                   | 262°                |
| 14:31   | 3.4                      | 6.5                   | 260°                |
| Average | 3.0 ± 1.1                |                       |                     |

The results from these studies indicate that multiple measurements in the mid to far field over multiple days are more representative of overall flux rates and reduce the amount of total measurement error. Having enough data points to calculate a statistical average is ideal for eliminating stochastic variances caused by micrometeorological disturbances.

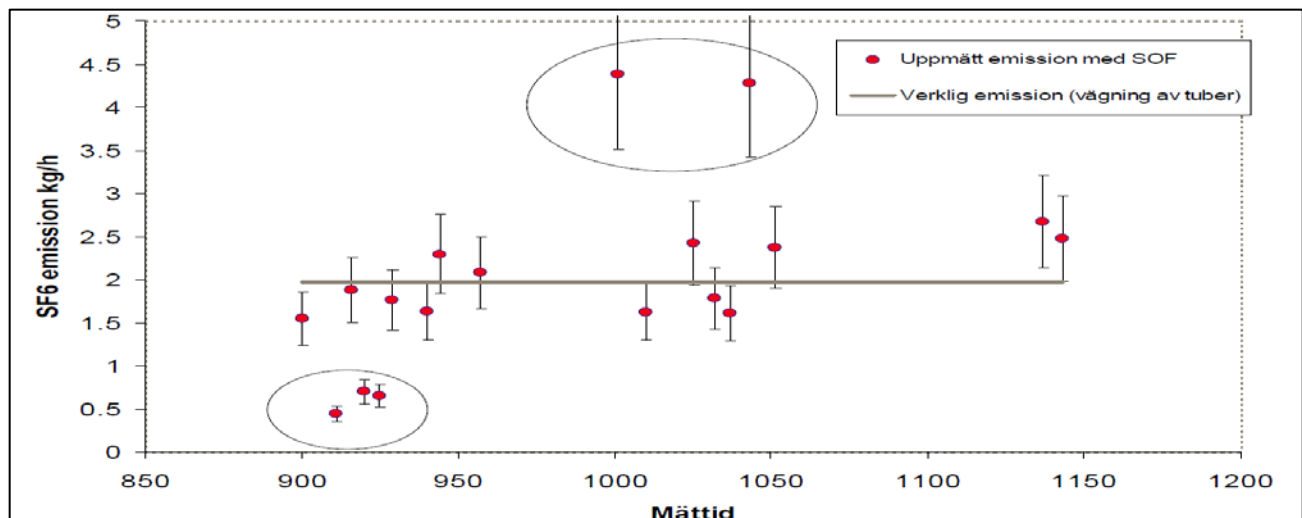


**Figure 3-11. Tracer gas/SOF experiment measuring SF<sub>6</sub> emissions in an open field over time of day. SOF measurements are depicted as red circles while the actual emission release rate is drawn as a grey line.**



### Typical QA/QC

To make emissions measurements with the SOF method, the operator needs to have meteorological information (distributed in height, surface, and time); a road to travel along that is relatively smooth, downwind of the emissions source and near perpendicular to the wind direction; stable wind conditions; and an unobstructed view of the sun. In addition to meeting these requirements, measurements can be further validated by calculating the expected and observed amounts of measurement error. The total amount of measurement error associated with SOF results is comprised of statistical and systematic error. Statistical error is described with a normal distribution as this type of error accounts for the natural, stochastic behavior of atmospheric variability. Researchers qualified this amount, which estimated the  $\sigma_S/N$  (or instrumental precision) from the standard deviation in the baseline of the plume column measurements during their VOC emissions study at oil refineries.<sup>5</sup> This value was about 0.3 to 0.6 mg/ m<sup>2</sup>, which corresponded to an uncertainty of 0.3 percent to 6 percent for a total column measurement of 100 to 10 mg/ m<sup>2</sup>. They also estimated the relative uncertainty in the total column due to wind direction variability ( $\sigma_\theta$ ) to be about 1 percent to 7 percent for eight scans. Researchers state that there is an 8 percent effect on column measurements when a plume is traversed at a 90° angle and that this error amount is sensitive to the ability to make measurements perpendicular to the wind direction such that angles of 80° and 70° contribute errors of 16 percent and 25 percent respectively.<sup>5</sup> Relative uncertainty in the wind speed due to plume height estimate uncertainties ( $\sigma_{uH}$ ) are discussed in more detail below.

Researchers calculated the statistical error assuming various typical scenarios encountered during measurements. The results displayed in Table 3-10 show that even between best and worst-case scenarios, the statistical error amount varies from 14 percent to 19 percent.<sup>5</sup> To determine the total error for a measurement, these statistical error values need to be added to the amount of systematic error. Output data recovered from SOF measurements do not contain information related to the height of the gas plume in the atmosphere. Plume height estimates are inferred from the corresponding temperature and pressure broadening of the spectral absorption lines if measured from high-resolution (< 0.125 cm<sup>-1</sup>) spectra.<sup>8</sup> This is the largest identified source of error in the SOF method, if the entire plume cross-section is captured and that the total amount of absorption equals the total concentration. As mentioned previously, the integrated concentration of the target species is multiplied by the mass average wind speed of the plume at plume height to

determine the emissions flux; therefore, accurate wind speed measurements are crucial to minimizing total flux measurement error. Increasingly complicated site conditions, such as a complex emissions source structure with unknown plume lift, will have larger amounts of systematic error.

One researcher states that measuring emission plumes with heights above 20-30 meters at distances greater than 500 meters downwind are ideal conditions to ensure minimal systematic errors associated with the wind field.<sup>1</sup> This is because of the increased predictability of the wind height profile that corresponds to the plume height while making measurements under these criteria. Figure 3-13 below shows the wind speed profile with height over developed land if a 5 m/s wind velocity was measured at 10 meters. It is clear from this figure that wind speeds above 20 meters from the surface during typical SOF conditions (i.e. sunny, which implies an unstable atmosphere) are past the major inflection point in the profile and have a less prominent height gradient with increasing height. Fransson and Mellqvist<sup>1</sup> made an estimation from data acquired at 17 meters that  $\pm 5$  meters is a realistic amount of error associated with the plume height estimation which translates to about 12 percent error in the wind speed measurement.<sup>5</sup> Further studies into the amount of error in the wind field by height concluded that about 14 percent systematic error in retrieved flux.

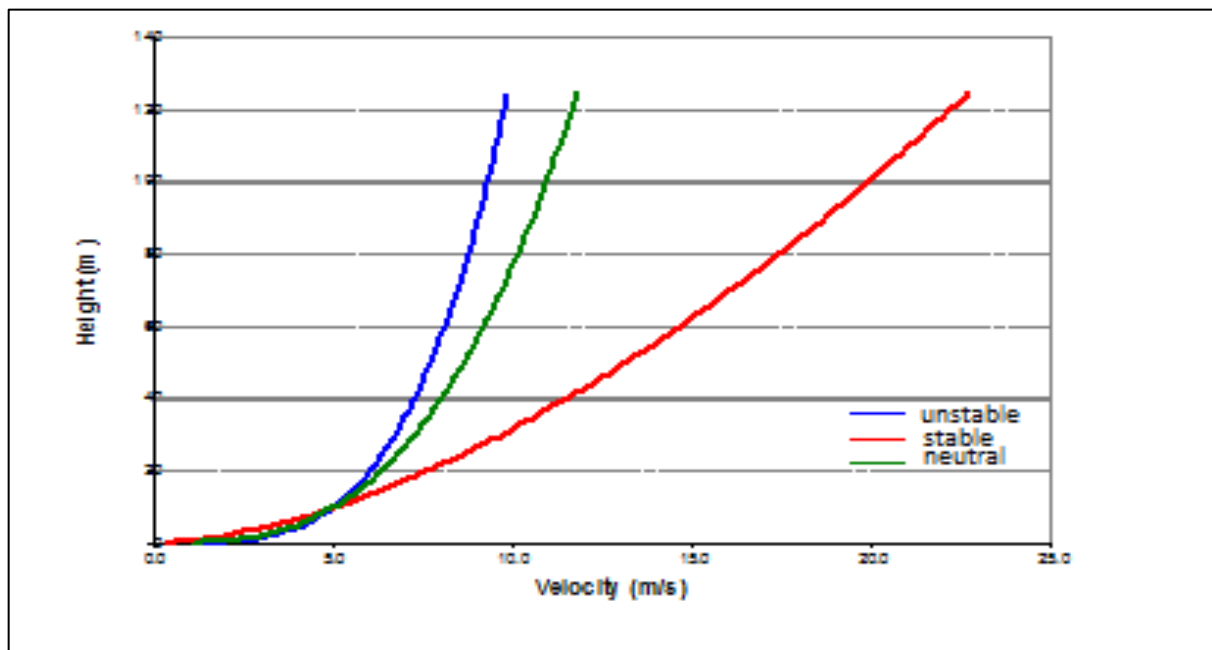


**Figure 3-12. Wind velocity profiles by height.**

### **Siting Concerns**

Since the instrumentation for the SOF method is mobile during analysis, issues originating from the site location are few. Most notably, the path of solar light through the plume to the instrumentation needs to be unobstructed, and excessive vibration during the mobile operations can cause noise originating from the interferometer. Therefore, measurement capabilities are constrained to weather conditions. In addition to the surrounding area of the mobile path, the line of sight needs to be clear of trees, shrubbery, and buildings that might impede the view of the sun. Moreover, the mobile path needs to be smooth and near perpendicular to the wind direction to minimize the amount of method error. SOF measurements are more representative in the mid and far field downwind from the emissions source where the plume is well-mixed and the solar transect of the plume will be higher in the wind profile. Plume traverses must be able to capture the entire plume cross-section plus open atmosphere on either side of the plume such that a representative background can be collected.

### **Strengths and Limitations**

One major advantage to the SOF method is also a disadvantage: the solar broadband light source. Using FTIR, the SOF method can precisely and accurately speciate and quantitate multiple gaseous emissions simultaneously using one instrument. The caveat to this advantage is that the method can only do so during specific climatic conditions (high sun and steady winds).<sup>4</sup> Other strengths and limitations associated with the SOF method are presented in Tables 3-11 and 3-12, respectively.

**Table 3-11. Feature strengths of using the SOF method.**

| Feature                              | Strength   |
|--------------------------------------|--|
| Direct Measurement                   | Increases measurement accuracy by reducing uncertainty.  |
| Passive Light Source                 | Decreases instrumental complexity for field operations and reduces amount of scattering errors in the UV.  |
| Broadband Light Source               | Multiple species detection over a wide range of wavelengths.   |
| Better Mobility                      | More suitable for frequent field application.  |
| Lower technical complexity           | Decreased cost and easier field application.   |
| FTIR Detection                       | Higher specificity and better signal-to-noise (relative to DIAL).  |
| Measurements during Sunny conditions | Corresponds to unstable meteorological conditions where wind gradients due to convection are smoothed out. |

**Table 3-12. Feature limitations of using the SOF method.**

| Feature   | Limitation  |
|---|---|
| Interferogram Vibration Sensitivity               | System requires vibration reduction platform and a smooth mobile path.  |
| Wind Speed Error                                  | Calculations based on wind speed measurements inherently add uncertainty due to the stochastic, uncontrollable, and highly variable nature of wind speed. |
| No Plume Height Measurement                       | Uncertainty of plume height increases measurement error from wind speed term.   |
| Solar Light Source                                | Inappropriate to make measurements in the presence of clouds.   |
| “Open Eye” Detection and Roadway Path Restriction | Difficulty in separating emissions sources that are close together.   |

**References**

1. Mellqvist, J., J. Samuelsson, C. Rivera, B. Lefer, and M. Patel, (2007), Measurements of industrial emissions of VOCs, NH<sub>3</sub>, NO<sub>2</sub> and SO<sub>2</sub> in Texas using the Solar Occultation Flux method and mobile DOA S, Final Report: HA RC Project H-53, retrieved off the World Wide Web on June 21, 2010 from [www.FluxSense.com](http://www.FluxSense.com).
2. Frisch, L., (2006), VOC Fugitive Losses: New Monitors, Emission Losses, and Potential Policy Gaps, 2006 International Workshop. Office of Air Quality Planning and Standards, Research

Triangle Park. Office of Solid Waste and Emergency Response, Washington, DC. October 25-27, 2006

3. Mellqvist, J., (2004), Quantifying fugitive emission of VOCs using the Solar Occultation Flux technique (SOF), Compliment to *Fransson and Mellqvist, 2002*, Chalmers University of Technology, Göteborg, Sweden.
4. Duffell, H., C. Oppenheimer, and M. Burton, (2001), Volcanic gas emission rates measured by solar occultation spectroscopy, *Geophysical Research Letters*, 28, 16, 3131- 3134.
5. Fransson, K., and J. Mellqvist, (2002), Measurements of VOCs at Refineries Using the Solar Occultation Flux Technique, Chalmers University of Technology, Göteborg, Sweden.
6. Kihlman, M., J. Mellqvist, J. Samuelsson, L. Tang, and D. Chen, (2005), Monitoring of VOC emissions from refineries in Sweden using the Solar Occultation Flux method, retrieved off of the World Wide Web on October 19, 2010 from [www.FluxSense.com](http://www.FluxSense.com).
7. Mellqvist, J., M. Kihlman, J. Samuelsson, and B. Galle, (2005), The Solar Occultation Flux (SOF) Method, a new technique for the quantification of fugitive emissions of VOCs, paper #1377 in proceeding of A&WMA's 98th Annual Conference & Exhibition, Minneapolis, USA.
8. Kihlman, M, (2005) Application of solar FTIR spectroscopy for quantifying gas emissions, Licentiate Thesis, Chalmers University of Technology, Göteborg, Sweden.
9. Mellqvist, J., M. Kihlman, B. Galle, K. Fransson, and J. Samuelsson, (2005), The Solar Occultation Flux (SOF) method: a nouvelle technique for the quantification of fugitive gas emissions, retrieved off the World Wide Web on March 10, 2010 from Fluxsense.com
10. Mellqvist, J., J. Samuelsson, J. Johansson, C. Rivera, B. Lefer, S. Alvarez, and J. Jolly, (2010), Measurements of industrial emissions of alkenes in Texas using the solar occultation flux method, *Journal of Geophysical Research*, 115.

### **3.4 Tracer Gas Correlation**

Challenges measuring emissions flux from a fugitive or area source such as a landfill, agricultural waste, industrial fugitive, waste water or oil and gas production source include spatial, temporal variability of the emission sources and the uncertainty of the measurement technology. Emissions source variability includes defined and undefined sources like unknown emissions points, delocalized emissions sources, the timing of periodic or episodic emissions, and atmospheric, diurnal, seasonal and process variations in emission flux. Defined fugitive sources cover smaller areas (i.e., less than 1 square kilometer down to a square meter) allowing emissions points to be identified for direct measurement. Undefined area sources typically originate from large areas (i.e., greater than 1 square kilometer). For either defined or undefined emissions sources, the sources of uncertainty cause emissions flux to be difficult to measure and model. Tracer gas correlation provides a ground based technique that can be applied to both well-defined area emissions sources and undefined fugitive sources.

Tracer correlation involves a common practice of measuring pollutant emission rates while releasing a known concentration of a tracer gas. The subsequent simultaneous measurement of this tracer gas and the pollutant of interest downwind from the release provide sufficient information to determine or validate the emissions flux measurements. The release of a known concentration of a tracer gas assists in tracking the plume and sources or sinks of the pollutant of interest into the plume. The majority of tracer gas studies use cell-based technologies, like CRDS and FTIR to measure the tracer gas and the compound of interest. However, some studies are expanding the use of tracer gas release to open-path techniques to evaluate the distribution over a large area.

#### **General Description of Approach**

The use of a tracer gas is common in projects that aim to study emission fluxes. Normally, emission fluxes are obtained by calculating fluctuations in the vertical and horizontal component of the wind ( $w'$ ), fluctuations in the tracer gas concentration ( $n'$ ) over either time (T) or space (S) and surface

roughness. The following equations provide a method for determining experimentally the surface fluxes of tracer gases by measuring meteorological parameters near the surface as well as the vertical gradient in the concentration of these calculate horizontal fluctuations, one must consider wind velocity ( $u(z)$ ) near the surface, friction velocity ( $u_*$ ), which is a measure of the drag exerted by the wind on the surface, and the displacement height ( $d$ ). The displacement height results from the canopy acting as a displaced lower boundary layer and whose value is typically 70-80 percent of the canopy height.

$$F = \frac{1}{T(orS)} \int_0^{T(orS)} w' n' dt$$

One must consider wind velocity ( $u(z)$ ) near the surface, friction velocity ( $u_*$ ), which is a measure of the drag exerted by the wind on the surface, and the displacement height ( $d$ ). The displacement height results from the canopy acting as a displaced lower boundary layer and whose value is typically 70-80 percent of the canopy height.

$$u(z) = \frac{u_*}{k} \ln \left[ \frac{z - d}{z_0} \right]$$

Where:

$k$  is the von Karman constant and is equal to 0.4 and  $z_0$  is the surface roughness.<sup>1</sup>

Using the Tracer Correlation Approach to measure total emissions over a large subject area is an alternative to standard dispersion modeling when attempting surface boundary layer methods as weather conditions are too difficult to measure or estimate accurately. Thus, releasing a tracer gas with known concentration and rate of release assists in calculating emission rates. If meteorological conditions affect both the tracer gas and the analyte in the same way, the analyte emission rate is calculated from simultaneous measurements of the tracer and analyte gas far downwind from the

plume emission source.

$$Q_m = \frac{Q_t \Delta C_m}{\Delta C_t}$$

Where:

$Q_m$  = analyte emission rate,

$Q_t$  is the tracer gas release rate,

$\Delta C_m$  is the concentration above the background of the analyte observed in the plume (plume – background concentration)

$\Delta C_t$  is the concentration above background in tracer concentration in the plume, relative to the background.

A tracer gas is released from a canister to transport in the plume along with the analyte. Usually a tracer gas is chemically stable with no significant sources or sinks while in transport and is expected to fully mix in the plume. Typical tracer gas field measurements are performed with cell-based instruments that utilize specific spectroscopic properties to characterize chemical species like CRDS and FTIR. These instruments can be setup as stationary or mobile to obtain one-point or multiple-point samples. Figure 3-13 shows a cartoon of tracer gas release setup. Normally, the tracer gas is released upwind from the source and the cell-based instrument is downwind from the source to measure a well-mixed plume with the analyte and tracer gas.



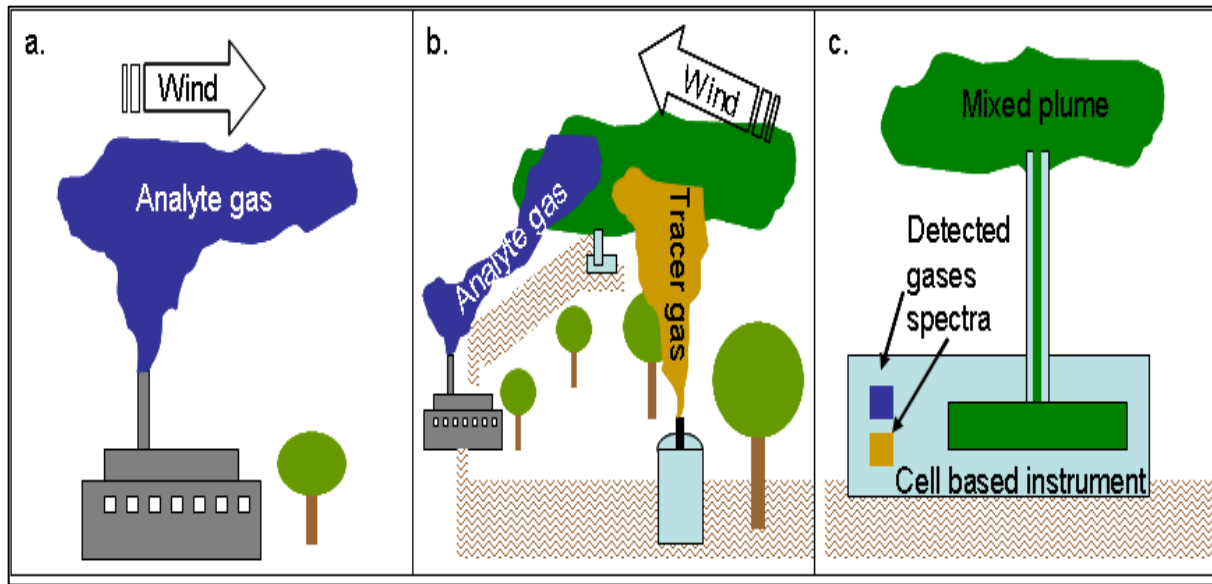


**Figure 3-13 Tracer gas release setup cartoon.**

**Note:** Panel a shows the source with the analyte gas been released to the ambient air. Panel b shows the tracer gas been released and pushed by the wind into the analyte gas area to mix in the plume. Panel c shows the cell-base instrument measuring gases, analyte and tracer.

### Verification/Validation Studies

Because the tracer gas release concentration is known and there are no significant sources or sinks, the mixing ratio should remain constant while in transport. Thus, verification of correct measurements by the cell-based instrument is done by measuring the known tracer gas concentration with accuracy. Validation is performed depending on the DQOs of the study.

Normally, the study will say how accurate the retrieval of the known concentration of tracer gas must be to obtain emission fluxes and the quality of the meteorological parameters to measure. Following are some examples of studies performed to verify and validate the use of tracer gas to calculate emission fluxes, utilizing CRDS and FTIR.

Mobile plume tracer dilution measurements were taken from May 18 – 21, 2009, driving on Interstate 36 and East Main Street in Danville, IN. Acetylene ( $C_2H_2$ ) tracer gas was released from four sites located on or near to the center of each landfill facility. The stationary measurements for gas tracer correlation measurements, the analyzer was located in the plume sufficiently downwind of the  $CH_4$  source and  $C_2H_2$  tracer gas release locations for plumes to be well-mixed and appear as

a single point emission source. During the measurements, the analyzer is stationary and continuously measures  $\text{CH}_4$  and  $\text{C}_2\text{H}_2$  concentrations. The CRDS Picarro Model G1203 methane ethylene ( $\text{C}_2\text{H}_2$ ) analyzer used in this study is a self-contained, stand-alone unit that provides continuous measurements of  $\text{C}_2\text{H}_2$  and  $\text{CH}_4$  concentrations, ambient temperature, and analyzer location (via high resolution GPS). The  $\text{C}_2\text{H}_2$  tracer gas was released from bottles through a mass flow controller (Alicat Scientific MC Series 16-Bit Mass Gas Flow Controller, model MCP-50SLPM-DIO-SG-30PSIA/5m) which was attached to the gas cylinder line to ensure a constant release rate throughout the study. The range of tracer gas release for the test was 20 L/min to 40 L/min. The release rates were automatically recorded. The following parameters were measured: horizontal wind speed, horizontal wind direction, temperature, vertical and lateral turbulence, and net solar radiation. Results from the study shown in Figure 3-14 demonstrated that the Tracer Correlation Approach can measure highly correlated, (correlation coefficient of 0.84) tracer gas to  $\text{CH}_4$  emissions over a wide range of atmospheric and dispersion conditions.<sup>4</sup>

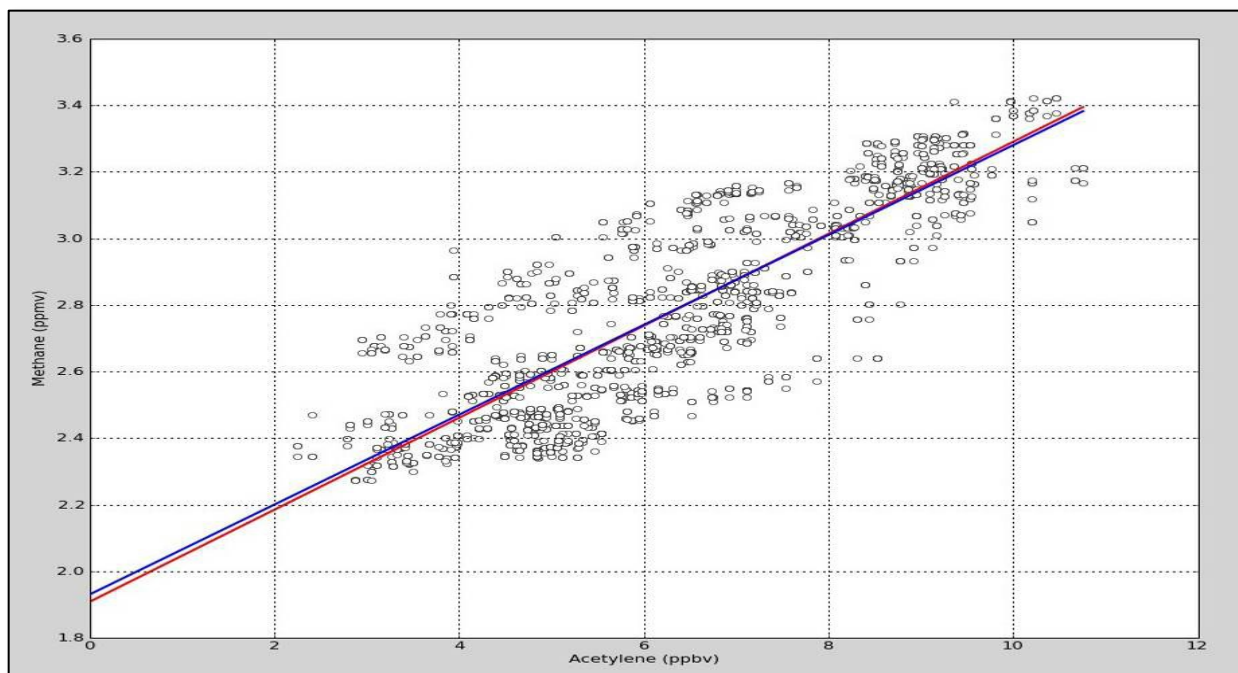


**Figure 3-14 Methane concentration versus acetylene concentration Tracer gas characterization using FTIR: Samuelsson et al., 2001**

FTIR was used to obtain time resolved concentration measurements of methane in the downwind plume of a landfill and  $\text{N}_2\text{O}$  was selected as the tracer gas.<sup>4</sup> FTIR spectroscopy is an optical

technique allowing a wide spectral region to be recorded simultaneously, thus the detection of  $\text{CH}_4$  and  $\text{N}_2\text{O}$  could be done at the same time. Low detection limits and sensitivity of ppb were obtained using a long optical path. In this study, a medium resolution ( $1\text{ cm}^{-1}$ ) FTIR spectrometer was connected to an optical multiple-reflection gas cell with an adjustable pathlength, ranging from 9 to 107 meters. Normally a pathlength of 96 m was used, selected to optimize optical throughput and absorption levels. The system was built into a well-tempered and mechanically stabilized optical bench and was in a normal transport van. The recorded spectra were analyzed by multiple-regression techniques, fitting synthetically derived calibration spectra of all present compounds.  $\text{CH}_4$  was analyzed in the wave number region at  $\sim 2950\text{ cm}^{-1}$ , and  $\text{N}_2\text{O}$  around  $2200\text{ cm}^{-1}$ .<sup>4</sup>

The methodology used to couple the concentration measurements to an actual emission is the Time Correlation Tracer method.  $\text{N}_2\text{O}$  was released in a controlled way from the methane emitting area by use of several point sources distributed over the landfill.  $\text{N}_2\text{O}$  mixed with the emitted  $\text{CH}_4$  in the landfill plume, and the emission rate was derived by time resolved analysis of the  $\text{CH}_4$  and tracer concentrations collected far enough downwind the landfill. The part of the time series where the concentrations correlate, can be assumed to have its origin in the area where the tracer is released, and can be quantified using the known tracer flux according this Equation.

$$Q_{\text{CH}_4} = Q_{\text{Tracer}} \cdot \frac{C_{\text{CH}_4} \cdot M_{\text{CH}_4}}{C_{\text{Tracer}} \cdot M_{\text{Tracer}}}$$

Where:

C = the concentration in the mixing ratio and M to the molecular weight.

A correlation plot between tracer concentration and analyte helps to identify if sampling is within the plume or outside. If the slopes of the concentration curves coincided as the plume swept in and out of the location, it could be assumed that the tracer release simulated the entire methane release. An estimate of the total landfill emission was obtained using the slope of the regression line

of methane. Depending on the meteorological conditions, it is estimated that an accuracy of 15-30 percent in the emission estimate is achievable.<sup>4</sup>

### **Typical QA/QC**

This section describes the QA/QC steps that pertain to the applications described above. QA/QC for applications steps normally depend on pre-determined data quality indicators that address the project unique objectives. The technology used for the applications presented above have their own QA/QC associated to specifics of the instruments.

When using the tracer gas approach, it is important to consider a gas that is stable and has low reactivity; thus, no significant sources and sinks that will alter the released concentration or, at least, good knowledge of the background concentrations. Spurious releases of tracer gases that reach 20 percent of the known concentration are easily identified CRDS, but anything below is probably not significant. Background levels of the analyte gas must be known to track the boundaries of the plume and to determine whether the measurements are in or out of the plume. The time delay between release and arrival at measurement site needs to be carefully determined before total methane emission results are considered acceptable. Flow rate of tracer gas released from all bottles be carefully monitored and recorded if total methane emissions from a landfill are to be accurately determined. A comparison (correlation plot) of analyte and tracer gas measurements taken close and far away from the source provide a correlation coefficient and the percentage difference or the total emission rate at close and far locations. Large percentage differences indicate insufficient overlap of the analyte plume and the tracer gas plume during stationary tracer-dilution measurements.

### **Siting Concerns**

In general, concerns regarding the use of tracer gases to obtain emission fluxes are associated with possible loss or gain of the tracer gas while in transport, not fully mixing within the plume, and changing weather conditions (wind speed and direction for the most part). Other concerns are

associated with calculations of the emission fluxes when estimating surface roughness or assessing vertical and horizontal fluctuations.

**Strength and Limitations**

A key strength of using a tracer gas correlation technique is the ability to determine if varying weather conditions affect the calculation of emission rates, which is possible by knowing release rates and concentration. An additional strength is that emission rates are calculated within 15-30 percent precision. However, stationary and mobile setups have their challenges in terms of logistics, location and whether available roads are near perpendicular to the flow of the plume.

Other limitations are cost of tracer gases cylinders and transportation of these, as well as changing weather conditions affecting the calculation of emission rates. Tables 3-12 and 3-13 summarize these strengths and limitations.

**Table 3-12. Tracer Gas Correlation Strengths**

| Feature                   | Tracer Gas Correlation Strengths  |
|---------------------------|---|
| Addresses Meteorology     | Can determine if varying weather conditions affect the calculation of emission rates. |
| Relatively precise Method | Emission rates are calculated within 15 - 30 percent precision.                       |
| Portable instrumentation  | Field units are lightweight, rugged, and relatively easy to transport and operate.    |

**Table 3-13. Tracer Gas Correlation Limitations**

| Feature                 | Tracer Gas Correlation Limitations   |
|-------------------------|--|
| Meteorological Concerns | Changing weather conditions affect the calculation of emission rates.                  |
| Logistical Concerns     | Location and the availability of roads perpendicular to the plume create difficulties. |
| Related Expenses        | Tracer Gas cylinders can be expensive to purchase and ship.                            |

## **References**

1. Brasseur, G. P., J. J. Orlando and G. S. Tyndall. 1999. Atmospheric Chemistry and Global Change. New York, NY: Oxford University Press.
2. Eastern Research Group, Inc. 2010. Evaluation of Large Area Methane Emission Source Methods: Mobile and Stationary Plume Measurements Using the Tracer Correlation Approach. Final Report for U.S. EPA. May 30.
3. Crosson, E. and S. Tan. 2009. Report on the work undertaken at the Twin Bridges Recycling and Disposal Facility under an agreement with Eastern Research Group, Inc. August 1.
4. Samuelsson, J., G. Börjesson, B. Galle and B. Svensson. 2001. The Swedish landfill methane emission project.

### ***3.5 Backward Lagrangian Stochastic Inverse-Dispersion model***

Identifying and quantifying gaseous emission rates from a fugitive or area source to air (e.g., emissions from an open-air waste lagoon, confined animal feeding operations, biofuel production facilities, landfills, etc.) is difficult. Several meteorological techniques are available (e.g., eddy covariance and flux gradient), but they involve complex instrumentation (e.g., concentration measurements at many heights and fast-response concentration sensors). They also require the measurement site to be on a flat location. There is a separate technique that can be used called the Integrated Horizontal flux that can be used for non-flat locations, but can only be used for small source areas because it requires vertical and horizontal concentration measurements for the entire plume. Because many emission sources do not meet these criteria, other techniques must be implemented to estimate emission rates.<sup>1</sup>

#### **General Description of Approach**

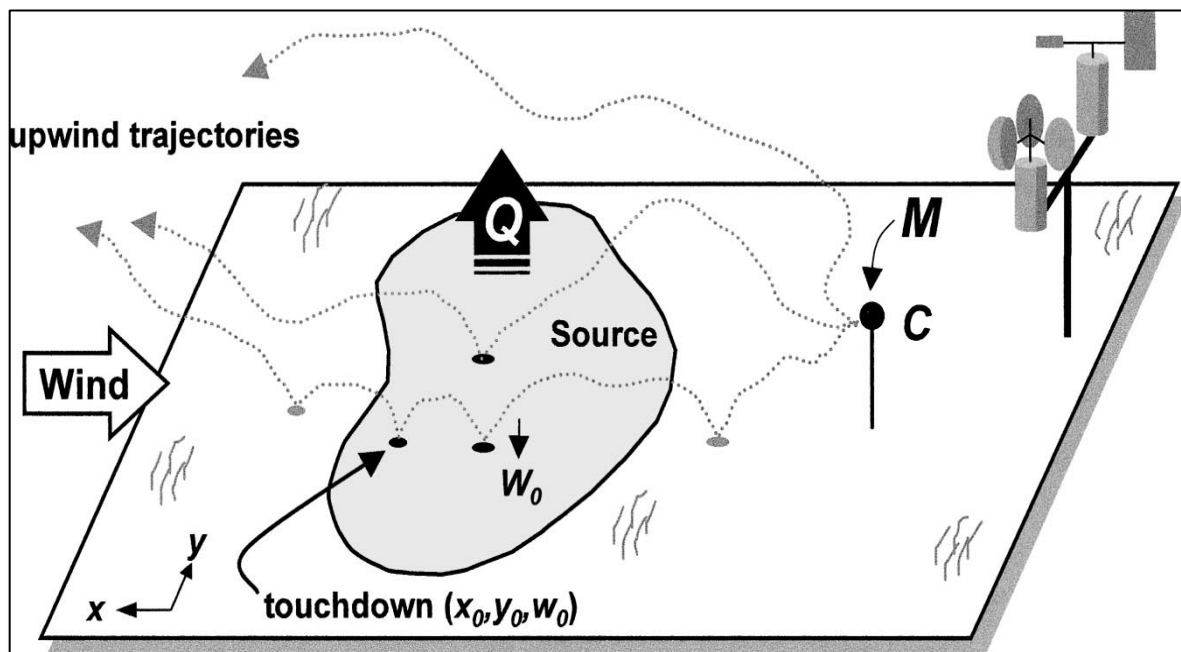
The limitations of traditional meteorological techniques can be addressed by using an atmospheric dispersion model to calculate the emission rate indirectly. The “inverse-dispersion” technique provides an accurate and economical alternative for measuring emissions. The technique uses a mathematical model of the dispersion of target gas from an emission source to a downwind location, so that a downwind concentration measurement can establish the emission rate.<sup>1,2</sup> This approach has the advantage of requiring only a single concentration measurement and basic wind information, with substantial freedom to choose convenient measurement locations. Theoretically, the technique assumes idealized wind conditions; however, with careful selection of measurement locations, inverse-dispersion modeling can provide a simple means of calculating emissions even in non-ideal conditions.<sup>1,2</sup>

Figure 3-15 illustrates the bLS model for estimating emission rates. An area source of known configuration emits gas at a uniform, but unknown, rate  $Q$  in kilograms per meter<sup>2</sup> per second ( $\text{kg}/\text{m}^2/\text{s}$ ). A time-average gas concentration  $C$  is measured at point  $M$  within the plume. The gas concentration  $C$  can be determined by ORS measurement methods such as open-path FTIR, TDLAS,

UV-DOAS, or point measurements such as CRDS. With a model prediction of the ratio of concentration at  $M$  to the emission rate  $(C/Q)_{sim}$ , the emission rate can be inferred as indicated in the Equation below. where  $C_b$  is the background pollutant concentration.<sup>1,2,3,4,5</sup>

$$Q = \frac{C - C_b}{(C/Q)_{sim}}$$

The inverse-dispersion model calculates the ratio of the concentration rise to the emission rate  $(C/Q)_{sim}$  at point  $M$ . This is the basis of the inverse-dispersion modeling technique. It requires only a single pollutant concentration measurement (assuming  $C_b$  is known) with flexibility in the choice of the measurement location  $M$ . The accuracy of the technique rests on the calculation of  $(C/Q)_{sim}$



**Figure 3-15. Illustration of an inverse-dispersion model for estimating emission rate  $Q$ .**

Note: Average concentration  $C$  is measured at point  $M$  downwind of the source.<sup>3</sup>

One of the most accurate models used to calculate  $(C/Q)_{sim}$  is a bLS model. The model follows the path of a fluid element (e.g., “particle”) from a given location backward in time to determine its origin. Particles in the context of the model are carriers.



Depending on the trajectory, the particle may or may not sample the target source (i.e., "touchdown" within the source). The term Lagrangian indicates that the model releases individual particles and follows them along their paths through the air, rather than performing calculations at fixed locations in space. Stochastic indicates that the model mimics the random, turbulent motion of each particle. As these particles travel through the air, they move through different regions of interest. Some particles will touch down in the source region and move to the concentration sensor, contributing to a measured concentration increase.<sup>1,2,6</sup>

For surface area emission sources, all that is needed to invoke the bLS model to calculate  $(C/Q)_{sim}$  are wind statistics, which can be determined from a few key meteorological observations.<sup>1,2</sup> In general, the bLS inverse-dispersion method of modeling emissions is cost-effective, requires only a single field measurement of  $C$ , and, under the conditions described in this section, generates emission rates with accuracy adequate for many applications.

**Backward LS Dispersion Model for Calculating  $(C/Q)_{sim}$**

In a bLS dispersion model, the upwind trajectories of model particles are calculated from location  $M$  (Figure 3-15). The important information from the backward trajectories is the set of "touchdown" locations  $(x_0, y_0)$  where particles impact the ground, and vertical "touchdown velocities" at impact  $w_0$ . From the set of trajectories, the equation below is used to calculate  $(C/Q)_{sim}$  by summing the reciprocal of  $w_0$  for touchdowns occurring within the source boundary.<sup>3</sup>

$$(C/Q)_{sim} = \frac{1}{n} \sum \left| \frac{2}{w_0} \right|$$

Where:

$n$  = the total number of computational particles released from  $M$  and the summation covers only touchdowns within the source area. In the bLS model, thousands of trajectories are calculated upwind of the prevailing wind conditions.

Commercially-produced software developed and distributed by WindTrax (Thunder Beach Scientific, Nanaimo, Canada) is available to solve bLS equations. WindTrax combines the bLS model with a graphical interface, allowing sources and sensors to be conveniently mapped (see Figure 3-16).<sup>6</sup> To calculate unknown source emission rates and/or concentrations, WindTrax requires the following information:

- upwind and downwind gas concentrations ( $C_b$  and  $C$ ),
- wind statistics (e.g. wind speed and wind direction),
- roughness of the surface ( $z_o$ ), and stability of the atmosphere near the ground (Monin-Obukhov stability parameter,  $L$ ).

The latter wind statistics may be obtained from sonic anemometry or estimated within Windtrax. If concentration is measured in units of ppm or ppb, air temperature and pressure are also needed (pressure is often estimated from elevation). The particle models used in WindTrax are time-independent, so the input data must be values averaged over a period, typically 15-30 minutes. This averaging eliminates the unpredictable variability due to turbulence in the atmosphere on short time-scales. Conversely, if the averaging time is too long, the more gradual diurnal variation typical of the surface layer will not be resolved.<sup>6</sup>

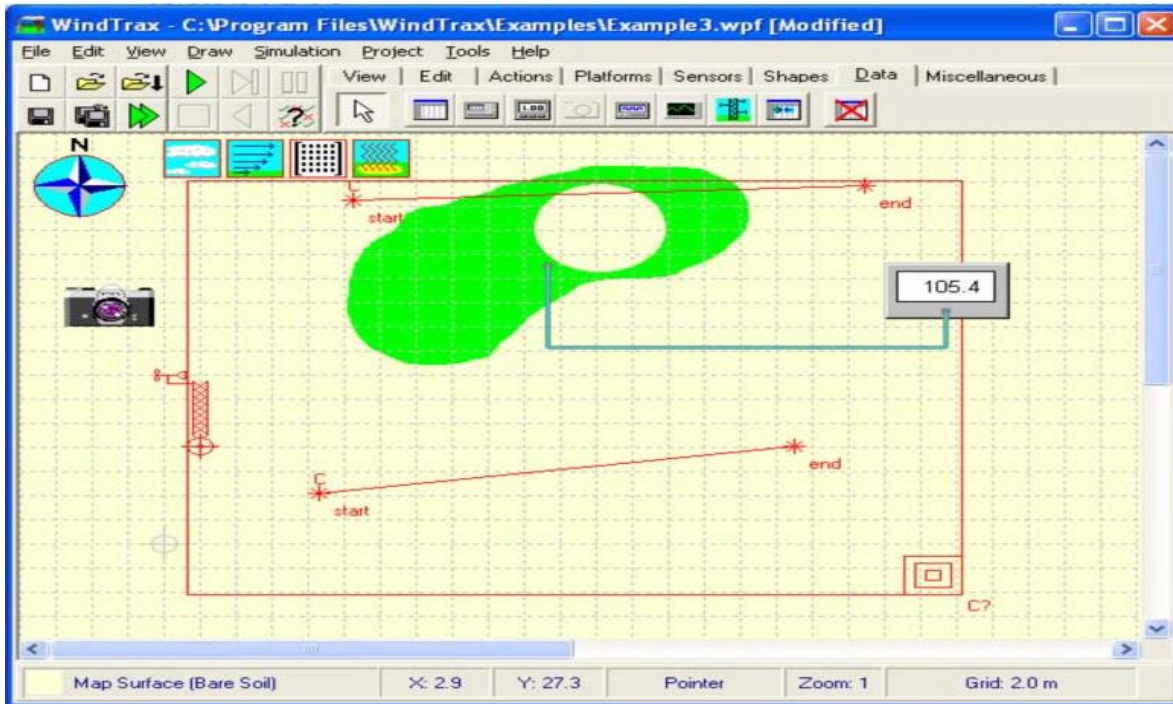


**Figure 3-16. Illustration of the WindTrax bLS Modeling Software Graphical Interface**

**bLS Model Output Units**

Open-path ORS (OP-ORS) measurement techniques such as open-path FTIR or TDLAS can be used to make the concentration measurement in a bLS application. Also, point-measurement sensors such as closed-cell sensing techniques including CRDS or cell-based FTIR could be used to measure plume concentration. These techniques provide concentration in units of ppm or ppb over the optical path used in the measurement (ppm\*m or ppb\*m). Specific temperature and pressure data are needed to convert to absolute concentration (i.e. g/m<sup>3</sup>), which is used to determine the mass emission rate. The bLS calculation itself produces an emission rate (flux),  $Q_{bLS}$ , with units of kg/m<sup>2</sup>/s (for example), but sometimes the emission rate is multiplied by the source area and  $Q_{bLS}$  becomes an area integrated emission rate with units of kg/s or kg/h.<sup>1,2,8,9</sup>

**Verification/Validation Study**

One of the foremost leaders in the development and application of bLS modeling as it applies to gaseous emissions for large area sources is Thomas Fleisch at the University of Alberta, Canada. He conducted numerous studies using bLS. In this section, a bLS field trial entitled *Deducing Ground-*

*to-Air Emissions from Observed Trace Gas Concentrations: A Field Trial* is summarized as an example of the bLS application.<sup>1</sup> The summary briefly illustrates how bLS can be used and describes the quality of data that can be generated by the model.

In 2004, Flesch *et al.* reported a bLS field trial experiment in which the inverse-dispersion technique was used to determine  $Q_{\text{bLS}}$  in an ideal surface-layer setting. A small area source from which methane was released at known rates over a wide range in meteorological conditions was constructed. An open-path laser measured the methane concentration  $C$  at positions located up to 100 meters downwind of the source as shown in Figure 3-17. A corresponding  $(C/Q_{\text{sim}})$  was calculated using a bLS dispersion model, and the resulting estimate of the emission rate  $Q_{\text{bLS}}$  was compared with the known  $Q$ . The study objectives were the following: 1) to quantify the accuracy and uncertainty in  $Q_{\text{bLS}}$  in an ideal setting; 2) to probe the conditions under which a dispersion model based on the Monin–Obukhov similarity theory (MOST) performs poorly; and 3) to validate an experimental system (i.e., source, sensors, bLS model) for examining the robustness of a bLS estimate in non-ideal conditions.

### **Flesch et al. Conditions and Setup**

The experiment took place over a 6-day period in May and June of 2001, near Ellerslie and Edmonton, Alberta, Canada, in a large clover field. From a meteorological perspective, the site was nearly ideal—wind conditions were uniform, temperatures were not high enough to cause thermal convection of the plume out of the measurement window, and the nearest significant change in land cover was more than 500 m from the source.

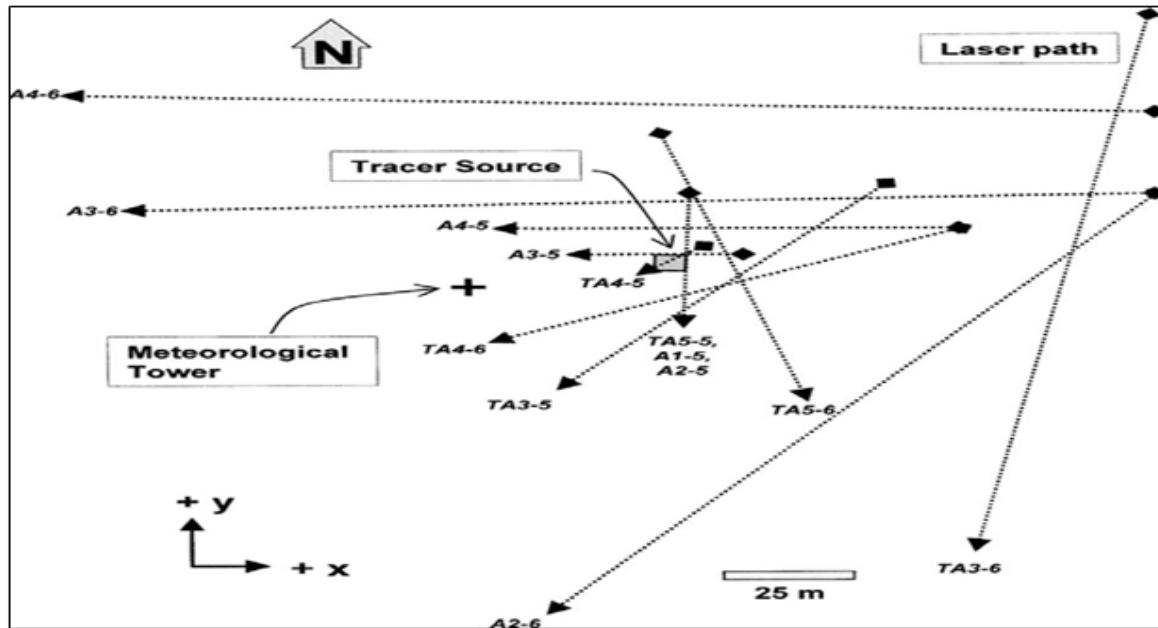


**Figure 3-17. Map of the laser paths used in the 2004 Flesch et al experiment.**

Note: The shaded square on the map represents the methane tracer source and the large “+” symbol indicates the location of the meteorological tower with the 3-D sonic anemometer.

A synthetic source was created to approximate a 6 m × 6 m square area source. A manifold was constructed out of polyvinyl chloride pipe and 36 0.5 mm outlet holes were drilled into the pipe. A gas cylinder was coupled to the manifold through a regulator and rotometer (flow meter). The methane tracer gas was released from high pressure cylinders (99.1 percent purity) at flow rates between 15 and 50 L/min. Each release lasted from 1 to 3 hours. The cylinder valve was manually adjusted to maintain a nominally constant flow rate, with adjustment occurring every minute or two as necessary. The study estimates a 10 percent uncertainty in  $Q$  due to flow-rate fluctuations, observer error in reading the rotometer scale, and gas temperature variability inside the rotometer (which affects calibration).

Methane concentration measurements were made using two open-path lasers. A focused beam from a tunable IR laser was aimed at a distant retro-reflector where it was reflected back to the receiver optics and a detector. The returning signal strength was proportional to the methane concentration  $C$  between the laser and the retro-reflector. Background methane  $C_b$  was periodically measured at 1.95 ppm. This measured value closely correlated with the average

methane background for the Edmonton region during the experiment, as routinely measured by the provincial government of Alberta. The laser units recorded  $C$  every minute. These readings were averaged into 15, 30, or 120-minute values. To convert concentrations from ppm to absolute concentration in  $\text{g/m}^3$ , Flesch *et al* used the measured air temperature and atmospheric pressure for each observation period. A 3-D sonic anemometer was placed on a tower approximately 2 m above ground and was used to determine values of  $u^*$ ,  $L$ ,  $z_0$ , and  $\beta$  for the bLS simulations. Figure 3-17 shows a map of the various laser paths (dotted lines with arrows) used in the experiment. The code at the tip of each arrow head is associated with the experimental conditions for that trial measurement. The wind direction on the map is from west to east and all laser measurements were made downwind.

### **Flesch et al Results and Conclusions**

When periods of extreme stratification or MOST failure were excluded, the bLS inverse-dispersion technique diagnosed the strength of a small ground-level source with small bias (mean value of  $Q_{\text{bLS}}/Q$  within 2 percent of unity). Poor results were excluded when using a laser path over the source because this study dealt with a very small area source, meaning the laser path was not always sufficiently inside the plume. In situations involving a large source area, a measurement location above the source is acceptable. The period-to-period variability in  $Q_{\text{bLS}}$  was acceptably small (standard deviation of  $Q_{\text{bLS}}/Q$  is approximately 0.2). Using path-integrated values of  $C$  enhanced the accuracy with which  $Q_{\text{bLS}}$  was diagnosed and rendered the experimental procedure very forgiving (the laser could be positioned without being overly concerned about changing wind direction). Based on their field experiments, Flesch *et al* made several recommendations for using a bLS model to infer  $Q_{\text{bLS}}$  from an area source in an ideal surface layer problem:

- PIC measurement is preferable to a point measurement because PIC gives results that are integrated over the entire beam path length and are, therefore, more representative than a single point source measurement of the actual plume concentration.

- Distance of the detector from the source should be small enough that the concentration rise over background is accurately measured.
- Meteorological averaging times of 10–30 minutes are ideal for calculating concentration and meteorological statistics. Shorter averaging times may not capture an equilibrium state of the atmosphere, a requirement for the application of MOST.
- Periods of extreme atmospheric stability should not be used in assessing  $Q_{\text{bLS}}$ . An example of an acceptable limit is  $|L| \geq 10\text{m}$ .<sup>4</sup>
- Disregard periods of low  $u^*$  (e.g.,  $u^* \leq 0.15$  m/s).

Because all testing sites are different, the bLS modeling system has been used with varying site locations such as ponds, pastures, and other scenarios. More detailed information pertaining to different types of site locations can be researched in the literature.

### **Typical QA/QC**

For the bLS dispersion model to accurately calculate the emission rate of a source, it is important to verify that the instrumentation used to collect concentration data for target analytes is appropriate for bLS calculations. QA/QC guidelines identified in this protocol or other EPA literature for the technology used should be followed for optimal performance.

Because meteorological measurements are required for the bLS model, it is important to ensure that accurate measurements are used. Meteorological data collected on site should be collected with appropriate instrumentation, and applicable EPA guidelines should be followed. More information on the technology used to collect meteorological data can be found in the *Quality Assurance Handbook for Air Pollution Measurement Systems, Volume IV:*

*Meteorological Measurements, Version 2.0.*<sup>7</sup> If meteorological data are not collected on site, it is necessary to ensure that the data used in the bLS model are taken from a trusted source and the location of the measurements is near the test site. Wind stability determination requires more sophisticated instrumentation (e.g., 3-D sonic anemometer, or temperature measurements at two or more heights).

WindTrax and other modeling software are available for use to perform the bLS calculations. A simplistic data set with known results should be used to test the modeling software before use for field data calculations to verify the software's performance. In special cases, it may be preferable for the user to develop its own software program to perform the necessary calculations, though it is not recommended for accurate modeling. It is necessary to test all bLS software on a simplistic data set for which the results are known to verify the software. In all cases, input data should be reviewed for accuracy and possible transcription errors.

### **Siting Concerns**

The bLS dispersion model utilizes the average wind and turbulence statistics of the atmosphere to calculate  $(C/Q)_{sim}$ . MOST states that the statistical properties of the wind in the surface layer are determined by a few key parameters: the friction velocity  $u^*$ , which is determined by the vertical transport of horizontal momentum near the surface; the Obukhov stability length  $L$ , which quantifies the stability of the atmospheric surface layer; the surface roughness  $z_0$ , which is related to the height of the plants, soil, or other elements covering the ground; and the wind direction  $\beta$ . In the field, these parameters are typically determined with the use of sensors such as a 3-D sonic anemometer. The placement of sensors relative to sources can have a major effect on the quality of the predictions generated by the models. If no concentrations are measured downwind of a source, then emission rates cannot be determined.<sup>6</sup> Upwind ambient gas concentrations must also be measured that may be coming onto the site. The variability of wind direction might cause some simulations to fail while others succeed. When multiple unknown sources are present, the calculations are very sensitive to sensor placement and measurement error. Where flow obstacles such as buildings or fences are present, measurements are often better made further downwind of the source, well away from the obstacles; at least 10 obstacle heights downwind are a useful rule of thumb for measurement location (M) placement.<sup>1,2,5,6</sup>

If the source and the detection point  $M$  lie within a horizontally homogeneous surface layer, the application of the bLS dispersion model technique is reasonably straightforward. Many agricultural



and environmental source estimation problems potentially fit this category. These problems may include emissions from small soil research plots, feedlots, ponds, industrial grounds, and so on, that often occur in circumstances for which it is reasonable to assume that the local wind flow is uniform (i.e., wind statistics that do not deviate more than 10 to 20 percent from their spatial average over the region from source to detector).<sup>1</sup>

An important advantage of bLS models is the ease with which complex source shapes can be handled. One of the most important factors affecting model error is the size of the regions of interest through which the analytes travel. As more analytes travel through a given region (i.e., the concentration is higher), more samples of the region are taken and the model error is reduced. In practice, this means that the larger the source target, the smaller the error, and conversely, the smaller the source target, the greater the potential for error.<sup>1,2,3</sup> However, the use of bLS within large source areas has been very successful in many studies.

### **Strengths and Limitations**

bLS models have several advantages over Gaussian and Eulerian models. For example, bLS models are more physically valid than Gaussian models, which do not incorporate wind shear or other meteorological information, and they do not require artificial diffusivity, as do the Eulerian models for convective transport. A traditional disadvantage of bLS models is their computation time requirements, which can be several orders of magnitude larger than those required to solve algebraically reduced Gaussian models or even Eulerian models. This is because of the need to calculate thousands of unique atmospheric trajectories. However, modern computing power has rendered this problem to be of limited concern for most users. Tables 3-15 and 3-16 summarize the bLS model's strengths and limitations in more detail.

**Table 3-15. bLS Model Strengths**

| Feature                    | bLS Strengths   |
|----------------------------|---|
| Simplicity of Measurements | Requires only a single concentration measurement – as opposed to many concentration measurements made in the vertical or horizontal plane of the plume.   |
|                            | Flexible input requirements: various wind statistics can be entered into software and needed conversions are done internally; different types of concentration observations are possible (point or line average). |
| Siting Concerns            | Substantial freedom to choose convenient measurement locations  |
|                            | Handles complex source shapes and sizes with relative ease  |
|                            | Can be used in locations with wind disturbances if sensor locations are chosen with care  |
| Economical                 | An economical alternative for determining emissions   |
|                            | Free downloadable software available online   |

**Table 3-16. bLS Model Limitations**

| Feature                 | bLS Limitations   |
|-------------------------|---|
| Meteorological Concerns | Assumes idealized atmospheric conditions unless care is taken with sensor placement.  |
|                         | Rapid atmospheric changes or extreme stability invalidate MOST and cause $Q_{bLS}$ estimates to be inaccurate   |
| Training Requirements   | Some judgment required to identify poor measurement locations (for both winds and concentration). Poor measurements locations (e.g., close to building) can significantly impact the quality of emission calculation. |
|                         | Some basic experience or training in micrometeorology or atmospheric gas transport is required to generate high-quality data from the bLS model   |
| Siting Concerns         | When multiple unknown sources are present, the calculations are very sensitive to sensor placement  |
|                         | Where flow obstacles such as buildings or fences are present, measurements are often better made further downwind of the source, well away from the obstacles.  |
| Time Limitations        | Can require lengthy computational time.   |

## References

1. Flesch, T.K., J.D. Wilson, L.A. Harper, B.P. Crenna, and R.R. Sharpe. 2004. Deducing ground-air emissions from observed trace gas concentrations: A field trial. *J. of Applied Meteorology*. 43:487-502.
2. Flesch, T.K., J.D. Wilson, and L. A. Harper. 2005a. Deducing ground air emissions from observed trace gas concentrations: A field trial with wind disturbance. *J. of Applied Meteorology*. 44:475-484.
3. Flesch, T.K., J.D. Wilson, and E. Yee. 1995. Backward-time Lagrangian stochastic dispersion models, and their application to estimate gaseous emissions. *J. of Applied Meteorology*. 34:1320-1332.
4. Wilson, J.D., T.K. Flesch, and L.A. Harper. 2001. Micro-meteorological methods for estimating surface exchange with a disturbed wind flow. *J. of Agricultural and Forest Meteorology*. 107:207-225.
5. McBain, M.C. and R.L. Desjardins. 2005. The evaluation of a backward Lagrangian stochastic (bLS) model to estimate greenhouse gas emissions from agricultural sources using a synthetic tracer source. *J. of Agricultural and Forest Meteorology*. 135:61-72.
6. Thunder Beach Scientific, Nanaimo, British Columbia, Canada, 2009.  
<http://www.thunderbeachscientific.com>.
7. U.S. EPA, Quality Assurance Handbook for Air Pollution Measurement Systems, Volume IV: Meteorological Measurements, Version 2.0, EPA-454/B-08-002, March 2008.
8. Harper, L.A., T.K. Flesch, J.M. Powell, W.K. Coblenz, W.E. Jokela, and N.P. Martin. 2009. Ammonia emissions from dairy production in Wisconsin, *J. of Dairy Science*. 92:2326–2337.
9. Flesch, T.K., L.A. Harper, J.M. Powell, and J.D. Wilson. 2009. Use of dispersion analysis for measurement of ammonia emissions from Wisconsin dairy farms. *Agric. Eng.* 52:253–265.
10. Harper, L.A., T.K. Flesch, K.H. Weaver, and J.D. Wilson. 2010. The effect of biofuel production on swine farm ammonia and methane emissions. *J. Environ. Qual.* (accepted for publication, August 5, 2010)

### ***3.6 Geospatial Measurement of Air Pollution, Remote Emission Quantification – Other Test Method 33***

Identifying and quantifying gaseous emission rates from a fugitive or area source to air (e.g., emissions from an open-air waste lagoon, confined animal feeding operations, biofuel production facilities, landfills, etc.) is difficult. The challenges encountered trying to measure area source emissions flux include spatial and temporal variability of the emission sources and the uncertainty of the measurement technology. As discussed in previous sections, emissions source variability includes defined and undefined sources such as unknown emissions points, delocalized emissions sources, the timing of periodic or episodic emissions, and atmospheric, diurnal, seasonal, and process variations in emission flux. Defined fugitive sources cover smaller areas (i.e., less than 1 square kilometer down to a square meter) allowing emissions points to be identified for direct measurement. Undefined area sources typically originate from large areas (i.e., greater than 1 square kilometer) and attempts at measuring the air quality have included ambient air monitoring.

Traditional ambient air quality measurements are primarily collected from fixed-placement monitoring stations and provide information on long-term trends of air pollutants over the larger air shed region. Direct (on-site) measurements of air pollutants are conducted at the immediate source of the emission. By contrast, the methods of geospatial measurement of air pollution utilize source assessment schemes that provide data for air quality conditions in the spatial and temporal ranges in between for both defined and undefined areas. Figure 3.18 illustrates the operation regime of the geospatial methods.<sup>1</sup>

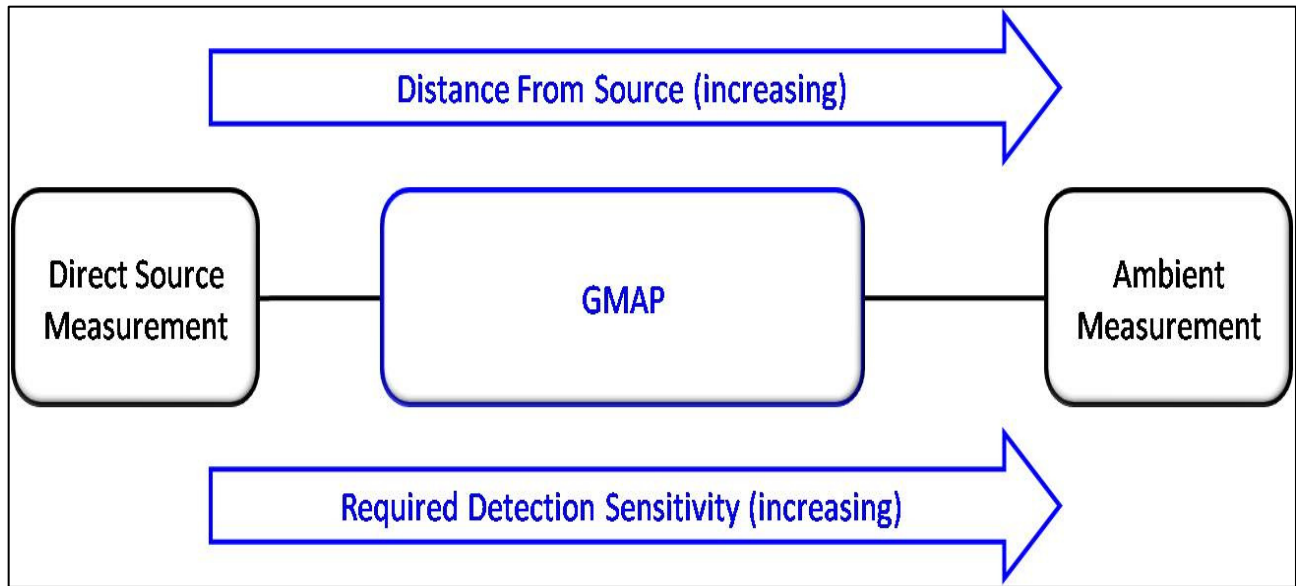


**Figure 3-18. GMAP Operational Regime.**

Since 2006, EPA has investigated the use of mobile measurement systems under its Geospatial Measurement of Air Pollution (GMAP) program for a variety of air quality assessment applications, including those involving complex, undefined, or large area sources.<sup>1</sup> The GMAP vehicle instrumentation system combines fast response analytical instruments with precise global positioning systems (GPS) to characterize pollution emissions. Other Test Method 33 (OTM 33) is a mobile measurement method series that resulted from the GMAP efforts using approaches that are designed to quantify source emissions on scales ranging from near-field inspections of small fugitive releases to whole facility mass emission rate measurements.<sup>2</sup>

OTM 33 systems typically have two possible modes of operation: (1) downwind mapping surveys to detect and locate emission sources, and (2) quantification procedures to characterize concentrations and mass emission rates. Because the OTM 33 techniques can be applied to many different situations with different approaches, sub-methods OTM 33a, 33b, 33c, and 33d are in development to address more details and specifics regarding the different assessment approach schemes. This OTM 33 method series allows for the use of many different instrumentation configurations and vehicle mobility schemes to assess air quality concerns at a variety of spatial scales.

The OTM category of measurement methods contains methods that have not undergone the federal

rulemaking process, but have been reviewed by the EPA's Emission Monitoring Center (EMC) and are potentially useful to the emission measurement community. Such methods may be considered for use in federally enforceable state and local programs and can also be considered as candidates for alternative methods to meet federal requirements under 40 CFR Parts 60, 61, and 63 through an approval process.

### **General Description of Approach**

Geospatial measurements of air pollution, or GMAP, is a general term defined in OTM 33 as “referring to the use of fast-response instruments and precise global positioning systems (GPS) in mobile formats to spatiotemporally-resolve air pollution patterns in a variety of use scenarios.”<sup>1</sup> The geospatial measurement of Air Pollution-Remote Emissions Quantification (GMAP-REQ) measurement method series (OTM 33) uses ground-based vehicle platforms fitted with instrumentation to make mobile measurements proximal to a driving route. OTM 33 is a general description of instruments, approaches, and assessment schemes that are further defined in sub-methods. The source assessment schemes covered in these sub-methods include:

- Concentration Mapping (CM) – Used to find the location of unknown sources and to evaluate the impact these source emissions may have on local air shed pollution concentrations.
- Source Characterization (SC) – Used to improve the understanding of known or discovered sources through the collection of secondary measurements (such as remote imaging or canister grab sample speciation).
- Emissions Quantification (EQ) – Used to measure (or estimate) the source emission rate.

Emission information on gas-phase criteria pollutants, particulate matter and ultrafine particles, volatile organic compounds (VOCs), hazardous air pollutants (HAPs), and greenhouse gases (GHGs) is collected when a vehicle outfitted with appropriate analytical and auxiliary equipment is driven around the target facility. This information is spatially and temporally resolved, meaning that the

data can be analyzed for leak detection and repair programs, periodic fence line monitoring, gradient-type local air shed concentration mapping, and source emission rate characterization. As the instrumented vehicle is driven around the facility, air pollution concentration levels are recorded both inside the emission plume and outside the plume, capturing background levels and the location where the plume intersects the vehicle pathway.

Figure 3.19 illustrates a limitation of the method based on wind direction and path of the instrumented vehicle.<sup>1</sup> Also, if the wind conditions are not favorable, or there are other interferences such as buildings or topographic obstacles to the path of the emission plume, then representative measurements of pollutants in the plume may be difficult.

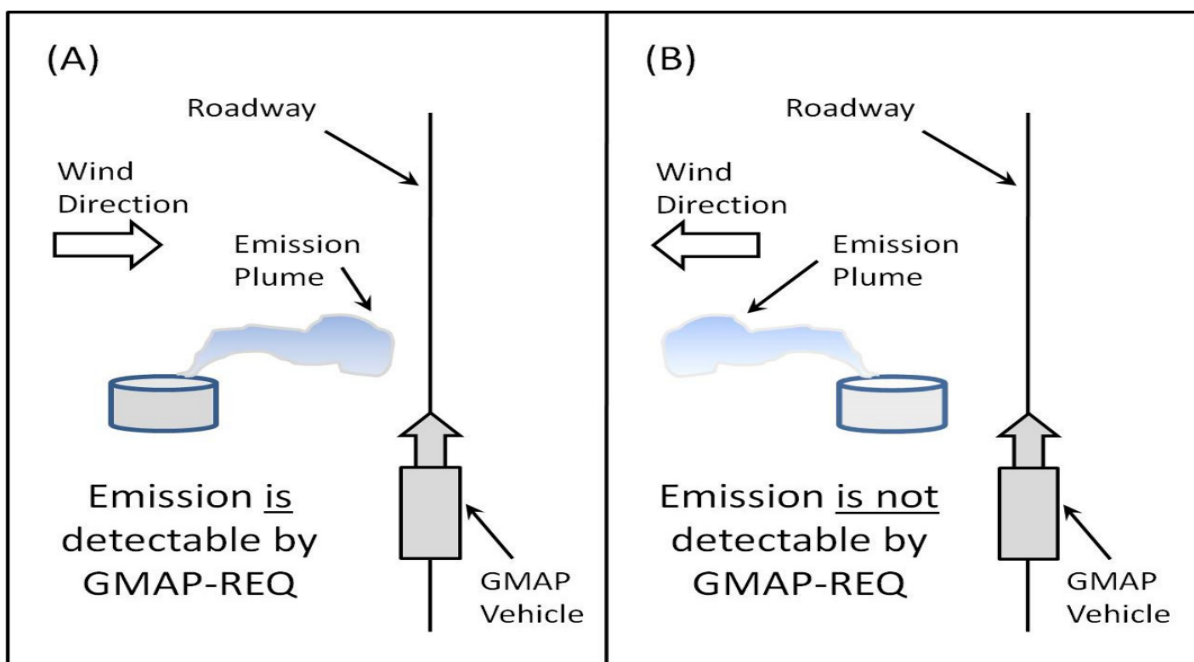


**Figure 3-19. GMAP (OTM 33) Limitations**

The analytical instruments included in the design of the GMAP vehicle must be robust enough to withstand mobile applications in remote areas. Unpaved or rough roads will likely be encountered during the course of a facility survey. The pollutant measurement instrumentation must have near-ambient level detection capabilities with an appropriate dynamic range. Because OTM 33 sub-methods typically use a combination of data measurements (such as GPS location, pollutant concentration, wind information, etc.) to determine source detection, emission source location, and

mass emission rate, the instruments should also be time-synchronized to the second.

Currently, only OTM 33A is promulgated by EPA while other sub-methods are in development (and are, therefore, not final). Following are the anticipated sub-methods for OTM 33:<sup>1-10</sup>

- OTM 33A – Discovery/Characterization of Near-Field Fugitive Sources  
See Section 3.7 for a more in-depth discussion.
  
- OTM 33B – Mobile Tracer Correlation  
See Section 3.4 for more discussion.
  
- OTM 33C – Solar Source Techniques  
See Section 3.3 for more discussion.
  
- OTM 33D – Regional Mobile Sensing Approach  
This method will be like OTM 33A, but will be designed for a broader geographical survey.

Details on the method procedures, quality assurance requirements, and performance specifications are (or will be) available in the sub-methods, however, EPA expects that project-specific quality assurance project plans will be developed according to EPA requirements for each measurement event. Table 3.16 presents a brief overview of the performance characteristics of various mobile measurement approaches that can be used for OTM 33 sub-methods.



**Table 3.16. Summary of mobile measurement approaches.**

|                             | OTM 33A                                 | OTM 33B (Near-field)         | OTM 33B (Far-field)          | Mobile SOF                        | Mobile Flux Plane               | Work Truck                          |
|-----------------------------|---|------------------------------|------------------------------|-----------------------------------|---------------------------------|-------------------------------------|
| CM, SC (various types)      | ✓                                       | ✓                            | ✓                            | ✓                                 | ✓                               | ✓                                   |
| EQ Approach                 | Stationary single point / inverse model | Tracer correlation           | Tracer correlation           | Extended flux plane / integration | Finite flux plane / integration | Mobile single point / inverse model |
| Primary Source Type         | Point-like                              | Point-like                   | Large area / facility        | Large area / facility             | Point-like                      | Point / area                        |
| Distance to Source (m)*     | 20 – 150                                | 50 – 300                     | 300 – 4000                   | 500 – 3000                        | 20 – 150                        | 20 – 500                            |
| Elevated Source             | –                                       | Possible                     | Possible                     | ✓                                 | –                               | –                                   |
| EQ Observation Mode         | 20 min. stationary                      | Drive-by                     | Drive-by                     | Drive-by                          | Drive-by                        | Drive-by / stationary               |
| Analyte Limitations         | CMI-limited                             | CMI-limited                  | CMI-limited                  | Column background limited         | CMI and storage tube-limited    | CMI / sensor cost limited           |
| Site Access Required        | –                                       | ✓                            | ✓                            | –                                 | –                               | –                                   |
| Key Use Limitation          | Open areas / meteorological             | Road access / meteorological | Road access / meteorological | Road access / sunny conditions    | Open areas / meteorological     | Meteorological                      |
| Anticipated Accuracy Goals* | < 30%                                   | < 15%                        | < 15%                        | < 20%                             | < 20%                           | < 50%                               |
| Application Cost            | Low                                     | Mid                          | Mid                          | Low/mid                           | Low                             | Very low                            |

### **Verification/Validation Studies**

Verification/validation studies were conducted on the sub-methods to OTM 33. Therefore, see the referenced sections above to review studies specific to the different OTM 33 techniques.

### **Typical QA/QC**

Each sub-method to OTM 33 will have its own QA/QC parameters that are specific to the instrumentation used, measurement technique, field site, and purpose of the study. QA/QC for applications steps normally depend on pre-determined data quality indicators that are unique to

the project objectives. The technology components used for OTM 33 applications have their own QA/QC associated to specifics of the instruments. For the technology QA/QC for OP-FTIR, refer to section 2.1; for OP-TDLAS, refer to section 2.2; for UV-DOAS, refer to section 2.3; and for CRDS, refer to section 2.6.

Although EPA OTM 33 discusses potential interferences and QA/QC parameters for the various sub-methods, this section pertains only to the method overview. Readers should refer to the published sub-method for further discussion of potential interferences and QA/QC parameters.

### **Siting Concerns**

In general, concerns regarding the use of OTM 33 to make representative air pollutant measurements are associated with roadway access in and around the target facility, topography of the landscape, buildings around the facility, and meteorological conditions. Referring to Figure 3.20, it is easy to see how these factors could prevent a successful measurement survey. Having limited or no roadway access could eliminate a site from being a candidate for OTM 33 measurements altogether. On the other hand, complex site topography and/or meteorological conditions may make the acquisition of representative measurements difficult, but not entirely impossible. Each measurement survey at each individual site must have a project specific quality assurance plan that evaluates the characteristics of the target facility site.

Other factors may exist that would indicate the need for one OTM 33 sub-method over another. For example, if the leak source is suspected to be significantly elevated off the ground, then sampling via inlet may not be able to sample the source plume, and therefore, total column techniques that use the sun as the optical source (such as OTM 33C) would be more appropriate. Or, if there is the possibility for multiple overlapping sources (such as that shown in Figure 3.20), a near-field OTM 33 sub-method (such as OTM 33A) may be more appropriate than a farther-field (such as OTM 33D).<sup>1</sup>

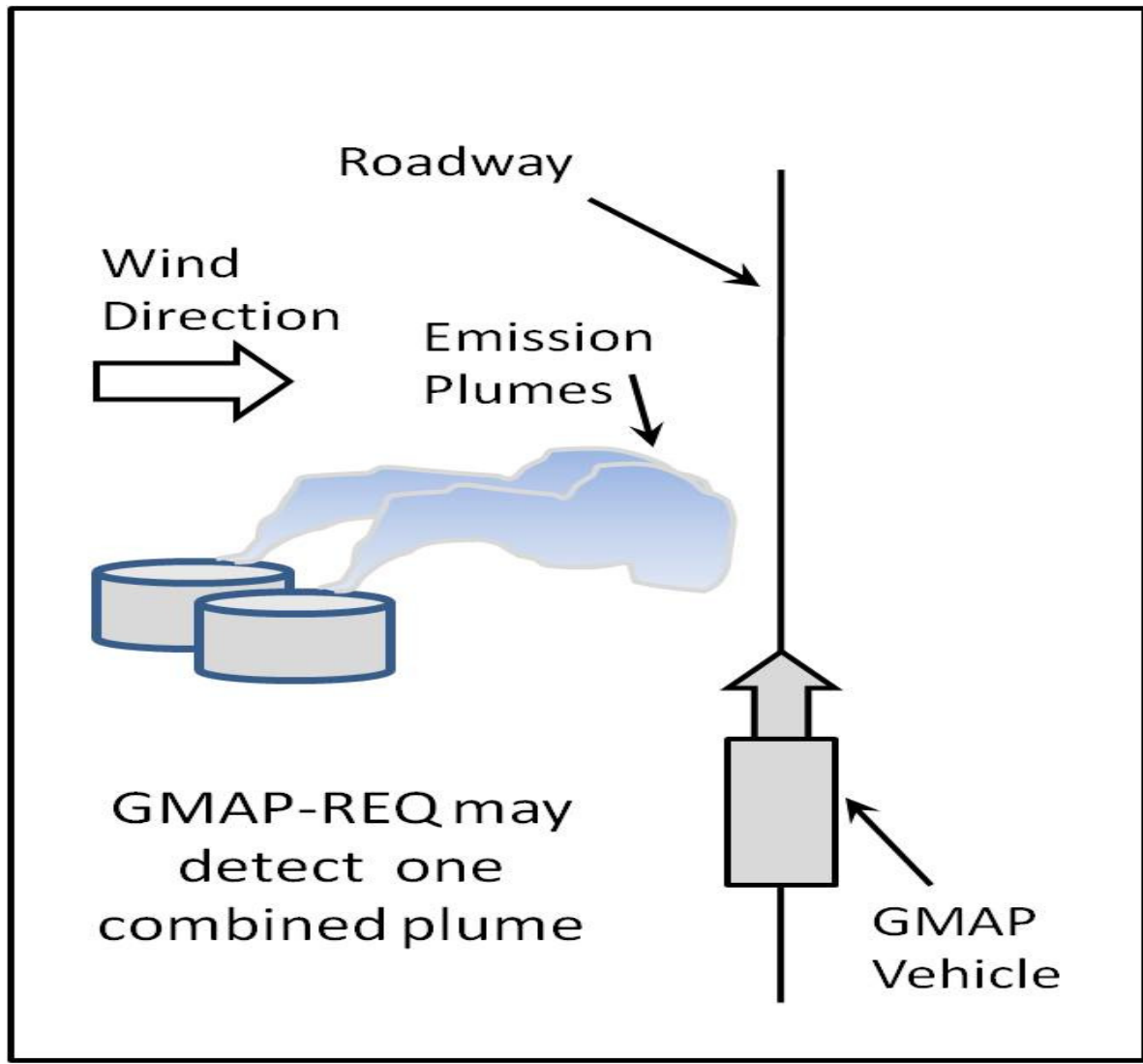


*Figure3-20. GMAP (OTM33) Overlapping Plume Sources*

**Strength and Limitations**

The OTM 33 method series is advantageous for the flexibility that the method and sub-methods allow. This flexibility means that one mobile sampling platform could be used in a wide variety of applications simply by adjusting method parameters.

OTM 33 methods fill an important gap in air quality measurement spatial and temporal scales, but can operate at the extremes as well (more locally at the source, to more regionally at ambient levels). The air quality measurement instruments installed in the mobile platform will, by design, have a broad dynamic range with a detection limit near ambient concentrations. An additional

strength of the OTM 33 methods is that emission rates are calculated within 15-50 percent precision.<sup>1,2</sup>

Although OTM 33 methods have their strengths, stationary and mobile setups have challenges in terms of logistics, location, and whether available roads are near perpendicular to the flow of the plume. For example, one major limitation of the OTM 33 method series is the requirement for roadway access. Not all target facilities will have ideal perimeter survey roadways that completely encircle the facility. If some roadway access exists on one side of the facility, but not on another, then measurements should be taken during times when the wind conditions favor plume transportation to the side with good roadway access. The representativeness of the emission estimates will heavily rely on a limited range of appropriate atmospheric conditions and an unobstructed transport pathway for the plume to travel from the source to the sampling location. Tables 3.17 and 3.18 list the general strengths and limitations of the general approach, respectively.

**Table 3.17. Strengths of the General OTM 33 Approach**

| Feature                  | OTM 33 Strengths   |
|--------------------------|--|
| Flexible application     | Is appropriate for a variety of applications with only simple adjustments.   |
| Good inspection approach | Individual emission rates are calculated within 60% accuracy (OTM 33A), improving with each replicate measurement. |
| Portable instrumentation | Field units are rugged with a high temporal resolution for real-time analysis and fast deployment.                 |
| Site access not required | OTM 33A does not require access to the surveyed site.  |

**Table 3.18. Limitations of the General OTM 33 Approach**

| Feature                              | OTM 33A Limitations  |
|--------------------------------------|--|
| Meteorological concerns              | Sustained and varying wind conditions are required to transport the emission plume.  |
| Susceptible to atmospheric stability | Atmosphere must be stable, but not overly stable.  |
| Absence of near-field obstructions   | Obstructions to proper plume transportation (such as trees, fences, etc.) can cause inaccurate estimates.                                |
| Logistical concerns                  | Location and the availability of roads that are perpendicular to the plume create difficulties.  |
| Distance from emission source        | Measurements must be made between about 10 and 200 m (OTM 33A). Accurate distance measurements are required for the emission estimation. |

**References**

1. U.S. Environmental Protection Agency (EPA). 2014. Draft “Other Test Method” OTM 33 Geospatial Measurement of Air Pollution, Remote Emissions Quantification (GMAP-REQ). Available online at <http://www.epa.gov/ttn/emc/prelim.html>.
2. Thoma, E.B., H. Brantley, B. Squier, J. DeWees, R. Segall, and R. Merrill. 2015. Development of Mobile Measurement Method Series OTM 33. Proceedings of the 108<sup>th</sup> Annual Conference & Exhibition of the Air & Waste Management Association, Raleigh, NC, June 22-25, 2015.
3. DeWees, J. 2014. Development of a Mobile Tracer Correlation Method for Assessment of Air Emissions from Landfills and Other Area Sources. Presented at the 38<sup>th</sup> SSSAAP Conference, Point Clear, AL.
4. Foster-Wittig, T.A., E.D. Thoma, R.B. Green, G.R. Hater, N.D. Swan, and J.P. Chanton. 2014. Development of a Mobile Tracer Correlation Method for Assessment of Air Emissions from Landfills and Other Area Sources. *Atmospheric Environment*, 102, 323 – 330.
5. Albertson, J.D., T. Harvey, G. Foderaro, P. Zhu, X. Zhou, S. Ferrari, M.S. Amin, M. Modrak, H. Brantley, and E.D. Thoma. 2016. A Mobile Sensing Approach for Regional Surveillance of Fugitive Methane Emissions in Oil and Gas Production. *Environmental Science & Technology*, 50, 2487 – 2497.

6. Rella, C.W., T.R. Tsai, C.G. Botkin, E.R. Crosson, and D. Steele. 2015. Measuring Emissions from Oil and Natural Gas Well Pads Using the Mobile Flux Plane Technique. *Environmental Science & Technology*, 49, 4742 – 4748.
7. Thoma, E.D., B.C. Squier, D. Olson, A.P. Eisele, J.M. DeWees, R.R. Segall, M.S. Amin, and M.T. Modrak. 2012. Assessment of Methane and VOC Emissions from Select Upstream Oil and Gas Production Operations Using Remote Measurements, Interim Report on Recent Survey Studies. Proceedings of the 105<sup>th</sup> Annual Conference of the Air & Waste Management Association, San Antonio, TX, June 19-22, 2012.
8. Brantley, H.L., E.D. Thoma, W.C. Squier, B.B. Guven, and D. Lyon. 2014. Assessment of Methane Emissions from Oil and Gas Production Pads using Mobile Measurements. *Environmental Science & Technology*, 48, 14508 – 14515.
9. Brantley, H.L., E.D. Thoma, and A.P. Eisele. 2015. Assessment of Volatile Organic Compound and Hazardous Air Pollutant Emissions from Oil and Natural Gas Well Pads using Mobile Remote and On-site Direct Measurements. *Journal of the Air & Waste Management Association*, 65:9, 1072 – 1082.
10. Foster-Wittig, T.A., E.D. Thoma, and J.D. Albertson. 2015. Estimation of Point Source Fugitive Emission Rates from a Single Sensor Time Series: A Conditionally-sampled Gaussian Plume Reconstruction. *Atmospheric Environment*, 115. 101 – 109.

### ***3.7 Geospatial Measurement of Air Pollution, Remote Emission Quantification: Direct Assessment – Other Test Method 33A***

Identifying and quantifying gaseous emission rates from a fugitive or area source to the atmosphere is difficult due to a source's spatial and temporal variability and measurement technology uncertainty. However, spatiotemporal measurements of air quality around a facility can be made with mobile measurement systems. Mobile measurements refer to the geospatial measurement of air pollution (GMAP) series of methods wherein a vehicle is outfitted with fast-response air quality instruments and precise global positioning systems (GPS) that can be deployed in a variety of scenarios.<sup>1,2</sup> Other test method (OTM) 33, or "Geospatial Measurement of Air Pollution-Remote Emissions Quantification (GMAP-REQ)," describes the general overview of the GMAP methods and serves as the background for method subsets. This section discusses the first of these sub-methods, OTM 33A, a GMAP-REQ approach called "direct assessment" (DA). The DA approach directly measures the concentration of atmospheric pollutants and then uses wind measurements to calculate the emissions flux rate. OTM 33B for comparison, requires the known release of a tracer gas to determine emissions flux as described in Section 3.4.

OTM 33A is a mobile measurement technique that is used to characterize emissions from near-field, ground-level point sources and is intended for rapid deployment without requiring auxiliary stationary instrumentation, site-specific modeling, or direct site access. Typically, this method is applied to sources that are small in spatial extent and are near (about 20 to 200 m) to the driving route.<sup>2,3</sup>

Emission sources are categorized as either "defined" or "undefined." Undefined area sources typically originate from large areas (i.e., greater than 1 square kilometer), whereas defined fugitive sources cover smaller areas (i.e., less than 1 square kilometer down to a square meter) allowing emissions points to be identified for direct measurement.<sup>1</sup> The types of sources targeted with OTM 33A are mostly categorized as defined sources.

### **General Description of Approach**

Conducting OTM 33A requires the deployment of a vehicle equipped with fast-response analytical instruments<sup>1</sup> and precise GPS to characterize pollution emissions as the GMAP vehicle is driven around the facility. Emission information on gas-phase criteria pollutants, particulate matter and ultrafine particles, volatile organic compounds (VOCs), hazardous air pollutants (HAPs), and greenhouse gases (GHGs) is collected when a GMAP vehicle outfitted with appropriate analytical and auxiliary equipment is driven around the target facility. This information is spatially and temporally resolved, meaning that the data can be analyzed to supplement regular air monitoring programs such as leak detection and repair programs, periodic fence-line monitoring, gradient-type local air shed concentration mapping, and source emission rate characterization.<sup>1</sup> As the GMAP vehicle is driven around the facility, air pollution concentration levels are recorded both inside the emission plume and outside the plume, depending on where the plume intersects the GMAP vehicle pathway (Figure 3.21).<sup>1</sup> If the wind conditions are not favorable, or there are other interferences such as buildings or topographic obstacles to the path of the emission plume, then representative measurements of pollutants inside the plume may be difficult. Measurements outside the plume are considered background levels.

---

<sup>1</sup> A suitable instrument example is cavity ring-down spectroscopy (CRDS) described in Section 2.6.



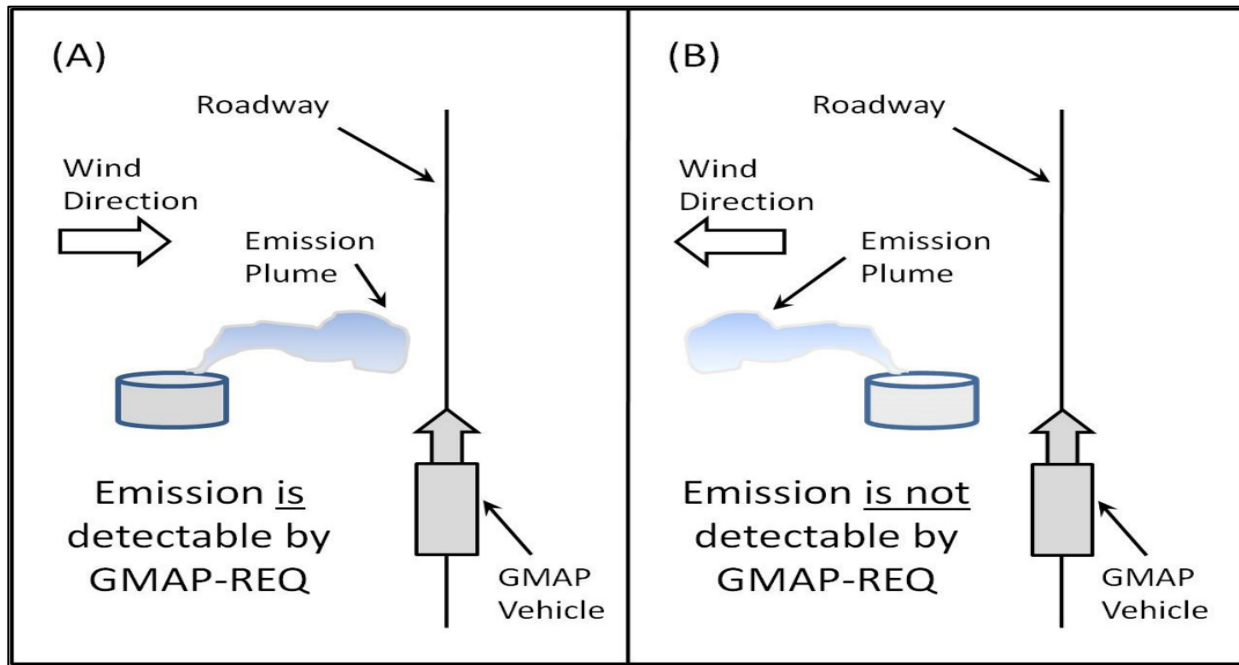


**Figure 3.21. GMAP (OTM 33) Limitations.**

The flexibility of OTM 33 methods allow for multiple source assessment schemes possible using one measurement system. The source assessment schemes possible for OTM 33A include:

- Concentration Mapping (CM) – Used to find the location of unknown sources and to evaluate the impact these source emissions may have on local air shed pollution concentrations.
- Source Characterization (SC) – Used to improve the understanding of known or discovered sources through the collection of secondary measurements (such as remote imaging or canister grab sample speciation).
- Emissions Quantification (EQ) – Used to measure (or estimate) the source emission rate.

Concentration mapping (CM) involves driving the GMAP vehicle around a target facility to determine the area of highest emission concentrations. As illustrated in Figure 3.22, the mobile measurements combined with wind information can identify a “hot spot” area (shown in red as higher concentration).<sup>2</sup>

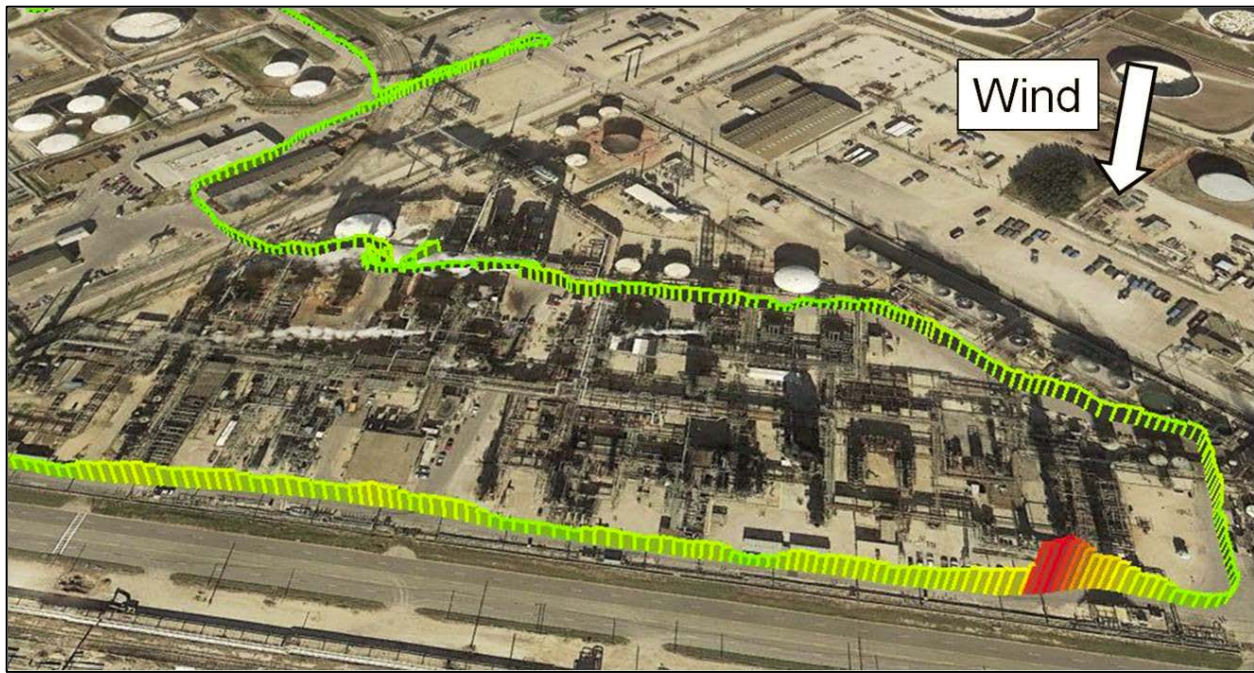


**Figure 3.22. GMAP-REQ-DA (OTM 33A) Concentration Mapping Survey of an Industrial Facility. Red bars indicate elevated emission concentrations.**

Once a hot spot area has been identified, further investigations (i.e., source characterization, leak detection and repair (LDAR)) may be conducted to provide additional information regarding the discovered emissions. As explained in the OTM 33A method, these source characterization activities can include multiple repeated transects of the GMAP vehicle through the emission plume or mapping upwind and downwind of the source to help refine the source location and observe any potential background interferences. Source characterization activities may also involve the collection of other data forms and samples such as recording infrared camera images or collecting a canister grab sample while in the emission plume. Auxiliary data can also be collected using the real-time measurement data to position the GMAP vehicle in the plume at a safe distance downwind of the emission source. If site access is limited and there is no other way to determine the source of the emission, then in-plume canister sampling may help inform the actual source by elucidating the chemical composition, which may indicate one component of the process over another.<sup>2</sup>

While positioned in the plume, EQ efforts can also be accomplished. Although it is possible to perform EQ measurements both in mobile and stationary scenarios, EQ measurements are typically acquired using a stationary approach such as Point Source Gaussian (PSG).<sup>2</sup> When conducting PSG

measurements, the GMAP vehicle is stationary at a location downwind of the emission source while the concentration measurement and wind measurement instruments of the vehicle collect data over a period of 15 to 20 minutes for one EQ measurement. A PSG-based computer program uses an inverse algorithm to estimate the strength of the source emissions and bin the concentration data by the wind angle at the time of sample collection (see example in Figure 3.23).<sup>2</sup> The combined information is then used to estimate the mass emission rate of the emission source assuming a point source release and using Gaussian plume dispersion tables.

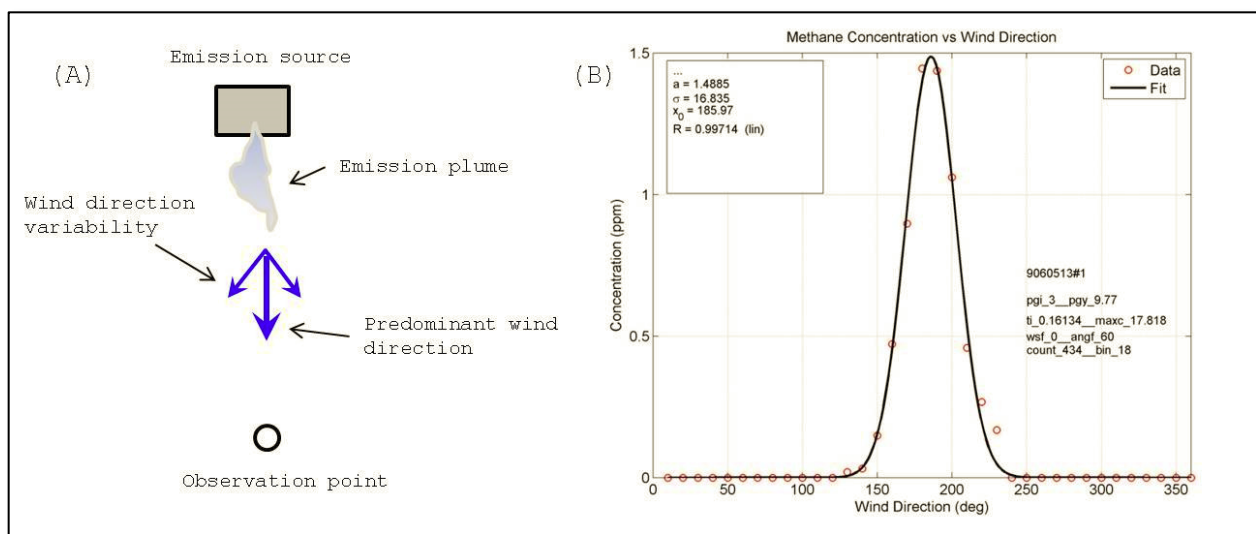


**Figure3-23. (A) An Illustration of a Stationary EQ Observation, and (B) the Resultant Time-Integrated, Wind Angle-Resolved Data File and Gaussian Fit.**

The analytical instruments included in the design of the GMAP vehicle must be robust enough to withstand mobile applications in remote areas. Unpaved or rough roads will likely be encountered during a facility survey. The pollutant measurement instrumentation must have near-ambient level detection capabilities with an appropriate dynamic range. Because OTM 33 sub-methods typically use a combination of data measurements (such as GPS location, pollutant concentration, wind information, etc.) to determine source detection, emission source location, and mass emission rate, the instruments should also be time-synchronized to the second. A typical GMAP vehicle includes a cavity ring-down spectroscopy instrument (e.g., 10 Hz G1301-fc or 0.5 Hz G1204 by Picarro Inc., Santa Clara, CA, USA; a 1 Hz GG-24-r instrument by Los Gatos Research, Mountain View, CA, USA; or similar) to provide real-time methane measurements. Common additional equipment includes a sonic anemometer (e.g., model 81000 3-D by R.M. Young, Traverse City, MI, USA), a compact auto-

north weather station (e.g., model AIO by Climatronics Corp., Bohemia, NY, USA), and a GPS system (e.g., Hemisphere Crescent R100 Series GPS by Calgary, AB, Canada or similar). A custom computer program (e.g., LabView by National Instruments, Inc., Austin, TX, USA) is also employed to time-align the wind and concentration data stream, while a custom analysis program (e.g., MATLAB by MathWorks, Natick, MA, USA) processes the data and calculates source emission rate estimates based on the PSG calculation approach.<sup>2,3,4,5,6,8</sup>

The PSG calculation uses the measured source distance from the mobile platform when stationary (determined using an optical gas imaging (OGI) camera and laser rangefinder) and a representative atmospheric stability indicator (ASI)—derived from the average turbulence intensity from the 3-D sonic anemometer and the standard deviation of the 2-D wind direction from the compact meteorological station—to input values for the horizontal ( $\sigma_y$ ) and vertical ( $\sigma_z$ ) plume dispersion as indicated in the PSG reference tables (EPA OTM 33A Appendix F1). The PSG emission estimate ( $q$ ) is a simple 2-D Gaussian integration (reflection term is omitted) where the plume dispersion is multiplied by the mean wind speed ( $u$ ) and the maximum plume concentration ( $c$ ), calculated as:<sup>2,3</sup>

$$q = 2 \pi \times \delta y \times \delta z \times u \times c$$

Through validation studies discussed in the section below, data quality indicators (DQIs) were developed to filter out data that were not ideally obtained. This process eliminates the potential for high or low biases in the concentration measurements due to skewed plume acquisition decreasing the representativeness of the plume measurement, plume concentrations too low for the method limits or incomplete plume capture, or improper wind conditions or plume channeling due to upwind obstructions. Such DQIs include (but are not limited to):

- Concentrations corresponding to wind directions that are  $\pm 30^\circ$  of the mean source wind direction
- An average in-plume concentration of 0.1 ppm or greater
- A Gaussian fit with an  $R^2 > 0.80$ .

For example, if the atmospheric boundary layer increases in height due to unstable atmospheric conditions, the emission plume height will increase such that the measured concentration is greatly reduced (Figure 3.24).<sup>2</sup> In this example, the change in atmospheric stability is typified by two emission plume mobile OTM 33A measurements taken about 2 hours apart on the same day. In the mid-morning (shown in the red trace), when the atmosphere is more stable, the advection (lateral) movement of the plume is more dominant than the convection (vertical) movement of the plume and the full representation of the gas emission concentration is captured. Conversely, as the ground warms towards mid-day (blue trace) and the energy in the atmosphere increases, the number of rising parcels of air increases and the convection movement strengthens, causing the plume to disperse more vertically and effectively dilute the gas emission concentration at the sample probe.<sup>2</sup> The measurement shown in the blue trace would be eliminated from the final data set after the application of the < 0.1 ppm DQI, thereby insuring that the data set analyzed by the end-user is of a known quality and certainty.

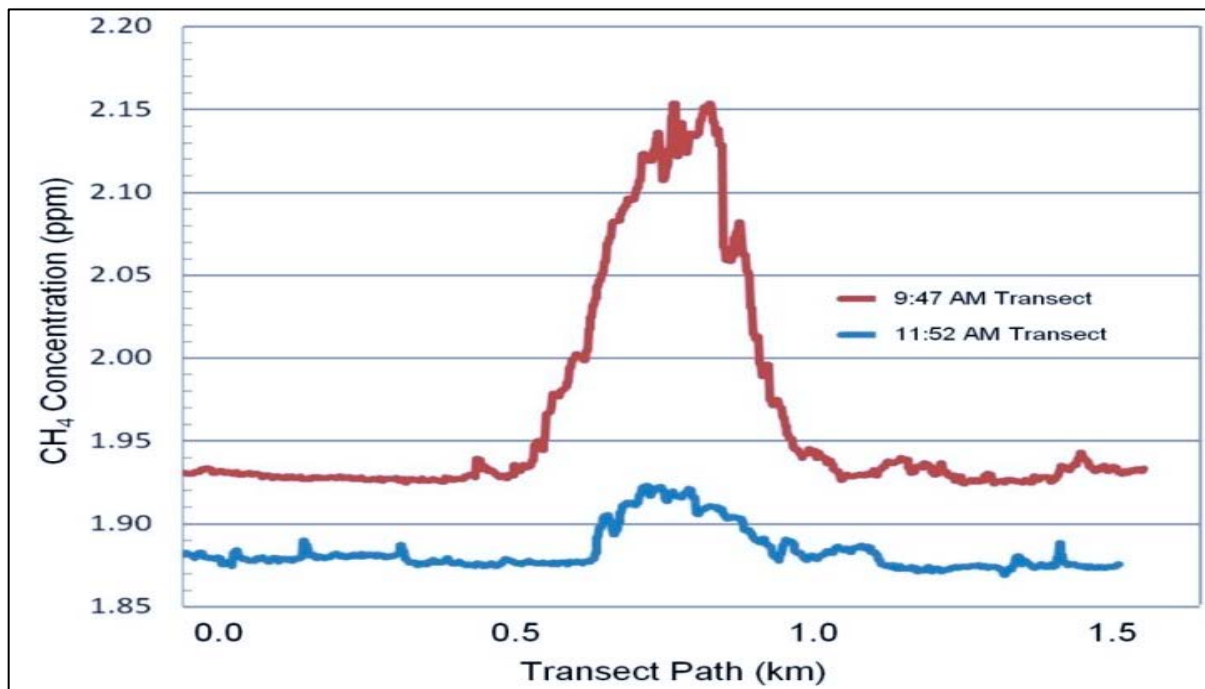


**Figure 3-24. Effect of varying atmospheric conditions with red showing stable atmosphere and blue showing unstable atmosphere.**

As mentioned in Section 3.6, the quality assurance project plan (QAPP) will identify the DQIs used and EPA’s OTM 33A document includes considerations for sampling technique and execution.

**Verification/Validation Studies**

Although many groups are actively developing OTM 33A GMAP vehicles and techniques, only a handful of have published the results of their studies and many of these are from EPA-directed research. What is now known as OTM 33A was first described by Thoma et al. in 2010 as a mobile method designed to locate fugitive emissions, estimate the methane emission rate, and use the methane result to calculate VOC emissions using the ratios of compound abundance relative to methane in evacuated canister samples. This preliminary study provided proof-of-concept and laid the groundwork for method development. An overview of the studies performed to date is available in Table 3.19 and are discussed in chronological order below

**Table 3.19. Summary of GMAP-REQ-DA Studies.**

|                             | Thoma et al., 2010 <sup>4</sup>   | Thoma et al., 2012 <sup>5</sup>  | Brantley et al., 2014 <sup>6</sup>   | Brantley et al., 2015 <sup>7</sup>  | Foster-Wittig et al., 2015 <sup>8</sup>   |
|-----------------------------|---|--|--|---|---|
| Study dates                 | 2009  | 2010 – 2011  | 2010 – 2013  | July 2011   | 2010 – 2013   |
| Chemical compounds measured | Methane & VOC   | Methane & VOC  | Methane  | VOC & HAPs  | Methane   |
| Study Focus                 | Proof-of-concept  | Interim Report   | Data statistics and comparison with direct, onsite measurements  | Comparison of onsite and remote VOC/HAP measurements  | Comparison of emissions calculation methods   |
| Key Results                 | <ul style="list-style-type: none"> <li>➤ There is potential for the approach</li> </ul> | <ul style="list-style-type: none"> <li>➤ Multiple repeat measurements are best.</li> <li>➤ Proper plume transport is important.</li> <li>➤ Accuracy = ± 60%</li> </ul> | <ul style="list-style-type: none"> <li>➤ Methane emissions mostly correlated with gas production.</li> <li>➤ OTM 33A captures large, stochastic emission events versus smaller leaks.</li> </ul> | <ul style="list-style-type: none"> <li>➤ Onsite and remote concentration measurements are similar.</li> <li>➤ OTM 33A can be used to identify when emissions are not effectively controlled.</li> </ul> | <ul style="list-style-type: none"> <li>➤ Although simplified, PSG estimates are good approximations.</li> <li>➤ Repeat measurements reduce estimate error.</li> </ul> |

As research progressed and the technique was applied in multiple field studies, Thoma et al.<sup>5</sup> released an interim report in 2012 that discussed different emissions estimation calculation methods and the potential use and limitations of the method. The data presented in this study included measurements from both field campaigns and controlled release experiments using a

preliminary DQI filter for the wind direction of  $\pm 60$  degrees from the predominant wind vector. The field campaign measurements indicated that the methane emission rates and VOC compositions for each basin are unique to that basin such that there is potential to determine the source of a measurement just from these two attributes, like a compositional fingerprint.<sup>5</sup> The controlled release experiments investigated the accuracy and precision of two emission calculation methods: PSG and backwards Lagrangian stochastic (bLs) modeling. Although individual measurements can exhibit a large amount of variability (see Figure 3.25a), repeat measurements can significantly reduce the measurement error and yield estimates for 0.6 grams per second (g/s) methane release of 0.56 g/s using PSG and 0.57 g/s using bLs calculation methods (with a 1 standard deviation ( $\sigma$ ) = 0.17 g/s and 0.23 g/s, respectively). In addition, the controlled release experiments showed that unstable, low wind speed conditions (< 1 meters per second (m/s)) do not produce much usable data and measurement farther away from the emission source than 100 m require more favorable wind conditions for sufficient plume transport to the sampling location.<sup>5</sup>

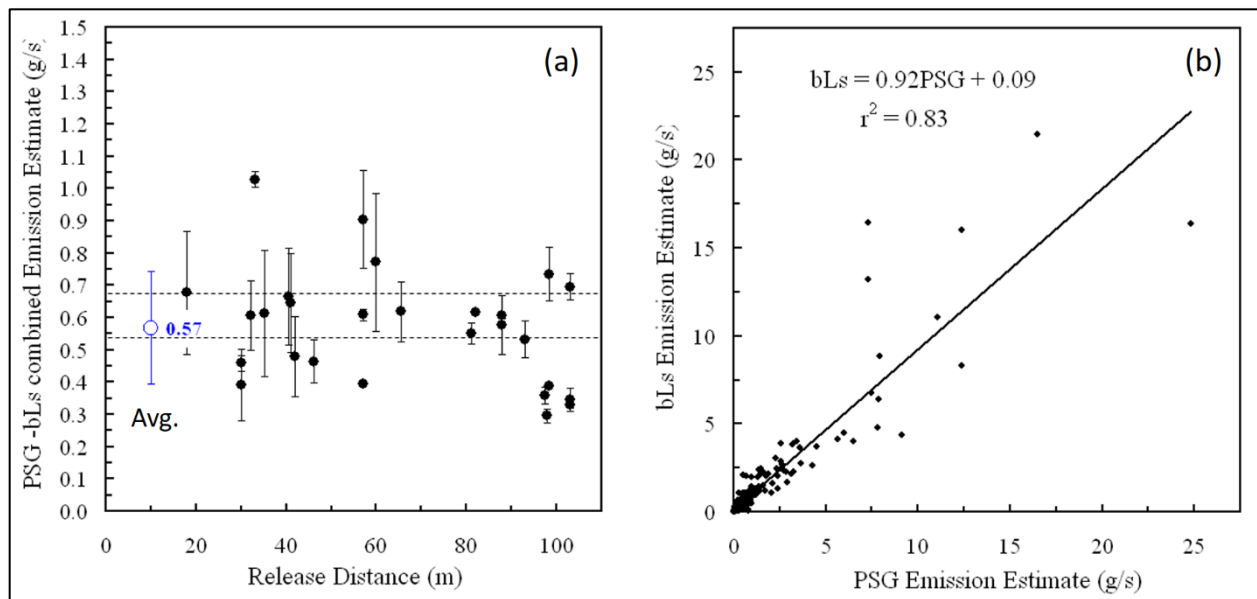


**Figure 3-25. results from controlled release experiments with (a) measurement results for both psg and bls calculation methods, and (b) a comparison between the two methods.**

The data plotted in Figure 3.25a represent the spread of the two calculation methods—PSG and bLs—using the error bars with the circle indicating the average of the two methods. The first data point in blue of panel (a) represents the average of all the data with  $\sigma = 0.18$  g/s as the error bars.<sup>5</sup>

The largest underestimates in panel (a) occur at the farther distances while the largest overestimate in the measurement series (1.03 g/s) occur where plume flow obstructions were observed and therefore indicate the effect of plume “channeling.” The overall measurement uncertainty between the two methods is quite small as evidenced by the data set average in panel (a) being very close to the actual release rate and the high  $r^2$  value of 0.83 in panel (b). Most notably, the data shows that individual measurements using the OTM 33A approach can have an accuracy of about  $\pm 60\%$ , while ensembles of repeat measurements tend to be much more accurate.<sup>5</sup>

Field studies using this approach continued to 2013, when the researchers of Brantley et al.<sup>6</sup> had enough data to evaluate the statistics of the data set. The data used for Brantley et al., 2014 resulted from the PSG calculations and were pre-screened using the following 3 DQI criteria:

- Peak concentrations that corresponded with wind directions that were within  $\pm 30^\circ$  of the source direction
- An average in-plume concentration greater than 0.1 ppm
- A Gaussian fit with an  $R^2 > 0.80$ .

The filtered data set was then subjected to multivariate linear regression analysis and comparisons with previous, onsite, direct measurement studies.

The Pearson correlation coefficients shown in Table 3-20 represent the results of the multivariate regression analysis. Here, the amount of correlation in the data set is shown as a fractional number, with +1.00 being the highest amount of positive correlation possible and -1.00 indicating the most negatively correlating variables (where, if one goes up, the other goes down at a rate that is inversely proportional). As illustrated in Table 3-20, the most correlating variable to methane emissions is the amount of gas production per day, and it is not a relatively strong correlation with a coefficient of only 0.29, accounting for only 10% of the emissions data set variation. The negative correlation of methane emissions with mean facility age indicates that the amount of methane emissions measured at a facility should decrease as the facility age increases. However, with only a correlation coefficient of -0.20, the age variable of a facility is not expected to predict methane emissions.<sup>6</sup>



**Table 3.20. Pearson Correlation Coefficients of Emission and Production.**

|  | Methane Emissions<br>(Mscf/day) | Gas Production<br>(Mscf/day) | Hydrocarbon<br>Liquids Production<br>(bbl/day) | Water Production<br>(bbl/day) |
|--|---------------------------------|------------------------------|--|-------------------------------|
| Methane Emission<br>(Mscf/day)                 | 1.00                            |                              |  |                               |
| Gas Production<br>(Mscf/day)                   | 0.29                            | 1.00                         |  |                               |
| Hydrocarbon<br>Liquids Production<br>(bbl/day) | -0.01                           | 0.44                         | 1.00   |                               |
| Water Production<br>(bbl/day)                  | 0.22                            | 0.77                         | 0.40   | 1.00                          |
| Mean Age (years)                               | -0.20                           | -0.59                        | -0.34  | -0.57                         |

In relation to direct, onsite, measurements, the data captured from OTM 33A appears to only represent the leaks with the highest emission rates. For the study comparison, Brantley et al.<sup>6</sup> compared OTM 33A field results with those from Allen et al. (2013)<sup>10</sup> and ERG (2011),<sup>11</sup> where the methane emissions were measured using three very different approaches. The results from the study comparison are shown in Figures 3.26 and 3.27, where the ERG study captured more of the very low leak rates relative to the other studies, and the OTM 33A study captured more of the higher leak rates.<sup>6</sup>

Although the studies collected measurements from different basins during different years (the OTM 33A study used data from 2010 to 2013) and from very different facility populations, some general observations are still possible. For example, the ERG study data in Figure 3.26 was conducted in the Barnett Basin and exhibits many more measurements that are well below the whiskers of the box plot (the boxes represent 1<sup>st</sup> and 3<sup>rd</sup> quartiles of the data and the whiskers extend to 1.5 times the interquartile range; the black circles and bars indicate the data means and 95% confidence intervals, respectively). The data mean for the ERG study is also much lower, accounting for the more measurements collected for leaks of smaller emission rates. Whereas, the OTM 33A study was only able to capture the larger emission rates at the farther sampling location. As discovered by Thoma et al. (2012),<sup>5</sup> each basin should have a distinct emission rate relative to its production type and region; however, the comparisons between similar facilities in the same basin should be similar.

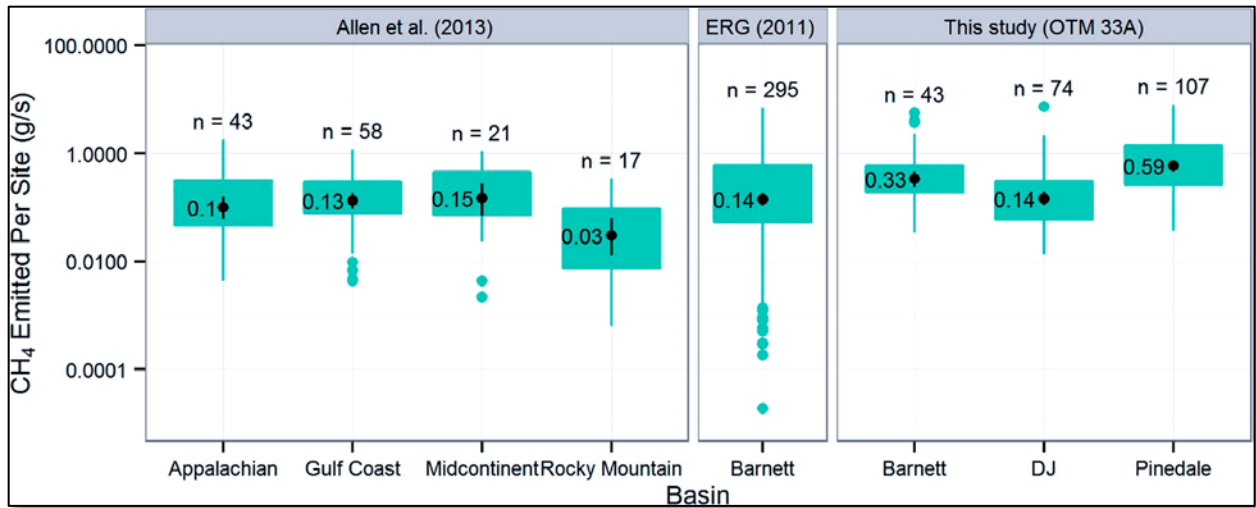


Figure 3-26. Comparison of methane measurements by basin.

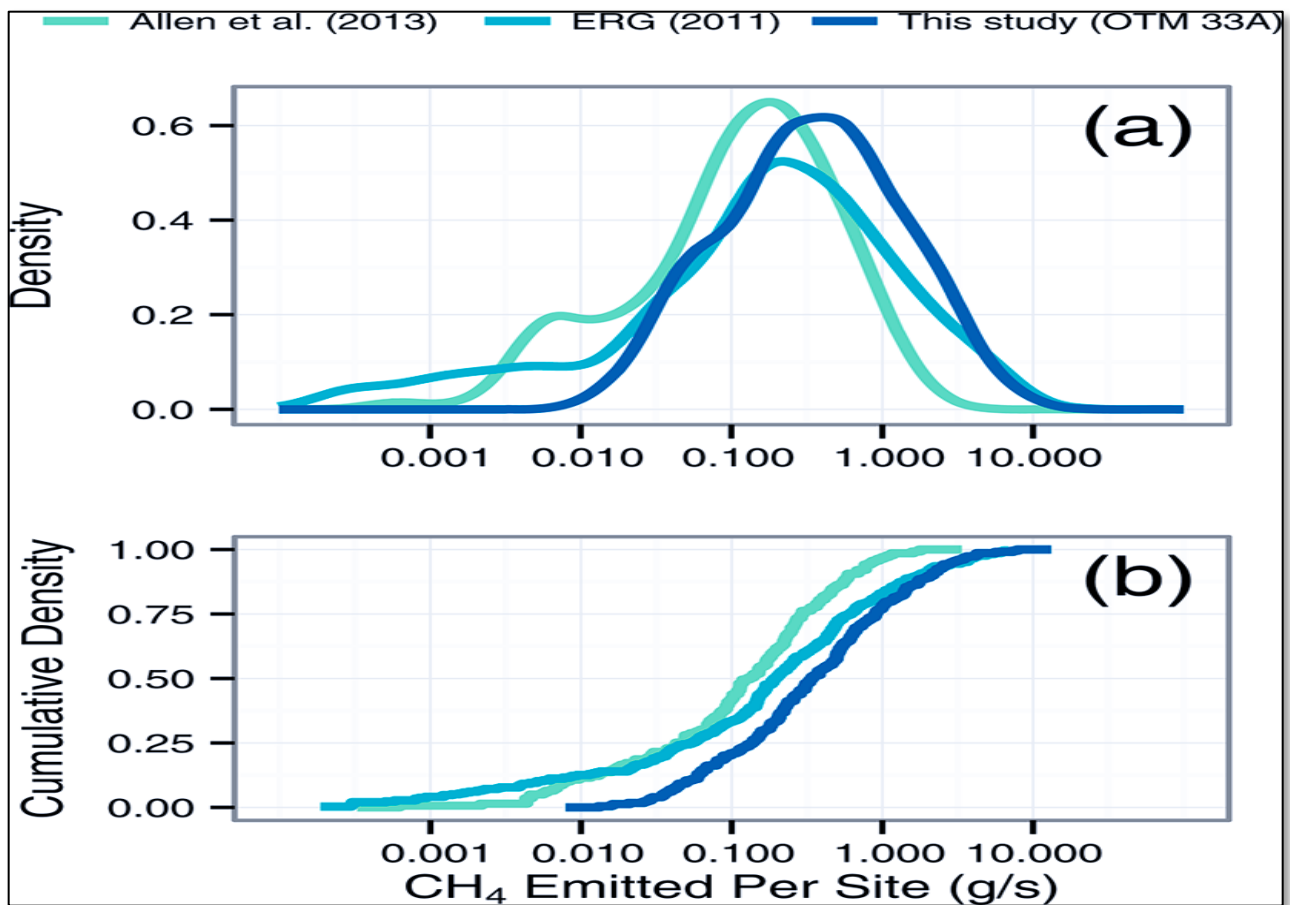


Figure 3-27. Density (a) and cumulative density (b) of methane emission measurements.

Figure 3.27 elucidates the potential reason for the discrepancy between the two Barnett Basin data sets. In panel (a), the ERG study represents many more measurements that are lower in emission

rate as seen by the “shoulder” in the left-hand part of the ERG line. The OTM 33A study used a DQI filter of only measurements at a concentration > 0.1 ppm, which limits the method to about 0.010 g/s compared to the < 0.0001 g/s measurement limit for the onsite sampling approaches. When looking at the cumulative density, the OTM 33A measurements do not start until a higher emission rate and do not peak until the very upper end of the measurement distribution. Therefore, Brantley et al. (2014)<sup>6</sup> not only revealed that OTM 33A captures the emissions from higher rate leaks, but also observed that many of the onsite measurements did not or were unable to represent these larger leaks in their data sets. Most likely, these leak omissions were due to the presence of stochastic emission events (such as tank flashing and malfunctioning equipment), which are not easily measured using onsite techniques.

Brantley et al. (2015)<sup>7</sup> continued analysis of OTM 33A measurements by investigating the concentration and composition of VOCs and HAPs collected using OTM 33A versus those measured onsite. During stationary measurements, when the GMAP vehicle was in the peak of the emission plume as indicated by the real-time methane concentration measurements, the GMAP vehicle operator initiated sample acquisition with a 30-second evacuated canister grab sample. After applying the same DQI criteria as for the previous study (Brantley et al., 2014<sup>6</sup>), the PSG method was used to estimate methane emission rates from the associated 20-minute OTM 33A sample and used the following ratio calculation to estimate the canister compound emission rate:

$$F_c = [(C_c \cdot F_o) / C_o] [M_c / M_o]$$

Where:

$F_c$  = Emission rate estimate of canister compound (g/s)

$C_c$  = Measured concentration of canister compound (ppb)

$F_o$  = Emission rate estimate of methane using PSG (g/s)

$C_o$  = Methane concentration measured from the canister sample that is above

background (ppb)

$M_c$  = Molecular weight of the canister compound (g/mol)

$M_o$  = Molecular weight of methane (g/mol)

Unexpectedly, this study discovered that the high-volume sampler (HVS) used for the onsite measurements has a now-documented (Howard et al., 2015)<sup>9</sup> malfunction when transitioning from lower to higher measurement categories. This is evidenced in Figure 3.28 where the measurements between the HVS (Hi-Flow) and OTM 33A (canister) are well correlated at concentrations of up to about 10.5% hydrocarbons (HC).<sup>7</sup>

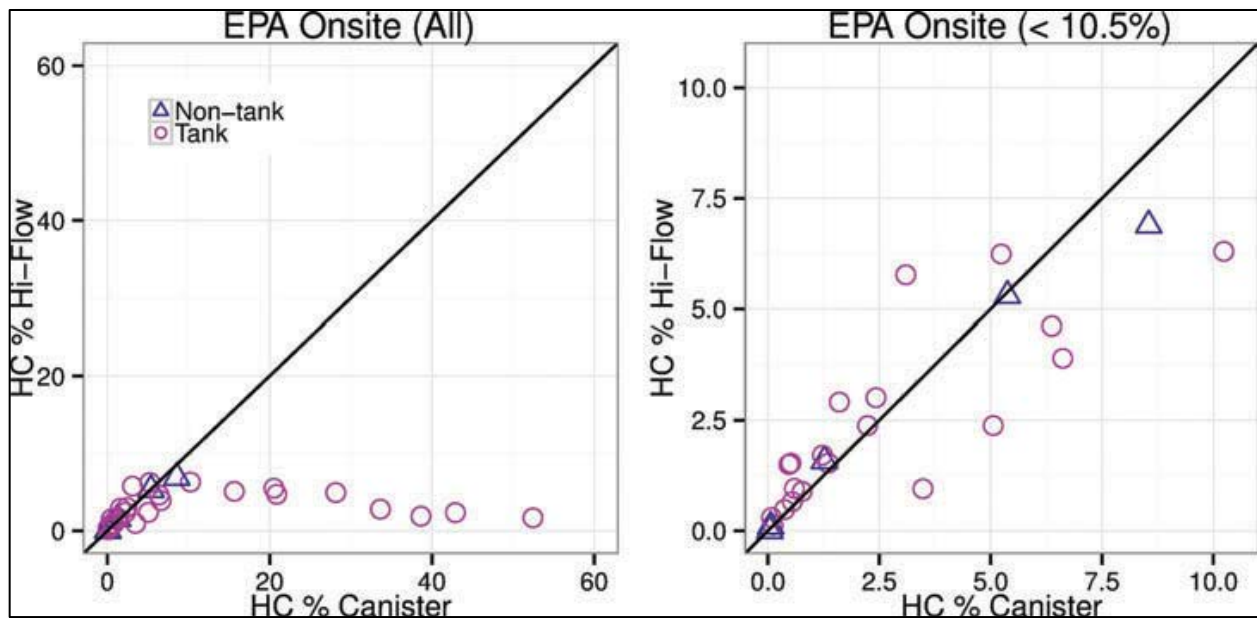


**Figure 3-28. Comparison of onsite measurements and remote (canister) measurements. The solid black line represents  $y=x$ .**

The presence of flash emissions during this study seem to correlate with higher methane, VOC, and HAP emissions and highlights the need for a cost-effective method that can identify significant leaks that have a larger amount of temporal variability. Brantley et al. (2015)<sup>7</sup> also compared the VOC and HAP emissions estimates from the canister samples to those modeled by the API E&P TANKS potential-to-emit estimates. By comparing the measured and modeled values, Brantley et al.<sup>7</sup> discovered that the OTM 33A remote sampling approach can be used to identify situations where

facility emissions are not being effectively controlled to the 95% control level. The overall results of this study show that the OTM 33A approach can be used as a remote inspection technique to survey facilities for large and/or intermittent fugitive emissions.<sup>7</sup>

Recently, a study by Foster-Wittig et al. (2015)<sup>8</sup> took a closer look at the methane emission estimate calculations by comparing PSG results with those from plume geometry inverse calculation approaches based on a wind field data model and plume geometry reconstruction from angle-resolved concentration data. The modeled and reconstructed calculation approaches attempt to produce more robust measurement results by calculating atmospheric dispersion and plume geometry in more detail than what is represented using the atmospheric stability look-up tables associated with the more simplistic PSG method. Controlled release data was filtered using the following DQIs:

- Data were acquired during a mostly neutral atmosphere (the absolute value of stability—source height divided by source distance—is less than 0.2).
- Measurements where the average concentration sorted by corresponding wind direction measurements were greater than 0.3 ppm for any wind angle category.
- The standard deviation of the wind direction over the measurement duration is greater than 20° to allow full plume capture.
- The mean wind direction over the measurement duration is within  $\pm 50^\circ$  of the measurement location direction relative to the plume source.

After DQI data filtering, 41 of the original 106 measurements were calculated using the modeled and reconstructed methods and compared to the PSG results.<sup>8</sup> Figure 3.29 illustrates these results, where the shaded bands indicate the controlled methane release amount with a  $\pm 5\%$  release rate accuracy.<sup>8</sup> In this figure, the circles represent the estimated emission rate as calculated by the modeled atmospheric dispersion approach ( $S_M$ ), the asterisk data points represent the reconstructed geometry approach ( $S_R$ ), and the triangles represent the conventional PSG estimates ( $S_E$ ). Similarly, the authors compared the calculated emission values average by study in Figure 3.30.<sup>8</sup>

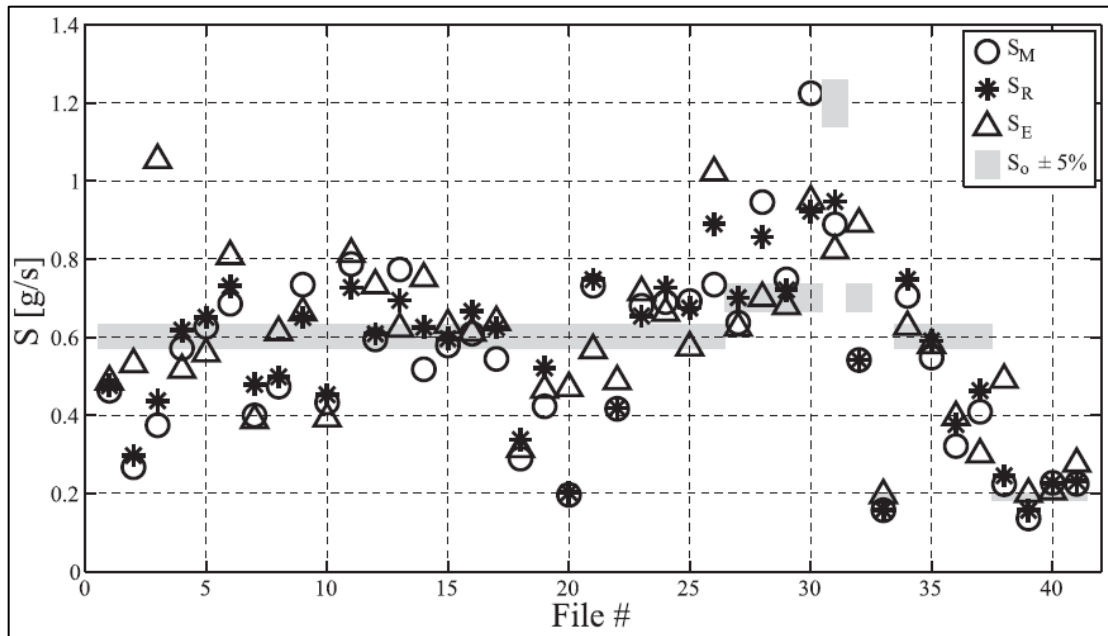


**Figure 3-29. Source emission strength calculations for each controlled release.**

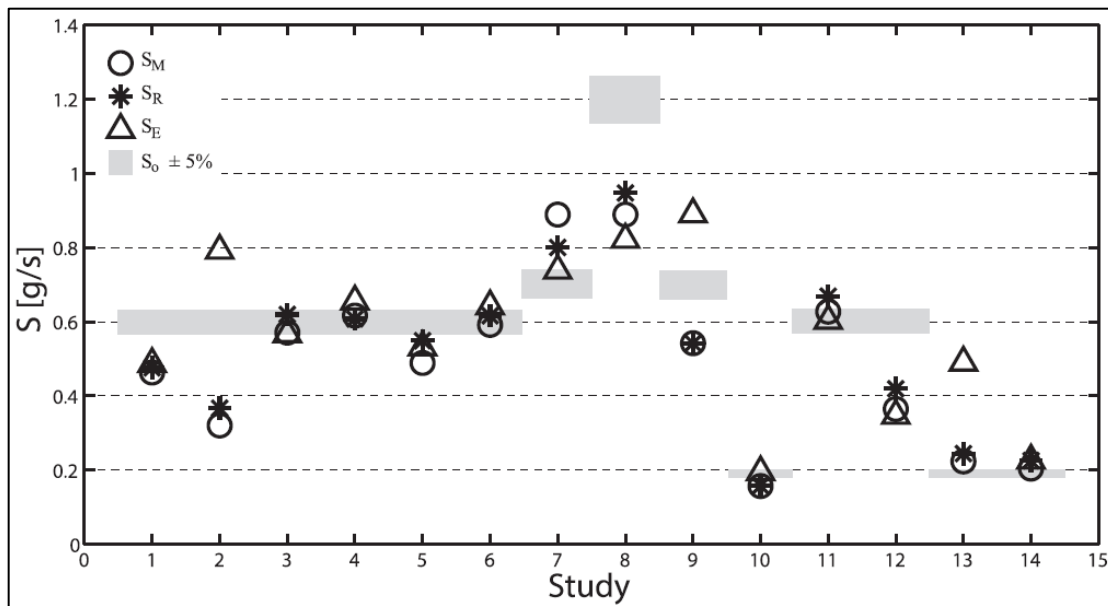


**Figure 3-30. source strength calculation averages by controlled release study.**

Note for Figure 3.30 that only studies 3, 4, 5, 6, 7, and 14 along the x-axis have three or more measurements in their averages.<sup>8</sup> Each study average represents at least one measurement and can have up to seven measurements. The amount of error represented by the data in Figures 3.30 and 3.31 for each calculation approach is -47 to 27%, -39 to 29%, and -42 to 158% for the modeled, reconstructed, and PSG results, respectively.<sup>8</sup> Overall, the mean percent error for the modeled,

reconstructed, and PSG results are -5%, -2%, and 6% with a standard deviation of 29%, 25%, and 37%, respectively. The mean percent error results show that the modeled and reconstructed measurements tend to underestimate the release rate whereas the PSG measurements tend to overestimate the release rate; however, it was observed that the largest error occurs when there are less than three measurements available for the study average, indicating that multiple repeated measurements with help to reduce the overall error in the source emission rate estimate. In conclusion, although the PSG calculation approach yields higher standard deviations versus more complicated calculation approaches, it will still provide a good estimation of source emission rates that become more accurate with repeat measurements.<sup>8</sup>

### **Typical QA/QC**

The OTM 33A approach involves many potential stages to application and, therefore, can be subject to multiple stages of QA/QC related to site characteristics, measurement execution, and acquired data quality. The facility type and expected emitted compounds must be able to be detected by the GMAP vehicle equipment, depending on the real-time concentration measurement instrument incorporated in the GMAP vehicle design. Because OTM 33A is a mobile approach, the site must have road access proximal to the target equipment (within 20 to 200 m), there must be a clear, open area between the potential source and the GMAP vehicle sample inlet, and the atmospheric conditions must be such that the plume is transported from the source to the GMAP vehicle with minimal uplift or dispersion (typically sustained wind speeds should exceed 2.0 m/s and the atmospheric stability indicator level of 3 or greater).<sup>2</sup> Repeated transection during mobile measurements or samples during stationary measurements are important to determine temporal variability and to provide confidence in the overall OTM 33A assessment. The application of auxiliary data, such as infrared camera videos, help to verify or pinpoint the source location and reduce the overall amount of measurement error. The number of repeated measurements is generally proportional to the importance of the study data, the temporal characteristics (constancy) of the emission, and the study measurement accuracy objectives.<sup>2</sup>

The GMAP vehicle must be outfitted with batteries such that the OTM 33A equipment can perform measurements while the vehicle is off, eliminating measurement interference from unintended sampling of vehicle emissions. The real-time concentration measurement instrument should have a time resolution of 1 Hz or better (about 10 Hz for the wind-field measurements), be within  $\pm 10\%$  of the actual concentration during an onsite accuracy test, and can resolve a sustained plume six times the standard deviation of a baseline (background) concentration level.<sup>2</sup>

The OTM 33 method series includes sub-methods that operate like the general OTM 33 design. As such, the general QA elements discussed in OTM 33 also apply to applications of OTM 33A and reader should be aware of these additional requirements. The OTM 33 sub-methods also allow for some flexibility in the choice and design of the GMAP vehicle equipment and application; therefore, detailed QAPPs that include discussion on engineering design, field application, procedures for operation and calibration and site-specific analysis of method applicability, potential interferences, measurement data quality objectives (DQOs) and DQIs are required.<sup>2</sup> An effective QAPP lists the measurement objectives, the intended use of the data, and the measurement error tolerances for the project through the definition of DQOs and infield and analysis DQIs. The project measurement objectives are defined in the DQOs, and the monitoring of field operations and performance against the DQOs are executed through DQIs. For example, to perform EQ measurements, the transportation pathway of the plume must be free from obstruction (DQO). If there are any trees or manmade structures in the near-field between the source and the GMAP vehicle, then the plume geometry will be affected and enforcing a DQI where the measurements must show a Gaussian distribution with an  $R^2 > 0.80$  when sorted into discrete bins based on wind direction can cause the measurement to fail the QA requirements.

The flexibility of the OTM 33A approach allows for a variety of GMAP vehicle engineering designs and equipment installed. As mentioned in the studies reviewed in Section 3.7.2, there are many infield DQIs that can be developed to monitor data quality and that may be applicable to all OTM 33A configurations, such as:



- Peak methane concentration within  $\pm 30^\circ$  of the source direction
- Average, in-plume concentration greater than 0.1 ppm
- Gaussian fit with an  $R^2 > 0.80$  for data binned by wind direction
- Standard deviation of the wind direction greater than  $20^\circ$  and less than  $60^\circ$
- Sufficient data acquisition rate as evidenced by the number of data points recorded per measurement duration.

Whenever deploying a newly developed GMAP vehicle for field use, it is good practice to validate the system for remote measurements by performing technique performance testing using a simulated leak source in a realistic environment (i.e., controlled release test). This primary QA tool helps to evaluate the system performance and develop in-field DQIs before the system is deployed for field use. With a combination of pre-deployment approach validation, in-field DQIs, and post-acquisition QA analysis procedures, in addition to proper operation of equipment and application of techniques, the OTM 33A method can provide an estimation of source emission strength from remote locations.<sup>2</sup>

### **Siting Concerns**

Many of the siting concerns associated with the application of the OTM 33A approach are discussed in the interferences section (Section 4) of the draft OTM 33A method. Because OTM 33A is a remote measurements method, these interferences are associated with the height of the emission source, the distance of the GMAP vehicle sample inlet to the emission source, the orientation of the GMAP vehicle inlet in relation to the emission source and predominant wind direction, and the presence of any near-field obstructions to the expected transportation of the emission plume to the GMAP vehicle sample inlet.<sup>2</sup>

At least three background source factors should be considered when making methane measurements from near-ground level, proximate sources: (1) potential for interference from mobile sources, (2) potential for interference from nearby methane sources, and (3) potential for interference from far away methane sources.<sup>2</sup> To mitigate the first potential interference, local

traffic patterns immediately proximal to the measurement route should be noted, the GMAP vehicle sampling inlet should be located in the front portion of the vehicle, and the vehicle must be turned off during stationary measurements. Making repeated mobile measurements around all aspects of the target facility help to elucidate multiple potential sources and/or far away background interferences, thus reducing the potential for the second and third categories of potential interferences. Auxiliary data such as site photos and infrared camera videos can help to verify or pinpoint the emission source and evaluate the upwind background for any potential interferences. Far away background sources should be stable enough to be considered a part of the background signal. However, if a background source is too close to the target equipment, the interference will show up in the variance of the 5% background determination used for the PSG calculation DQI analysis.<sup>2</sup>

When the GMAP vehicle is positioned for stationary measurements, the operator must use the real-time concentration display to ensure that stationary sampling occurs at the point of the predominant wind direction relative to the source location—this means finding the predominant area of peak concentration along the mobile measurement pathway. Once the location of predominant peak concentration is determined, the GMAP vehicle must be in proper orientation to avoid causing channeling interferences. Typically, this involves positioning the GMAP vehicle such that the sampling inlet is facing upwind towards the emission source and there are no obstructions from the vehicle between the inlet and the source location.

The site characteristics and expected emission source locations should also be considered during the pre-field assessment. For example, eddies and potential recirculation of emissions near to a tank source could overestimate the emission rate if the sampling location is not at least five tank diameters downwind. Other near-field obstructions may exist that will obscure the general transportation of the emission plume, such as a tank battery or other man-made structures. The use of an infrared camera can be helpful to positively identify the emission source so that an evaluation of any near-field obstructions can be made and mitigated, if possible.<sup>2</sup>

**Strengths and Limitations**

OTM 33A is a fast-deployable inspection approach that can be used to make source emission estimates without requiring onsite access or complex modeling. However, because the measurements are taken remotely, the representativeness of the emission estimates will heavily rely on a limited range of appropriate atmospheric conditions and an unobstructed transport pathway for the plume to travel from the source to the sampling location. Tables 3.XX3 and 3.XX4 list the general strengths and limitations of the approach, respectively.

**Table 3-21. Strengths of the OTM 33A Approach**

| Feature                  | OTM 33A Strengths  |
|--------------------------|--|
| Flexible application     | Is appropriate for a variety of applications with only simple adjustments.                               |
| Good inspection approach | Individual emission rates are calculated within 60% accuracy, improving with each replicate measurement. |
| Portable instrumentation | Field units are rugged with a high temporal resolution for real-time analysis and fast deployment.       |
| Site access not required | OTM 33A does not require access to the surveyed site.  |

**Table 3-22. Limitations of the OTM 33A Approach**

| Feature                              | OTM 33A Limitations  |
|--------------------------------------|--|
| Meteorological concerns              | Sustained and varying wind conditions are required to transport the emission plume.  |
| Susceptible to atmospheric stability | Atmosphere must be stable, but not overly stable.  |
| Absence of near-field obstructions   | Obstructions to proper plume transportation (such as trees, fences, etc.) can cause inaccurate estimates.                      |
| Logistical concerns                  | Location and the availability of roads that are perpendicular to the plume create difficulties.                                |
| Distance from emission source        | Measurements must be made between about 10 and 200 m. Accurate distance measurements are required for the emission estimation. |

**References**

1. U.S. Environmental Protection Agency (EPA). 2014a. Draft “Other Test Method” OTM 33 Geospatial Measurement of Air Pollution, Remote Emissions Quantification (GMAP-REQ). Available online at <http://www.epa.gov/ttn/emc/prelim.html>.
2. U.S. Environmental Protection Agency (EPA). 2014b. Draft “Other Test Method” OTM 33A Geospatial Measurement of Air Pollution, Remote Emissions Quantification – Direct Assessment (GMAP-REQ-DA). Available online at <http://www.epa.gov/ttn/emc/prelim.html>.
3. Thoma, E.B., H. Brantley, B. Squier, J. DeWees, R. Segall, and R. Merrill. 2015. Development of

Mobile Measurement Method Series OTM 33. Proceedings of the 108<sup>th</sup> Annual Conference & Exhibition of the Air & Waste Management Association, Raleigh, NC, June 22-25, 2015.

4. Thoma, E.B., B.A. Mitchell, B.C. Squier, J.M. DeWees, R.R. Segall, C. Beeler, M.T. Modrak, M.S. Amin, A.B. Shah, C.W. Rella, and R.L. Apodaca. 2010. Detection and Quantification of Fugitive Emissions from Colorado Oil and Gas Production Operations Using Remote Monitoring. Proceedings of the 103<sup>rd</sup> Annual Conference & Exhibition of the Air & Waste Management Association, Calgary, Alberta, Canada, June 22-25, 2010.
5. Thoma, E.D., B.C. Squier, D. Olson, A.P. Eisele, J.M. DeWees, R.R. Segall, M.S. Amin, and M.T. Modrak. 2012. Assessment of Methane and VOC Emissions from Select Upstream Oil and Gas Production Operations Using Remote Measurements, Interim Report on Recent Survey Studies. Proceedings of the 105<sup>th</sup> Annual Conference of the Air & Waste Management Association, San Antonio, TX, June 19-22, 2012.
6. Brantley, H.L., E.D. Thoma, W.C. Squier, B.B. Guven, and D. Lyon. 2014. Assessment of Methane Emissions from Oil and Gas Production Pads using Mobile Measurements. *Environmental Science & Technology*, 48, 14508 – 14515.
7. Brantley, H.L., E.D. Thoma, and A.P. Eisele. 2015. Assessment of Volatile Organic Compound and Hazardous Air Pollutant Emissions from Oil and Natural Gas Well Pads using Mobile Remote and On-site Direct Measurements. *Journal of the Air & Waste Management Association*, 65:9, 1072 – 1082.
8. Foster-Wittig, T.A., E.D. Thoma, and J.D. Albertson. 2015. Estimation of Point Source Fugitive Emission Rates from a Single Sensor Time Series: A Conditionally-sampled Gaussian Plume Reconstruction. *Atmospheric Environment*, 115, 101 – 109.
9. Howard, T., F. Thomas, and A. Townsend-Small. 2015. Sensor transition failure in the high-volume sampler: Implications for methane emission inventories of natural gas infrastructure. *Journal of the Air & Waste Management Association*, 65:7, 856-862.
10. Allen, D. T.; Torres, V. M.; Thomas, J.; Sullivan, D. W.; Harrison, M.; Hendler, A.; Herndon, S. C.; Kolb, C. E.; Fraser, M. P.; Hill, A. D. 2013. Measurements of methane emissions at natural gas production sites in the United States. *Proceedings of the National Academy of Sciences of the U.S.A.*, 110 (44), 17768–17773
11. ERG. 2011. City of Fort Worth Natural Gas Air Quality Study Final Report; Fort Worth, TX. Available online at <http://fortworthtexas.gov/gaswells/?id=87074>.

### ***3.8 Hyperspectral Imaging***

Hyperspectral imaging is a powerful measurement technique that produces a visual representation of a typically invisible fugitive gas plume and provide spectral information of that gas plume for chemical identification and quantification. Any remote sensing system is a hyperspectral imager if it collects spectral information for each pixel in an image and enables that information to be processed to help identify and measure objects in the scene.

Hyperspectral imaging developed alongside aeronautical advances in the defensive and space exploration programs starting around 1960 with multispectral imaging, and experienced a significant increase in development and application after the arrival of 2-dimensional (2D) charge-coupled device (CCD) detector arrays in the 1980s.<sup>1,2</sup> The technique is popular with agricultural, astronomical, biomedical, geological, and geospatial (land-use, land-cover) applications and has recently been deployed for environmental purposes. This section discusses specifics related to hyperspectral imaging for the detection and measurement of volatile organic compounds (VOC) and hydrocarbon gases for environmental monitoring of industrial locations.

Hyperspectral imaging is typically conducted in the infrared (IR) region of the electromagnetic spectrum using IR sensing principles and can oftentimes include multi- or ultra-spectral imaging. Multispectral, hyperspectral, and ultra-spectral imaging operate by essentially the same principles, the main difference being the spectral resolution and the amount of spectral information collected as shown in Figure 3.31.<sup>2</sup>

Hyperspectral imaging is slightly different from multispectral imaging by the amount of wavelength data captured at any given moment. With multispectral imaging, about 3 to 10 discrete wave bands are analyzed with bandwidths commonly between 50 to 120 or more nanometers (nm), whereas hyperspectral imaging collects information from hundreds of wave bands that are smaller in width (typically 1 to 15 nm) and, therefore, produces a higher resolution.<sup>1</sup> Figure 3.31<sup>3</sup> shows that there can even be ultra-spectral measurements in which thousands of wave bands are evaluated; however, this is not currently used for gas detection and is therefore beyond the scope of this

document. IR detection of hydrocarbon gases is typically conducted using the mid-wave IR (MWIR) region of 3 to 5 micrometers ( $\mu\text{m}$ ) or the longwave IR (LWIR) region of 8 to 12  $\mu\text{m}$  due to the presence of an atmospheric transmission window (a region in the electromagnetic spectrum where common atmospheric gases such as water vapor and carbon dioxide are not very electromagnetically active). The shortwave IR (SWIR) region is not typically used due to the lack of electromagnetic activity for VOC and hydrocarbon gases in that region.

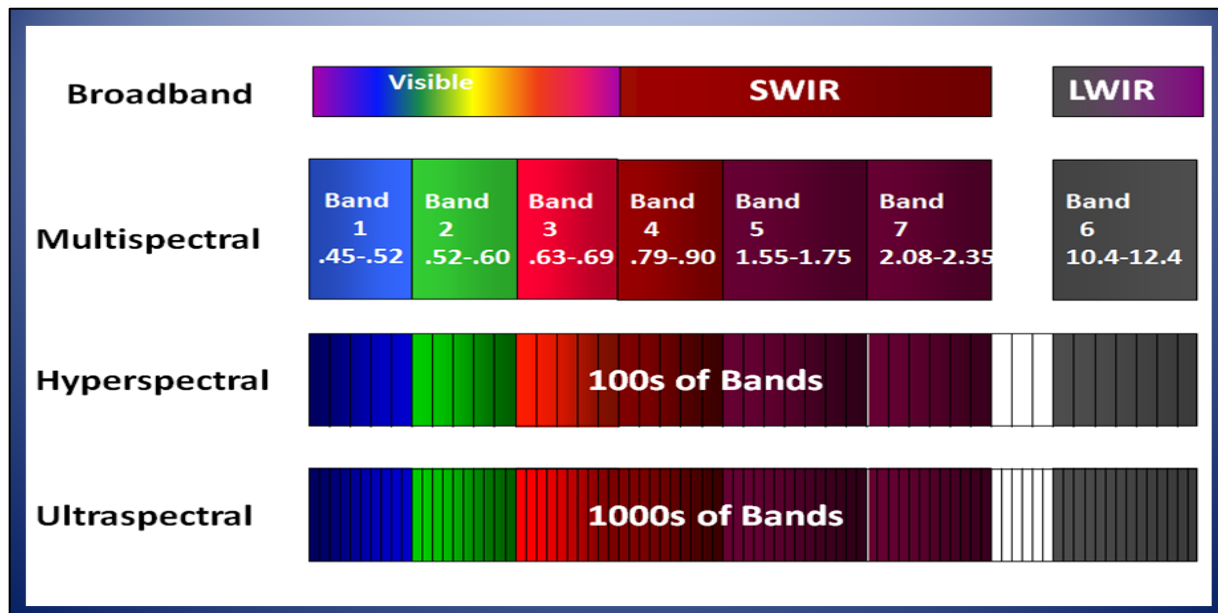


**Figure 3.31. Example of Differences between Multispectral, Hyperspectral, and Ultraspectral Data Resolution.**

These different spectral resolutions fall under the banner of hyperspectral imaging because, for as many applications that exist for the technology, so too do many systems exist that acquire hyperspectral information. These systems are described and discussed in the following section.

**General Description of Approach**

Hyperspectral imaging is a passive optical remote sensing technique that both provides a visual display of the measurement area and spectral information for each pixel of the image. The resulting data are therefore 3-dimensional (3D) “datacubes,” where the (x,y) coordinates correspond to the 2D image values and wavelength ( $\lambda$ ) is the spectral information in the third dimension (on the z-axis). Hyperspectral imaging is also a radiometric method, meaning that the measurement method

is based on the thermal properties of the elements in the field-of-view.

**Operating Principles**

As a radiometric method, the radiation perceived by the hyperspectral imaging device can be simplified into the radiative transfer model depicted in Figure 3.32.<sup>8</sup> For IR hyperspectral imaging devices discussed in this section, the spectral radiance reaching the device can be expressed as:

$$L_1 = (1 - \tau_1)B_1 + \tau_1[(1 - \tau_2)B_2 + \tau_2L_3]$$

Where:

$L_1$  = Spectral radiance reaching the hyperspectral imaging device

$\tau_1$  = The transmittance of layer 1

$\tau_2$  = The transmittance of layer 2

$B_1$  = The Planck function for a blackbody evaluated at layer 1

$B_2$  = The Planck function for a blackbody evaluated at layer 2

$L_3$  = Radiance entering the gas cloud from the background

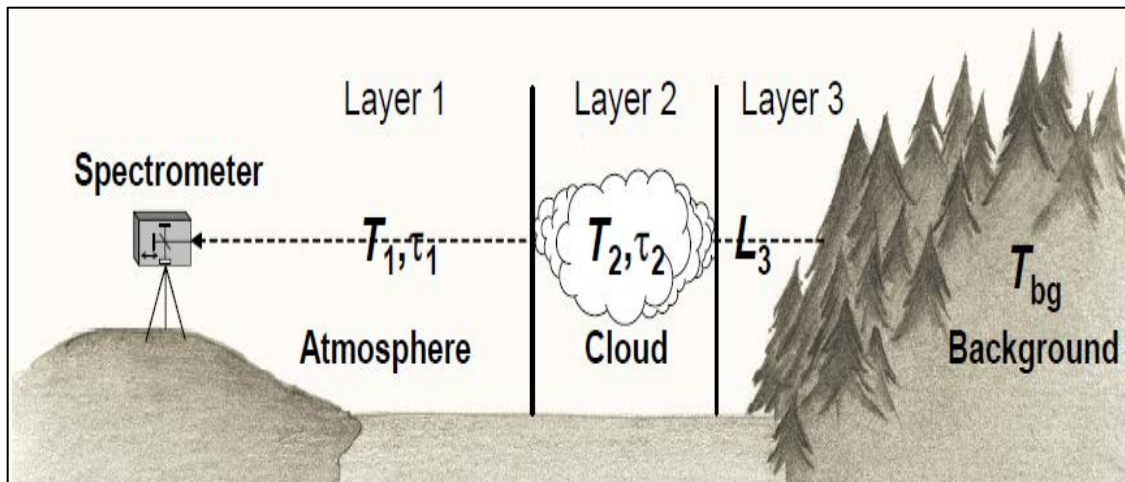


**Figure 3.32. Radiative Transfer Model Illustration for IR Remote Sensing of Airborne Pollutants.**



Many variations of hyperspectral imagers exist, but they all basically operate on the radiative transfer principle. In most designs, the instrument detects the spectral difference between the original background radiation and the radiation after it has passed through a gas cloud. Typically, the magnitude of this difference is converted into chemical species concentration using the Beer-Lambert Law, which relates the amount of transmittance of a material to its optical depth (concentration) and absorbance:

$$A = \varepsilon * c * l$$

Where:

A = Absorbance intensity (transmission = initial radiation – absorbance)

$\varepsilon$  = Absorption coefficient of the pollutant

c = Pollutant concentration

l = Measurement path length through the plume

Although a wide variety of system designs exist, most hyperspectral imagers fit into one of two categories: IR cameras with modified optics and imaging Fourier transform instruments (FTIR).<sup>5</sup> Occasionally, these two types of technology are combined. The basic operation principles of these types of technology (IR cameras and FTIR) can be found in Chapters 2.1 and 2.5 of this handbook, respectively.

Hyperspectral imagers based on IR camera technology will have additional filtering systems such as a Fabry-Perot etalon or an internal filter wheel. For example, the “Second Sight MS” system by Bertin Technologies uses luminance differentials between various optical cut-off filters to acquire multispectral information using an IR camera.<sup>6</sup>

## **Example Instruments**

### **Bertin's Second Sight MS System**

The Second Sight MS system operates by cycling through a specially designed filter wheel that contains one reference filter and five active filters to limit the spectral range of thermal radiation reaching the camera's detector. The scene information for each filter is captured sequentially in time to a 2D focal plane array (FPA) detector and then processed to subtract the background (or reference filter data) from the target (active filter) results. Figure 3.33<sup>6</sup> is an example schematic where the dark blue line represents the incident radiation being transmitted from the imaged scene to the instrument and the reference filter allows the spectral data from about 9.5  $\mu\text{m}$  and greater to reach the camera's detector (purple line). Active Filter 2 (orange line) captures the spectral data to almost 8  $\mu\text{m}$ , and Active Filter 3 (green line) captures data to about 7  $\mu\text{m}$ , which also includes the area of absorption for methane shown by the dip in the dark blue line. When the spectral luminance data from the reference filter and/or Active Filter 2 are subtracted from the data captured by Active Filter 1, pixel by pixel, the image of the methane gas plume is isolated (the 7 to 8.3  $\mu\text{m}$  region) and the plume composition can be identified. The resulting data from the Second Sight MS system is, therefore, not highly resolved spectrally but covers band segments and is a multispectral technique.

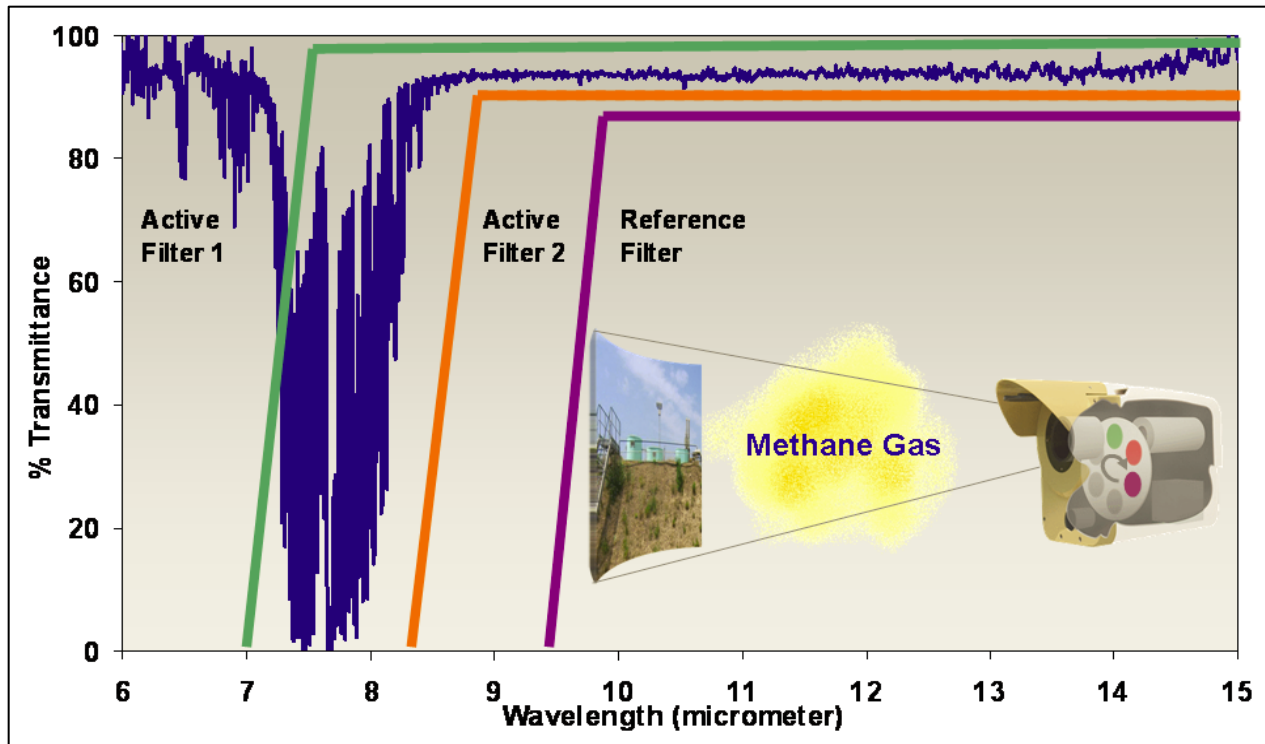


*Figure 3.33. Example of Multispectral Imaging using Spectral Differentiation of Methane Gas.*

### Physical Sciences' AIRIS

The Adaptive InfraRed Imaging Spectroradiometer (AIRIS) developed by Physical Sciences, Inc. is an IR camera that is fitted with a Fabry-Perot interferometer on the front (Figure 3.34).<sup>5</sup> The interferometer is tunable and can therefore select the wavelength of interest to reach the camera's detector. The MWIR model operates in the range of 3-5  $\mu\text{m}$  and the LWIR model operates between 8-12  $\mu\text{m}$ . Both models have a quick tuning velocity of 10-20 milliseconds (ms). The selected wavelength radiation enters through the camera's optics and is detected by a mercury-cadmium-telluride (HgCdTe) FPA, as seen with other, conventional IR cameras.<sup>7</sup>

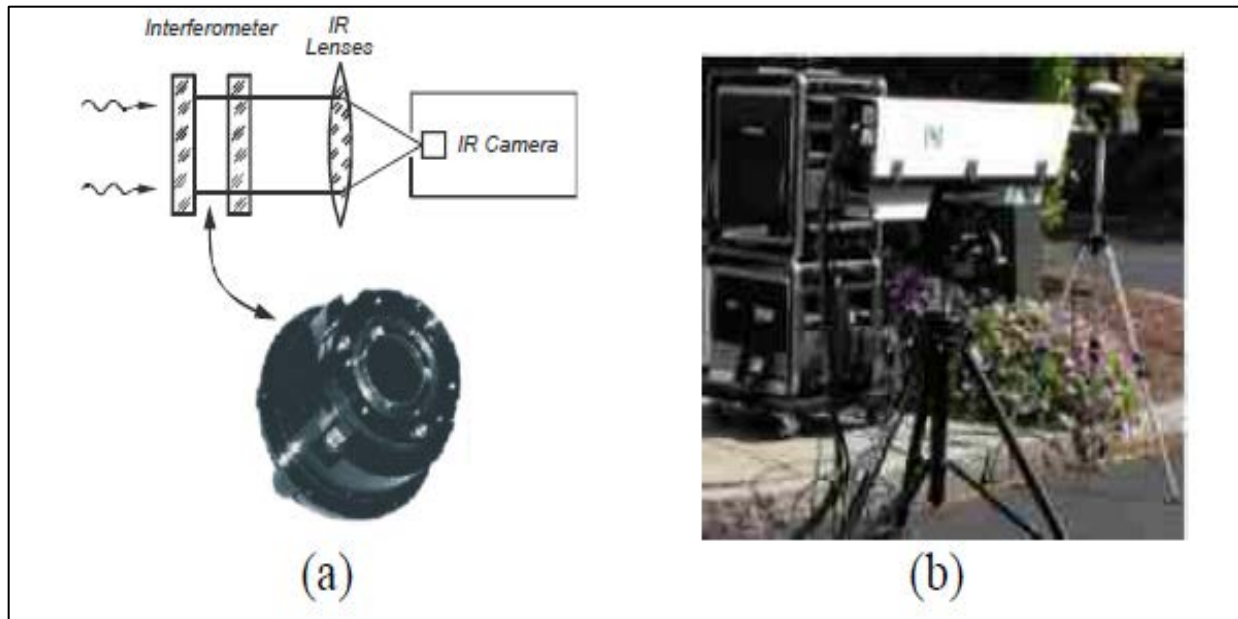


**Figure 3.34. AIRIS Interferometer Design where the Interferometer Lens (a) is Placed on the Front of the IR Camera (b).**

### **Rebellion Photonics' Gas Cloud Imager**

Rebellion Photonics, Inc. added subdivisional mirrors, an array of spectroscopes with dispersive elements, and a recombination scheme to develop their datacube in a system they call an image mapping spectrometer (IMS).<sup>9</sup>

Once the radiation enters through the lens optics, it encounters a mirror (called the “mapping mirror” in Figure 3.35) with a multifaceted surface that divides the image into numerous strip images. The mapping mirror directs each collection of strip images into its respective spectroscope (prism and lenslet arrays in Figure 3.35),<sup>9</sup> which disperses the bandwidths so that each bandwidth for each strip image is detected by a singular, coupled Sofradir microbolometer detector array. The 2D detector array image of multiple strip images are then recombined into the 3D datacube by a remapping algorithm. An example of the recombined image is provided in Figure 3.XX6.

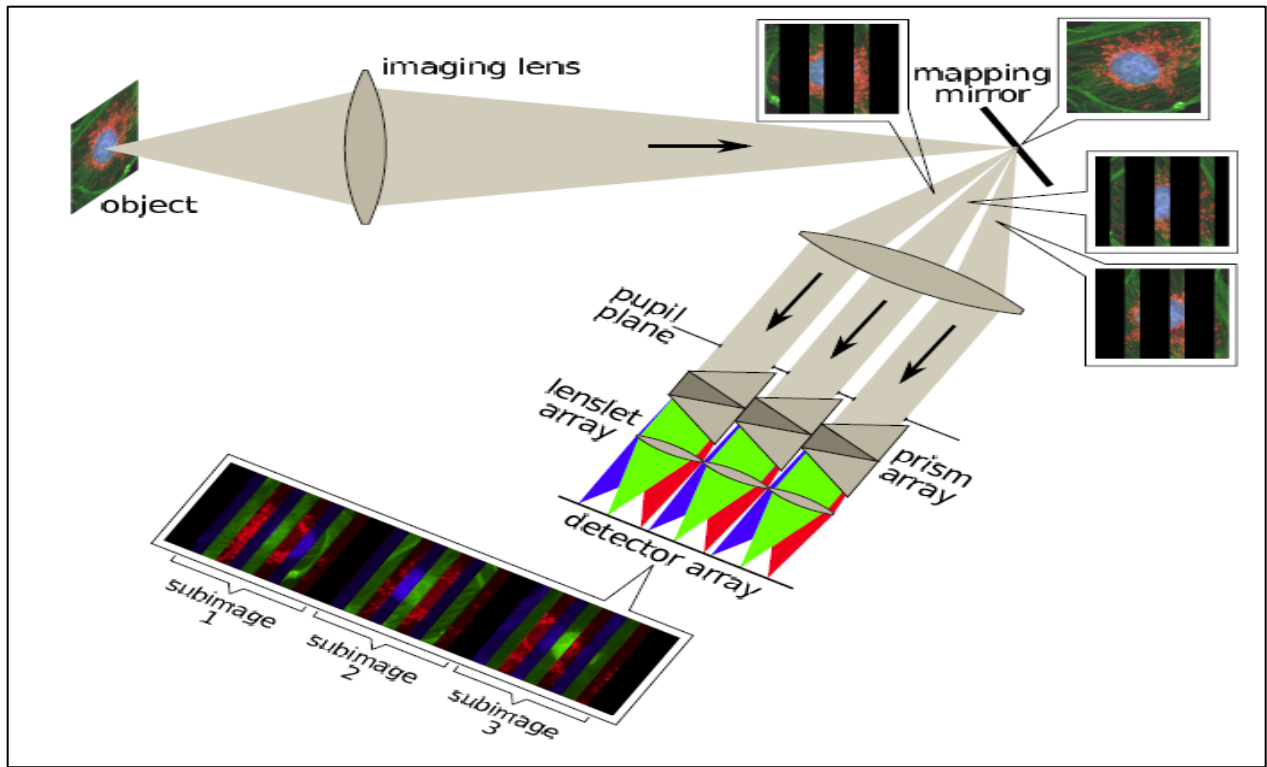


**Figure 3.35. Illustration of the IMS Optical Layout.**

The resulting image in Figure 3.36<sup>9</sup> panel (a) was first divided into strip images. Those strip images were reflected into the spectroscopy array where they were further divided by wavebands. The strip images of each waveband were recorded by the detector array and recombined using a remapping algorithm. Panels (b) through (e) in Figure 3.36 represent each waveband result after the recombination of the corresponding strip images. In this image, the four wavebands are spaced apart at (b) 463 nm, (c) 523 nm, (d) 595 nm, and (e) 622 nm. The IMS instrument typically has 8 to 20 spectral channels available, indicating that this is a multispectral technique.

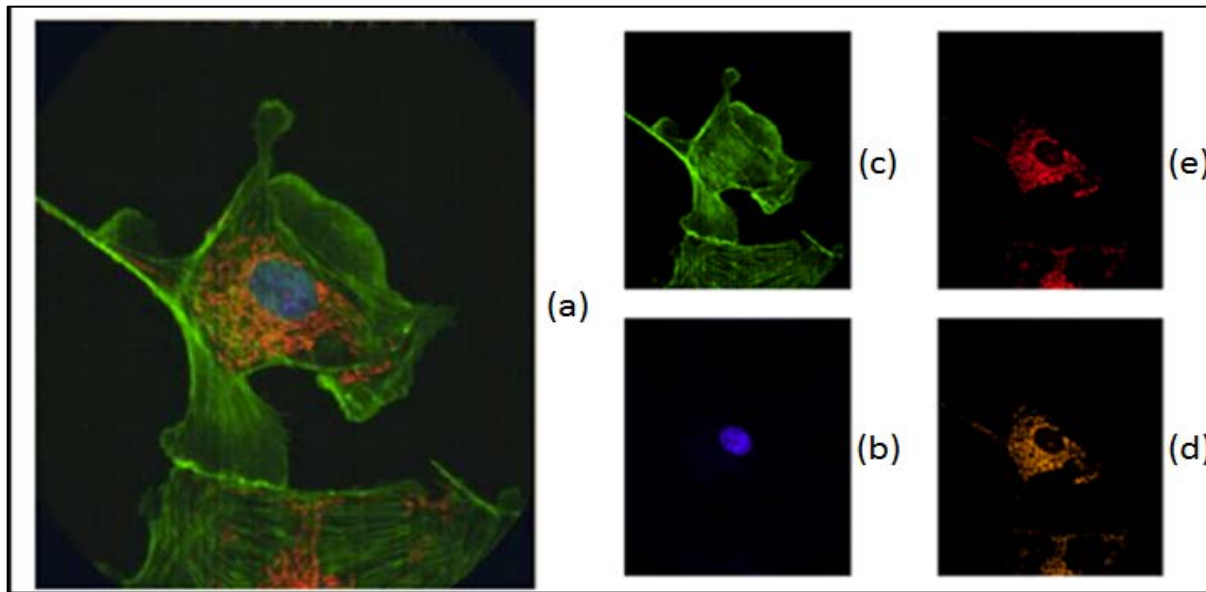


*Figure 3.36. Example Datacube (a) with Waveband Elements at (b) 463 nm, (c) 523 nm, (d) 595 nm, and (e) 622 nm.*

### Telops' HyperCam and MS-IR

A true imaging Fourier transform spectrometer (iFTS) was developed by Telops, Inc. over a period of about 20 years. The current name for this iFTS system is the HyperCam (Figure 3.37, left panel).<sup>12,14</sup> The HyperCam uses a Michelson interferometer to modulate the optical radiance allowed to pass to the FPA detector (see Section 2.1 for more detail on FTIR). The wave form of the radiance exiting the interferometer plotted over the scan location (optical path difference (OPD) value of the interferometer range) yields an interferogram. The interferometer conducts a single scan in time at one OPD setting for all pixels. The interferometer then moves to the next OPD setting and records for all pixels again. This is repeated for the full range of the interferometer so that a full interferogram is constructed for each pixel. The pixel interferograms are then mathematically converted from time-domain information to wavelength-domain information using Fourier transform algorithms and the spectrum for each pixel is thus developed. False color identification of plumes is produced by the Telops software highlighting the regions of gas cloud detection over a scene image that comprises the total radiance broadband information for each pixel from the datacube (Figure 3.38).<sup>10</sup>

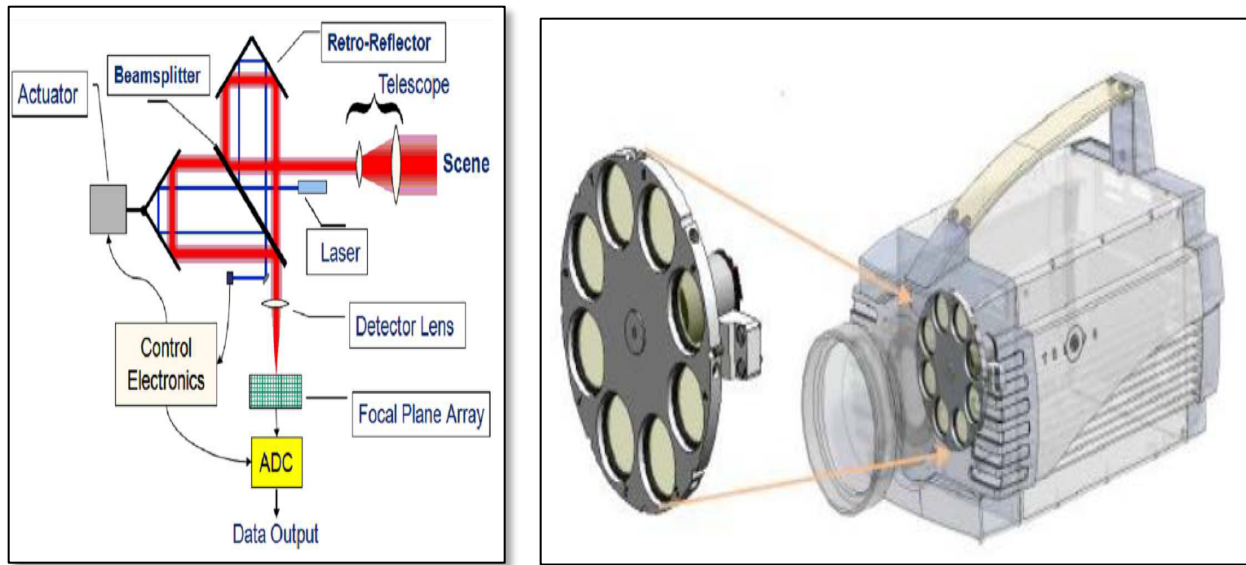


**Figure 3.37. Telops HyperCam (Left) Hyperspectral Imager and MS-IR Infrared Camera (Right) Multispectral Imager.**



**Figure 3.38. Example Telops Software Output Where the Detection View is the Total Radiance with the Gas Cloud Highlighted in False Color.**

Depending on the spectral resolution selected by the operator, the HyperCam can capture up to 320 wavelengths per pixel (the maximum for the size of the FPA), thus making this system a true hyperspectral imager. Telops has also developed a multispectral imager similar to the Second Sight system, where an IR camera has an added filter wheel to collect information at from up to 8 different wavelength regions (Figure 3.37, right panel).<sup>12</sup>

### Additional Considerations

How hyperspectral systems develop the resulting datacube is a key characteristic in the instrument's design. There are two main methods for acquiring a datacube: either by collecting 2D cube slices in rapid succession over time (scanning), or by collecting all information simultaneously and dividing it onto 2D elements to be recombined into a cube with post processing (snapshot). The scanning method is shown in panel (a) of Figure 3.39 as the "pushbroom spectrometer" and the snapshot method is represented by the "snapshot imaging spectrometer" in panel (b).<sup>4</sup>

The scanning detection method measures time-sequential 2D slices of the datacube, whereas the snapshot method takes one instantaneous measurement of the scene and divides the measurement information into multiple 2D elements on the FPA that can then be recombined into a datacube (Figure 3.40).<sup>2</sup>

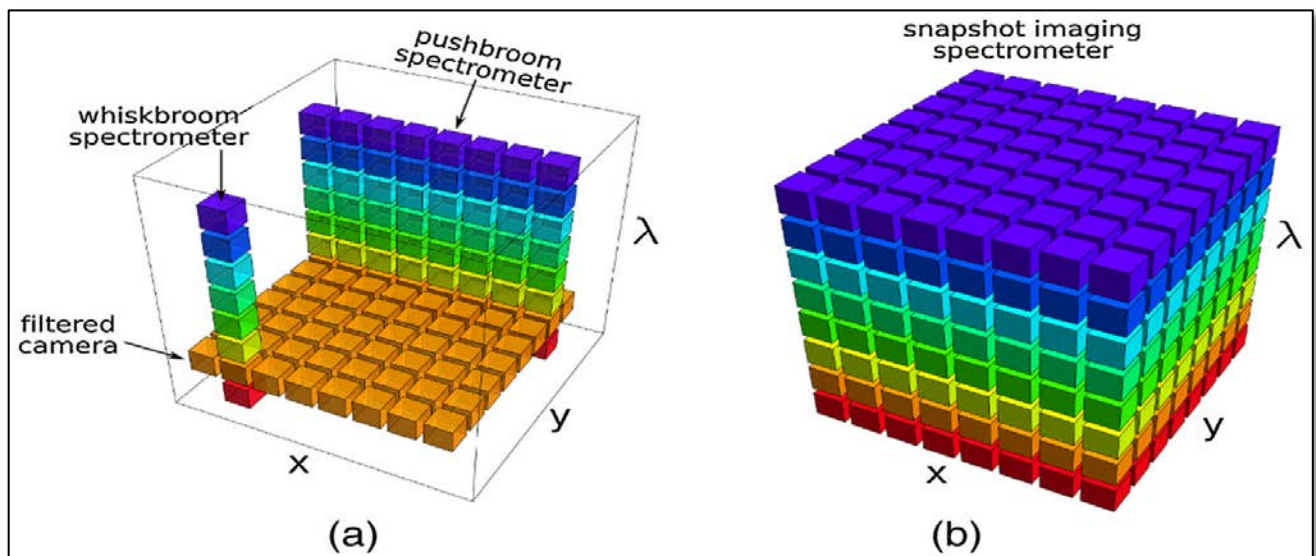


**Figure 3.39. Detector Methods for DataCube Acquisition.**



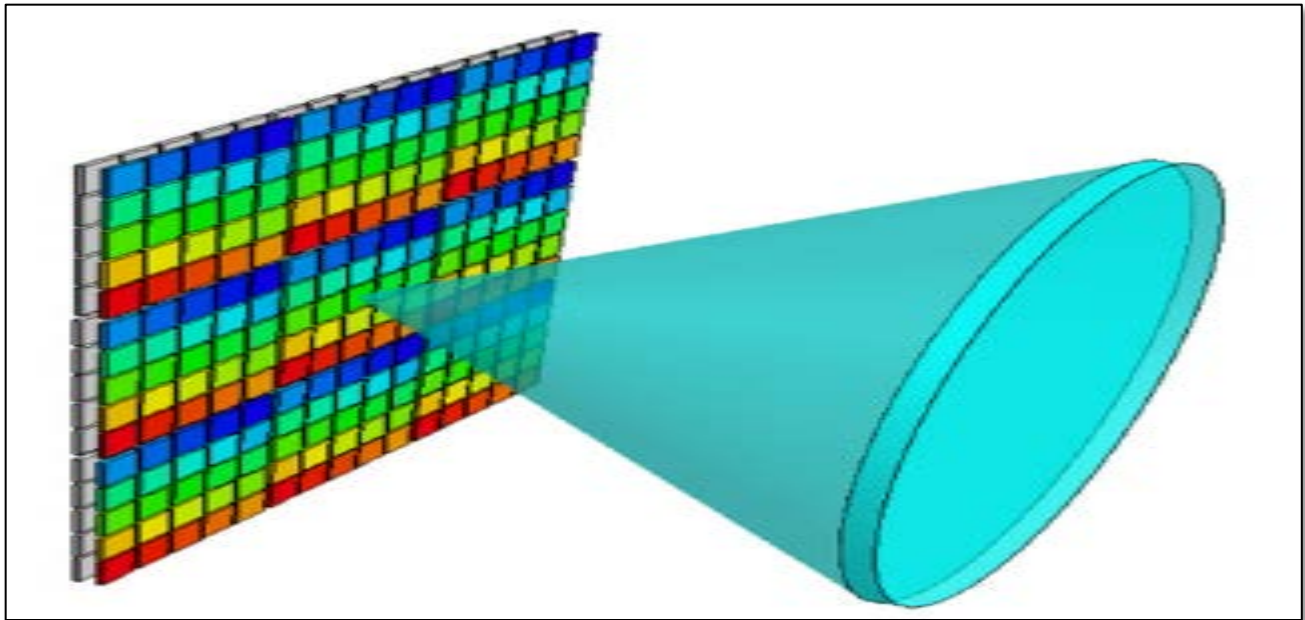


**Figure 3.40. Example SnapShot Detection with FPA Divided into smaller Collections.**

For the instruments used as examples for system designs, Table 3.23 lists their type of detection. The “Pushbroom spectrometer” depicted in panel (a) of Figure 3.39 illustrates how a scanning method would acquire the spectral information for each pixel by evaluating all spectral wavelengths across the x-axis for one row in the y-axis per scan over time. In Table 3.23, a similar concept is used to illustrate that the “Infrared Camera” detection scheme in Figure 3.39 is really a pushbroom spectrometer in the spectral domain (along the  $\lambda$ -axis). The designation of “Spectral Pushbroom” in Table 3.23 therefore indicates that all pixels are evaluated for the same wavelength per instrument measurement (scan).

**Table 3.23. Detection Method by Instrument.**

| Instrument       | Instrument Type | Detection Type     |
|------------------|-----------------|--------------------|
| Second Sight TC  | Multispectral   | Spectral Pushbroom |
| AIRIS            | Hyperspectral   | Spectral Pushbroom |
| Gas Cloud Imager | Multispectral   | Snapshot           |
| HyperCam         | Hyperspectral   | Spectral Pushbroom |
| MS-IR            | Multispectral   | Spectral Pushbroom |

There are documented advantages to using a snapshot detection method, most notably the higher light throughput and the simultaneous collection of all datacube information. The snapshot

technique has had some exposure in the astronomy community, but application has been limited to coupling with telescopes and very little attention has been given to the technique for other applications. To understand the advantage of using the snapshot technique, the rest of this section discusses the number of voxels (the “pixels” of the datacube) illuminated per measurement integration.<sup>4</sup> Simply, the amount of radiation collected through a filtering or scanning system (panel a in Figure 3.39) is significantly less than that of a full throughput snapshot collection (panel b in Figure 3.39). The light collection efficiency of a system is related to the number of elements in the datacube recording illumination for a single measurement integration according to the following equation:

$$LCE = \frac{1}{N_{x,y,\lambda}}$$

Where:

LCE = light collection efficiency

$N_{x,y,\lambda}$  = number of elements in the scan

Many more snapshot system architectures are reviewed in reference 4. However, limitations in the manufacturing of large FPAs and precision multi-aperture optical elements have slowed the advance of this technology for many applications, such as environmental monitoring.<sup>4</sup>

### **Verification/Validation Studies**

The technology for hyperspectral imaging is still being developed and therefore only a couple of studies are currently available. The complexity of FTIR instruments requires the regular verification of proper operation and measurement accuracy.

In June 2015, Rebellion Photonics participated in a validation study hosted by EPA in North Carolina. Two controlled release platforms were utilized to try and quantify the accuracy of the Rebellion hyperspectral method while also noting any limitations on its application. The first release platform had two release positions that varied in height (Figure 3.41) and the

second was an industrial leak simulator custom-built by Eastern Research Group, Inc. (ERG) (Figure 3.42).



**Figure 3-41. High/Low Controlled Gas Release Platform**

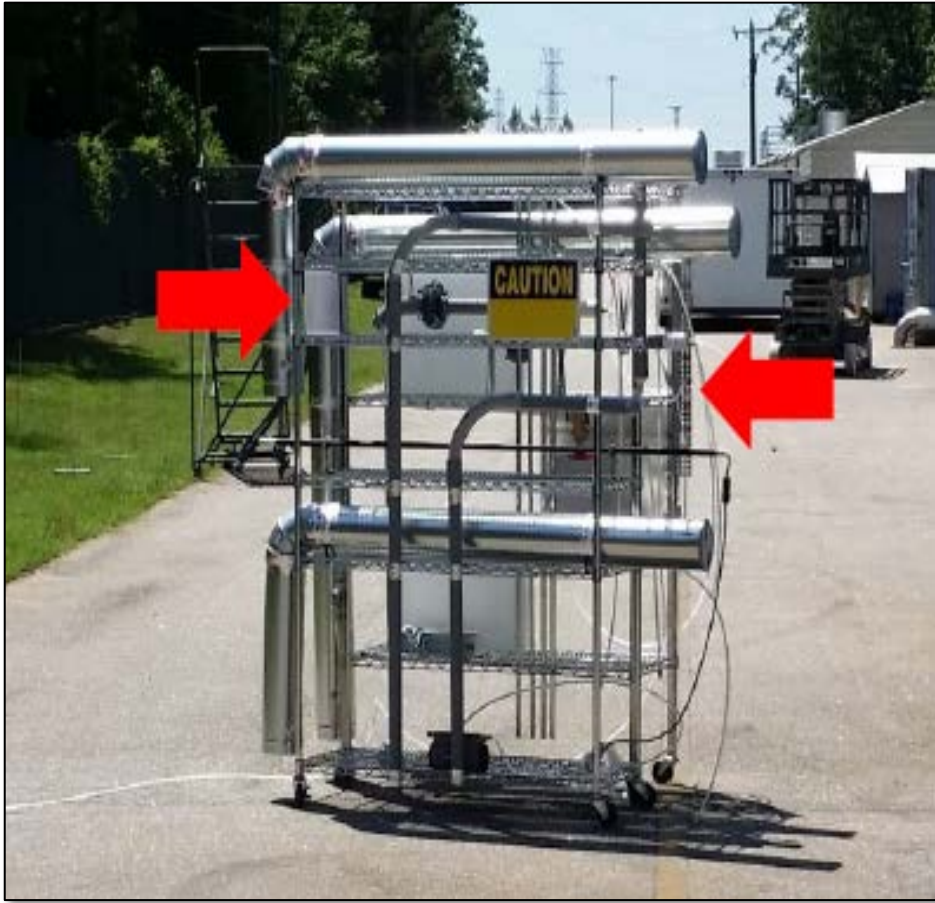


**Figure 3-42. ERG Controlled Leak Simulation Platform**

The Rebellion Gas Cloud Imager was able to detect the leaks from all platforms; however, the accuracy from the High/Low EPA platform (left panel of Figure 3-43) was better than that achieved from the partially obscured ERG platform (right panel of Figure 3-43). The data in Table 3.XX2 illustrate that the average error for the unobstructed view with the High/Low platform was about  $\pm 10\%$  and about  $\pm 31\%$  for the partially obstructed view with the leak simulation platform.<sup>15</sup>

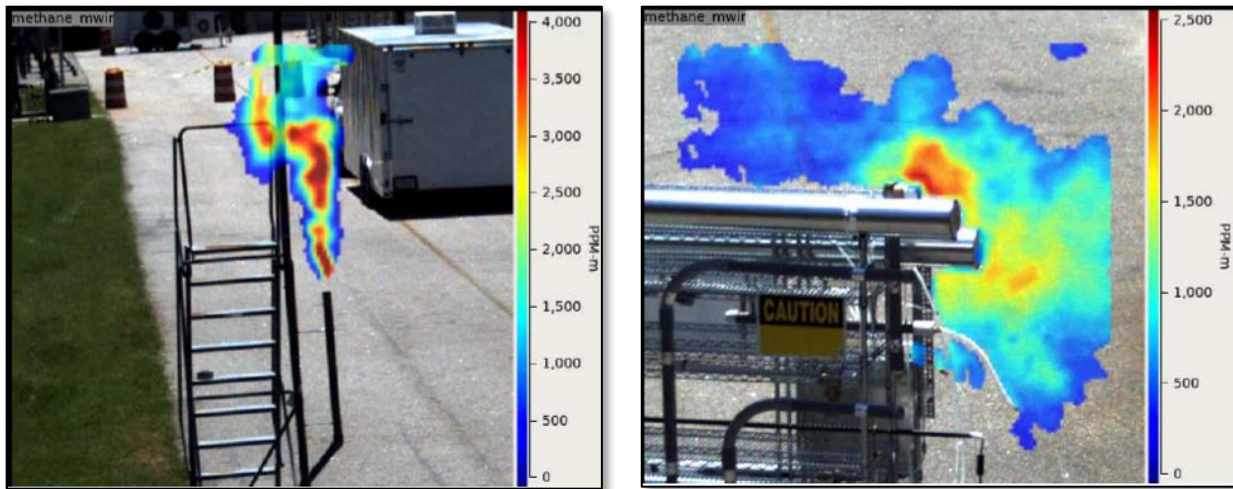


**Figure 3-43. Example Releases as Seen from the GCI for the (Left) High/Low Platform and (Right) Leak Simulation Platform.**

**Table 3.24. Summary of Rebellion GCI EPA Controlled Release Results.**

| Trial | Test Gas        | Viewing Distance (m) | Release Rate (g/s) | Measured Rate |        |         |
|-------|-----------------|----------------------|--------------------|---------------|--------|---------|
|       |                 |                      |                    | (g/s)         | Error  | Error % |
| 1     | Methane         | 30                   | 0.20               | 0.193         | -0.007 | -3.4    |
| 2     | Methane         | 30                   | 1.20               | 1.020         | -0.180 | -15.0   |
| 3     | Methane         | 30                   | 0.02               | 0.018         | -0.002 | -9.6    |
| 4     | Methane         | 30                   | 0.12               | 0.123         | 0.012  | 10.3    |
| 5     | Methane         | 17                   | 0.20               | 0.207         | 0.007  | 3.3     |
| 6     | Methane         | 17                   | 1.20               | 0.983         | -0.217 | -18.1   |
| 7     | Methane         | 17                   | 0.02               | 0.022         | 0.002  | 10.5    |
| 8     | Methane         | 17                   | 0.12               | 0.107         | -0.013 | -10.5   |
| 9     | Propane, hidden | 16                   | 0.02               | 0.028         | 0.008  | 38.7    |
| 10    | Propane, hidden | 16                   | 0.12               | 0.088         | -0.032 | 26.7    |
| 11    | Propane, hidden | 16                   | 0.02               | 0.027         | 0.007  | 33.1    |
| 12    | Propane, hidden | 16                   | 0.12               | 0.084         | -0.036 | -29.7   |
| 13    | Methane, hidden | 16                   | 0.02               | 0.028         | 0.008  | 39.7    |
| 14    | Methane, hidden | 16                   | 0.12               | 0.096         | -0.024 | -20.0   |

**Typical QA/QC**

The typical quality assurance/quality control (QA/QC) associated with each hyperspectral imager will be dependent on the base technology for that instrument. See Section 2.1.3 for the typical FTIR QA/QC for the Telops Hypercam or Section 2.5.3 for the typical thermal

camera QA/QC for many of the other hyperspectral imagers discussed. As the technology continues to advance, methods will be developed that contain more specific quality objectives.

### **Summary of Thermal IR Camera QA/QC**

Thermal IR cameras are less complex and, hence, so are the QA/QC procedures associated with using these instruments. If the IR camera is used for temperature measurements, then the instrument should have the temperature calibration settings verified annually by the manufacturer or other appropriate service. When preparing the instrument at the beginning of the day, the IR camera must be allowed to cool and reach a sort of thermal equilibrium. The design of an IR camera will typically not allow the camera to be used until the desired temperature is reached, but it is also important to allow an additional 10 to 15 minutes after this point to allow for thermal stabilization. Once the camera indicates it is ready and some additional time has passed to allow for thermal stabilization, if possible, reset the detector values by performing a non-uniformity correction (NUC) with the lens cap still in place. When the lens cap is still in position over the lens, the camera should theoretically see a completely uniform image. The FPA of an IR camera is known to suffer from fixed-pattern noise—where there is a spatial non-uniformity in the photo-response of the detectors in the array—and so the NUC homogenizes the FPA output by measuring the amount of difference perceived for each pixel and mathematically correcting the pixel response to appear identical across the entire array. The fixed-pattern noise phenomena common for FPA responses can drift over time so it is suggested that a NUC is performed a couple times throughout the imaging duration, if longer than 1-2 hours.

The IR camera operator may wish to record evidence of proper operation before beginning a survey if the IR camera results may potentially be required in a legal proceeding. However, this step is not necessary for the camera preparation and a survey may begin at this time. It was determined that the gas emission rate of butane from a standard, non-adjustable, BIC® lighter is constant at 4.00 g/hr, and so this may be used as evidence of proper operation by recording video footage of the butane release. Similarly, if the IR camera has additional optics that will allow for the measurement

of a gas release, then the standard BIC® lighter can be used as a calibration gas check as well.<sup>15</sup>

### **Siting Concerns**

The siting concerns for hyperspectral imaging techniques are dependent on the technological design. For example, if the instrument is a modified IR camera, then the siting concerns will be like those for thermal cameras in Section 2.5 of this document. The same is true for FTIR-based systems; they will be subject to restrictions like those for the FTIR technology in Section 2.1 of this document.

Regardless of the base technology, performing hyperspectral imaging will absolutely require the ability to have an unobstructed view of the gas leak emission. As evidenced by the study discussed in Section 3.8.2 using the Rebellion Photonics Gas Cloud Imager, measurements derived from gas plumes that are partially hidden from view lead to greater error in the overall measurement. Therefore, the hyperspectral system must be mobile enough to allow for optimal positioning with respect to the target plume location and transport direction.

### **Strengths and Limitations**

As mentioned for typical QA/QC and siting concerns, the strengths and limitations for each system will be influenced by the base technology that the hyperspectral imager is designed around. However, in general, the hyperspectral imaging technique has specific strengths and limitations as listed in Table 3.24.

**Table 3.25. Strengths and Limitations of Hyperspectral Imaging.**

| Strengths   | Limitations   |
|---|---|
| Faster and easier to deploy than traditional active techniques                | High cost   |
| Nondestructive acquisition of all spectral data preserved for post-processing | Can be subject to wind speed and other meteorological conditions      |
| Results in an image of the pollutant plume for superior spatial resolution    | About one order of magnitude less accurate than laboratory techniques |
| Mobile/portable design for better maneuverability and optimum siting angles   | Requires a complete view of the emission plume                        |

**References**

1. Hungate, W.S., R. Watkins, and M. Borengasser. 2007. *Hyperspectral Remote Sensing: Principles and Applications*. CRC Press, Boca Raton, FL, USA. Print ISBN: 978-1-56670-654-4.
2. Hagen, N., and M.W. Kudenov. 2013. "Review of Snapshot Spectral Imaging Technologies." *Optical Engineering*, 52(9). DOI: 10.1117/1.OE.52.9.090901.
3. Altigator. 2017. Webpage: *Multispectral and Hyperspectral Drone Imagery*. Last accessed on February 7, 2017 from <http://altigator.com/multispectral-and-hyperspectral-drone-imagery/>.
4. Hagen, N., R.T. Kester, L. Gao, and T.S. Tkaczyk. 2012. "Snapshot Advantage: a Review of the Light Collection Improvement for Parallel High-Dimensional Measurement Systems." *Optical Engineering*, 51(11). DOI:10.1117/1.OE.51.11.111702.
5. Kastek, M., T. Piątkowski, P. Lagueux, M. Chamberland, and M.A. Gagnon. 2015. "Passive Optoelectronics Systems For Standoff Gas Detection: Results Of Tests." *WIT Transactions on Ecology and the Environment*, 198, 89—104. DOI: 10.2495/AIR150081.
6. Naranjo, E., S. Baliga, and P. Bernascolle. 2010. "IR Gas Imaging in an Industrial Setting."



*Proceedings of SPIE, Thermosense XXXII*, 7661, 76610K. DOI: 10.1117/12.850137.

7. Gittins, C.M., W.J. Marinelli, and J.O. Jensen. 2002. "Remote Sensing and Selective Detection of Chemical Vapor Plumes by LWIR Imaging Fabry-Perot Spectrometry." *Proceedings of SPIE*, 4574, 63-71.
8. Harig, R., M. Grutter, G. Matz, P. Rusch, J. Gerhard. 2007. "Remote Measurement of Emissions by Scanning Imaging Infrared Spectrometry." CEM2007, 8th International Conference on Emissions Monitoring, Zürich, 34-39, 2007.
9. Hagen, N., R.T. Kester, and C. Walker. 2012. "Real-time quantitative hydrocarbon gas imaging with the gas cloud imager (GCI)." *Proceedings of SPIE*, 8358. DOI: 10.1117/12.919245.
10. Chamberland, M., and M.-A. Gagnon. 2017. Personal communication.
11. Gagnon, M.-A., J.-P. Gagnon, P. Tremblay, S. Savary, V. Farley, E. Guyot, P. Lagueux, M. Chamberland, and F. Marcotte. 2016. "Standoff Midwave Infrared Hyperspectral Imaging of Ship Plumes." *Proceedings of SPIE*, 9862. DOI: 10.1117/12.2218643.
12. Telops. 2014. "Application Note: Time-resolved Infrared Multispectral Imaging of Gases." Last accessed on January, 4, 2017 from <http://telops.com/products/multispectral-cameras>.
13. Chamberland, M., P. Lagueux, P. Tremblay, S. Savary, M.-A. Gagnon, M. Kastek, T. Piątkowski, and R. Dulski. 2014. "Standoff gas detection, identification and quantification with a thermal hyperspectral imager." *WIT Transactions on Ecology and The Environment*, 181. DOI: 10.2495/EID140571.
14. Kastek, M., T. Piatkowski, M. Zyczkowski, M. Chamberland, P. Lagueux, and V. Farley. 2013. "Hyperspectral Imaging Infrared Sensor Used for Environmental Monitoring." *Acta Physica Polonica A*, 124(3), 463-467.
15. Footer, T.L. (ERG). 2015. "Draft Technical Support Document: Optical Gas Imaging Protocol (40 CFR 60, Appendix K)." Technical document posted as docket ID: EPA-HQ-OAR-2010-0505-4776. Last accessed on 1/24/2017 from <https://www.regulations.gov/document?D=EPA-HQ-OAR-2010-0505-4949>.
16. Hagen, N., S. Rajaraman, R.P. Mallery, and R.T. Kester. 2016. "Quantifying gas cloud emission rates with the Gas Cloud Imager." *Proceedings of the A&WMA 2016 Air Quality Measurement Methods and Technology Specialty Conference*, March 15, 2016, Chapel Hill, NC.

### **3.9 Fenceline Passive Sampling – Method 325 A/B**

A variety of industrial facilities, including energy production and refining operations, can emit greenhouse gases and other pollutants due to equipment leaks and process malfunctions. Of specific interest is monitoring of volatile organic compounds (VOCs) such as benzene. For example, in 2015 the Environmental Protection Agency (EPA) amended the petroleum refinery rules (40 CFR part 63, subpart CC) to add fenceline monitoring provisions for fugitive benzene emissions (80 FR 75178).

One method to monitor fenceline emissions gaining considerable interest is the deployment of diffusive samplers. The samplers collect gas or vapor pollutants at a controlled rate via physical process (diffusion) rather than pumped air. Samplers have been developed specifically to collect emissions of benzene and several other VOCs. Method 325A and 325B (325A/B) were created to outline proper sampling and analysis, respectively, of passive samplers to help manufacturers comply with the new ruling.

#### **General Description of Approach**

Qualitative versions of diffusive samplers were first introduced in the 1930s. The diffusion and permeation processes through which the samplers collect pollutants of interest can be described through derivations of Fick's first law of diffusion:

$$J = -D \frac{d\varphi}{dx}$$

Where:

- J = Diffusion flux of amount of substance per unit area per time (mol/m<sup>2</sup>s)
- D = Diffusion coefficient (m<sup>2</sup>/s)
- φ = Concentration of ideal mixture (mol/m<sup>3</sup>)
- x = Position of the mixture (m)

The derived expressions from Fick's law relate the sampler's mass uptake to the concentration gradient, the sample time, and the surface area of the sampler to ambient air.<sup>1</sup>

Because pollutant concentrations are directly proportional to the sampler's mass uptake, it is important that the sampling rate is constant and does not change due to the sampler deployment time or the concentration of pollutant it is exposed to. Concentrations are also positively correlated to the diffusion coefficient of the pollutant, the time of exposure, and the cross-sectional area of the diffusion path. Conversely, the pollutant concentration is inversely proportional to the length of the diffusion path. It is important to note that the sampling rate can be negatively affected as the sampler's sorbent reaches saturation.

It is generally necessary to expose the sampler over a period of days to collect sufficient concentrations of the target pollutant for analysis in environmental samples because the sampling rate is relatively low compared to active (i.e., pumped) methods.

### **Passive Tube Samplers**

The first quantitative application for diffusive samplers occurred in 1973 when E.D Palmes<sup>2</sup> developed a tube-type sampler that collected sulfur dioxide.<sup>1</sup> Since then, a variety of passive samplers have been developed for the quantification of a variety of pollutants. Method 325 A/B uses a tube-type sampler similar to the one described by Palmes. Please see example of a passive tube design that was proposed for Method 325 A/B in Figure 3-43.<sup>3</sup>

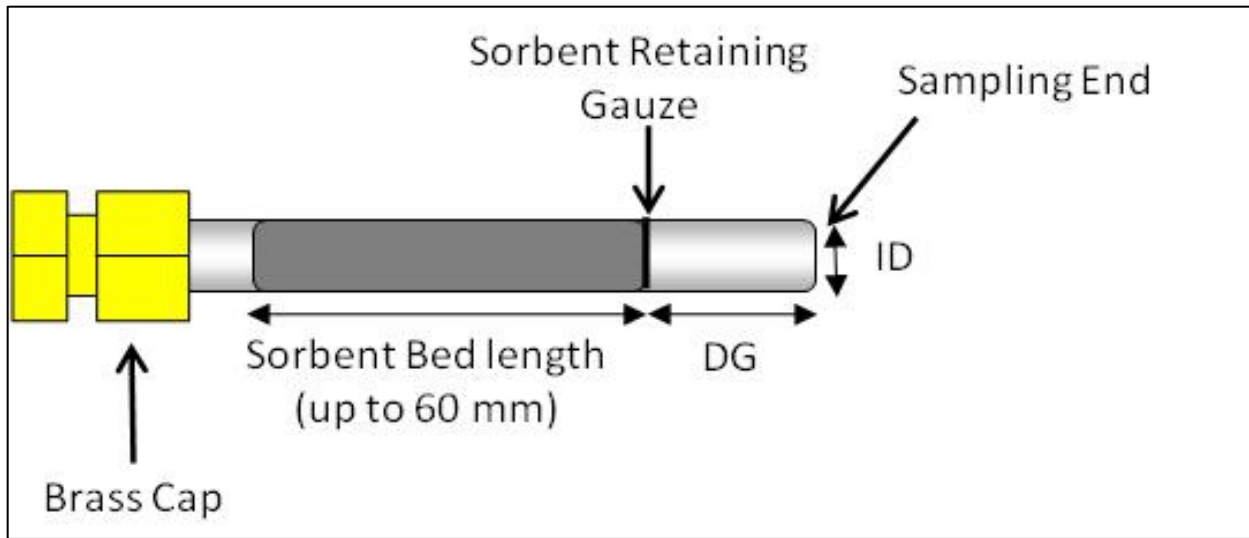


**Figure 3-43. Cross-Section of the PS Tube.**

A passive sampler (PS) uses a thermally de-absorbable carbon-based sorbent packed in a stainless-steel tube (approximately 3.5" long and ¼" internal diameter). The cross-sectional area of the tube is 19.6 mm<sup>2</sup> with an internal diffusion gap (DG) of 1.5 cm between the diffusion cap and the sampling end. Each tube is equipped with leak-proof storage caps to prevent contamination during both storage and transport. Several laboratory equipment manufacturers create tubes appropriate for Method 325 A/B sampling. Table 3.26 lists the manufacturers that currently sell passive samplers.

**Table 3.26. Passive Sampler Manufacturers**

| Manufacturer  | Website Information                                |
|---------------|--|
| Camsco        | <a href="http://www.camso.com">www.camso.com</a>   |
| Markes        | <a href="http://www.markes.com">www.markes.com</a> |
| Sigma-Aldrich | www.sigmaaldrich.com                               |
| SKC           | www.skcinc.com                                     |

Although Method 325 A/B is written specifically for the measurement of fugitive emissions for

benzene, the PSs are suitable for sampling a variety of pollutants. Each pollutant has a different diffusion coefficient, therefore the maximum concentration collected over the same time period may differ significantly between different pollutants. Table 3.27 lists pollutants that can be sampled using Passive Samplers.

**Table 3.27. Pollutants that can be Collected with Passive Diffusive Samplers**

| Pollutants                            |                       |
|---------------------------------------|-----------------------|
| 1,1-Dichloroethane                    | Carene                |
| 1,1-Dichloroethene                    | Chlorobenzene         |
| 1,1,1-Trichloroethane                 | Ethylbenzene          |
| 1,1,2-Trichloro-1,2,2-trifluoroethane | Labile Sulfur         |
| 1,1,2-Trichloroethane                 | Limonene              |
| 1,2-Dichloroethane                    | p-Dichlorobenzene     |
| 1,2-Dichloropropane                   | Styrene               |
| 1,3-Butadiene                         | Tetrachloroethene     |
| 3-Chloropropene                       | Trichloroethene       |
| Benzene                               | Toluene               |
| bis-Chloromethyl Ether                | Xylenes (m,p- and o-) |
| Carbon Tetrachloride                  |                       |

## **Sampler Deployment**

Prior to deployment, passive samplers received from the manufacturer must be conditioned as described in EPA Method 325B, Sections 6.2 and 9.2. This can be accomplished with a dedicated tube conditioning unit or an analytical thermal desorber (TD) system. The TD system should be used only if it supports a dedicated tube conditioning mode that allows effluent from the tubes to vent without passing through the system's sample flow path. Alternatively, if a tube conditioning unit is used, the unit must be leak-tight and allow for reproducible temperature selection within a 5 °C range that is at least that of the thermal desorber. The unit must also allow inert gas flows up to 100 mL/min.<sup>3</sup>

Great care must be taken to avoid contaminating the passive tube samplers during transport, sample deployment, and analysis. Each tube must be capped with brass long-term storage caps that are fit with polytetrafluoroethylene (PTF) ferrules. While capped, the tubes must be stored in a clean, air-tight container that is designated for un-sampled passive tubes (un-sampled tubes must never be stored in the same container as sampled tubes.) Tubes should be handled while wearing cotton or nitrile gloves to prevent contamination on the surface of the tubes themselves, especially if the analytical thermal desorption equipment used to extract the tubes does not exclude contamination from the surface of the samplers.<sup>3,4</sup>

Upon arrival at the sampling location, the tubes should be allowed to equilibrate with local ambient conditions for 30 minutes to an hour before removal from their transport container. After inspecting the tube for any potential damage or contamination sources, the tube should be secured to a pole or other structure so that the bottom of the sampling cap is approximately 5 to 10 feet above the ground. The passive tube should be oriented vertically with the sampling end pointing down. To protect the tube from bad weather, a sorbent tube protection cover, as shown in Figure 3.44,<sup>4</sup> should be used. The storage cap on the sampling end of the tube must be replaced with a diffusive

sampling cap and the start time and sampling location for the passive sampler must be recorded. Method 325A recommends a minimum sampling period of 14 days for passive tube samplers.<sup>4</sup>

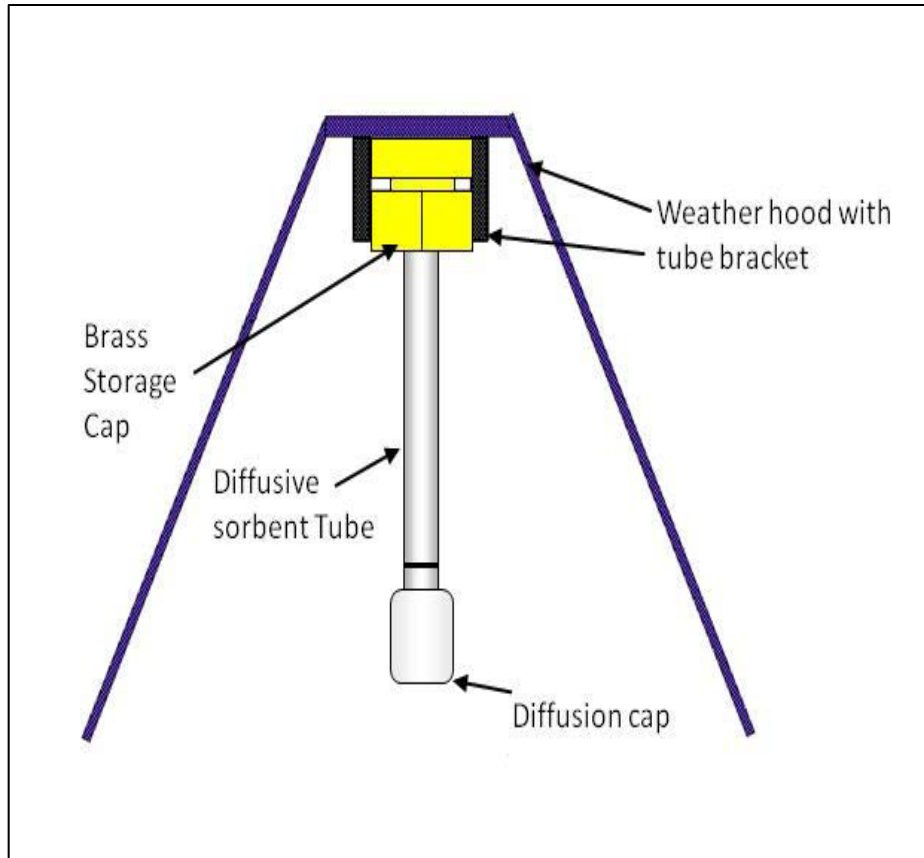


**Figure 3-44. Sorbent Tube Protection Cover.**

**Note:** Tubes must be labeled for identification purposes; however, many labeling substances may cause contamination. See EPA Method 325A, Section 8.6.2, for specific information about sampler labeling. Radio-frequency identification (RFID) labels compatible with many TDs are commercially available and allow each sample to be programmed with relevant sample information.

### **Passive Sampler Recovery**

After the 14-day sampling period is complete, the diffusion cap must be removed from the PS and replaced with the storage cap. The storage cap must be tightened sufficiently to prevent further exposure during transport. The date and time the end cap was replaced must be recorded and the tube must be placed in an air-tight container that is not used for clean conditioned tubes. If the tubes are being shipped to the laboratory for analysis, they may be shipped at ambient

temperature.

### **Meteorological Data Collection**

Time-resolved meteorological data used in conjunction with concentration measurements from the passive samplers can be used to determine both the source of pollutants and calculating the mass flux of the plume. Therefore, a meteorological station must be deployed at or near the monitored facility in locations that are representative of the conditions to which the passive sample is exposed. These stations must be equipped to monitor ambient temperature, barometric pressure, and wind speed and direction.<sup>4</sup> Specific information about meteorological station siting can be found in Section 8.3 of EPA Method 325A; more information about meteorological instrumentation can be found in Meteorological Monitoring Guidance for Regulatory Modeling Applications (EPA-454/R-99-005).<sup>5</sup>

### **Passive Sampler Analysis**

Due to the variety of analytical equipment available for this analysis, analysis procedures will vary between laboratories. For specific procedures, reference EPA Method 325B, Section 11. Presented here is a general overview of the analysis of PSs. The samples must be analyzed no later than 30 days from the end of sampling to ensure accurate concentration results for benzene. It should be noted that if quantification is desired for certain compounds that are reactive in nature, analysis should occur no more than 10 days from the end of sample collection.

The gas chromatographer/mass spectrometer (GC/MS) must be tuned to the manufacturer's specifications using a 50-ng injection of bromofluorobenzene. Tuning must be completed prior to the start of each analytical run and every 24 hours thereafter for continuing analysis. Tuning criteria is summarized in Table 3.28.



**Table 3.28. GC/MS Tuning Criteria.<sup>3</sup>**

| Target Mass | Rel. to Mass | Lower Limit % | Upper Limit % |
|-------------|--------------|---------------|---------------|
| 50          | 95           | 8             | 40            |
| 75          | 95           | 30            | 66            |
| 95          | 95           | 100           | 100           |
| 96          | 95           | 5             | 9             |
| 173         | 174          | 0             | 2             |
| 174         | 95           | 50            | 120           |
| 175         | 174          | 4             | 9             |
| 176         | 174          | 93            | 101           |
| 177         | 176          | 5             | 9             |

The TD system must also be checked for system integrity and go through additional steps prior to each analysis. Many commercial TD systems implement these procedures automatically. A leak check must be performed of the PS tube, the GC carrier gas pressure, and the sample flow path. A dry purge of the PS may also be performed to remove water vapor and other interferences, and internal standards must be added to the PS, either automatically or manually. Each sampler is then pre-purged to remove oxygen to prevent damage to the analytical system.

The TD/GC/MS system must be calibrated using at least five concentrations that represent the expected monitoring range of the samples for each compound monitored with sampling. PS tubes prepared as described in Section 10.7 of EPA Method 325B can be used for calibration and may be stored up to 30 days when refrigerated. The TD/GC/MS system must be calibrated prior to the start of PS analysis, following any significant instrument maintenance, or if the instrument fails continuing calibration verification (CCV).

The preferred analytical sequence is detailed in Section 11.1 of EPA Method 325B. If an automated TD GC/MS, then the end caps of each sample can be removed and loaded into the instrumentation. However, if a manual system is used, each sample must be uncapped and analyzed individually. A CCV must be analyzed at the beginning and end of each analysis and every 10 samples throughout. Step-by-step procedures for operating the TD and the GC-MS are included in Section 11.3 of EPA Method 325B, although instrument-specific operating manuals should also be used.

### **Recordkeeping and Data Analysis**

Throughout each step, records must be maintained to both verify a sample's validity and to provide optimal analytical results for data analysis. The following information should be available for each PS tube:

- The sorbent lot used for each PS, as well as records of tube packing if the tubes are manually prepared.
- Information about the conditioning and blanking of each tube, including the measured background.
- A chain of custody that documents each tube's sampling location and start and end times. Duplicate copies must be maintained for both field and laboratory staff purposes.
- Meteorological data records collected during the sampling period for each sample.
- The day the sample was received at the laboratory, as well as the day it was analyzed.
- Analytical method data and sample results must be maintained by laboratory personnel.

The calculations required for this method are included in EPA Method 325B, Section 12.2. This section includes both the calculations necessary to verify calibration performance, as well as the calculations used to determine the target compound's concentration in micrograms per cubic meter ( $\mu\text{g}/\text{m}^3$ ). Valid VOC concentrations determined by this method are expected to be between 0.5 and 5.0  $\mu\text{g}/\text{m}^3$ , although that is dependent upon such factors as the split ratio used, the dynamic range and noise provided by the analytical instrumentation, and any interfering background of VOCs on the PS tube.

### **Verification/Validation Studies**

#### **Flint Hills West Refinery<sup>6</sup>**

At the end of 2008, the EPA was permitted access to Flint Hills West Refinery by Flint Hills Resources. Production at Flint Hills West Refinery, which refines up to 260,000 barrels per day of crude oil, was typical during the sampling period described. With the aid of the on-site leak detection and repair contractor hired by Flint Hills Resources, a total of 26 PS sets were deployed between December 3, 2008 and December 2, 2009. Each PS was exposed for 14 days while attached to the boundary fence

line at approximately 5 feet above the ground. In addition to the 18 locations along the fence line, PSs were also deployed at two continuous air monitoring stations (CAMS) south and east of the facility. The CAMS sites perform automated GC benzene measurements on an hourly interval; therefore, the PS collection data could be compared to the GC results at both sites. In total, 579 samples were collected at or near Flint Hills West Refinery, including 56 duplicates and 49 field blanks.

Meteorological data were collected at the CAMS site located south of the facility. The wind data from the site indicates a six-month period of mixed wind directions, as well as another six-month period where the wind direction is typically from the southeast. These periods of high wind speeds with a uniform direction can affect comparison analysis results with time-integrated monitors significantly.

The benzene concentration data collected by the PSs was compared to the 14-day average of the hourly concentration data collected by the GCs at both CAMS sites. The MDL for the PS was slightly lower than that of the GC, at 35 parts per trillion by volume (pptv) as opposed to 50 pptv. A linear regression of PS and GC data correlated well, with an unconstrained  $R^2$  value of 0.86 and a slope of 0.90. Unfortunately, due to the distance from the refinery, the range of concentrations collected at the CAMS sites were not truly representative of the data collected at the fence line sites, and therefore not optimal for validation of the data collected at those sites.

The average benzene concentration of PSs collected at the facilities fence line was 1,075 pptv, with a median value of 709 pptv over a range of 122 to 29,280 pptv. Duplicate samples were collected at two sites for the entire study period and a third duplicate site was added towards the end of the study. This data also correlated well, with an average relative percent difference (RPD) of 8.5%. The maximum RPD (33%) occurred for a set of samples with a low concentration reading. Field blanks were also collected at two sites. Analysis yielded results that averaged 8.0 pptv, which is well below the 35 pptv MDL calculated for the study.

Further analysis of the data from the study showed that the PS results are very likely a result of emissions from the facility, rather than an outside emission source. The benzene data also showed

that the two-week sampling period was able to reflect changes in wind direction around the facility. Additionally, it was determined that changes in temperature in humidity due to seasonal changes at the facility had little bearing on the performance of the PSs. Overall, the study verified that benzene concentrations collected by PS tubes are in fact reflective of emissions from the target facility, have good precision and accuracy, and yield time resolved data that reflects meteorological conditions at the site.

### **South Philadelphia PS and Sensor Study<sup>7,8</sup>**

To continue its monitoring efforts, the EPA performed a PS study in South Philadelphia from June 18, 2013 to March 25, 2015. Carbopack X passive sampling tubes were deployed at 17 locations that included fence-line locations around a petroleum refinery (Philadelphia Energy Solutions) and sites near other oil and natural gas operations in the area. Samplers were also installed in community areas near the refinery. Passive samplers were deployed in duplicate at each location for a two-week sampling period. EPA Method 325A was used for sample collection, with the exception of Section 8.0, which describes the procedures for determining sampling locations, and a modified version of EPA Method 325B was used for analysis. After duplicate averaging, 41 valid sampling periods yielded 655 total PS results. Each PS was installed between 2 and 4 m from the ground on stakes, light poles, or billboards. In addition to benzene, the samples were also analyzed for ethylbenzene, toluene, styrene, and xylene isomers.

Meteorological conditions during the study were variable, though the prevailing wind direction was from the west. Northerly winds were more common during the winter months. To capture downwind emissions, most of the samplers were situated to the east of the petroleum refinery. However, other sources such as traffic and other facilities that emit VOCs did impact the sampling locations.

In addition to the PSs, AMS also deployed an open-path ultra-violet differential optical absorption spectrometer (UV-DOAS) at one of the PS locations. The EPA also tested two prototype leak detection sensors called SPod and Sentinel to further investigate the viability of low-cost leak

detection options for fenceline monitoring.

Benzene concentrations from each of the 17 monitoring sites ranged from 540 pptv to 5,020 pptv, with an overall study mean of 700 pptv. Analysis of the data shows that nearly all the minimum concentrations were collected at the community sites furthest away from the refinery, while the majority of the maximum concentrations for each study period were collected at or near the fenceline of the facility. Coupling the PS data with the distance from the facility and the collected meteorological data allowed the researchers to determine a general concentration gradient, where the highest concentrations of benzene were seen downwind (generally, east) of the refinery, while lower concentrations were seen at sampling locations north of the refinery. Further examination of the data yielded time-resolved concentration data that clearly indicates the source of pollution.

### **Typical QA/QC**

#### **Field Sampling QA/QC<sup>3</sup>**

EPA Method 325A/B requires the collection of both collocated or duplicate samples as well as field blanks. One collocated or duplicate sample must be collected for every 10 field samples so that precision measurements can be calculated for the sampling period. The relative percent difference (RPD) is calculated between sample pairs; if the RPD exceeds 30%, then the sample data must be qualified.

One field blank must be collected per sampling period (no less than two for an entire study) to verify PSs were not contaminated during sampler transport to and from the sampling locations or during the sampling period. Field blanks must be conditioned at the same time as the correlating PSs used for field samples. They are deployed at the sampling location during the entire two-week period under a protective hood; however, the long-term sample caps are not removed. Field blank must have less than one-third the target analyte concentration of the field samples. If a field blank fails to meet these criteria, all associated criteria for the sampling period must be qualified as such.

**Laboratory QA/QC<sup>3</sup>**

Most of QA/QC for EPA Method 325 is carried out in the laboratory. EPA Method 325B describes the QA/QC requirements for the method in detail. Table 3.29 below lists the required analytical control procedures that must be performed frequently throughout a PS study.

**Table 3.29. Analytical QA/QC Procedures for EPA Method 325B<sup>3</sup>**

| QC/QA Parameter  | Frequency   | Acceptance Criteria  |
|--|---|--|
| Analytical Precision                                       | During initial method setup and once per year thereafter.   | ±20% RPD between two spiked tubes of the same concentration.   |
| Desorption Efficiency and Compound Recovery                | During initial method setup.  | Repeat analysis of the same standard tube must have > 95% recovery.  |
| Audit Samples  | As available.   | ± 30% of known spike concentration.  |
| Tube Conditioning Blank                                    | Blank values must be verified on each new sorbent tube and 10% of each batch of re-conditioned tubes.   | The larger of:<br>1. ≤ 0.2 ppbv, or<br>2. < 3x the detection limit, or<br>3. < 10% of target compound mass at the regulated limit.                       |
| Five Point Calibration                                     | Every three months, or following any major repair to the analytical system or if the daily CCV analysis does not meet criteria.   | 1. Percent deviation of response factors must be ± 30%.<br>2. Relative retention times (RRTs) for target peaks must be ±0.06 units from the average RRT. |
| Instrument Tune Performance Check                          | Prior to the analysis of samples.   | Described in Table 3.XX3.  |
| Analytical Bias (Initial calibration verification and CCV) | The initial calibration verification (ICV) must be analyzed immediately following the calibration curve.<br><br>CCVs must be analyzed prior to the analysis of samples, every ten samples thereafter, and | The response factor must be within 30% of the average response factor for the calibration curve.   |

| QC/QA Parameter  | Frequency                                     | Acceptance Criteria   |
|------------------|---|---|
| Laboratory Blank | Beginning of each analysis following the CCV. | Must meet the same criteria as the tube conditioning blank. |

Method detection limits (MDLs) are determined by calculating as described in Method 301, Section 15. Seven PSs are spiked with a concentration of pollutant within a factor of five of the estimated detection limit. The standard deviation of the seven measurements is determined and then multiplied by three to calculate the MDL. The MDL should be around 50 parts per trillion (ppt), or no more than one-third of the lowest concentration of interest.

**Siting Concerns**

Section 8 of EPA Method 325A<sup>4</sup> contains detailed instructions for determining the number and location of optimal PS deployment locations around a facility. This section presents a general overview of considerations that should be made when planning PS deployment around a facility.

Prior to any sampler deployment, a site visit should be made to note the size and shape of the facility, any potential obstructions that could impede air flow, and any potential source interferences from off-site locations. Obstructions that impede air flow include large groups of trees, buildings, and changing topography. Both air flow obstructions and external emissions sources can cause the PSs to report elevated levels of VOCs not related to the monitored facility.<sup>6</sup>

During the site visit, potential locations for a meteorological station should be identified as well. The meteorological station should be placed in a location that has representative air flow and ambient temperatures for the facility, and thus should be sited in open terrain far removed from buildings and at least 30 meters from large paved areas. In the case of facilities located within complex topography, more than one meteorological station may be required to accurately represent different sampling locations around the facility.<sup>4</sup>

PSs should be deployed in a perimeter around the source location along the internal boundary of the facility. Locations may circle the facility's geometric center at different angles, or placed at

different distances based on the length of the facility's perimeter. Method 325A discusses PS locations around a facility of both regular and irregular shape. In some cases, monitored facilities have permanent monitoring stations close by that are run by state or local agencies. If access is available, it may be beneficial to deploy a PS at this location as the emissions data

### **Strengths and Limitations**

EPA Method 325A and 325B have several strengths and limitations; however, it is the strengths of the sampling and analysis methods that have made PSs attractive to facilities that need to meet the EPA's new requirements for fenceline detection of benzene. Primarily, PSs can be deployed for much cheaper cost compared to other methods currently available for fenceline monitoring of VOCs. The sampling method is easy to deploy; current facility staff (such as leak detection and repair contractors) can successfully perform this sampling method without extensive training.<sup>5</sup> The PSs themselves are robust and can be deployed for two-week periods while exposed to a variety of weather conditions.

Because of the required two-week sampling period, PSs are not suitable for immediate leak detection and repair purposes. Additionally, the samplers must be transported and analyzed at an off-site laboratory that is able to do the analysis described in EPA Method 325B. Fenceline monitoring with PSs may also prove challenging for facilities with complex topographies or facilities that are closely surrounded by external emissions sources such as busy highways or other oil and gas facilities. Finally, meteorological data must be collected throughout the sampling period to accurately assess the sample data. Table 3.30 lists the strengths and limitations of EPA Method 325A/B.



**Table 3.30. Strengths and Limitations of EPA Method 325A/B**

| Strengths   | Limitations   |
|---|---|
| Inexpensive to deploy.  | Not suitable for more immediate leak detection and repair.                            |
| Minimal training required for monitoring staff.                             | Samplers must be analyzed at an offsite laboratory.                                   |
| Samplers are robust and can withstand a wide variety of weather conditions. | Challenging to use with complex site topography and close external emissions sources. |
|   | Meteorological data are required for data analysis.                                   |

**References**

1. Brown, R.H. The Use of Diffusive Samplers for Monitoring of Ambient Air. *Pure & Appl. Chem.*, Vol. 65, No. 8, pp. 1859-1874, 1993.
2. Palmes, E.D. and A.F. Gunnison. Personal Monitoring Device for Gaseous Contaminants. *American Industrial Hygiene Association Journal*. Vol. 34, pp. 78-81. 1973.
3. US EPA. Method 325B-Volatile Organic Compounds from Fugitive and Area Sources: Sampler Preparation and Analysis.
4. US EPA. Method 325A-Volatile Organic Compounds from Fugitive and Area Sources: Sampler Deployment and VOC Sample Collection.
5. US EPA. 2000. Meteorological Monitoring Guidance for Regulatory Modeling Applications. EPA-454/R-99-005. Office of Air Quality Planning and Standards, Research Triangle Park, NC. February 2000.
6. Thoma, Eben D., Michael C. Miller, Kuenja C. Chung, Nicholas L. Parsons, and Brenda C. Shite. Facility Fence Line Monitoring Using Passive Samplers.
7. Thoma, Eben D., et al. South Philadelphia Passive Sample and Sensor Study. *Journal of the Air & Waste Management Association.*, Vol. 00, No. 00, 1-12. 2016.
8. Mukergee, Shaibal, et al. Spatial Analysis of Volatile Organic Compounds in South Philadelphia Using Passive Samplers. *Journal of the Air & Waste Management Association.*, Vol. 66, No. 5, 492-498. 2016.

### ***3.10 Method to Quantify Particulate Matter Emissions from Windblown Dust – Other Test Method 30***

Dust emissions from arid playa sources<sup>1,2</sup> affect not only human health, but also create environmental concerns around loss distribution<sup>3</sup>, mineral cycling, and even cloud formation.<sup>1,2</sup> Sources of dust emissions in the United States include Owens and Mono Lakes, both of which are exposed lake beds in California that were the result of water being diverted from the lakes into populous areas. Other Test Method (OTM) 30 was developed so that particulate matter (PM) emissions can be monitored downwind of places susceptible to wind erosion and potentially remedied through characterization of high emission sources.

#### **General Description of Approach**

The basic premise of OTM 30 is that PM emissions can be quantified by comparing saltation flux to the difference in upwind and downwind ambient PM concentrations.<sup>3</sup> Saltation is sand-sized particles hopping over erodible surfaces caused by wind. The saltating particles bombard the ground surface, releasing tiny particles of dust. It is this saltation bombardment, not aerodynamic lift, that is the primary mode by which dust particle movement is initiated.<sup>4</sup> When the tiny dust particles are lofted by bombardment, winds can carry those particles many kilometers downwind. Figure 3.45<sup>3</sup> is an illustration from OTM 30 that shows the transport of dust particles through the saltation process.

---

<sup>2</sup> Playa is the flat bottom of a desert basin that can become a shallow lake at times.

<sup>3</sup> Loess is an unstratified loamy deposit found in North America, Europe, and Asia and is chiefly deposited by the wind.

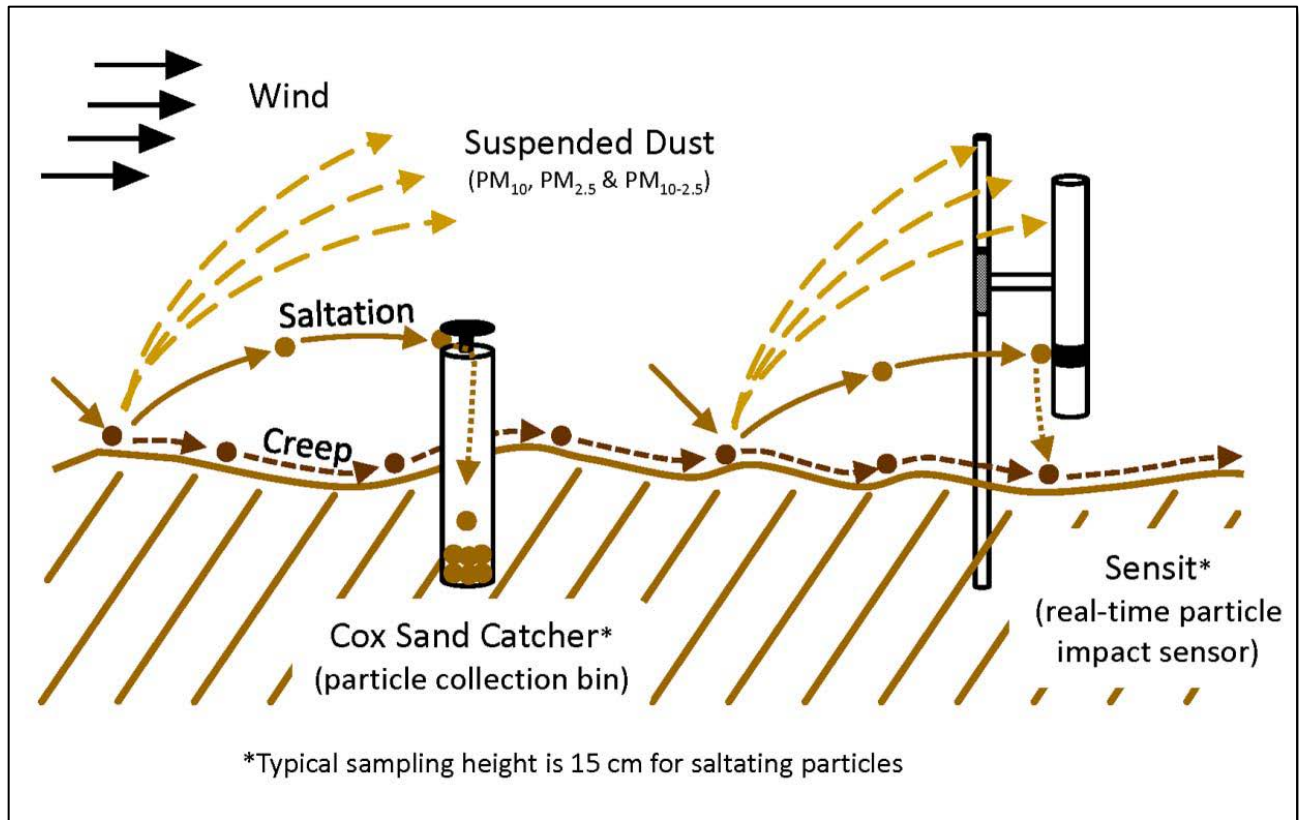


**Figure 3-45. Saltation and Dust Production Process for Windblown Dust.**

Theoretical and experimental evidence indicates that the vertical flux of windblown dust is proportional to the horizontal flux of saltating sand-sized particles for soils with the same binding energy. The following equation shows the two components are proportional by a factor of K:

$$F = K_f \times q_{15}$$

Where:

F = Vertical PM<sub>10</sub> emission flux [g/cm<sup>2</sup>-s]

K<sub>f</sub> = Seasonal K-factor; Non-dimensional proportionality constant

q<sub>15</sub> = Horizontal sand flux 15 cm above the surface [g/cm<sup>2</sup>-s]

Studies have shown that surface moisture and temperature changes that occur seasonally affect the binding energy of the soil, thereby affecting K<sub>f</sub>, or proportionality constant. Dispersion models such

as CALPUFF or AERMOD are used to determine the  $K_f$  for changing surface characteristics.

### **Instrumentation**

OTM 30 requires the deployment of two instruments to calculate sand flux measurements: (1) a passive instrument that monitors sand catch over a sampling period, and (2) a real-time particle impact sensor to time-resolve the sand catch data.

The sand catch instrument recommended by OTM 30 is the Cox Sand Catcher (CSC) manufactured by the Great Basin Unified Air Pollution Control District (GBUAPCD) in California. The sand catchers are deployed so that the inlet is 15 cm above the surface of the source as seen in Figures 3.46<sup>6</sup> through 3.46. Sample tubes that collect the sand inside the CSC are collected monthly to be weighed in a laboratory. Another sand catch instrument that has been used successfully in the Big Springs Number Eight (BSNE), manufactured by Custom Products in Big Springs, TX (Figure 3.47).<sup>7</sup> The BSNE, however, has a smaller capacity than the CSC, and daily site trips may be required to prevent overloading the instrument.

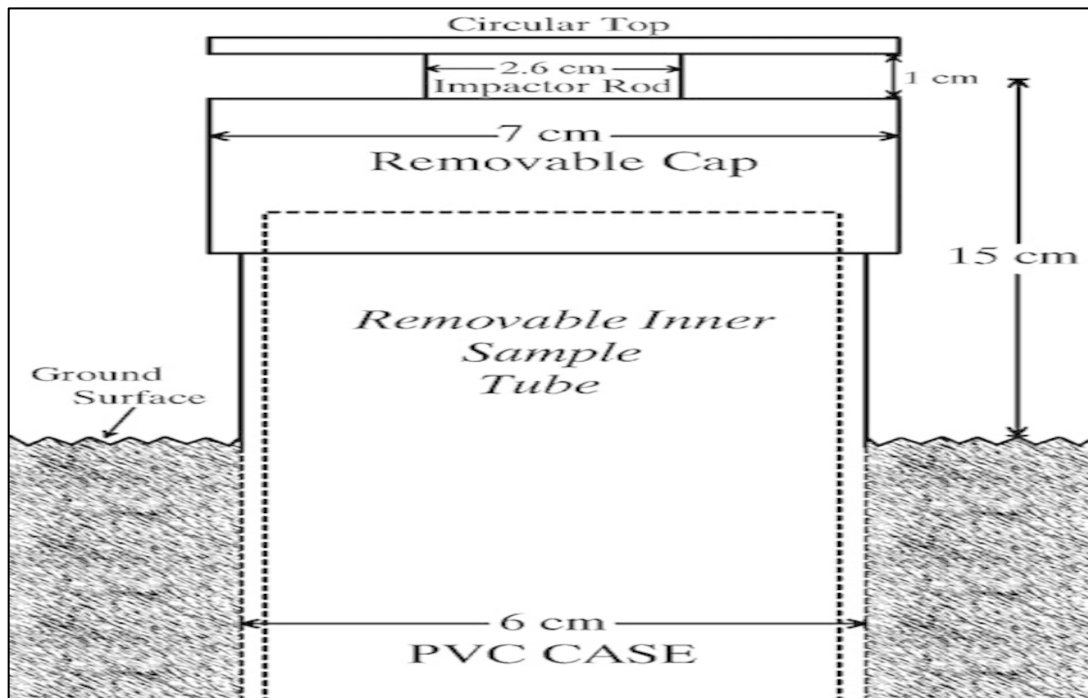
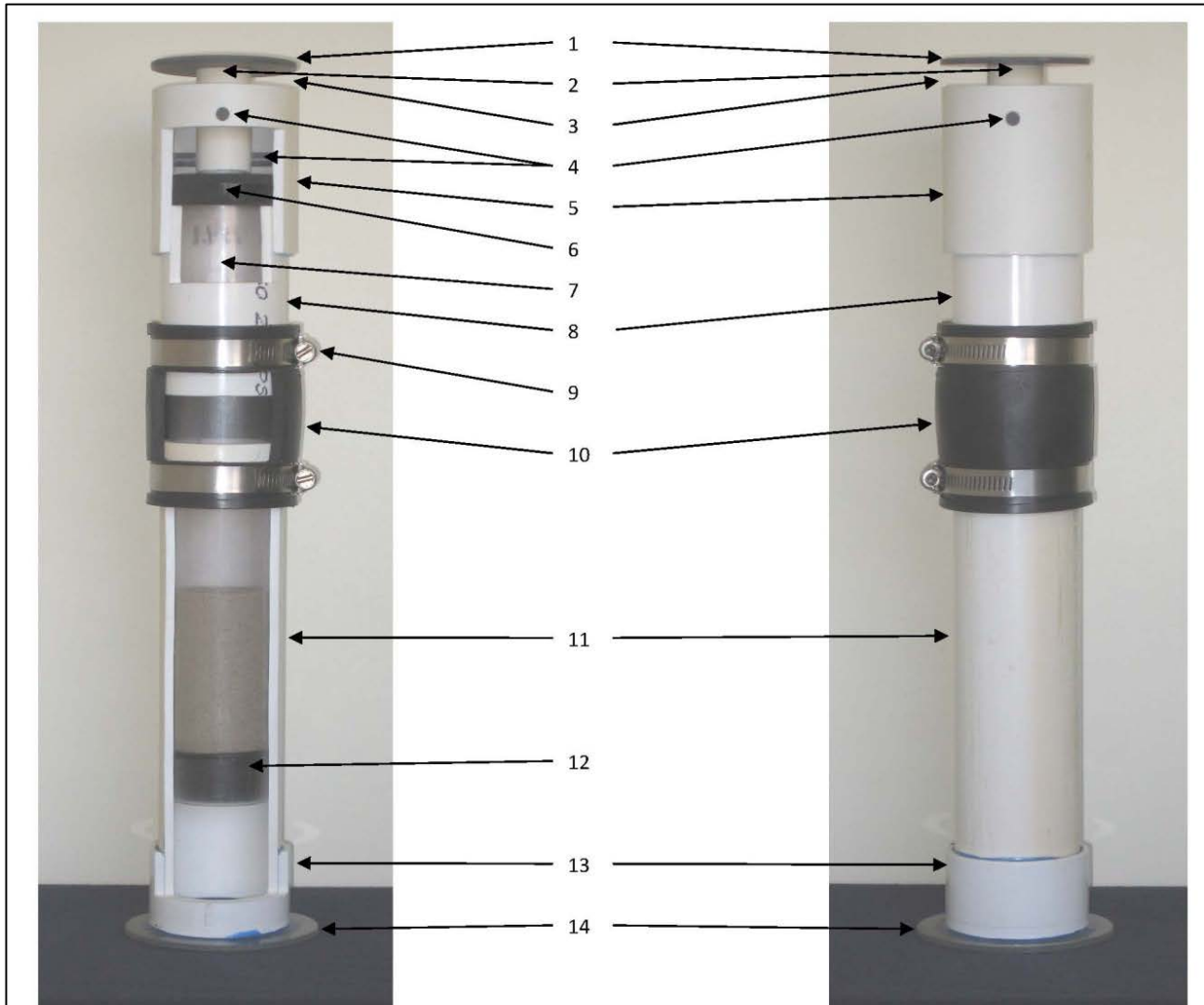


**Figure 3.46. Schematic of CSC Placement for Sampling.**



| Reference # | Feature              | Description   |
|-------------|----------------------|---|
| 1           | Roof                 | 1/8" thick by 2 3/4" diameter PVC sheet   |
| 2           | Roof Support         | 3/4" schedule 40 PVC pipe 2" in length  |
| 3           | Sample Inlet Opening | 1 cm from bottom of roof to top of PVC coupling. Tolerance is 0.5 mm.             |
| 4           | Support Pins         | 1/4" diameter PVC rod glued in place  |
| 5           | Head                 | 2" schedule 40 PVC coupling, specify long coupling approximately 2 3/4" in length |
| 6           | Catch Tube Seal      | rubber shank washer cut to fit  |
| 7           | Catch Tube           | 2" diameter clear plastic soil sample tube variable length to fit application*    |
| 8           | Connecting Pipe      | 2" schedule 40 PVC pipe** 3 1/2" in length  |
| 9           | Stainless Pipe Clamp |   |
| 10          | Adjustment Coupling  | 2" diameter rubber plain and flexible pipe coupling 3 1/2" in length              |
| 11          | Body                 | 2" schedule 40 PVC pipe** variable in length to fit application, 25" for 2' CSC   |
| 12          | Catch Tube Stopper   | rubber stopper or plug  |
| 13          | Bottom Cap           | 2" schedule 40 PVC cap with a flat top  |
| 14          | Bottom Plate         | 1/8" thick by 3 7/8" diameter PVC sheet   |

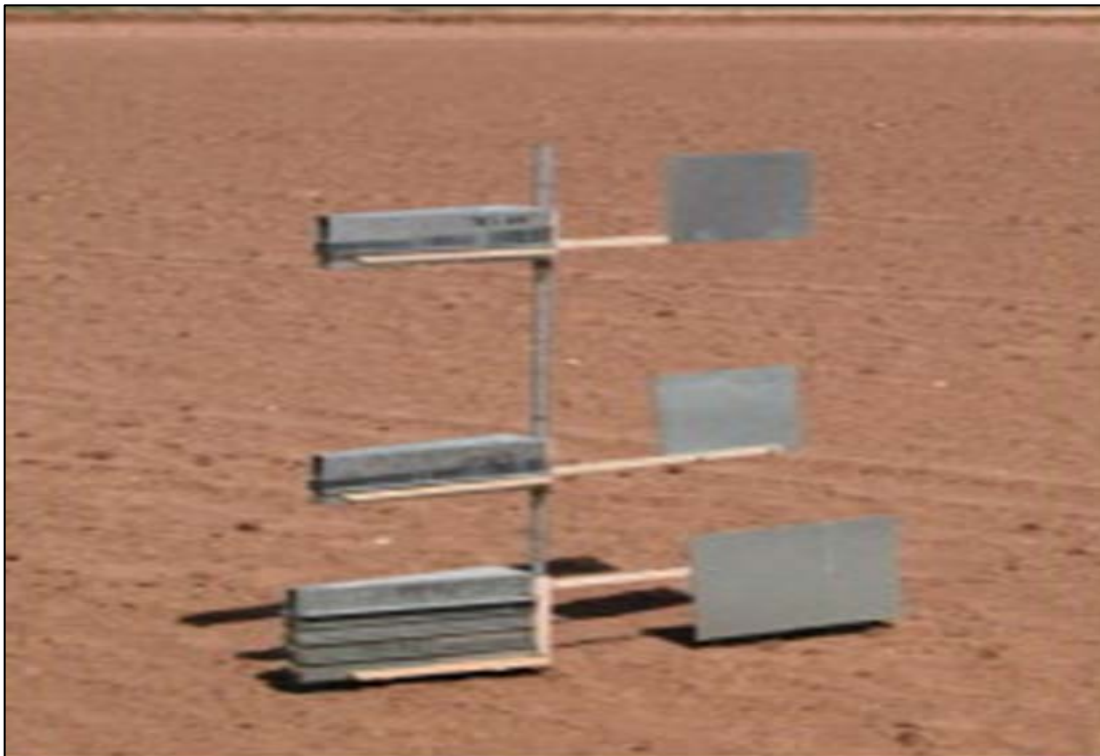
\*Note: The Catch Tube shown here is partially filled with sand.

\*\*Note: The inner diameter of PVC pipe varies with manufacture. Make sure the sample catch tube slides freely into the pipe before purchasing.

**Figure 3.47. Cut-out of a CSC and Construction Specifications**



**Figure 3.48. CSC Placement in the Field with a Height Adjustment Tool.<sup>3</sup>**



Th

**Figure 3.49. BSNE Sampler Shown Sampling in the Field.<sup>7</sup>**

The only real-time particle impact sensor to be successfully used for an OTM 30 study is the Sensit, manufactured by Sensit Company in Portland, ND. Sensits use a piezoelectric crystal to detect and measure saltation activity. The resulting particle count and kinetic energy measurements are proportional to the mass flux of PM. When co-located with CSCs and installed at the same height, hourly Sensit readings are used to time-resolve sand catch data over a sampling period to determine hourly sand flux.

OTM 30 also requires that PM is monitored with instruments capable of collecting hourly data; tapered element oscillating microbalance (TEOM) PM<sub>10</sub> monitors have proven to have good success in existing OTM 30 studies. Beta-gauge and beta-attenuation monitors that provide hourly PM data should also work with this method.

A 5-10 m meteorological tower that measures scalar wind speed, direction, and sigma-theta (the standard deviation of the wind direction over the period of measurement) is also required to be near the study area. The meteorological tower must be able to record hourly average data and should be sited and operated in accordance with the federal monitoring guidelines described in US EPA Quality Assurance Handbook for Air Pollution Measurement Systems, Volume IV: Meteorological Measurements.

A complete list of supplies and equipment needed to perform OTM 30 is available in Section 6.0 of the test method.

### **Dispersion Modeling and K-factors**

Both the AERMOD and CALPUFF dispersion models are EPA-approved and have been demonstrated to work well with OTM 30. Both are applied following the EPA modeling guidelines detailed in 40 CFR, Part 51, Appendix W. Both dispersion models calculate  $K_f$  using the PM emissions calculated from the horizontal flux assuming an initial K-factor,  $K_i$ , of  $5 \times 10^{-5}$ . The hourly  $K_f$  is then determined post-processing using the following equation:

$$K_f = K_i \left( \frac{C_o - C_b}{C_m} \right)$$

Where:

$K_i$  = Initial K-factor ( $5 \times 10^{-5}$ )

$C_o$  = Observed hourly concentration

$C_b$  = Background concentration

$C_m$  = Modeled concentration

OTM 30 offers specific guidance on hourly K-factors that should be screened due to varying conditions that affect PM emission data. Once K-factors are screened, the seasonal K-factors can be calculated based on the geometric mean of the hourly K-factors calculated above. It is the seasonal K-factor that is used in the calculation that determines vertical PM<sub>10</sub> emission flux from horizontal sand flux. More specific instructions for data analysis and calculations are discussed in Section 10.0 of OTM 30.

### **Sample Collection**

Prior to the start of monitoring, the meteorological instrumentation and PM monitor should be calibrated in accordance with EPA monitoring guidelines and all data logger functionalities should be checked. A tare weight must be determined for the empty sand catcher sampling tubes used in the CSCs and recorded. After installing the empty sampling tube in the CSC, the height must be adjusted to 15 cm. The Sensit functionality can be tested by simply tapping on the sensor. Once the height of the sensor is verified to be 15 cm, sampling and recording can be initiated. OTM 30 recommends that site visits occur monthly when no erosion event is occurring. It is important to note that maintenance activities may be required more frequently depending on the conditions the



instruments are exposed to. Specific procedures about the collection of CSC samples and Sensit data are listed in OTM 30, Section 7.4. Verification/Validation Studies

### **Owens (dry) Lake, Inyo County California<sup>1</sup>**

The goal of the study was to characterize the dry lake bed to determine which areas within the area create the highest PM emissions, therefore needing dust controls. The methodology used in this study is the basis on which OTM 30 was written.

In all, 135 sand flux sites were installed to monitor sand flux rates on an hourly basis. Each site was spaced approximately 1 km apart. The sites were separated into four sampling zones based on different geological characteristics and source activity that seemed to affect PM emissions. Each measurement site included a CSC, which collects saltating sand-sized particles, and a collocated Sensit electronic sensor that provided hourly sand flux rates. *K* factors were determined using the Calpuff dispersion modeling system at six representative monitoring sites. Using this system, researchers could quantitate PM emissions for each of the square kilometer measurement sites and determined that approximately 77 square km of the lake bed required dust controls to reduce PM emissions to within federal standards.

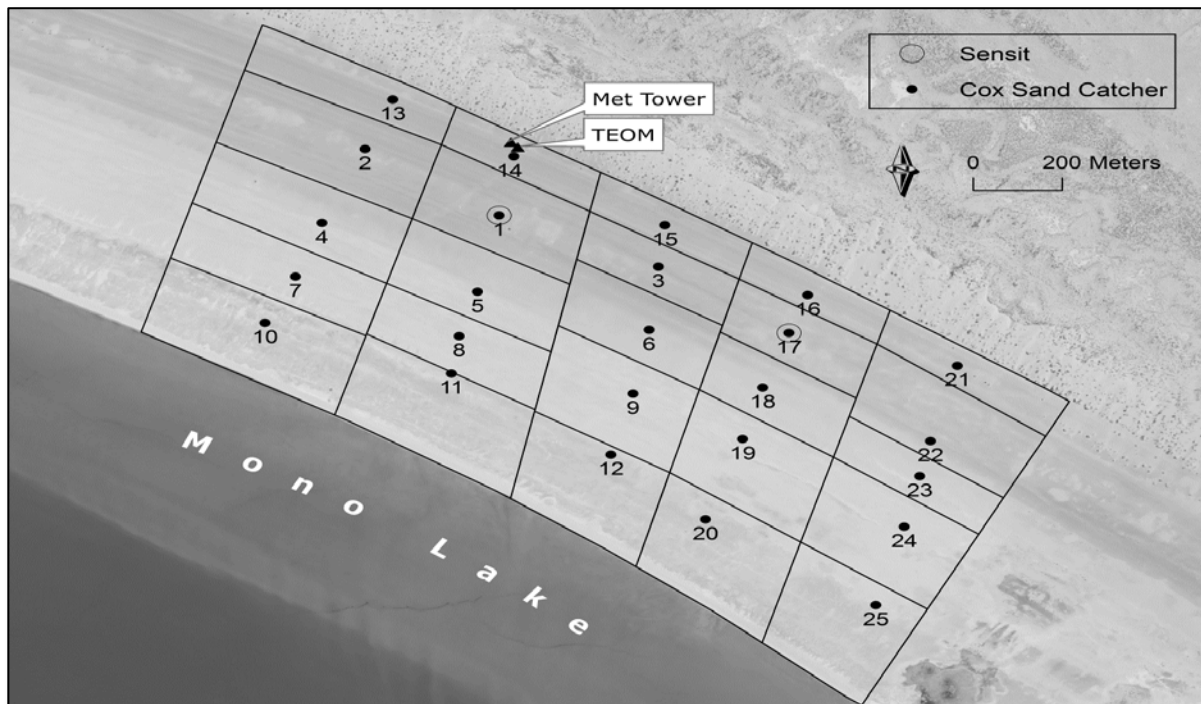
### **Mono Lake, California<sup>6</sup>**

A second large source of windblown dust is Mono Lake, California. The lake is a large shallow lake in the Great Basin of Yosemite National park in Mono County, north of Los Angeles. Diversion of water from the lake to the City of Los Angeles between 1941 and 1989 lowered the lake level, exposing over 24 square km of lakebed to wind erosion. Though an air quality analysis completed in 1994 determined that a lake level of 6,391 feet above sea level would reduce PM emissions to within federal standards, the lake level only reached 6385 feet twice, in 1999 and 2006. PM concentrations continued to exceed federal standards even at the highest lake levels.

The GBUAPCD implemented a refined method for estimating PM emissions from Mono Lake based on the methodology used to characterize PM emissions from Owens (dry) Lake. The monitoring effort started in July 2009 and ended in June 2010. The monitoring network, shown in Figure 3.50<sup>3</sup>,

included 25 CSCs, two Sensits, a meteorological tower, and one TEOM PM<sub>10</sub> monitor, all of which were operated on the north shore of Mono Lake. Hourly data were collected from each network component so that time-resolved PM<sub>10</sub> concentration data could be calculated. Researchers at Mono Lake used the AERMOD dispersion modeling system to determine K-factors. The AERMOD system differs from the CALPUFF model in that its AREAPOLY area source algorithm is better suited for irregularly-shaped area sources.

**Figure 3-50. Monitoring Network at Mono Lake, CA.**



Over the 1-year study period, the 24-hour federal PM<sub>10</sub> standard was violated 25 times, with the highest 24-hour average concentration measuring 14,147  $\mu\text{g}/\text{m}^3$ , nearly 10 times the federal standard. Predicted PM<sub>10</sub> concentrations calculated via dispersion modeling compared well to the concentrations recorded by the TEOM PM<sub>10</sub> monitor throughout the study period.

### **Typical QA/QC**

All data logged by the monitoring instrumentation must be examined for missing or anomalous data. In the case of missing data, which may be caused by a low battery or a data logger malfunction, data from the nearest operating Sensit can be used to replace the missing data and time-resolve the CSC sand catch data. Anomalous data, which includes sensor responses not caused by suspended dust

(such as operators tapping on sensors to check functionality) should be removed from the dataset. The ratio of the individual Sensit readings to sand catch ratio for each monitoring site and sampling period should be examined for consistency between sampling events. Large changes in this ratio may be an indication that a Sensit should be replaced.

Data logged by the meteorological station and PM monitors must also be examined for missing and anomalous data. Any anomalous data should be investigated and removed as needed. While operation staff conduct calibration activities at the site on a routine basis, OTM 30 requires that a third-party quality assurance audit be performed as well. For example, meteorological equipment must be audited within 30 days of the start of monitoring and every six months thereafter.

All balances used to weigh sample tubes and particulate collected in the CSCs must be checked before and after each weighing session with certified National Institute of Standards and Technology (NIST) Class-F weights. All weights must be recorded in a balance log. The balances must be certified and calibrated annually through a third-party.

### **Siting Concerns**

Section 7.0 of OTM 30 contains specific recommendations about creating a monitoring network using OTM 30. This section summarizes the major recommendations and specific concerns.

Monitoring networks can range in scope from one sand flux, meteorological, and PM monitoring site for small source areas to over 100 sand flux sites with a representative number of meteorological and PM monitoring sites. While measurement accuracy does improve with the number of monitoring sites, data yielded by few sites are also beneficial.

CSC and Sensit monitoring locations should include all significant windblown dust sources between the upwind and downwind PM monitors. Dust sources that are not included in the background concentration measured at an upwind monitoring site could bias hourly K-factor calculations, including dust sources that do affect the downwind monitoring site. Thus, it is very important to include all potential sources of PM in the dispersion model. Each CSC and Sensit monitoring site

should be between 100 and 1,000 m apart and each should have a designated source boundary.

PM monitors should be installed upwind and downwind of the site per the prevailing wind direction for high wind events. A collocated PM monitor should be positioned at the site of maximum impact, or a downwind position, to produce the most accurate K-factor, as well as enhance the defensibility of data collected during the study. The meteorological tower and PM monitor must be sited in an area that avoids structures and topographical features that interfere with wind flow patterns between the dust source and the downwind monitors.

**Strengths and Limitations**

The methodology provided in OTM 30 has several strengths and limitations. This flexible method allows all windblown dust events at a monitoring site to be sampled, flux calculations can determine specific sources of PM that require remediation, and the on-site instrumentation is simple to operate. OTM 30 does, however, require all potential PM sources that affect an area to be monitored. Extensive data analysis is also required to yield accurate results. Table 3.31 summarizes the strengths and limitations of OTM 30.

**Table 3.31. Strengths and Limitations of the OTM 30 Approach**

| Strengths   | Limitations   |
|---|---|
| All windblown dust events during a sampling period are sampled.               | All PM sources that contribute downwind concentration must be included in the dispersion model. |
| Sand flux measurements indicate specific locations where emissions originate. | Extensive data analysis is required to achieve accurate results.                                |
| Emissions vary hourly based on changing conditions that affect erosion rates. |   |
| Instrumentation is simple to operate.   |   |
| Flexibility in monitoring network size.                                       |   |

**References**

1. Gillette, D., D. Ono and K. Richmond. 2004. A Combined Modeling and Measurement Technique for Estimating Windblown Dust Emission at Owens (dry) Lake, California. *Journal of Geophysical Research*. 109:F01003.
2. Koehler, K. A., S.M. Kriedenweis, P.J. DeMott, A.J. Prenni, and M.D. Petters. 2007. Potential Impact of Owens (dry) Lake Dust on Warm and Cold Cloud Formation. *Journal of Geophysical Research*. 112:D12210.
3. U.S. Environmental Protection Agency (EPA). 2012. Other Test Method–30: Method to Quantify Particulate Matter Emissions from Windblown Dust. Available online at <https://www.epa.gov/emc/emc-other-test-methods>
4. Shao, Y., M.R. Raupach, and P.A. Findlater. 1993. Effect of Saltation Bombardment on the Entrainment of Dust by Wind. *Journal of Geophysical Research*. 98:12719–12726.
5. Office of Air and Radiation, EPA. 2016. Clean Air Excellence Awards Ceremony Booklet. Available online at <https://www.epa.gov/caaac/clean-air-excellence-awards-ceremony-booklet>.
6. Ono, D., P. Kiddoo, C. Howard, G. Davis, and K. Richmond. 2011. Application of a Combined Measurement and Modeling Method to Quantify Windblown Dust Emissions for the Exposed Playa at Mono Lake, California. *Journal of the Air & Waste Management Association*. 61:1036-1045.
7. Acosta-Marinez, V., S. Van Pelt, J. Moore-Kucera, M.C. Baddock, and T.M. Zobeck. 2015. Microbiology of Wind-eroded Sediments: Current Knowledge and Future Research Directions. *Aeolian Research*, 18, 99-113.

### **3.11 Determination of Emissions from Open Sources by Plume Profiling – Other Test Method 32**

#### **General Description of Approach**

Other Test Method 32 (OTM 32)<sup>1</sup> utilizes plume profiling to characterize particulate matter (PM) emissions from open sources—specifically from roadways. Plume profiling, synonymous with the terms exposure profiling or plume flux profiling, is an open source emissions test method based on the exposure profiling concept.<sup>2</sup> This concept describes how exposure can be defined as the mass flux of a pollutant at a sampling point, where mass flux is calculated as the product of pollutant concentration and wind speed.

OTM 32 uses a “conservation of mass” approach to calculate emissions factors and rates,<sup>3</sup> where the quantity of emissions (concentration) is determined by the spatial integration of mass over the cross section of the plume. The PM concentration is calculated by the following formula:

$$C = \frac{m}{QT}$$

Where:

- C = PM concentration (lb/VMT<sup>4</sup>)
- m = Mass collected on the filter or substrate (lb)
- Q = Flow rate of the sampler (VMT)
- T = Sampling time

Exposure is the net particulate mass that passes through a unit area during the test. Exposure is calculate using the following formula:

$$E = (C - C_b) U T$$

Where:

- E = Exposure (mass/area)
- C = Downwind PM concentration (mass/volume)
- C<sub>b</sub> = Background PM concentration (mass/volume)
- U = Approaching wind speed
- T = Sampling time

Because exposure values are determined at specific points within the plume, those values will vary

---

<sup>4</sup> VMT = Vehicle-mile traveled. This value is defined as the product of the vehicle count during the sampling period and the length of the road segment being represented by the profiling data.

over the vertical length. A one-dimensional integration is used to obtain the total PM emissions from a line source according to the following equation:

$$A1 = \int_0^H E dh$$

Where:

- A1 = Integrated exposure (mass/length)  
E = Exposure (mass/area)  
h = height from the ground (length)  
H = vertical height of the plume (length)

PM emission factors are then determined by normalizing the integrated exposure against a measure of source activity, such as dividing the integrated exposure by the number of passing vehicles.

### **Sampling Equipment**

To determine pollutant (PM) concentrations, an array of samplers is deployed to provide time-averaged concentration data at points within the plume. In the case of PM emissions, the sampler is fitted with a removable sample collection substrate, such as a filter, that is submitted to a laboratory for analysis after sampling is completed. The PM fraction of interest will determine the specific sampler used in the study, as described in Section 6.1 of OTM 32. Because sampler flow must be maintained at a sufficient level to ensure adequate sample collection, a flow measurement device is typically incorporated into the sampler. Figure 3.51<sup>1</sup> illustrates the configuration of a traditional PM sampler. All samplers should be maintained and calibrated as recommended by the manufacturer prior to sampling.

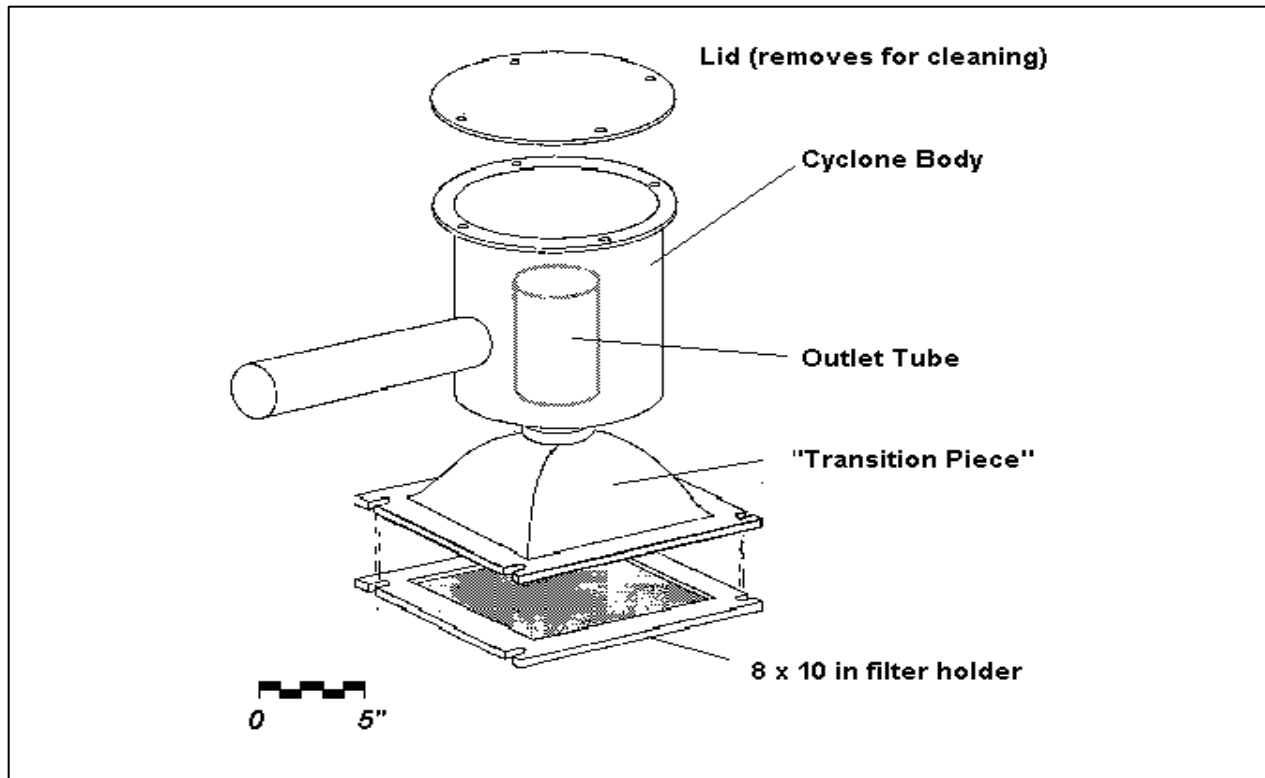


**Figure 3.51. Traditional PM Sampler Configuration.**

Filters used for sampling must be prepared in the laboratory before sample collection begins as described in OTM 32 Section 8.1.2. To summarize, a clean filter with no imperfections must be equilibrated in a controlled room with an analytical balance for at least 24 hours. Ideal room conditions for gravimetric analysis are 40% relative humidity with a temperature of 34° C (93° F). Once the balance's calibration is verified, each filter is weighed, providing an initial tare weight for the sample. At least three blank filters should be weighed and handled as a blank for each test day to assess the handling effects of the study. Each filter is then placed in a glassine envelope, followed by a numbered file folder. The folders are stored for submittal to the field in a heavy-duty cardboard box.

Because wind speed is an integral part of the mass flux calculation, meteorological equipment is also needed at the sampling location. The meteorological monitors should provide time-averaged wind speed data at 5 to 15 minute intervals. Ambient temperature and relative humidity are also collected at the sampling site. Barometric pressure data can be obtained from a local weather station to report concentration data in local conditions, or can be approximated based on elevation to report data in standard conditions. All meteorological equipment should be maintained and calibrated in accordance with Volume IV of EPA's QA Handbook series.<sup>4</sup>



### Sample Deployment

Because OTM 32 relies on both pollutant concentration and wind speed data to generate mass flux concentrations, simultaneous multi-point measurements are made over the emission plume in a sampling plane perpendicular to the pollutant's (PM) direction of transport. Figure 3.52<sup>1</sup> illustrates the ideal sampler array for a point source, where  $W$  is about 75% of the observed visible plume width and  $H$  is about 75% of the observed visible plume height at a distance  $D$ .<sup>1</sup> For mobile (or line) sources, the samplers are oriented in a vertical array at equal points along a support tower with a maximum height of seven meters (Figures 3.53 and 3.54).<sup>1</sup> Wind speed monitors are typically deployed at a height of 2 to 3 meters from the ground. If the length of the line source is at least ten times the downwind distance to the sampling array, only a single vertical array is needed to adequately characterize the emissions plume.

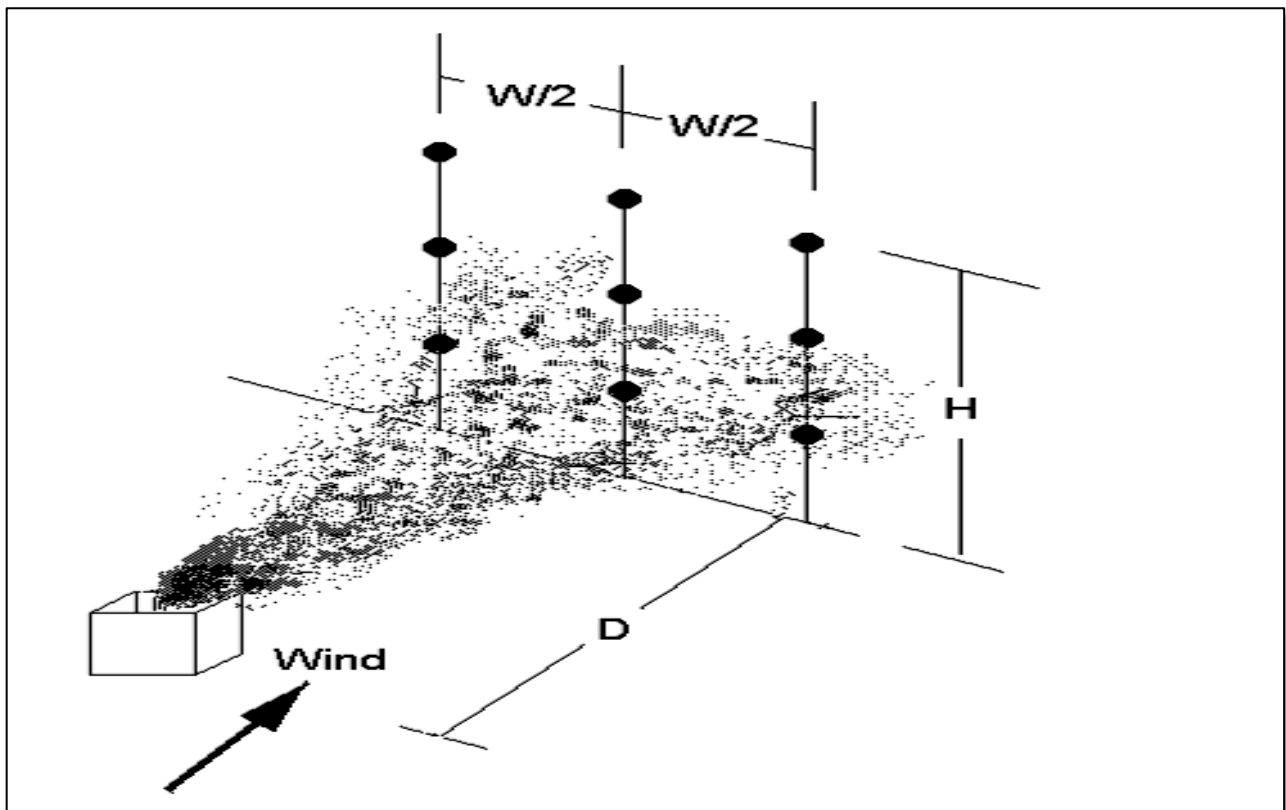


**Figure 3-52. Illustration of Fixed Point Source Sampling Array.**

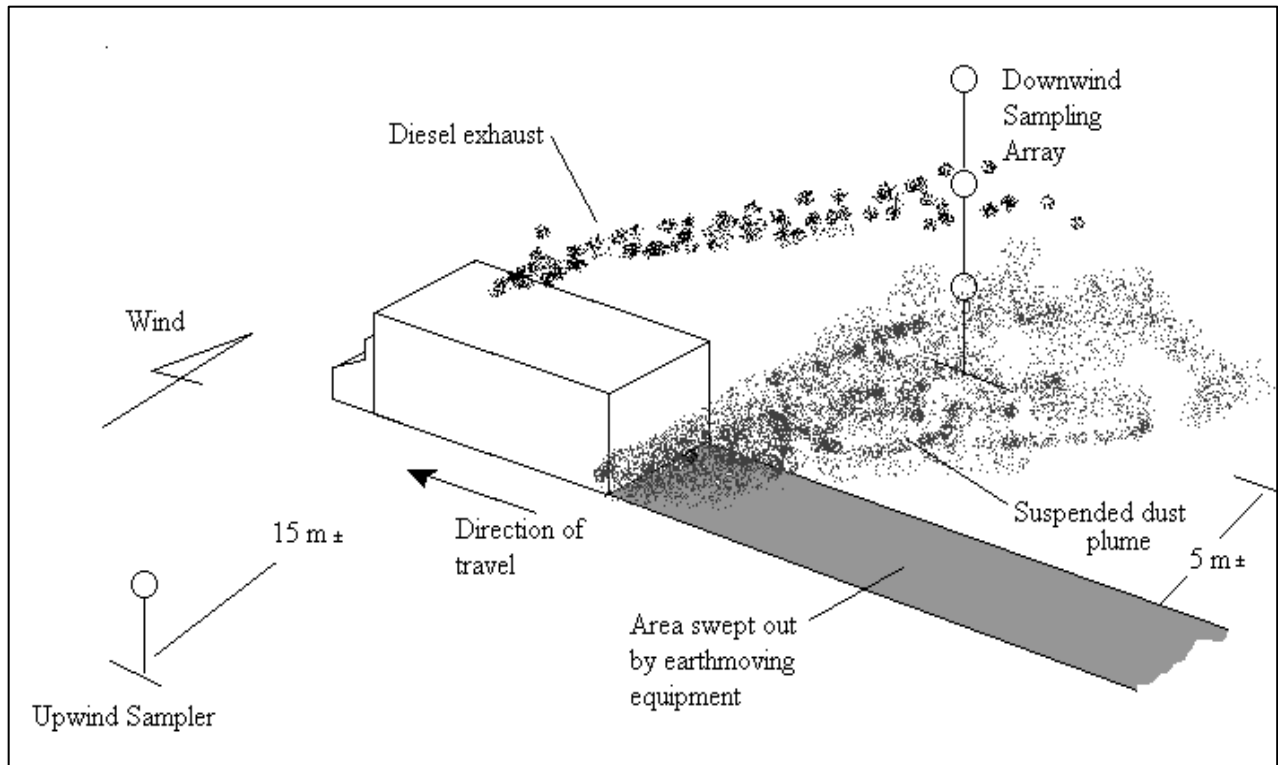


**Figure 3-53. Illustration of Moving Point Source--Unpaved Road Dust Emissions.**

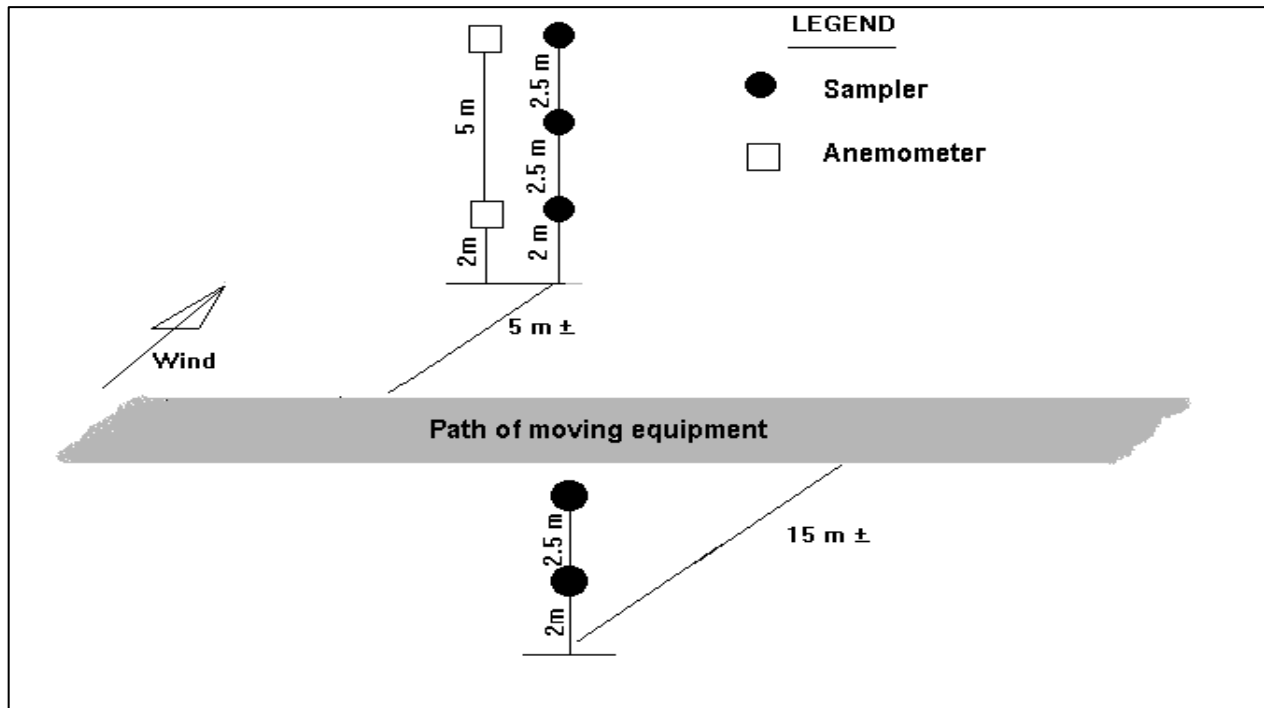


**Figure 3-54. Example Sampling Array for Moving Point Source.**

Sampling must be conducted at specific meteorological conditions. Specifically, if measurable precipitation is forecast, sampling should not occur. Additionally, average wind speed must be between 3 and 20 miles per hour (mph) in a direction that creates a 0 to 45-degree angle to the

perpendicular of the line source for at least two consecutive 5-minute time-averaged periods. If either condition drifts outside of these requirements for more than two consecutive 5-minute time-averaged periods, sampling must be suspended until acceptable meteorological conditions return.

Once the sampling event has concluded, sample substrates may be removed from the samplers. Filters used for PM collection are inserted into a glassine envelope upon sample collection, then further protected by a file folder and/or heavy-duty plastic bag. Sampled filters should be stored separately from clean filters to prevent contamination.

### **Sample Analysis**

Once clean filters are exposed and returned to the laboratory, gravimetric analysis is required to determine final weights for each filter. Once the filters are equilibrated as described above for the tare weight, and the balance's calibration is verified, an analyst weighs each filter and the final weight recorded. Then, a second analyst independently verifies ten percent of exposed filter weights. If the second measurement does not agree with the first within three times the standard deviation of the reweighs for the filter blanks, then the entire batch must be reweighed and verified a second time.

### **Verification/Validation Studies**

#### **United Taconite and U.S. Steel Minntac<sup>3</sup>**

Midwest Research Institute (MRI) conducted a field tests at United Taconite and U.S. Steel Minntac in the Mesabi Iron Range in northern Minnesota to characterize the PM emissions factors for fugitive dust emissions that result from haul truck operations at taconite<sup>5</sup> mines in January and July of 2007. The plume profiling method was performed in July to calibrate results from mobile monitoring efforts. The study objectives included developing PM<sub>2.5</sub>/PM<sub>10</sub> ratios for haul road dust emissions, and developing water control methods to reduce PM emissions. MRI implemented both mobile monitoring and the plume profiling method simultaneously at haul road sites for each mine. Sampling towers as described above were deployed at each reference site in the study downwind from the near edge of the haul road. Upwind PM<sub>10</sub> samplers were deployed upwind to

---

<sup>5</sup> Taconite is a low-grade iron ore.

determine background PM emissions. Sampling periods were typically between 1 and 2 hours long. The sampling sites were located at road segments where there was unobstructed wind flow over the road and there were no interferences from other PM sources. To prevent interference from truck exhaust emissions, the grade of the road segments was very small.

A mixture of haul trucks, maintenance vehicles, and light-duty vehicles passed through the sampling locations during the sampling periods. To account specifically for haul truck emissions, MRI converted the other vehicles into haul truck equivalents and determined the other vehicles accounted for less than 10 percent of the total haul truck passes through the sampling site. Six plume profiling tests were conducted at each facility, resulting in twelve total tests. Both PM<sub>10</sub> and PM<sub>2.5</sub> samplers were deployed to determine PM<sub>2.5</sub>/PM<sub>10</sub> emissions ratios for each of the reference test sites. Overall, emissions factors for the United Taconite facility were determined to be lower than those at U.S. Steel Minntac, which can be explained in part by rainy conditions at United Taconite and watering of the road segment overnight.

The average uncontrolled emission factors (both daytime and nighttime combined) were determined to 6.0 lb/VMT for United Taconite, and 8.4 lb/VMT for U.S. Steel Minntac. Annual emission factors previously estimated by the Taconite Industry Working Group based on literature and emissions factors determined at other facilities (6.2 lb PM<sub>10</sub>/VMT) compared well with the emission factors determined at the test sites when considering that the Working Group numbers were derived from daytime values only. Overall, MRI determined the average PM<sub>10</sub> emission factor for taconite mine roads to be 7.2 lb PM<sub>10</sub>/VMT, while the average PM<sub>2.5</sub> emission factor is 0.72 lb PM<sub>2.5</sub>/VMT.

### **Typical QA/QC**

Several types of quality assurance and quality control methods are utilized in OTM 32 to ensure accurate measurements and sample traceability.

### **Quality Control Samples**

Blanks are collected minimally for 10 percent of samples collected in the field. A blank is collected in the same manner as a sample, however, no ambient air is passed through the collection substrate or filter, as is the case for PM. Blank recoveries demonstrate that filters or other sampling media were not contaminated during sample handling.

### **Quality Assurance**

OTM 32 recommends performance audits be conducted routinely by an independent operator during the study period. The auditor reviews the flow rate calibration, re-analyzes the exposed substrate (filter), and reviews the data processing.

It is also necessary to ensure each sample is traceable throughout the sampling process. Each substrate, or filter, should receive a unique identification number that is recorded along with the date the filter was obtained. Each sample must also be coded with the sample location and test series, as well as any other data pertinent to sample collection. All sample transfers, such as from the field to a laboratory, should also be recorded.

### **Precision**

To determine method precision for mobile or line sources, vertical sampler towers can be collocated on the road segment of interest or by repeating tests on a single sampler tower under constant source conditions. An example of a collocated tower for mobile (line) source sampling is showing in the image of Figure 3.55.<sup>1</sup> A minimum of three tests is required to estimate method precision; however, due to the cost of deploying multiple sampler towers, method precision is often estimated based on the precision of previous studies with similar source configurations.

Les pass



**Figure 3.55. deployment of Collocated Plume Profiling Towers at Roadside Location.**

### **Siting Concerns**

In the case of OTM 32, the contract under which the sampling occurs may dictate a specific location. If this is not the case, the method outlines recommended site selection criteria in Section 8.2, which are summarized as follows:

- The sampling area should be flat, open terrain where:
  - The height of the nearest downwind obstruction is less than the distance from the obstruction to the sampler.
  - The height of the nearest upwind obstruction is less than one-third the distance from the obstruction to the sampler.
- The site should be at least 15 meters from the upwind edge of the source and at least 10 meters from the downwind edge of the source.
- For mobile sources treated as a line source, the mean wind direction should be a 0 to 45-degree angle from a line drawn perpendicular to the source at the time of sampling.

- Average wind speed should be greater than 3 mph at the time of sampling.
- Adequate source activity, i.e., traffic, should be present at the time of sampling to provide sufficient pollutant (PM) mass for sampling.
- To prevent interference from PM emissions due to vehicle exhaust, the road grade should be near zero.

OTM 32 recommends the use of a portable weather station to assess wind conditions at the sampling location at the time of sampling. The guidance provided in Volume IV of EPA’s QA Handbook series<sup>4</sup> should be followed when collecting meteorological data for flux emissions calculations.

**Strengths and Limitations**

Table 3.32 summarizes the strengths and limitations of OTM 32.

**Table 3.32 Strengths and Limitations of the OTM 32 Approach**

| Strengths   | Limitations   |
|---|---|
| Cost effective for determining PM emissions factors when used in conjunction with other test methods. | Potential interferences due to upwind pollutant (PM) concentrations.                      |
| Sampling array set up allows for the entire plume to be characterized.                                | Specific meteorological conditions are required for sampling.                             |
| OTM 32 isolates a single emission source in ambient conditions to provide accurate emissions factors. | Accuracy of testing results is highly dependent on wind conditions during sample periods. |
| Does not require interference of traffic patterns.  |   |
| Direct measurements do not utilize generalized atmospheric dispersion models to estimate results.     |   |

## **References**

1. U.S. EPA. 2013. Other Test Method – 32: Determination of Emissions from Open Sources by Plume Profiling. June 2013.
2. Cowherd, C., Jr., K. Axetell, Jr., C. M. (Guenther) Maxwell, and G. A. Jutze. 1974. "Development of Emission Factors for Fugitive Dust Sources," EPA Publication EPA-450/3-74/037, NTIS Publication PB-238 262, June 1974.
3. Cowherd, C., Jr., Donaldson, J. Kies, R., and Murowchick, P. 2008. "Field Study of Emissions from Haul Roads." Prepared for the Iron Mining Association of Minnesota, Duluth MN, October 30, 2008.
4. U.S. EPA. 2008. "Quality Assurance Handbook for Air Pollution Measurement Systems, Volume IV: Meteorological Measurements Version 2.0 (Final)." EPA-454/B-08-002. March 2008.



### ***3.12 Method to Quantify Road Dust Particulate Matter from Paved and Unpaved Roads – Other Test Method 34***

#### **General Description of Approach**

Other Test Method 34 (OTM 34)<sup>1</sup> is a mobile monitoring method used to quantify road dust particulate matter (PM) emissions from vehicles travelling on paved and unpaved roads. Although this method can be applied to any particulate size fraction in principal, this method specifically quantifies emissions for PM<sub>2.5</sub> (PM less than 2.5 microns) and PM<sub>10</sub> (PM less than 10 microns.) To accurately quantify emissions, OTM 34 relies on an increase of PM emissions from background levels caused by the interaction of vehicle tires with the road surface. Measurements are collected at one or more locations along a stretch of paved or unpaved road at least 100 meters long.

PM emissions are created primarily by the aerodynamic and mechanical suspension of roadway particles caused by the interaction of vehicle tires with the road surface. Roadway particles include loose, erodible soil, dust from brake or tire wear, and dust from erosion of the road surface (i.e., asphalt or cement.) As road dust PM is suspended, a PM plume disperses behind each tire and in the wake of the vehicle. The test method quantifies the increase of PM above ambient conditions at a known travel speed and fixed distance from the PM source. Background or ambient PM emissions are measured at a location not influenced by the test vehicle's own emission plume, such as the hood of the vehicle. Application of this test method relies on four key assumptions:

1. The speed of the vehicle determines the degree to which the emission plume disperses behind the vehicle tires;
2. The degree of plume dispersion is not measurably affected by other vehicles on the road, the magnitude of PM emissions, or the mechanism of PM emissions;
3. PM emissions are solely the result of the interaction of vehicle tires with the road and the contribution of PM from turbulence created by the vehicle is negligible; and
4. The additional PM created by a vehicle other than the test vehicle is either small or can be accounted for through known mathematical relationships.

Beginning in 1999, two concurrent mobile monitoring methods were tested for the measurement of road dust emissions. One, Fitz<sup>2</sup>, estimated the profile of the dust plume in the wake of the vehicle while the other, Kuhns et al<sup>3</sup>, measured PM concentrations directly behind the vehicle's front tire and related those concentrations to emission factors determined as prescribed in the US EPA AP-42

Guidance document (4<sup>th</sup> edition.)<sup>4</sup> The latter study that found that for the same roadway, PM emissions behind a vehicle tire increase exponentially with vehicle speed. The relationship between road speed and PM emissions is described in the following equation:

$$EF_{PS} = MSC_{i,v,ps} \times K_i(v)$$

Where:

$EF_{PS}$  = Emission factor of PM road dust (g/km)

$MSC_{i,v,ps}$  = Measured PM concentration

$K_i$  = Constant specific to the mobile monitoring system

$v$  = Travel speed

In addition to determining emission factors for roadways of interest, measurements yielded by OTM 34 can be used to provide insight on what types of road conditions yield the highest PM measurements, as well as evaluate the effectiveness of dust control techniques currently in use like chemical treatments.

### **Instrumentation**

The mobile measurement system must provide PM concentrations with a high time resolution, on the order of seconds or less. Typically, this requires the use of PM monitors that estimate mass concentrations based on the light scattering properties of aerosols such as PM. OTM 34 specifically mentions the DustTrak 3563 nephelometer, however this instrument has been discontinued. The manufacturer, TSI, Inc., has introduced a newer product called the DustTrak Aerosol Monitor (<http://www.tsi.com/environmental-dusttrak-aerosol-monitor/>, models 8540 and 8543), both of which measure PM at various size fractions. However, any similar monitor that can provide sufficient time-resolved PM concentration data may be used.

PM monitors may also be equipped with a cut device or size-selective inlet (SSI) that allows for the measurement of a specific fraction of PM, such as PM<sub>10</sub>. Although manufacturer-specific SSI devices

do not typically meet National Ambient Air Quality Standard (NAAQS) compliance requirements for PM monitoring, the widely-used SSI option is considered acceptable for compliance provided the nominal cut size is within 5 percent of the size fraction being measured and the size cut characteristics of the SSI are documented.<sup>1</sup> In the case that a manufacturer-provided SSI is not sufficient per project requirements, another option is to subject the entire sample flow within the sample inlet to an SSI, such as a cyclone for PM<sub>2.5</sub>. This second option proves more difficult for PM<sub>10</sub> measurements, as the SSI for this size tend to be larger and may not fit well behind the test vehicle's tires.

Other common equipment needed for the mobile monitoring system includes pumps or blowers to pull sample air through the inlet lines. Flow meters such as pitot tubes are required to measure the air flow through the sample inlet.

Due to logistical and safety reasons, the PM monitor typically cannot be installed in the ideal location (behind the tire) on a test vehicle to measure PM emissions, therefore, a sample inlet line is used to channel sample air into the PM monitor. One common configuration is to install the sample inlet directly behind the front tire, as shown in Figure 3.56.<sup>1</sup> With this configuration, particle sampling loss and size biases are small because there is little difference between the air speed just outside the sample collection point and the air speed through the inlet. Typically, one sample inlet will be installed behind the left front tire and another behind the right front tire with both lines measured independently.



**Figure 3-56: Sample inlet installation behind the front tire.**

Another common sampling configuration is to install the measurement instruments and sample inlet line on a trailer that is pulled behind the test vehicle, as shown in Figure 3-57.<sup>1</sup>



**Figure 3.57. Sample inlet installation on a trailer pulled behind the test vehicle.**

The assumption is that PM emissions from both the left and right tires will affect the sampler simultaneously. Regardless of the instrumentation set up, there are several requirements that must be met to minimize particle loss between the inlet and the measurement instruments. These requirements are discussed in detail in Section 6.1.1 of OTM 34.

Because vehicle location and speed are critical to OTM 34, a global positioning system (GPS) capable of providing high time-resolved data should be used in conjunction with the test method. Because measurement collection is automated, a datalogger such as a laptop is required to collect the data provided by the various instrumentation. A laptop is ideal because the data can be viewed real-time so adjustments to the instrumentation can be made as needed. While not required to perform OTM 34, Geographical Information System (GIS) software is a useful tool to map the travel route, select subsets of data, and examine spatial trends.

### **Calibration**

To quantify the coefficient  $K_i(v)$  in the equation above, the mobile monitoring system must be calibrated against an external standard. The likely optical-based mobile monitoring system is related to PM horizontal flux measurements determined by mass-based instruments using a method such as OTM 32<sup>5</sup>, "Determination of Emissions from Open Sources by Plume Profiling." Calibration should occur under conditions like those expected during the mobile monitoring effort, especially the range of expected vehicle travel speeds.

The calibration procedure requires that the horizontal flux of PM is measured perpendicular to the road segment of interest, at points both upwind and downwind of the site. PM is measured at varying heights above ground level simultaneously with wind speed and direction. The values are combined to quantify the rate at which PM is added to the atmosphere by vehicular travel along the road segment. It is assumed for the purposes of this method that the road itself represents a homogenous emission source, therefore small variations in wind direction are insignificant to results. For more information about this method, see Section 3.11 of this document.

It is important to note that if no calibration data are available, mobile monitoring data collected using OTM 34 are still valuable for determining the ratio of PM emitted by different road segments, which is useful for determining the effectiveness of road dust mitigation efforts. Calibration is required, however, if absolute emissions data are required.

### **Data Collection**

Prior to testing, all PM monitors and flow measurement instruments should be calibrated according to manufacturer recommendations, or shown to have been cleaned, serviced, and recalibrated within one year (12 months) of the test. Sample lines should be inspected and cleaned as needed. The flow through the sample lines should be verified with an independent flow measurement device to ensure any pitot tubes in the sample line are measuring accurately. Field personnel should log all repair, calibration, and replacement information for the mobile monitoring system in a maintenance log that is kept in a field notebook that resides in the test vehicle. An example pre-test preparation checklist is provided in Appendix A of OTM 34. Please follow this Internet link:

<https://www3.epa.gov/ttnemc01/prelim/otm34.pdf>.

Once the mobile monitoring system is set up and fully functional, the measurement collection process is automated. All data are uploaded to two separate data storage locations for redundancy. Data files should be checked to ensure the time stamps for the first and last data points collected match the duration of the measurement effort. Any discrepancies should be noted in the field notebook.

### **Data Analysis**

Once data have been collected and stored, data analysis begins. OTM 34 outlines eight steps that are needed for appropriate data analysis. For more details about each of these steps, refer to Section 10 of OTM 34.

1. Review One-Second Raw Data Records: Review raw data for missing information and invalidate or remove data as discussed later in Section 3.12.3.
2. Calculate One-Second Net Raw PM Concentrations: Subtract the background PM concentrations from the measured PM concentrations collected at the same time.

3. Apply Time Delay Correction to Raw Data Records: Apply the time delay created by the movement from the sample inlet to the sampler to the data so that events recorded by the GPS can be accurately correlated with the correct PM measurements.
4. Apply GPS-based Validity Criteria: Exclude measurement periods where GPS data indicate a quality assurance issue in the sample data (see Section 3.12.3 for more information.)
5. Apply PM Mass/Optical Correction: If a filter-based method for measuring PM was performed in parallel with the mobile measurement study, the ratio of the two measurements should be applied to all raw signals calculated using step 2.
6. Calculate Emission Factors: Calculate the PM emission factors on a one-second basis using the equation above.
7. Calculate Road Segment-Average Emission Factors: Associate each data point with a road segment and calculate average emission factors.
8. Tabulate Results: Collect road segment emission factors in a spreadsheet or database for further review. It is also possible to use GIS software to illustrate this information.

### **Verification/Validation Studies**

#### **Clark County, Nevada**

In February 2005, road dust emission factors were measured on a 100-mile stretch of road in Clark County, NV.<sup>6</sup> Over four consecutive days, the same measurement route was completed using the Testing Re-entrained Aerosol Kinetic Emissions from Roads (TRAKER) mobile monitoring system. At the time measurements were collected, the TRAKER system was not calibrated. However, a larger study called the Clark County Stage IV study<sup>7</sup> was performed in 2006 that provided a calibration scheme that was retroactively applied to the data collected in 2005.

During the latter study, the calibration values were determined via the plume profiling method used during the Clark County Stage IV study. The profiling method used a tower equipped with five nephelometer-style PM<sub>10</sub> monitors at five different heights above the ground on the downwind side of the road. The data collected were then mass-corrected by comparing the values collected by a nephelometer and filter-based monitor when the same road dust material was suspended in the laboratory. The horizontal flux was then calculated by numerical integration. After examination of the data generated during Clark County Stage IV, it was determined that the ratio of the calculated emission factor to the raw measurement data collected by the mobile monitoring system was not

dependent upon the speed of the test vehicle. This means the value for  $K_i$ , shown in the above equation, is constant with speed.

The value for  $K_i$  determined during the Clark County Stage IV study was then retroactively applied to the measurement data collected during the Clark County study performed in February 2005. At the same times, silt loading measurements were performed in accordance with USEPA AP-42, 5<sup>th</sup> Edition.<sup>8</sup> Although the entire 100-mile measurement route was executed in three to four hours, it took the same amount of time to perform the silt loading measurements for each site.

Because the same measurement route was monitored four consecutive days, the repeatability of the TRAKER mobile monitoring system could be determined. Using the assumption that road dust emissions were constant over the four days of monitoring, the study showed that the average coefficient of variation (COV, a measurement of uncertainty) decreased as the test vehicle travel speed increased, as shown in Figure 3-58.<sup>1</sup>

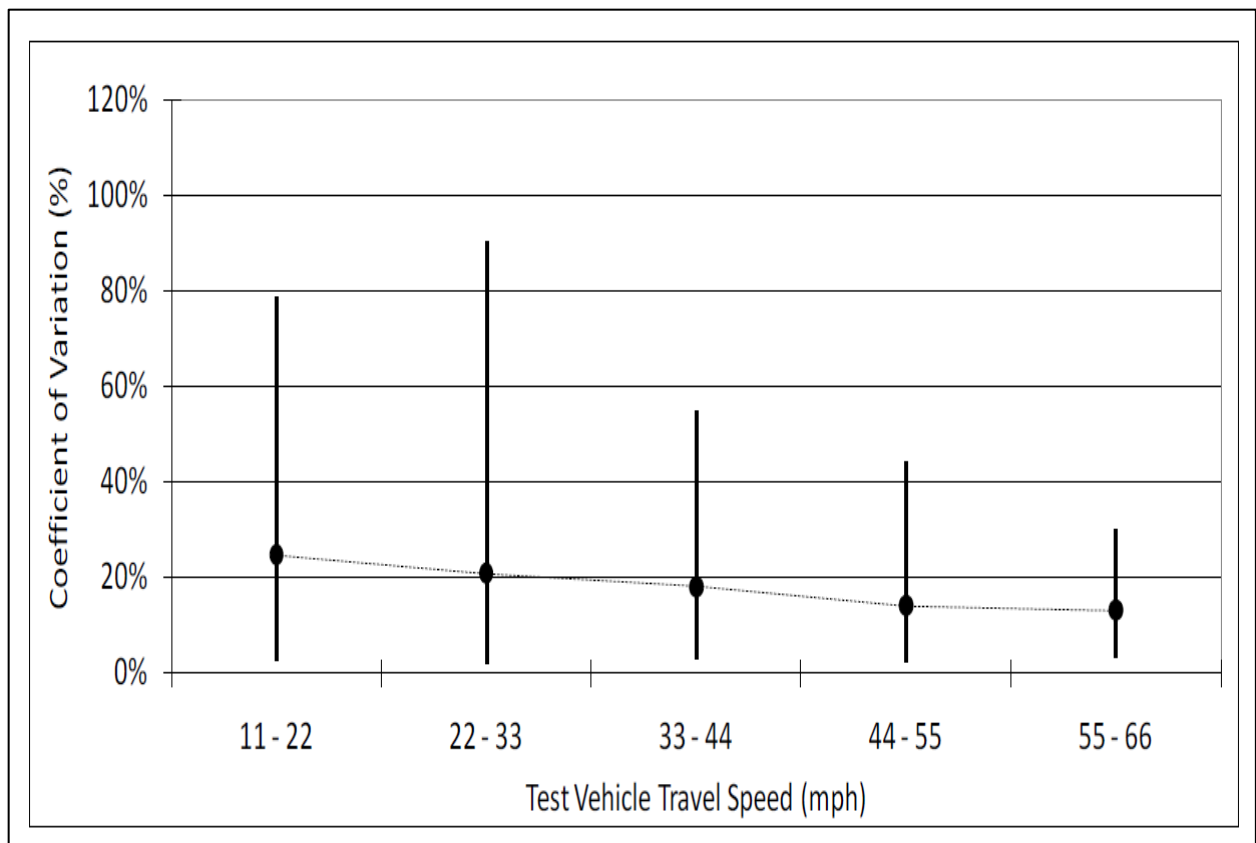


**Figure 3-58 Coefficient of Variation (COV) determined from data collected in Clark County, NV in February 2005.**



### **Typical QA/QC**

Several types of quality assurance and quality control methods are utilized in OTM 34 to ensure accurate measurements and sample traceability.

### **Screening Criteria**

Due to the variable nature of driving a test route, it may be necessary to screen, or eliminate, data associated with events not related to goals of the monitoring effort. OTM 34 recommends that data collected during the following events should be removed from the overall dataset:

- Travel speed is less than 11 miles per hour (mph);
- Acceleration or deceleration is outside of the prescribed range ( $\pm 1.3$  mph);
- The vehicle is performing a turn and the wheel angle is greater than  $3^\circ$  from the vehicle body;
- Exhaust or road dust plume from another vehicle interferes with measurement equipment;
- Corresponding GPS data are invalid;
- Measured concentrations are outside of the instrument's measurement range; and
- Correlating background concentrations indicate interference from other sources of PM.

Depending on the monitoring program, it may also be necessary to screen data collected during events such as the proximity to an intersection or location where excess road debris is present, such as a construction site.

### **Collocation**

The mobile monitoring system used to quantify emissions during testing should be collocated with a second identical mobile monitoring system, or other system that measures the same quantities with the same or better precision and bias. When the data are reviewed, PM concentration data changes should be recorded by both instruments within similar time periods. The data collected from each of the two systems correlate well when a regression line fit between two instruments of the same PM fraction yields a slope ranging from 0.8 to 1.2 for a dataset of 100 or more points.

Likewise, it is beneficial to compare concentration measurements collected from the left and right sides of the vehicle in mobile monitoring systems where the sample inlets are installed behind the front wheels. In general, PM concentrations from both sides of the vehicle will rise and fall at the same time. It is important to note that there may be periods where PM concentrations between the two sides of the vehicle are very different because the lane of a road is not considered homogenous.

**Siting Concerns**

The role of the testing operator is to drive a route within the road network of interest, ensuring that the route driven is consistent with the goal of the monitoring effort. Considerations when designing a measurement route include types of roads, type of activity studied, and time of year.

**Strengths and Limitations**

Table 3.33 summarizes the strengths and limitations of OTM 34.

**Table 3.32. Strengths and Limitations of the OTM 34 Approach**

| Strengths  | Limitations   |
|--|---|
| Dust emissions can be measured over many miles of roadway, allowing many measurements over a roadway network.  | Exhaust from nearby vehicles may result in higher PM concentrations than can be caused by road dust emissions.      |
| Many miles of roadway can be monitored in the time it takes to plan, set-up, and take measurements at a single site using stationary road dust monitoring methods. | Measurement data must be calibrated against an external standard.   |
| Meteorological data collection is not necessary, unlike stationary monitoring methods.   | Wet roadway conditions can cause erroneous estimates of PM emissions.   |
|  | Extensive maintenance and repair of PM measurement instruments may be required if allowed to get significantly wet. |

## References

1. U.S. EPA. Other Test Method – 34: Method to Quantify Road Dust Particulate Matter Emissions (PM10 and/or PM2.5) from Vehicular Travel on Paved and Unpaved Roads. January 2014.
2. Fitz, D.R. (2001) Measurements on PM10 and PM2.5 Emission Factors from Paved Roads in California. Final Report to the California Air Resources Board under Contract No 98-723, June 2001.
3. Kuhns, H., Etyemezian, V., Landwehr, D., MacDougall, C., Pitchford, M., and M. Green. (2001). Testing Reentrained Aerosol Kinetic Emissions from Roads (TRAKER): A New Approach to Infer Silt Loading on Roadways. *Atm. Env.* 35: 2815-2825.
4. U.S. EPA, 1993. Emission factor documentation for AP-42 4th edition, Section 13.2.1: Paved Roads. Report prepared for U.S. EPA, March 8, 1993 by Midwest Research Institute, 425 Volker Boulevard Kansas City, Missouri 64110-2299 USA.
5. U.S. EPA. Other Test Method – 32: Determination of Emissions from Open Sources by Plume Profiling. June 2013.
6. Etyemezian, V., H. Kuhns, and G. Nikolich (2005). The Las Vegas Road Dust Emissions Technology Assessment, Phase II: Final Report. Prepared for the Clark County Department of Air Quality and Environmental Management, Las Vegas, NV. July, 2005.
7. Langston, R., R.S. Merle Jr., V. Etyemezian, H. Kuhns, J. Gillies, D. Zhu, D. Fitz, K. Bumiller, D.E. James, and H. Teng (2008). Clark County (Nevada) Paved Road Dust Emission Studies in Support of Mobile Monitoring Technologies: Final Report, 122 pages.
8. U.S. EPA (1999). Compilation of Air Pollutant Emission Factors - Vol. I, Stationary Point and Area Sources. Report No. AP-42, 5th ed. U.S. Environmental Protection Agency, Office of Air Quality Planning and Standards, Research Triangle Park, NC.

## 4.0 Meteorological Measurements

Meteorological conditions at the site of optical remote measurements are an important component of many of the applications. Please note that in-depth description of meteorological measurements information can be found in Volume IV of EPA's QA Handbook series.<sup>1</sup> Quality of the meteorological parameters measurements is as important as the quality of the optical remote sensing results used in emissions flux calculations. The quality of meteorological parameters measurements includes topics such as:

- Meteorological tower siting and setup,
- Wind speed (horizontal and vertical) and direction,
- Relative humidity and dew point,
- Temperature,
- Solar radiation and
- Atmospheric pressure.

Historical meteorological parameters measurements are important to the applications of measurements because emission rates from open sources are affected by ambient conditions (e.g., high wind speed over the source can increase the emission rate). If the data are intended to evaluate exposure or determine emissions factors, the ultimate use of the measurements should include evaluation of how well the meteorological conditions encountered during the test compare to the annual average meteorological conditions for the sampling site. Ideally, the test report summary includes data or commentary that addresses the representativeness of the meteorological conditions. The meteorological conditions recorded during the test can be compared to the historical trends for a site. If site-specific meteorological measurements are not available, current local conditions can be compared to the average statistics available from the nearest National Weather Service (NWS) monitoring station. If there is more than one NWS station

near the measurement site, then the comparison should be made against the average measurement of the NWS stations.

Wind stability is often important to measurements and refers to atmospheric turbulence. Atmospheric stability or turbulence is the vertical and horizontal transportation of an air mass. Atmospheric turbulence is the collective differences between small-scale air motions driven by winds that vary in speed and directions for a given parcel of air. Measurements that lead to wind stability account for convection, diffusion, buoyancy, rapid variation of pressure and wind velocity. Turbulence is responsible for mixing the atmosphere and is what distributes water vapor, particulate matter and gases.

However, one does not measure or calculate turbulence directly to assess atmospheric turbulence; instead we examine the atmospheric stability and the potential for vertical and horizontal transport, as well as mixing while in transport. Vertical and horizontal transport is normally associated with atmospheric stability (although it is important to note that wind speed will play a major role in the horizontal plane).<sup>2,3,4</sup>

A practical use for “wind stability” or turbulence for ORS measurements is to examine atmospheric stability and assess the atmosphere’s potential to mix and transport (vertically and horizontally). Another concept that is associated with “wind stability” is surface roughness as it relates to topographical and landscape variability. Determining if one is under stable or unstable atmospheric conditions is an important step in evaluating when conditions are appropriate for sampling, depending on the objectives of the measurement application. For example, the combination of vertical and horizontal wind speed and direction with solar radiation can be used to determine the atmospheric stability class of the air parcel by stability categories.<sup>5</sup> These stability categories can be used as a quality indicator for representative ORS measurements.

#### ***4.1 Meteorological Station Siting***

Typically, the terrain associated with an optical remote monitoring measurement program is complex only to the extent that the local elevation provides an elevated or depressed land area

with sloped sides. A properly located meteorological monitoring station should provide meteorological measurements for an entire facility. For facilities or sites that exceed one square mile in area, an additional meteorological monitoring station may be required for each additional square mile of area to obtain accurate local meteorological conditions.

The meteorological monitoring station must be positioned at the center of the highest point near the measurement location. Winds blowing across the top of elevated areas and winds down the slopes contribute to transport and dispersion characteristics. By positioning the station at the center and highest land mass near the measurement site (i.e., as determined by Google earth® map elevations), all upwind wind patterns sweeping the source emissions are represented in the wind speed and direction measurements.

Obstructions must also be considered during siting of a meteorological monitoring station. There is no specified distance that the station must be positioned away from the measurement location. By positioning the station at the center of the highest elevation, effect/contribution of the winds blowing over elevated areas are normalized with respect to the direction of the wind to the greatest extent possible.

Meteorological measurement sensors are typically setup or positioned at 2 meters above ground level. The wind/speed direction sensors must be positioned so that they are located no closer than 2 meters from the temperature sensor. Wind direction sensors are oriented to true north using a digital compass. The timers/clocks on the meteorological station and the optical measurement equipment should be synchronized to allow the concentration data and meteorological data to be directly compared to the measurement data during post-processing. If synchronization is not possible, the offsets between the clocks will be recorded at the start and end of data collection of each day to estimate any differences in the clock times or rates.

### **Horizontal Wind Speed and Direction**

Compact weather stations<sup>6</sup> can provide all-in-one measurement of temperature, horizontal wind speed, and horizontal wind direction at optical remote measurement sites. The compact weather

station typically uses 2-D ultrasonic measurement technology for wind speed. For wind direction measurements, the system automatically and continuously self-aligns to magnetic North. Typical units can provide the following performance measurements:

- Wind speed range from 0-50 m/s with an accuracy of  $\pm 0.5$  m/s
- Wind direction range  $0^{\circ}$  -  $360^{\circ}$  with an accuracy of  $\pm 5^{\circ}$

### **Vertical Wind Speed and Lateral Turbulence**

If wind stability is required as an ancillary measurement for the optical remote measurement application, then a 3-D Ultrasonic Anemometer may be necessary. Typical accuracy of this instrument is  $\pm 2$ -degree compass (1 to 30 m/s) or  $\pm 5$  degrees compass (30 to 40 m/s).

### **Relative Humidity**

Relative humidity (RH) is important to measurements because it provides information on water interference and predicting cloud or fog formation which interfere with many techniques. Of the many atmospheric variables describing water vapor content in the atmosphere, RH is the most common for routine monitoring programs. RH is the ratio (percent) of actual vapor pressure of moist air to the saturation vapor pressure at the same temperature. A corollary measure, dew-point temperature (or dew point) is the temperature to which a moist air parcel must be cooled to achieve saturation over water at constant pressure and water vapor content. RH and dew point are measured with electrical hygrometer, chilled mirror, or psychrometric instruments. Typical accuracy of this equipment is  $\pm 0.5\%$  RH.

### **Temperature**

Temperature is important because it determines or controls vertical transport of air which changes portion of the plume measured by the ORS technology. Standard meteorological equipment includes a thermocouple or thermistor temperature sensor with a temperature range -  $50^{\circ}\text{C}$  to  $+50^{\circ}\text{C}$  and an accuracy of  $\pm 0.2^{\circ}\text{C}$ .

### **Net Solar Radiation**

Net Solar Radiometer is required for wind stability determination. The typical accuracy of these units is > 90 percent of the Daily Total Solar Radiation.

### **Atmospheric Pressure**

For air quality and meteorological purposes, atmospheric pressure is generally measured with mercury, aneroid, or electronic barometers. Most, if not all, of the atmospheric pressure sensors available provide analog or serial output that is directly interfaced with a data acquisition system.

A mercury barometer measures the height of a column of mercury that is supported by the atmospheric pressure. It is a standard instrument for many climatological observation stations, but it does not afford automated data recording. An aneroid barometer consists of two circular disks bounding an evacuated volume. As the pressure changes, the disks flex, changing their relative spacing which is sensed by a mechanical or electrical element and transmitted to a transducer. Most electronic barometers of recent design use transducers which transform the sensor response into a pressure-related electrical quantity in the form of either analog or digital signals. Current digital barometer technology employs various levels of redundancy to achieve long-term stability and accuracy of the measurements. One technique is to use three independently operating sensors under centralized microprocessor control. Even higher stability and reliability can be achieved by using three completely independent barometers, incorporating three sets of pressure transducers and microprocessors. Each configuration has automatic temperature compensation from internal-mounted temperature sensors. Triple redundancy ensures excellent long-term stability and measurement accuracy, even in the most demanding applications.<sup>7</sup>

### **Differential Global Positioning for Tracking Monitoring Locations**

Global position information using a high-resolution Differential Global Positioning System (DGPS) is required for mobile tracer correlation optical measurements and temporary stationary



measurement locations.<sup>8</sup> Global position high resolution accuracy of <0.6 meters will meet most application requirements. The DGPS data collection includes a time stamped data stream acquired in real time. The DGPS clock should be synchronized with the measurement system clock to simplify measurement location and concentration information.

In the field coordinates measured by the DGPS, unit results should be compared to known Google Earth<sup>®</sup> coordinates for known geodetic marks as a quality check of the location system.

### **Collection of Process Information**

Process information is site-specific data on factors or activities that affect the production or release of pollutants to be measured. Process parameters are measured indicators of process performance such as duct flow, operation temperature, or fuel use. The measurement of emissions rate, also called emission flux, may be extended beyond mass per unit air volume to determining emissions factors when the flux can be related to activity factors of the source.

Emission flux is often converted into an emission factor to estimate air pollutant emissions from a process or activity (e.g., fuel combustion, chemical production). The simplest form of an emission factor is an expression of the mass of pollutant emitted per unit of activity generating the pollutant (e.g., pounds of particulate matter emitted per ton of coal burned). Typically, emission factors for stationary point sources are developed by dividing the source's emission rate by an appropriate parameter (e.g., number of widgets made per hour) that represents the activity responsible for generating the emissions. Therefore, gathering process information related to production, chemical use, energy use, heat or power generation is important to assess the relative rates of pollution produced by a stationary source. Once process information is available, ORS flux measurements of open source activity can yield meaningful emission factors.

In developing emission factors for point sources, identification of the underlying activity that generates the emissions is typically straightforward. For example, particulate matter emissions from fuel combustion are a direct function of the type and amount of fuel burned. However, for open sources (e.g., landfills) the pollutant generation and emission release mechanisms tend to be

more complex. This complexity can make the selection of appropriate underlying activity, emission precursor, or process parameter(s) for use as an emissions surrogate more difficult than for point sources. Consequently, emission factor developers should have a thorough understanding of the pollutant generation and emission release mechanisms for a given open source to accurately interpret the results from the ORS test and to properly apply the ORS data for emission factor development.

One strength of the techniques in this Handbook is measurement of fugitive emissions from open sources such as landfills, wastewater treatment systems, agriculture operations, and equipment leaks at petrochemical and industrial facilities. At landfills, wastewater treatment systems, and animal agriculture operations, fugitive emissions are generated by biological decay of organic matter present in the waste. The rate of biological activity is affected by ambient conditions (e.g., bioactivity increases with increasing temperature) and process parameters such as chemical conditions (pH, reduction/oxidation potential) in the waste. Pollutant emissions are also affected by site-specific parameters such as the process information on the configuration of the source and the process steps involved in handling and disposing of the waste. At petrochemical and industrial facilities, fugitive emissions from equipment leaks are a function of process information such as the type of equipment; the number of equipment components; the concentration and vapor pressure of pollutants in the in-service gas; and process parameters such as temperature and pressure. The complex transport and diffusion mechanisms, and the chemical/biological reactions inherent in certain types of open sources, mean that the emissions from the open source may not be easily related to an industrial process or activity. For example, an industrial process generates a liquid waste stream that is discharged to an open wastewater treatment system. Although the pollutant loading to the treatment system may be relatively constant over time, the emissions from the system may not consistently track the loading rate due to changes in the rate of pollutant formation caused by increases/decreases in process parameters of the treatment system such as temperature.

The output ultimately obtained from a test is an emission rate in terms of mass of pollutant

emitted per unit of time. For point sources, the activity typically selected for emission factor development has a time component such that the use of the activity in the denominator of the factor cancels out the time units of the measured emission rate. For example, the use of a boiler's fuel feed rate (Mg coal/hr) as the activity converts the measured emission rate (g pollutant emitted/hr) into an emission factor in terms of g pollutant emitted/Mg of coal fired. The activity data selected for use in development of an emission factor based upon measurements may or may not have a time component.

Simple emission factors for a specific site can be developed using the emission rate measured by one of several of the technologies described in Chapter 2 and a characteristic activity factor related to the emissions factor of interest. However, the source characteristic is not necessarily a simple time-dependent activity independent of the site. The addition of site-specific or process-specific information improves emissions factors estimates. For example, a simple emission factor (kg of pollutant/ft<sup>2</sup> of landfill surface area) could be developed using test data and the surface area of the landfill. However, because landfill fugitive emissions are also dependent on the type of cover and gas collection system (if applicable), the type of material contained in the landfill, the retention time of the material, and the size and number of landfill cells, the applicability of the simple emission factor to other landfills based solely upon surface area would be limited. A more refined landfill emission factor (e.g., in terms of mass of pollutant emitted/mass of pollutant generated) could be developed using the measured emission rate and an estimated pollutant generation rate, such as one calculated from the site specific biological decay model discussed in Section 2.4.4.1 (Municipal Solid Waste Landfills) of EPA's AP-42, as the activity. This refinement (i.e., emission factor) would be an intermediate estimate and more site-specific than the simple factor, yet less specific than uniquely measuring the emissions flux for every landfill of interest. The additional value of the process parameters necessary to utilize the decay model (e.g., pollutant generation potential of the waste, time since initial waste placement in the landfill) is less costly than multiple field sampling episodes at different landfills.

### **Attribution of Emissions to Source of Intent**

Results from an ORS sampling episode can be used in a dispersion modeling analysis conducted in reverse. In dispersion modeling for point sources, the emission rate from the source is known and the concentrations at receptor points downwind of the source are estimated based on the release characteristics of the source (e.g., stack height, exit velocity, gas temperature) and the meteorological data (e.g., wind speed and atmospheric stability parameters) used in the modeling analysis. In ORS sampling, the sampling path or plane effectively serves as a downwind receptor and the emission rate from the open source is back-calculated based upon measured downwind concentrations and the wind speed and atmospheric stability data measured during the test. Consequently, the open source emission rate is directly dependent upon the ambient conditions encountered during the test.

The emission rates determined using ORS techniques can also be affected by background pollutant concentrations in the atmosphere surrounding the open source, and by how well the placement of the instrumentation (e.g., transmitters, receivers, retro-reflectors) captures the area source emissions. Consequently, data users should determine whether background concentrations were accounted for in the measurements. Typically, background emissions are determined by measuring pollutant concentrations in sampling paths or planes located upwind of the emission source and subtracting those concentrations from the concentration values measured at the downwind locations. For assessing the effectiveness of the instruments to capture the source emissions, the developer should review the placement of the instrumentation, and any assumptions made regarding the prevalent wind direction, relative to the emission source to be measured. The technique could be applied properly, but the configuration of the sampling equipment relative to the emission source and the prevailing wind direction may not adequately capture the source emission plume under varying meteorological conditions.

### ***4.2 References***

1. Quality Assurance Handbook for Air Pollution Measurement Systems, Volume IV: Meteorological Measurements Version 2.0 (Final), EPA-454/B-08-002 March 2008.

2. Daniel J. Jacob, Introduction to atmospheric chemistry, Princeton University Press, 1999.
3. John M. Wallace and Peter V. Hobbs, Atmospheric Science an introductory survey, Academic Press, 1977.
4. David G. Andrews, An introduction to atmospheric physics, Cambridge University Press, 2000.
5. EPA 2000. Meteorological Monitoring Guidance for Regulatory Modeling Applications, EPA-454/R-99-005.
6. A Climatronics Corporation AIO compact weather station A 2-D Ultrasonic Anemometer (AIO Compact Weather Station, Model 102780, Climatronics, Bohemia, NY).
7. World Meteorological Organization. Guide to meteorological instruments and methods of observation; Draft seventh edition ed.; Secretariat of the World Meteorological Organization; Geneva, Switzerland, 2006.
8. DGPS, Cressent R100 Series, Hemisphere GPS, Calgary, AB, Canada.

## 5.0 Data Validation and Verification

This section provides information on validation and verification of remote optical measurements starting from field observation through test report review. The emphasis in this section is how an optical technology report recipient can evaluate and verify the quality of the reported data. Information is provided on how data quality indicators can be used to assess and verify optical monitoring data in the most general way.

Data review, verification, and validation are techniques used to accept, reject, or qualify data in an objective and consistent manner. Verification can be defined as the process of evaluating the completeness, correctness and conformance of a specific data set against the data quality requirements.<sup>1</sup> Verification can be done by examination and objective evidence that the final data meets specified QC recommendations or requirements and fulfills the data users' requirements.

Validation can be defined as a confirmation by examination and objective evidence that the recommendations for a specific intended use are fulfilled. The criteria for deciding the degree to which each data item has met its quality specifications should be described in an organization's site specific QAPP. The QAPP should clearly indicate the plan to meet the end user's DQO. The DQO process was described in Chapter 1 Section 1.4.

This data validation and verification section describes the techniques used to make assessments of the application of remote optical air methods to field measurements. In general, the initial assessment activities are performed both by persons implementing the environmental data operations and by personnel "independent" of the operation, such as post test data reviewers and the organization's QA personnel. The procedures, designated personnel, and frequency of assessment should be included in an organization's QAPP. These activities should occur prior to submitting the final data report and before they are used in models or emissions factors development. Field testers should verify results from a field test program before data users validate measurement results and use them to make decisions.

## **5.1 General Approach**

Specific QC specifications for each optical technique are provided in the individual technology or applications sections in Chapters 2 and 3. The general information in this section can be used for most optical remote measurement projects. How closely a measurement represents the actual environment at a given time and location is a complex issue that must be considered during development of the sampling design. Testers check (verify) each measurement for conformity to the specifications, including type and location (spatial and temporal). Modelers and other secondary data users should compare project quality specifications to their data needs and determine (validate) if the optical remote measurement data is useful for their purpose. By noting the deviations in sufficient detail, modelers and secondary data users will be able to determine the data's usability for scenarios different from those included in project planning.

Remote sensing methodology and meteorological data are often linked. Pollution enters the atmosphere directly, or is formed by chemical reactions in the atmosphere, or it is the result of a process. Photochemical pollutants, such as O<sub>3</sub> and sulfates, are generally produced over a period of time. Ozone forms by the interaction of VOCs and NO<sub>x</sub> under the right meteorological conditions when low wind speeds, variable wind directions, and relatively high temperatures are present. Other pollutants are generated by point, mobile, and area sources. Winds, a meteorological variable, can transport pollutants from their sources to affect populated areas.

## **5.2 Data Validation Methods**

Therefore, if possible, meteorological data should be verified and validated at the same time as remote sensing data, not separately. Figure 5-1 is an illustration of a typical verification and validation process. The left column shows the "levels of data review." These levels of data are described in this Section. The right column illustrates the type of verification or validation that usually occurs during the process. The numbers in parentheses reference the section numbers in this document that provide additional details on the data review process at each step in the hierarchy.

### Levels of Data Quality Review

Generally, there are four “levels” of air quality measurements data review. These levels are similar to those defined by Mueller and Watson<sup>2</sup> and Watson et. al.<sup>3</sup> When a data set has undergone each level of review, it passes on to the next level. The entire process is used to determine the validity of the data.

Level 0 verification includes raw calibration data and initial setup observation prior to collecting field data. Testing staff should report results of manufacturer calibration and verification that they perform prior to a field campaign. These data can include background and noise measurements made to establish a baseline for sensitivity of the measurements. Level 0 verification also includes field observation of the equipment setup and function. At this level, the data may be reduced and possibly reformatted, but are unedited and un-reviewed. These data have not been adjusted for known biases due to interfering components in the air at the test site or other problems that may have been identified during field maintenance checks or audits. These observations and data may be used to monitor instrument operations during the measurement episode but should not be used for regulatory purposes. Section 5.2 provides more details on this level of validation.

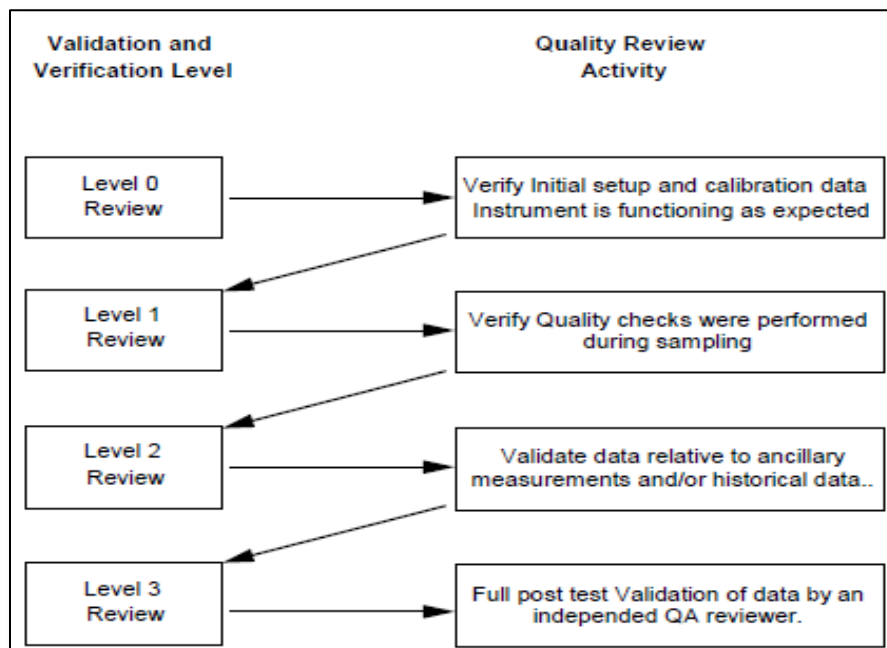


**Figure 5-1. Generalized Data Verification and Validation Process Flow**



- Level 1 data verification involves quantitative and qualitative reviews for accuracy, completeness, and internal consistency. Quantitative checks are performed by instrument software screening programs, and qualitative checks are performed by field staff who manually review the data for outliers and problems. Quality control flags are assigned, as necessary, to indicate the data quality. Data are only considered verified at Level 1 after final QC checks have been completed and any adjustments, changes, or modifications to the data have been made. Section 5.2.2 provides more details on this level of data validation.
- Level 2 data validation involves comparisons with independent data sets. This function includes, for example, making comparisons to other simultaneous emissions measurements or historical data on the source emissions.
- Level 3 data validation involves a more detailed analysis and final screening of the data. The purpose of the final step is to ensure that there are no inconsistencies among the primary optical data and related data (such as meteorological measurements). The reviewer examines the overall consistency of the data and the consistency of related data (i.e., checking emissions patterns against time of day or wind speed and wind direction).

### ***5.3 Data Verification Methods***

Data verification is defined as the confirmation by examination and objective evidence that specified quality requirements have been fulfilled according to the standard procedure for the method. This verification contributes to the confidence that the data will be valid for the original decision or purpose of the data collection. These recommendations should be included in the organization's QAPP as part of the method quality indicators. The data verification process involves two basic steps: visual inspection and analysis and verification performed by data review. Both techniques are needed to verify optical measurements data. Each is described in the following sections.

### Visual Data Verification

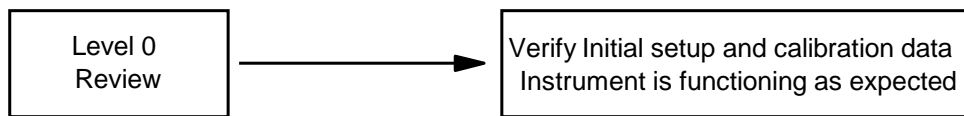


**Figure 5-2. Level 0 Verification Checks the Most Fundamental Quality Requirements**

The monitors and equipment used for remote sensing rely upon a radiation source (UV, visible, or IR) and a detector used together to identify and quantify the levels of certain chemicals in the atmosphere. These monitors are typically used in a continuous monitoring mode and monitor one or several compounds simultaneously. Although the overall design requirements for the different spectral ranges are significantly different, the basic components of these technologies are similar. In general, these monitors contain at least the following components:

- Radiation source
- Optics
- Detector
- Data processing algorithms

The radiation sources for these technologies belong to one of three distinct groups. The monitors operating in the UV region of the spectrum use a continuous or non-continuous lamp that provides broad-band radiation in the UV and visible regions. The monitors, using TDL technology, use a laser to provide radiation over a very narrow spectral range in the near-IR. That spectral range can be tuned over a small range with a single TDL and is selectable over a wider range using multiple TDLs. The FTIR monitors use a broadband IR source. Passive technologies such as IR cameras and Passive FTIR measure natural IR radiance from the compounds being measured. The optical components of these monitors typically are used to guide the radiation from the source, through the atmospheric path to be monitored, to the detector. The detectors and configurations for these monitors vary according to specific applications. They are typically chosen to maximize signal-to-

noise ratio for the spectral region and operating temperature.<sup>4</sup>

Level 0 verification includes review of calibration of instruments and equipment. Periodic calibration and/or calibration checks must meet MQOs identified in project QAPPs. Typical MQOs are listed Chapter 2 for each measurement technology. Calibration data should be reviewed by field test staff and data validation staff. The following questions should be answered:

- Were the calibrations performed within an acceptable time prior to generation of data?
- Were they performed in the proper sequence?
- Were they performed using standards at the conditions expected during field measurements?
- Were acceptable linearity checks and other checks made to ensure that the measurement system was stable when the calibration was performed?

Level 0 verification can also include field inspections to visually verify optical measurement technologies performance during field acquisition of data. Field verification can be technical systems audits (internal or external) or simple inspections by field operators. For example, optical equipment often generates visible light as a direct or indirect result of the measurement process. Field inspection can verify measurement equipment is aimed correctly and operating if reflected visible light is apparent from the optical path. Optical equipment and associated reflectors can gather dust or moisture, and observation of these two interferences can be made visually during field inspection. Several questions might be asked during a visual verification process:

- Is the equipment operational? Verification is performed by observing that the optical equipment is collecting and storing data.
- Was the equipment aimed correctly to make measurements? Verification is performed by observing that the data collected is different from zero or full saturation.

- Part of the verification process is a review of the optical remote data over a period of time. A quick visual inspection may reveal some anomalies that do not match other parameters.

Continuous long term optical measurement verification programs should include documentation of periodic field observations that ensure equipment is operating. Figure 5.3 is an example of a visual observation records. Many environmental samples can be flagged (qualified) during the periodic visual inspections.

|   |
|---|
| <p><b>Weekly Visual Quality Control Check Sheet</b></p> <p>Optical Remote Instruments</p> <p>Site__ Month/Year __ Site Number__ Technician ____ Date: _</p> <p><input type="checkbox"/> System is powered and operating</p> <p><input type="checkbox"/> Source is generating a adequate radiation for measurements</p> <p><input type="checkbox"/> Optical alignment is correct allowing beam detection</p> <p><input type="checkbox"/> Detector is maintained at the proper temperature and generating spectral signal</p> <p><input type="checkbox"/> Calibration, span, zero checks are performed as appropriate</p> <p><input type="checkbox"/> Standard Gas mixtures are available if required</p> <p><input type="checkbox"/> System operation includes periodic QC</p> |
| <p>All comments must be noted in the system log.</p> <p>Reviewed by _____ Date _____</p>  |

**Figure 5.3 Example of Optical Remote Measurement Visual Check List**

### **Data Review and Verification**

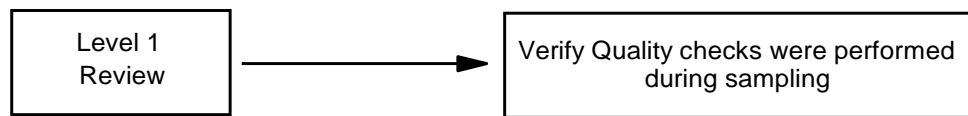


***Figure 5.4 Level 1 Verification Process***

In the late 1990s, optical remote systems were developed with personal computer compatible data collection routines. Many optical remote instruments offer remote access and download of data from systems that are in continuous use. Steps preparatory to data validation should include the daily transfer of raw data (e.g. signal averaged processed data) to a central data processing facility and the transfer of raw data files to create an edited database. The raw data files should be stored separately to insure data integrity. Backup copies of the data should be prepared and maintained on-site and off-site.

For continuous optical remote monitoring systems, data can be processed and QC operations parameters can be evaluated to determine if equipment maintenance is required. These types of verification techniques can be extremely useful because the program can “sense” a change in operating conditions or instrument response and a prediction of the possibility of equipment failure.

Data reviewers should answer some typical questions during their remote download data review such as:

- Did the signal intensity drift or diminish significantly since the last equipment maintenance?
- Did the regular QC check for noise and or calibration exceed acceptable limits?
- Did the optical system trip any electronic limits or indicate data collection failure?
- Does the data fall within the measurement range of the instrument or was the data saturated or zero?

- Does the system have a minimum detectable limit?

### **Validation of Primary and Ancillary Measurements**

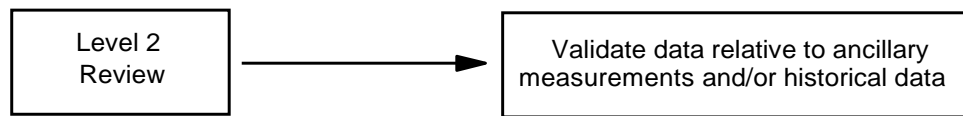


***Figure 5-5 Level 2 Quality Checks Start the Data Validation Process***

Both manual and computer-oriented systems require individual reviews of all data tabulations. As with all environmental measurements, it is necessary to keep accurate records during measurement periods to ensure a complete data collection. A site logbook and calibration sheets should be maintained at the data collection site. The site logbook will include information such as meteorological conditions, path lengths, UV filter numbers, lamp type, light intensities and measurement times. Light intensities must be recorded any time an optical source or receiver is adjusted and compared to the intensities measured when the equipment was installed.

Calibration sheets include the record and results of system calibration checks or audits performed with known concentrations of a target or surrogate analyte.

Initial data verification steps should be performed by the station operator and later by data validation staff. All necessary supporting material, such as audit reports and site logs, should be available for Level 2 validation. Access to daily ancillary measurements such as wind speed, direction, should be provided for use in relating suspect data to local and regional conditions. If measurements are taken down wind of a facility, process information and production schedules are useful to interpret trends or excursions in optical remote data. Questionable data, such as data flagged in an audit, manual review should be corrected or invalidated during Level 2 data validation.

For long-term continuous measurements programs, the data should be reviewed on a regular schedule and at least monthly. For short-term measurements programs, the data should be reviewed by the site operators at the end of each day. Optical measurement instruments typically

include onboard personal computers that allow operators to view and evaluate data visually. Graphs or plots of data or a summary table of data can be evaluated for outliers or obvious data collection failures. Graphing data can be a quick method of visualizing the data relative to other parameters. Graphs can show longer term trends and relationships that are difficult to see when data validation staff are looking at large amounts of tabular data.

The purpose of manual data inspection is to spot unusually high (or low) values (outliers) that might indicate a gross error in the data collection and to verify signal intensity. Manual review of data tabulations also allows detection of uncorrected drift in the zero baseline of an optical sensor. Zero drift may be indicated when the daily minimum values tend to deviate (increase or decrease) from the expected minimum value over a period of several days.

In an automated data processing system, procedures for data validation can be incorporated into the basic software. As noted in Section 5.2.2, the computer can be programmed to scan data for extreme values, outliers, or ranges. These checks can be further refined to account for time of day, time of week, and other cyclic conditions. Questionable data values flagged on the data tabulation may or may not indicate possible errors. The system operator should check all the data flagged by the acquisition system program and investigate whether the data flagged should remain flagged. In some cases, extreme conditions can occur rapidly and the data may reflect real values. For example, if a spill or leak occurs and moves through a measurement area the optical monitor may record high values or extreme interference in the data. The system operator should note such excursions and alert the data validation and reporting staff that these data may reflect real conditions. Data validation in Level 2 evaluates the data completeness and representativeness against the project DQO requirements to ensure sufficient data is collected for data users to draw conclusions or make decisions.

A useful data validation method is to compare the difference between successive data values. Logic dictates that rapid changes in values in a 1 to 15 minutes acquisition period would normally not be expected. When the difference between two successive values exceeds a predetermined value,

the data in question can be flagged for further evaluation. Screening is an iterative process in which range checks and other screening criteria are revised as necessary based on experience. For example, an initial QA pass of a data set using default criteria may result in flagged values which, upon further investigation, are determined to be valid for a particular site. In such cases, one or more follow-up QA passes using revised criteria may be necessary to clearly segregate valid and invalid data.

### **Final Validation and Evaluation of Measurements for Data Users**

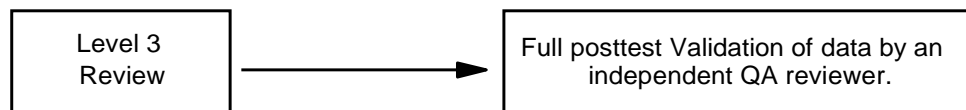


***Figure 5-6 Level 3 Quality Checks Ensure the Data is Usable for the Purpose Intended***

Data validation is a routine process designed to ensure that reported values meet the quality goals and objectives of environmental data operations. A progressive, systematic approach to data validation must be used to ensure and assess the quality of data. The purpose of this step in the process is to detect, compare, and perform a final screening on all data values. Any final data that may not represent actual conditions at the sampling site will be detected at this stage. Effective data validation procedures usually are handled independent of the procedures of initial data verification, that is, by different staff. It is important that data validation staff be independent of field operators.

If data assessment results clearly indicate a serious response problem with the optical technology, the agency should review all related information to determine whether the optical remote assessment data, should be invalidated. Some problems that may escape detection during an audit are often easily identified during data validation. Data validation should be performed by a person **with appropriate training in the optical technology who has a basic understanding of instrument operation and typical results from similar measurement projects.**

Data flagged by the QC screening should be evaluated by personnel with optical measurement



expertise. Reasons for changes in the data resulting from the validation process should be documented. If system problems are identified, corrective actions should also be documented. Edited data should continue to be flagged so that their reliability can be considered in the interpretation of the results of modeling analyses for which the data are used. Flags can be used in the field and by the data reviewers to signify data that may be suspect due to calibration or audit failure, special events, or failed QC limits. When calibration problems are identified, data produced between the suspect calibration event and subsequent recalibration should be flagged. Because flag combinations can be overwhelming and cannot always be anticipated, an organization needs to review these flag combinations to determine whether single values or values from a site over a period should be invalidated. Procedures for screening data for possible errors or anomalies should also be implemented. When calibration problems are identified, data produced between the suspect calibration event and any subsequent recalibration should be flagged to alert data users.

#### **5.4 References**

1. Guidance on Environmental Data Verification and Data Validation, EPA QA/G-8, EPA/240/R-02/004, November 2002.
2. Mueller, P. K.; Watson, J. G. " Eastern regional air-quality measurements. Volume 1, Section 7" ;EPRI-EA -1914-Vol.1, final report prepared for Environmental Research and Technology, Inc., Concord, MA , by Electric Power Research Institute, Palo A lto, CA. 1982.
3. Watson, J. G.; Lioy, P. J.; Mueller, P. K. " The measurement process: precision, accuracy, and validity" . In Proceedings, Proceedings, Air Sampling Instruments for Evaluation of Atmospheric Contaminants; 7th ed.; Hering, S. V., Ed.; American Conference of Governmental Industrial Hygienists: Cincinnati, OH, 1989, pp 51- 57.
4. Battelle ETV Generic Verification Protocol for Optical Open-Path Monitors 2002.

---

United States  
Environmental Protection  
Agency

Office of Air Quality Planning and Standards  
Air Quality Assessment Division  
Research Triangle Park, NC

Publication No. EPA-454/B-18-008  
August 2018

---